National Park Service
U.S. Department of the Interior

Science Report NPS/SR—2024/141
https://doi.org/10.36967/2303786

# Divergent Trends in Distribution and Abundance of Landbirds in Low and High Elevation Habitats of the Ka‘ū Rainforest



‘Akiapōlā‘au (*Hemignathus wilsoni*)
© JACOB DRUCKER

# Divergent trends in distribution and abundance of landbirds in low and high elevation habitats of the Ka‘ū Rainforest

Science Report NPS/SR—2024/141

Seth W. Judge, [1] Kevin W. Brinck, [2] Ayesha S. Genz, [2] Lainie Berry, [3] Jacqueline M. Gaudioso, [4] Alexander X. Wang, [4] and Richard J. Camp[5]

[1]Pacific Island Network Inventory and Monitoring Program
National Park Service
P.O. Box 52
Hawai‘i National Park, HI 96718

[2]Hawai‘i Cooperative Studies Unit
University of Hawai‘i at Hilo
200 West Kawili Street
Hilo, HI 96720

[3]Division of Forestry and Wildlife
State of Hawai‘i Department of Lands and Natural Resources
1151 Punchbowl Street
Honolulu, HI 96813

[4]Division of Forestry and Wildlife
State of Hawai‘i Department of Land and Natural Resources
19 East Kawili Street
Hilo, HI 96720

[5]United States Geological Survey
Pacific Island Ecosystems Research Center
P.O. Box 44
Hawai‘i National Park, HI 96718

Please cite this publication as:

Judge, S. W., K. W. Brinck, A. S. Genz, L. Berry, J. M. Gaudioso, A. X. Wang, and R. J. Camp. 2024. Divergent trends in distribution and abundance of landbirds in low and high elevation habitats of the Ka‘ū Rainforest. Science Report NPS/SR—2024/141. National Park Service, Fort Collins, Colorado. https://doi.org/10.36967/2303786

NPS 124/193811, June 2024

The National Park Service Science Report Series disseminates information, analysis, and results of scientific studies and related topics concerning resources and lands managed by the National Park Service. The series supports the advancement of science, informed decision making, and the achievement of the National Park Service mission.

All manuscripts in the series receive the appropriate level of peer review to ensure that the information is scientifically credible and technically accurate.

Views, statements, findings, conclusions, recommendations, and data in this report do not necessarily reflect views and policies of the National Park Service, U.S. Department of the Interior. Mention of trade names or commercial products does not constitute endorsement or recommendation for use by the U.S. Government.

The Department of the Interior protects and manages the nation's natural resources and cultural heritage; provides scientific and other information about those resources; and honors its special responsibilities to American Indians, Alaska Natives, and affiliated Island Communities.

This report is available in digital format from the National Park Service DataStore and the Natural Resource Publications Management website. If you have difficulty accessing information in this publication, particularly if using assistive technology, please email irma@nps.gov.

# Contents

Page

Figures....vi

Tables....x

Appendices....xiii

Abstract....xiv

Acknowledgments....xv

Introduction....1

Methods....4

Survey Area....6

Point-Transect Distance Sampling Methods....7

Habitat Survey Methods....8

Computer Data Entry and Verification Methods....8

Data Analysis....8

Indices....8

Density Estimation....8

Vegetation Covariates....10

Abundance Estimates and Inference Areas....10

Population Trend....11

Results....12

2019 Landbird Detections....12

Population Densities, Abundance, and Trends of Native Species....14

Native Species Summaries....16

ʻAkiapōlāʻau....16

ʻAlawī....16

ʻApapane....17

Hawaiʻi ʻĀkepa....19

Hawaiʻi ʻAmakihi....19

# Contents (continued)

Page

Hawai‘i ‘Elepaio....21
‘I‘iwi....22
‘Io....24
‘Ōma‘o....24
Population Densities, Abundance, and Trends of Non-Native Species....26
Non-Native Species Summaries....28
Chinese Hwamei....28
Common Myna....28
Common Waxbill....28
Erckel’s Spurfowl....28
House Finch....28
Japanese Bush Warbler....28
Kalij Pheasant....28
Northern Cardinal....28
Red-billed Leiothrix....31
Red Junglefowl....33
Warbling White-eye....33
Western Meadowlark....35
Wild Turkey....35
Yellow-fronted Canary....35
Habitat Surveys....35
Vegetation Covariates....36
Discussion....38
Landbirds....38
Habitats....41
Conclusion....42

# Contents (continued)

Page

Literature Cited ..... 43

# Figures

Page

**Figure 1.** The 2019 Kaʻū Rainforest survey area, including the Kahuku Unit of Hawaiʻi Volcanoes National Park, the adjacent Kaʻū Forest Reserve, Kapāpala Forest Reserve, Kapāpala Cooperative Game Management areas; as well as parcels managed by The Nature Conservancy and the Kamehameha Schools Land Assets Division. ..... 5

**Figure 2.** The 2019 Kaʻū Rainforest survey area and transects surveyed in 2019. ..... 54

**Figure 3.** Legacy transects 1, 2, 3, and 4 and stations surveyed during the 2019 Kaʻū Rainforest landbird survey (in green). ..... 60

**Figure 4.** Exit routes for the bottom of Transect 2 and Transect 3 within the Kaʻū Forest Reserve. ..... 61

**Figure 5.** Exit route for Transect 4 and The Nature Conservancy Kaiholena Unit Preserve. ..... 63

**Figure 6.** Transects 5, 6, and 7 and stations surveyed during the 2019 Kaʻū Rainforest landbird survey (in green). ..... 64

**Figure 7.** Exit routes for Transect 6 and Transect 7 surveyed in 2019. ..... 66

**Figure 8.** Kaʻū Rainforest Transects 8, 9, 10, and 11 and stations surveyed in 2019 (in green). ..... 67

**Figure 9.** Exit route of Transect 8 surveyed in 2019. ..... 69

**Figure 10.** Access and exit routes of Transect 9 surveyed in 2019. ..... 70

**Figure 11.** Access and exit routes of Transect 10 surveyed in 2019. ..... 71

**Figure 12.** The 2019 Kaʻū Rainforest landbird survey inference area. ..... 74

**Figure 13.** ʻAkiapōlāʻau detection history and estimated ranges within the Kaʻū Rainforest survey area. ..... 75

**Figure 14.** ʻAlawī detection history and estimated ranges within the Kaʻū Rainforest survey area. ..... 76

**Figure 15.** Hawaiʻi ʻĀkepa detection history and estimated ranges within the Kaʻū Rainforest survey area. ..... 77

**Figure 16.** ʻIʻiwi detection history and estimated ranges within the Kaʻū Rainforest survey area. ..... 78

**Figure 17.** ʻAkiapōlāʻau (*Hemignathus wilsoni*) detections during the 2019 Kaʻū Rainforest landbird survey. ..... 103

# Figures (continued)

Page

**Figure 18.** ʻAlawī (*Loxops* mana) detections during the 2019 Kaʻū Rainforest landbird survey. ..... 104

**Figure 19.** ʻApapane (*Himatione sanguinea*) detections during the 2019 Kaʻū Rainforest landbird survey.. ..... 105

**Figure 20.** Hawaiʻi ʻĀkepa (*Loxops coccineus*) detections during the 2019 Kaʻū Rainforest landbird survey. ..... 106

**Figure 21.** Hawaiʻi ʻAmakihi (*Chlorodrepanis virens virens*) detections during the 2019 Kaʻū Rainforest landbird survey. ..... 107

**Figure 22.** Hawaiʻi ʻElepaio (*Chasiempis sandwichensis*) detections during the 2019 Kaʻū Rainforest landbird survey.. ..... 108

**Figure 23.** ʻIʻiwi (*Drepanis coccinea*) detections during the 2019 Kaʻū Rainforest landbird survey. ..... 109

**Figure 24.** ʻIo (*Buteo solitarius*) detections during the 2019 Kaʻū Rainforest landbird survey. ..... 110

**Figure 25.** ʻŌmaʻo (*Myadestes obscurus*) detections during the 2019 Kaʻū Rainforest landbird survey. ..... 111

**Figure 26.** Chinese Hwamei (*Garrulax canorus*) detections during the 2019 Kaʻū Rainforest landbird survey. ..... 113

**Figure 27.** Common Myna (*Acridotheres tristis*) detections during the 2019 Kaʻū Rainforest landbird survey. ..... 114

**Figure 28.** Common Waxbill (*Estrilda astrild*) detections during the 2019 Kaʻū Rainforest landbird survey. ..... 115

**Figure 29.** Erckel's Spurfowl (*Pternistis erckelii*) detections during the 2019 Kaʻū Rainforest landbird survey. ..... 116

**Figure 30.** House Finch (*Haemorhous mexicanus*) detections during the 2019 Kaʻū Rainforest landbird survey ..... 117

**Figure 31.** Japanese Bush Warbler (*Horornis diphone*) detections during the 2019 Kaʻū Rainforest landbird survey. ..... 118

**Figure 32.** Kalij Pheasant (*Lophura leucomelanos*) detections during the 2019 Kaʻū Rainforest landbird survey. ..... 119

# Figures (continued)

Page

**Figure 33.** Northern Cardinal (*Cardinalis cardinalis*) detections during the 2019 Kaʻū Rainforest landbird survey. ..... 120

**Figure 34.** Red-billed Leiothrix (*Leiothrix lutea*) detections during the 2019 Kaʻū Rainforest landbird survey. ..... 121

**Figure 35.** Red Junglefowl (*Gallus gallus*) detections during the 2019 Kaʻū Rainforest landbird survey. ..... 122

**Figure 36.** Warbling White-eye (*Zosterops japonicus*) detections during the 2019 Kaʻū Rainforest landbird survey. ..... 123

**Figure 37.** Western Meadowlark (*Sturnella neglecta*) detections during the 2019 Kaʻū Rainforest landbird survey. ..... 124

**Figure 38.** Wild Turkey (*Meleagris gallopavo*) detections during the 2019 Kaʻū Rainforest landbird survey. ..... 125

**Figure 39.** Yellow-fronted Canary (*Crithagra mozambica*) detections during the 2019 Kaʻū Rainforest landbird survey. ..... 126

**Figure 40.** ʻAkiapōlāʻau (*Hemignathus wilsoni*) population estimates from surveys conducted in the Kaʻū Rainforest from 1976 to 2019. ..... 127

**Figure 41.** ʻAlawī (*Loxops mana*) population estimates from 1976 to 2019 and trends from 2002 to 2019. ..... 128

**Figure 42.** ʻApapane (*Himatione sanguinea*) population estimates from 1976 to 2019 and trends from 2002 to 2019. ..... 129

**Figure 43.** Hawaiʻi ʻĀkepa (*Loxos coccineus*) population estimates from 1976 to 2019 and trends from 2002 to 2019. ..... 130

**Figure 44.** Hawaiʻi ʻAmakihi (*Chlorodrepanis virens virens*) population estimates from 1976 to 2019 and trends from 2002 to 2019. ..... 131

**Figure 45.** Hawaiʻi ʻElepaio (*Chasiempis sandwichensis*) population estimates from 1976 to 2019 and trends from 2002 to 2019. ..... 132

**Figure 46.** ʻIʻiwi (*Drepanis coccinea*) population estimates from 1976 to 2019 and trends from 2002 to 2019. ..... 133

**Figure 47.** ʻŌmaʻo (*Myadestes obscurus*) population estimates from 1976 to 2019 and trends from 2002 to 2019. ..... 134

# Figures (continued)

Page

**Figure 48.** Northern Cardinal (*Cardinalis cardinalis*) population estimates from 1976 to 2019 and trends from 2002 to 2019. ..... 135

**Figure 49.** Red-billed Leiothrix (*Leiothrix lutea*) trends population estimates from 1976 to 2019 and from 2002 to 2019. ..... 136

**Figure 50.** Warbling White-eye (*Zosterops japonicus*) population estimates from 1976 to 2019 and trends from 2002 to 2019. ..... 137

**Figure 51.** Environment classifications recorded at stations surveyed in 2019 and in previous years. ..... 139

**Figure 52.** Forest cover classifications recorded at stations surveyed in 2019 and in previous years. ..... 142

**Figure 53.** Canopy height classes recorded at each station during the 2019 Kaʻū Rainforest landbird survey and for transects surveyed in previous years. ..... 143

**Figure 54.** The predominant canopy species recorded at each station surveyed in 2019 and for transects surveyed in previous years. ..... 145

**Figure 55.** The predominant understory species or class recorded at each station surveyed in 2019 and for some transects surveyed in previous years. ..... 148

**Figure 56.** The Jacobi (1989) vegetation code recorded for each station surveyed in 2019 and previous survey years. ..... 150

# Tables

Page

**Table 1.** Management units surveyed during the 2019 Kaʻū Rainforest landbird survey. 6

**Table 2.** Models and parameters used to derive population densities by species for the 2019 Kaʻū Rainforest landbird survey. 9

**Table 3.** Inference areas (hectares) used to determine abundance estimates for broadly occurring species and for smaller range-restricted and wide-spread species detected during the 2019 Kaʻū Rainforest landbird survey. 11

**Table 4.** List of species detected during the 2019 Kaʻū Rainforest landbird survey. 12

**Table 5.** Indices of native and non-native bird detections for the 2019 Kaʻū Rainforest landbird survey. 13

**Table 6.** Native landbird trends within the Kaʻū Rainforest (2002–2019) by species range or survey strata and total surveyed area. 15

**Table 7.** ʻAkiapōlāʻau density and abundance estimates (± standard error [SE] and 95% confidence interval [CI]) in the species' estimated restricted range within the Kaʻū Rainforest survey area. 16

**Table 8.** ʻAlawī density and abundance estimates (± SE and 95%CI) in the species' entire estimated range within the Kaʻū Rainforest survey area. 17

**Table 9.** ʻApapane density and abundance estimates (± SE and 95%CI) in the low elevation (<1,500 m), high elevation (≥1,500 m), and total area combined. 18

**Table 10.** Hawaiʻi ʻĀkepa density and abundance estimates (± SE and 95%CI) in the species' entire estimated range within the Kaʻū Rainforest survey area. 19

**Table 11.** Hawaiʻi ʻAmakihi density and abundance estimates (± SE and 95%CI) in the low elevation (<1,500 m), high elevation (≥1,500 m), and total area combined. 20

**Table 12.** Hawaiʻi ʻElepaio density and abundance estimates (± SE and 95%CI) in the low elevation (<1,500 m), high elevation (≥1,500 m), and total area combined. 21

**Table 13.** ʻIʻiwi density and abundance estimates (± SE and 95%CI) in the low elevation (<1,500 m), high elevation (≥1,500 m), and total area combined. 23

**Table 14.** ʻŌmaʻo density and abundance estimates (± SE and 95%CI) in the low elevation (<1,500 m), high elevation (≥1,500 m), and total area combined. 25

**Table 15.** Non-native landbird trends within the Kaʻū Rainforest (2002–2019). 27

**Table 16.** Northern Cardinal density and abundance estimates (± SE and 95%CI) in the low elevation (<1,500 m), high elevation (≥1,500 m), and total area combined. 30

# Tables (continued)

Page

**Table 17.** Red-billed Leiothrix density and abundance estimates (± SE and 95%CI) in the low elevation (<1,500 m), high elevation (≥1,500 m), and total area combined. ..... 32

**Table 18.** Warbling White-eye density and abundance estimates (± SE and 95%CI) in the low elevation (<1,500 m), high elevation (≥1,500 m), and total area combined. ..... 34

**Table 19.** Vegetation covariates used to improve detection function model. ..... 36

**Table 20.** Bird models and species detection functions that were improved with vegetation covariates. ..... 37

**Table 21.** PACN legacy transect numbering in the Kahuku Tract during the 2010 and 2016 landbird monitoring surveys and the new relabeled numbers updated during the 2019 survey. ..... 57

**Table 22.** Model selection based on AIC for ʻAkiapōlāʻau (*Hemignathus wilsoni*) ..... 80

**Table 23.** Model selection based on AIC for ʻAlawī (*Loxops mana*). ..... 80

**Table 24.** Model selection based on AIC for ʻApapane (Himatione sanguinea). ..... 81

**Table 25.** Model selection based on AIC for Hawaiʻi ʻAmakihi (*Chlorodrepanis virens virens*) ..... 82

**Table 26.** Model selection based on AIC for Hawaiʻi ʻElepaio (*Chasiempis sandwichensis*). ..... 83

**Table 27.** Model selection based on AIC for Hawaiʻi ʻĀkepa (*Loxops coccineus*) ..... 84

**Table 28.** Model selection based on AIC for ʻIʻiwi (*Drepanis coccinea*). ..... 85

**Table 29.** Model selection based on AIC for Northern Cardinal (*Cardinalis cardinalis*). ..... 86

**Table 30.** Model selection based on AIC for ʻŌmaʻo (*Myadestes obscurus*). ..... 86

**Table 31.** Model selection based on AIC for Red-billed Leiothrix (*Leiothrix lutea*). ..... 87

**Table 32.** Model selection based on AIC for Warbling White-eye (*Zosterops japonicus*). ..... 88

**Table 33.** Model selection based on AIC for ʻAkiapōlāʻau (*Hemignathus wilsoni*) ..... 91

**Table 34.** Model selection based on AIC for ʻApapane (*Himatione sanguinea*). ..... 91

**Table 35.** Model selection based on AIC for Hawaiʻi ʻĀkepa (*Loxops coccineus*) ..... 92

**Table 36.** Model selection based on AIC for Hawaiʻi ʻAmakihi (*Chlorodrepanis virens virens*) ..... 93

# Tables (continued)

Page

**Table 37.** Model selection based on AIC for Hawai‘i ‘Elepaio (*Chasiempis sandwichensis*). ..... 94

**Table 38.** Model selection based on AIC for ‘Alawī (*Loxops mana*). ..... 95

**Table 39.** Model selection based on AIC for ‘I‘iwi (*Drepanis coccinea*). ..... 96

**Table 40.** Model selection based on AIC for ‘Ōma‘o (*Myadestes obscurus*). ..... 97

**Table 41.** Model selection based on AIC for Northern Cardinal (*Cardinalis cardinalis*). ..... 98

**Table 42.** Model selection based on AIC for Red-billed Leiothrix (*Leiothrix lutea*). ..... 99

**Table 43.** Model selection based on AIC for Warbling White-eye (*Zosterops japonicus*). ..... 100

**Table 44.** Moisture zones of 2019 Ka‘ū Rainforest survey stations per each study area. ..... 138

**Table 45.** Canopy height and cover classes recorded during the 2019 Ka‘ū Rainforest Survey. ..... 140

**Table 46.** Dominant canopy classes recorded within each survey area during the 2019 Ka‘ū Rainforest landbird survey. ..... 144

**Table 47.** Understory classes recorded within each survey area during the 2019 Ka‘ū Rainforest landbird survey. ..... 146

**Table 48.** Vegetation classification codes (Jacobi 1989) recorded for each station surveyed in 2019. ..... 149

# Appendices

Page

Appendix A. Hawai‘i Volcanoes National Park and Ka‘ū Forest Reserve Landbird Monitoring Field Report (2019) ..... 52

Appendix B. Methods for Determining Inference Area of Range Restricted Species ..... 73

Appendix C. Akaike’s Information Criterion (AIC) Statistics- Weather, Temporal, and Observer Covariates ..... 79

Appendix D. Akaike’s Information Criterion (AIC) Statistics- Vegetation Covariates ..... 90

Appendix E. Landbird Occurrence Maps ..... 102

Appendix F. Ka‘ū Rainforest Landbird Trend Graphics ..... 127

Appendix G. 2019 Habitat Survey Results ..... 138

# Abstract

Federal, state, and non-governmental partners resurveyed landbirds in the Kaʻū Rainforest on the Island of Hawaiʻi in 2019. Point-transect distance sampling was conducted in Hawaiʻi Volcanoes National Park, Kaʻū Forest Reserve, Kapāpala Forest Reserve, and Kapāpala Cooperative Game Management Area. This is the first comprehensive survey of the region since 2008. Through a collaborative effort, monitoring transects were consolidated to provide a consistent, repeatable sampling frame for future surveys. We estimated landbird distribution, density, and abundance for eight surveys since 1976. Changes in species-specific densities were assessed using a log-linear regression to determine trends of the six most recent surveys since 2002. Trends were assessed in three strata: low elevation (<1,500 m), high elevation (≥1,500 m), and total survey area.

We detected 23 species and there were sufficient detections of 11 species to estimate density and abundance. We provided indices of relative occurrence for the remaining 12 species detected. Native birds vulnerable to avian malaria (*Plasmodium relictum*) were absent or trended downward in the low elevation stratum. The federally endangered ʻAkiapōlāʻau (*Hemignathus wilsoni*), ʻAlawī (Hawaiʻi Creeper, *Loxops mana*), and Hawaiʻi ʻĀkepa (*Loxops coccineus*) were restricted to areas above 1,500 m elevation, likely due to the low prevalence of the cold-intolerant vector of avian malaria, the southern house mosquito (*Culex quinquefasciatus*). However, downward trends of the federally threatened ʻIʻiwi (*Drepanis coccinea*) above 1,500 m elevation may indicate an expansion in range of mosquitoes due to warming trends. Thought to be more resilient to avian malaria, the ʻApapane (*Himatione sanguinea*) and Hawaiʻi ʻAmakihi (*Chlorodrepanis virens virens*) trended upward in all three strata. The Hawaiʻi ʻElepaio (*Chasiempis sandwichensis*) trended downward in each stratum. The ʻŌmaʻo (*Myadestes obscurus*) trended upward in the low stratum and downward in high. Trends were inconclusive for Hawaiʻi ʻĀkepa, but favorable for ʻAlawī, which trended upward in its restricted range. There were insufficient detections of ʻAkiapōlāʻau in 2019 to estimate density, but the 2008 abundance estimate of 691 ± 410 (SE) birds was the lowest since 1976. Trends were mixed for the non-native Warbling White-eye (*Zosterops japonicus*), Red-billed Leiothrix (*Leiothrix lutea*), and Northern Cardinal (*Cardinalis cardinalis*). Overall, upward trends of ʻApapane and Hawaiʻi ʻAmakihi throughout the survey area, ʻŌmaʻo in the low stratum, and ʻAlawī in the high stratum, suggests management actions to protect native forest bird habitat are having a positive benefit. Nevertheless, avian malaria is predicted to have an increasing impact on vulnerable species as mosquitoes expand into higher elevations.

# Acknowledgments

We would like to thank Ryan Monello, Kelly Kozar, and Mark Wasser of the Pacific Island Network Inventory and Monitoring Program, as well as the State of Hawai‘i Division of Forestry and Wildlife (DOFAW) land managers Steven Bergfeld and Jay Hatayama, Hilo branch operations staff, and administrators for access, funding, and support of the project. Many thanks to Hawai‘i Volcanoes National Park's Rhonda Loh, David Benitez, and Ryan Deacy for facilitating permits and coordination. Thanks to pilot David Okita of Volcano Helicopters for safe transport and logistical advice. We would also like to thank the staff and volunteers from the following agencies and organizations for their diligent work establishing transects and conducting surveys over challenging terrain and, at times, inclement weather: DOFAW Forestry and Wildlife crews, the Hawai‘i Island Natural Area Reserve System program, Three Mountain Alliance, Research Cooperation of the University of Hawai‘i, Kupu Hawai‘i, Maui Forest Bird Recovery Project, the Plant Extinction Prevention Program, The National Park Service, The Nature Conservancy, U.S. Fish and Wildlife Service, the University of Hawai‘i at Hilo, and the generous volunteers with no formal affiliation. The groundwork and resources needed to conduct this project would have not been possible without the participation and coordination provided from these entities. Many thanks to Steve Kendall and Marcos Gorresen who provided comments that improved this report. This study was conducted through the Hawai‘i-Pacific Islands Cooperative Ecosystem Studies Unit, Task Agreement P14AC00637 between the National Park Service and the University of Hawai‘i at Hilo; as well as the Hawai‘i Cooperative Studies Unit, Task Agreement G13AC00125 between the U.S. Geological Survey and the University of Hawai‘i at Hilo. Any use of trade, firm, or product names is for descriptive purposes only and does not imply endorsement by the U.S. Government.

# Introduction

The Hawaiian Islands harbor a disproportionate number of federally listed threatened and endangered species in the United States. There are approximately 500 federally listed species of plants and animals in Hawai‘i—comprising >30% of all listed species in the country (USFWS 2023a). There are 27 species of seabirds, shorebirds, and landbirds listed (USFWS 2023a). In 2023, eight species of landbirds were delisted due to extinction (USFWS 2023b), totaling to about 110 of 142 known endemic bird species that have gone extinct since human colonization of the islands (James and Olson 1991, Olson and James 1991, Banko and Banko 2009a, Pyle and Pyle 2017). The subfamily of Hawaiian honeycreepers (Carduelinae) suffered the most losses; of the more than 50 documented species and subspecies, only 17 currently persist in the island chain and all but six are federally endangered or threatened (VanderWerf et al. 2018, Chesser et al. 2023).

The history of Hawai‘i’s imperiled avifauna can be tracked spatially along an elevational gradient, starting at low elevations with the first arrival of Polynesians between 1,000 and 1,200 common era (Kirch 2011). Lowland forests were degraded through the pressures of agriculture and development (Kirch 1982). Birds were harvested for food and feathers, and the predatory pressures of introduced dogs (*Canis lupus familiaris*), and Polynesian rats (*Rattus exulans*) resulted in the extinction of an estimated 71 bird species and sub-species before Western contact (Olson and James 1982, 1984, Banko et al. 2001). The first European arrivals were in the late 1770s and by 1825 that influence culminated in more lowland deforestation and increased numbers and varieties of stressors. Domestic cats (*Felis catus*) were intentionally introduced, and the Norway rat (*R. norvegicus*), black rat (*R. rattus*), and house mouse (*Mus musculus*) were accidentally introduced and quickly naturalized within most landbird habitat where they posed persistent threats through predation and competition of resources (Atkinson 1977, Witmer and Shiels 2017). In 1883, the small Indian mongoose (*Herpestes javanicus*) was intentionally introduced (Tomich 1986), and the predator became nearly ubiquitous on the islands of Hawai‘i, O‘ahu, Moloka‘i, and Maui, ranging from sea level to as high as 3,000 m elevation (Kaholoaa et al. 2019). Mongooses are effective predators and cause direct threats to nesting seabirds, water birds, and forest birds (Banko 1992, Hays and Conant 2007, VanderWerf 2020).

Threats to avifauna extended into predominantly native forest with the introduction of the Southern house mosquito (*Culex quinquefasciatus*) in 1826, a species that is a competent vector for avian malaria (*Plasmodium relictum*; Warner 1968). Hawaiian honeycreepers are highly vulnerable to the parasite, and avian malaria has contributed to many extinctions and significant reductions in range (Warner 1968, van Riper et al. 1986, Atkinson et al. 1995). The impact of avian malaria is worsened by the effects of climate change. In Hawai‘i, mean air temperature has warmed significantly by 0.052°C/decade over the last 100 years (McKenzie et al. 2019). Higher mean temperatures increase altitudinal range of both cold-intolerant *C. quinquefasciatus* and *P. relictum* (Ahumada et al. 2004, LaPointe et al. 2010, Samuel et al. 2011, Atkinson et al. 2014). The upper limit of mosquito distribution and malaria transmission was historically around 1,500 m elevation where mean temperatures were approximately 14°C (Ahumada et al. 2004). The island of Kaua‘i, with a maximum elevation of 1,598 m, has suffered catastrophic collapse of the avian community due to

avian malaria (Paxton et al. 2016). With no higher elevation habitat available and no immediate plan or method to control avian malaria, models predict several more landbird extinctions in the coming decades (Paxton et al. 2016). Under current climate change scenarios, Fortini et al. (2015) projected that honeycreepers will lose more than 50% of current projected range by 2100 in the main Hawaiian Islands. After this time, only islands with native habitat higher than 1,500 m are projected to still have some (limited) refugia for honeycreepers vulnerable to malaria.

The Kaʻū Rainforest on the Island of Hawaiʻi, at approximately 35,000 hectares (ha), is one of the largest native forests in the state. This forest habitat is critically important to native bird populations, and many of the island's other indigenous, endemic, and endangered flora and fauna. The Kaʻū Rainforest ranges in elevation from wet mesic forest near 600 m upward to montane woodland at 2,300 m elevation. The high elevation forests provide refugia for native birds vulnerable to avian malaria. Located on the windward side of Mauna Loa volcano, the forest's natural resources benefit from protection by the National Park Service (NPS), the State of Hawaiʻi Department of Land and Natural Resources (DLNR), The Nature Conservancy (TNC), and parcels owned by Kamehameha Schools Land Assets Division (KS). During the late 1970s and early 1980s, the U.S. Fish and Wildlife Service (USFWS) conducted surveys of bird and plant communities on the main Hawaiian Islands as part of the Hawaiʻi Forest Bird Survey (HFBS; Scott et al. 1986). The 1976 HFBS was conducted in the Kaʻū Rainforest, on transects within the Kaʻū Forest Reserve (KFR) and Kapāpala Forest Reserve (KPFR), which are managed by the State of Hawaiʻi Division of Forestry and Wildlife (DOFAW). The upper portions of the 1976 HFBS surveyed in what is now the Kahuku Unit of Hawaiʻi Volcanoes National Park (HAVO). DOFAW continued landbird surveys (on transects established by the HFBS) in 1993, 2002, and 2008 (Gorresen et al. 2007, Camp et al. 2009a). In 2004, the U.S. Geological Survey (USGS) conducted surveys in areas of KFR and Kapāpala Cooperative Game Management Area (KCGMA; Gorresen et al. 2007). The Kahuku Unit was surveyed for landbird occurrence, distribution, and population densities in 2005 (Tweed et al. 2007). The NPS Pacific Island Inventory and Monitoring Program (PACN) began conducting landbird monitoring in the Kahuku Tract in the Kahuku Unit and the upper forest habitat of KFR in 2010 and repeated those surveys in 2016 (Judge et al. 2011, 2017a). In 2019, PACN, DOFAW, TNC, USGS, the Three Mountain Alliance Watershed Partnership (TMA), and additional partners collaborated to align overlapping and disjunct transects into a single set and resurvey and analyze the entire area (Kahuku Unit, KPFR, KCGMA, and KFR) as a single dataset.

We report on the distribution and relative abundance of forest bird species detected during the 2019 survey, and for species with sufficient detections, we estimate density, abundance, and trends in the entire survey area or within the distribution of range-restricted species. We reanalyzed data of six surveys since 2002 to update density estimates and assess trends. We include population estimates and trends for four federally endangered or threatened native Hawaiian Honeycreepers: ʻAkiapōlāʻau (*Hemignathus wilsoni*), ʻAlawī (Hawaiʻi Creeper, *Loxops mana*), Hawaiʻi ʻĀkepa (*Loxops coccineus*), and ʻIʻiwi (*Drepanis coccinea*). We also report on population trends of four additional native species: ʻApapane (*Himatione sanguinea*), Hawaiʻi ʻAmakihi (*Chlorodrepanis virens virens*), Hawaiʻi ʻElepaio (*Chasiempis sandwichensis*), and ʻŌmaʻo (*Myadestes obscurus*); as

well as three non-native passerines:  Northern Cardinal (*Cardinalis cardinalis*), Red-billed Leiothrix (*Leiothrix lutea*), and Warbling White-eye (*Zosterops japonicus*).

# Methods

The 1976 HFBS applied point-transect distance sampling methods for surveying landbirds in the State of Hawai‘i (Scott et al. 1986). DOFAW adopted those methods and continued surveys in KFR, KPFR, and other important conservation areas (Camp et al. 2009b). PACN began surveys in 2010 and conducts point-transect distance sampling-based surveys in HAVO, Haleakalā National Park, and the National Park of American Samoa once every five years (Camp et al. 2011). Eight monitoring tracts were surveyed within HAVO in 2010, 2015, and 2016 (Judge et al. 2011, 2017a); five of which are within the Kahuku Unit of HAVO. The largest of the tracts, the Kahuku Tract covers portions of both HAVO and KFR, where five permanently established Legacy Transects are surveyed. In this collaborative effort, we realigned previously surveyed DOFAW transects to extend from the five PACN transects. Transects were numbered 1–11 and the Kahuku Tract transects were renumbered accordingly (Figure 1). Details considering the realignment, transect locations, transect logistics, and summary of the 2019 field effort are provided in Appendix A. To make the distinction between federally managed land and state land, we refer to the survey area only within HAVO as the Kahuku Unit. Scott et al. (1986) reported population densities and abundance in the 32,900 ha Ka‘ū survey area, which is a portion of the 2,388 $km^2$ Ka‘ū District of Hawai‘i County. We refer to the 2019 survey area colloquially as the Ka‘ū Rainforest, which primarily consists of wet and mesic montane native forest, and includes all areas surveyed. Non-HAVO lands are designated by their management entity and associated name (KFR, KPFR, and KCGMA, as well as parcels managed by TNC and KS).

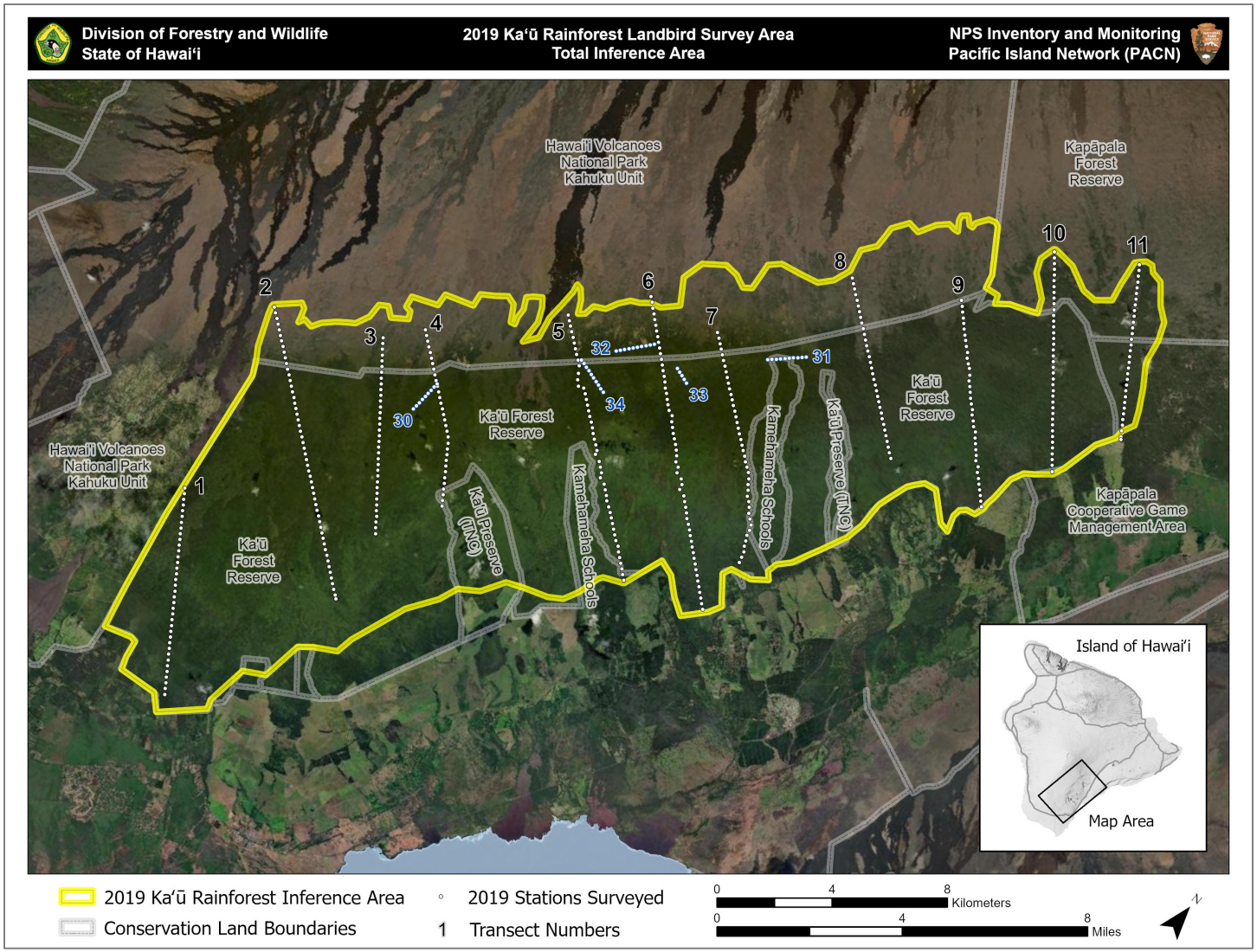



**Figure 1.** The 2019 Ka'ū Rainforest survey area, including the Kahuku Unit of Hawai'i Volcanoes National Park, the adjacent Ka'ū Forest Reserve, Kapāpala Forest Reserve, Kapāpala Cooperative Game Management areas; as well as parcels managed by The Nature Conservancy and the Kamehameha Schools Land Assets Division. Numbers in blue denote randomly prescribed transects surveyed in 2019 and numbers in black are permanently established Legacy Transects. Base map source: World Imagery (Esri, Maxar, Earthstar Geographics, and the GIS user community).

## Survey Area

The 2019 Kaʻū Rainforest survey area included landbird monitoring transects in portions of the Kahuku Unit, KFR, KPFR, and KCGMA (Table 1; Figure 1). The survey area also includes portions of privately managed land, including three TNC managed units collectively called the Kaʻū Preserve, and two separate parcels managed by KS. Methods for determining total inference area and areas of range restricted landbirds areas are described in methods below and in Appendix B. Total inference area equaled 32,917 ha, the largest portion of 23,665 ha was within KFR, with an additional 5,775 ha within the Kahuku Unit. The remaining units were each ≤800 ha each.

**Table 1.** Management units surveyed during the 2019 Kaʻū Rainforest landbird survey.

| Management Unit | Subunit | 2019 Survey Area (ha) |
|---|---|---|
| Kaʻū Forest Reserve | – | 23,665 |
| HAVO Kahuku Unit | – | 5,775 |
| Kapāpala Forest Reserve | – | 800 |
| Kapāpala Cooperative Game Management Area | – | 426 |
| The Nature Conservancy Kaʻū Preserve: | Kaiholena Unit | 772 |
| | Keaīwa Unit | 229 |
| | Kāhilipali Unit | 41 |
| **Total** | **–** | **32,917** |

There was a total of 11 permanently established transects with stations spaced at 200-m intervals. Five random transects were designated from a random sample of legacy station numbers, with a randomly selected azimuth in degrees selected to define direction of transect. The random transects had stations spaced at 150-m intervals, with the first station located 150 m from the randomly selected legacy station. The 200 m spacing of legacy transects was established by Tweed et al. (2007) and followed recommendations by Reynolds et al (1980), which considered time increments of surveys and the "area effect," or the probability of double counting an individual bird, which is reduced with greater station spacing. The reduced area effect is also applicable with the 150 m spacing of sampling points on legacy and random transects and allows surveyors to complete more stations during the sampling window (Reynolds et al. 1980, Scott et al. 1986, Buckland et al. 2001). A total of 488 distinct stations were sampled and 86 stations were surveyed twice or more for a total effort of 603 counts in 2019. The elevation of sampling stations ranged between 630 m and 2,270 m, with a diversity of substrate ages ranging from <200 to approximately 10,000 years old (Wolfe and Morris 1996). The study area spanned the moist mesic and moderately wet climate zones (Price et al. 2007) and was primarily montane ʻōhiʻa lehua (hereafter ʻōhiʻa; *Metrosideros polymorpha*) woodland, montane dry shrubland, and mesic closed-canopy ʻōhiʻa-koa (*Acacia koa*) forest. Montane woodlands (1,700–2,300 m) were an open-canopy mosaic of ʻōhiʻa trees, shrubland, and bare lava. Shrublands were co-dominated by native pūkiawe (*Leptecophylla tameiameiae*), ʻōhelo ʻai (*Vaccinium reticulatum*), hinahina (*Geranium cuneatum*), ʻaʻaliʻi (*Dodonaea viscosa*), and *Dubautia* spp., with scattered sedges (*Carex* spp.) and grasses (Poaceae, including non-native *Cenchrus*

*clandestinus* and native *Deschampsia nubigena*). There was a sharp transition from montane woodland into closed-canopy ʻōhiʻa forest near 1,700–1,800 m elevation. Large old-growth ʻōhiʻa formed a closed canopy and the understory was a dense mixture of native and non-native shrubs, ferns, and trees. Native shrubs and small trees included kanawao (*Hydrangea arguta*), ʻākala (*Rubus hawaiensis*), pilo (*Coprosma* spp.), ʻamaʻu (*Sadleria* spp.), kōlea lau nui (*Myrsine lessertiana*), kāwaʻu (*Ilex anomala*), and the matted fern uluhe (*Dicranopteris linearis*). The montane and subalpine portions of the Kahuku Unit, KFR, and KCGMA support introduced populations of European mouflon sheep (*Ovis aries musimon*; Hess et al. 2006). Non-native wild pigs (*Sus scrofa*) occur throughout the KFR, KPFR, and KCGMA; and to a lesser extent within the Kahuku Unit, where HAVO Resource Management actively control for ungulates (Judge et al. 2017b). Both Mouflon sheep and wild pigs degrade native habitat through browsing, grazing, trampling, and digging (Leopold and Hess 2017). HAVO continues to maintain and construct fences in the Kahuku Unit to exclude ungulates (National Park Service 2016).

### Point-Transect Distance Sampling Methods

Landbird surveys were conducted using point-transect distance sampling, where a detection function is fitted to distance measures between station center points and individually detected birds to estimate densities accounting for individuals that are undetected (Buckland et al. 2015). Robust estimates are reliant upon the critical assumptions that all birds are detected with certainty at or near the station center point, birds are detected prior to any movement, and distances are measured accurately. The sampling design is described in Camp et al. (2011).

Landbird surveys were conducted from 5 March 2019 through 18 April 2019. In weeks prior to the start of the survey, primary and secondary surveyors from NPS, DOFAW, and other partners were trained to calibrate for distance estimation and learn bird vocalizations, thereby minimizing variability among observers and standardizing for local conditions (Camp et al. 2011). During surveys, the detection type (heard, seen, or both) and horizontal distance from the station center point to individual birds detected were recorded during an 8-minute count. Birds only flying over or through the survey area were excluded. Detections of both male and female birds singing and calling were recorded, although the sex of individuals was not noted. Most of the birds encountered were adults because counts occurred during the breeding season and most juveniles had not yet fledged (Camp et al. 2011).

Observers also recorded cloud cover, rain, wind, gust, and time of day at each station (Camp et al. 2011). Sampling was conducted between dawn and 11:00 a.m. and halted when rain, wind strength, or gust exceeded prescribed levels (light rain and wind level 3 on the Beaufort scale). Weather variables and time of day were included as covariates in the analyses to account for possible differences in the detection probabilities due to the conditions when the count was conducted.

The detectability of forest birds varies throughout the year, due to changes in vocal activity associated with breeding (Best 1981), and birds may move in or out of the study area in response to phenology of food resources (Simon et al. 2002). To minimize biases associated with seasonal differences, surveys were conducted during the breeding season, which extends from November

through May (Ralph and Fancy 1994), with the Kaʻū Rainforest surveys usually conducted in April and May.

## Habitat Survey Methods

Landbird habitat data within the survey area were collected at each of the point-transect sampling stations. A 50-m radius plot was established at each station using the station as the center. At each plot the dominant canopy species composition, canopy height and cover, and dominant understory species composition were described. In addition to habitat characteristics, topographical attributes were collected at each station. Moisture regime zones (e.g., dry, mesic, or wet; Wagner et al. 1990) were assigned to survey stations *post hoc* using the Geographic Information System (GIS) layers provided by Jacobi (1989) and Green et al. (2015) and were summarized to describe each survey area. Habitat surveys were collected during transect preparation prior to conducting bird counts in most situations. Details of habitat sampling can be found in Camp et al. (2011). Sign of feral ungulates (pigs, goats [*Capra hircus*], and cattle [*Bos taurus*]) was documented opportunistically while hiking transects—either directly or by observing evidence of browsing, scat, and footprints.

## Computer Data Entry and Verification Methods

Microsoft Access was used as the primary software environment for landbird data and the associated metadata. Three separate Access databases with front-end, back-end configuration were developed for the landbirds monitoring data: (1) Avian Monitoring Entry Database, (2) Hawai'i Forest Bird Interagency Database, and (3) Habitat Monitoring Database.

Raw data were verified by comparing data sheets to the electronic version on a line-by-line basis to correct transcription errors. After line-by-line proofing was completed, individual data sets were certified by checking for errors. Lastly, field books (copies and originals) and digital data were archived according to PACN standards (Camp et al. 2011).

## Data Analysis

### *Indices*

Indices of bird occurrence and relative abundance were calculated for each species. Percent occurrence was calculated as the number of stations occupied divided by the total number of stations sampled. Similarly, birds per count was calculated as the total number of individuals detected divided by the total number of station counts. We computed relative abundance as birds per station (BPS) based on the total number of detections divided by the total number of stations surveyed. Birds per count (BPC) was computed because some stations were sampled more than once, either counted repeatedly by one surveyor or by multiple surveyors.

### *Density Estimation*

Species-specific density estimates (birds $ha^{-1}$) were calculated for each year for 11 species that had sufficient detections to adequately characterize detectability (Table 2; >75–100 detections; Buckland et al. 2015) using program DISTANCE, version 7.3, release 1 (Thomas et al. 2010; retrieved August 2019 from http://www.ruwpa.st-and.ac.uk/distance/). The candidate detection function models were limited to half-normal and hazard-rate detection functions with expansion series of order two (Buckland et al. 2015). Following recommendations by Buckland et al. (2015), the half-normal was

paired with cosine and Hermite polynomial adjustments, and the hazard-rate was paired with cosine and simple polynomial adjustments. Model precision was improved, by incorporating sampling covariates in the multiple covariate distance sampling engine of DISTANCE (Marques and Buckland 2004, Thomas et al. 2010). Covariates include habitat, observer, detection type (1=heard, 2=seen, 4=heard and seen), and time of detection; as well as weather variables including cloud cover, rain, wind, and gust (Table 2; Appendix C). All covariates were treated as a factor, except time of detection which was treated as a continuous covariate. Assessing time of detection as a continuous covariate helped to determine if the detection rate varied during the morning. Each detectability model in the candidate set was fit to survey data pooled across the timeseries, and the model selected was that with the lowest Akaike's Information Criterion (AIC) (Buckland et al. 2015). A total of 3,599 detections recorded during the 2008 survey of KFR and KPFR were evaluated in the detectability model. Numbers of detections for the remaining survey years for estimating detectability and densities are provided in Camp et al. (2009a) and Judge et al. (2011, 2017a). Data were truncated at a distance where detection probability was <10%. This procedure facilitates modeling by deleting outliers and reducing the number of parameters needed to modify the detection function. Species-specific densities were estimated from the global detection function using the post-stratification approach, and variances and confidence intervals (CI) were derived by bootstrap methods in DISTANCE from 999 iterations (Appendix C; Thomas et al. 2010).

**Table 2.** Models and parameters used to derive population densities by species for the 2019 Kaʻū Rainforest landbird survey. Models examined included half-normal and hazard-rate key detection functions and with cosine (Cos), Hermite polynomial (Hpoly), and simple polynomial (Spoly) series expansions. Detection type (1=heard, 2=seen, 4=heard and seen) was also evaluated as a categorical variable, indicated as "Detection", and based on pooling detection type by combination of types (e.g., "Detect 2, 4" pools all detections that were seen, and both heard and seen). Time of day (Time) and survey year (Year [continuous]) were evaluated as continuous variables. Truncation is the distance at which the detection probability was <10% using a preliminary half-normal detection function model.

| Species | Model | Series Expansion | Covariate | Truncation |
|---|---|---|---|---|
| ʻAkiapōlāʻau | Half-normal | Cos (1) | none | none |
| ʻAlawī | Half-normal | None | Detect 2,4 | none |
| ʻApapane | Hazard-rate | Cos (2,3) | Detect 2,4 | 10% |
| Hawaiʻi ʻĀkepa | Hazard-rate | None | Year (Factor) | none |
| Hawaiʻi ʻAmakihi | Hazard-rate | None | Detection | 10% |
| Hawaiʻi ʻElepaio | Hazard-rate | None | Detection | none |
| ʻIʻiwi | Half-normal | None | Detection | 5% |
| ʻŌmaʻo | Hazard-rate | None | Detect 2,4 | 10% |
| Warbling White-eye | Hazard-rate | None | Detection | 10% |
| Northern Cardinal | Hazard-rate | None | Detection | 5% |
| Red-billed Leiothrix | Hazard-rate | None | Detection | 5% |

### *Vegetation Covariates*

In addition to fitting models using the observation and sampling condition covariates described above, we examined the potential of using vegetation covariates to improve model fit. Fitting vegetation covariates was an exploratory analysis, and because vegetation information was not available for the entire study period these models were not used for inference. We used 12 measurements of the vegetation structure as vegetation covariates from vegetation surveys done in 1983 (Jacobi 1989), a PACN GIS-based classification by Green et al. (2015), and the habitat surveys (described above) collected at the 488 stations during the 2019 survey. Jacobi (1989) used classifications described by (Wagner et al. 1990) to map plant community types that were described by moisture regimes, elevation, and vegetation composition and structure (Appendix D). In the Kaʻū Rainforest, moisture regimes were identified by three annual rainfall categories: Dry (<1,200 mm rain/year), Mesic (1,200–2,500 mm rain/year), and Wet (>2,500 mm rain/year). Elevation was categorized in three elevation bands: Lowland (15–2,000 m), Montane (500–2,700 m), or Subalpine (1,700–3,000 m; Wagner et al. 1990). In addition to habitat variables collected during surveys in 2019, we used the maps produced by Jacobi (1989) and Green et al. (2015) to classify each station and explored those community types as covariates. There was strong correlation (> |0.5|) among the variables because many of them were subsets or simplifications of variables. Some of these categorical predictors had many discrete values in the raw data.

To simplify the model selection, we looked at the subset of stations where all the vegetation covariates were available. We re-fit the detection functions on the subset of observations where all the vegetation covariates were available, testing the vegetation covariates using the best-fit models from Table 2 with the vegetation covariates. Key detection functions were taken to be the same as in the best-fit models. We used a forward selection process to sequentially add the vegetation covariate that produced the greatest reduction in AIC and stopped when no additional covariates improved model fit. We then compared abundance estimates obtained from the vegetation covariate models with abundance estimated from the non-vegetation covariate models applied to the same subset of survey stations.

### *Abundance Estimates and Inference Areas*

Once the best-fit detection function was selected, we calculated annual abundances by multiplying mean density by the inference range area for each species by year. Inference ranges for the entire survey area and range restricted species (i.e., threatened and endangered species) were defined by station location, survey history, landowner boundaries, elevation contours, and vegetation classes defined by Jacobi (1989) and Green et al. (2015). The survey area was also subset to assess trends in upper and lower elevation habitat using the 1,500 m contour, an elevation threshold below which mosquito-borne diseases are prevalent (Atkinson et al. 2000, 2005). For wide-spread species such as ʻApapane, Hawaiʻi ʻAmakihi, Ōmaʻo, Northern Cardinal, Red-billed Leiothrix, and Warbling White-eye, inference was made to the entire surveyed area (Table 3). Four species were restricted in range within the total survey area: ʻAkiapōlāʻau, Alawī, Hawaiʻi ʻĀkepa, and ʻIʻiwi. For those species we estimate densities and abundance for their respective range within Kaʻū Rainforest based on detection history and survey coverage. ʻIʻiwi ranged within substantial portions (>90%) of the low and high elevation survey areas, thus we provide density and abundance estimates within each

stratum, as opposed to more range restricted species that occur primarily within the high stratum. We also provide density and abundance estimates for each of the species mentioned above in the previous seven survey years if there were sufficient detections to do so. For example, there were enough detections of the endangered ʻAkiapōlāʻau to estimate density in only 1976, 2005, and 2008. Detailed methods for determining entire inference area and area for range-restricted species are described in Appendix B.

**Table 3.** Inference areas (hectares) used to determine abundance estimates for broadly occurring species and for smaller range-restricted and wide-spread species detected during the 2019 Kaʻū Rainforest landbird survey. Total ranges and ranges by land management (HAVO or KFR), and by elevation strata (low elevation or high elevation) are provided.

| Species | HAVO | KFR[A] | Low (<1,500 m) | High (≥1,500 m) | Total |
|---|---|---|---|---|---|
| ʻAkiapōlāʻau | 629 | 4,101 | 498 | 4,232 | 4,730 |
| ʻAlawī | 656 | 9,018 | 3,002 | 6,672 | 9,674 |
| Hawaiʻi ʻĀkepa | 4,952 | 7,544 | 1,440 | 11,055 | 12,495 |
| ʻI'iwi | 3,226 | 18,600 | 10,829 | 10,998 | 21,826 |
| *Widespread Species* [B] | 5,775 | 27,142 | 19,369 | 13,548 | 32,917 |

[A] KFR includes portions of the private and state managed properties described in survey area.

[B] Widespread species: ʻApapane, Hawaiʻi ʻAmakihi, Hawaiʻi ʻElepaio, ʻŌmaʻo, Northern Cardinal, Warbling White-eye, and Red-billed Leiothrix.

### *Population Trend*

Population trend was assessed using log-linear regression on the bootstrap abundance estimates from the 2002–2019 surveys. Using 1,000 bootstrap-resamples of stations within years (and regions as necessary) we generated a distribution of slopes. We then examined the distribution of slopes in an equivalency framework, using a threshold of a 25% change over 25 years to calculate the proportion of slopes that fell into a downward, upward, or neutral trend (Camp et al. 2008). We considered ≥50% of the bootstrap slopes falling into a category (downward, upward, or neutral) as weak evidence for that trend, ≥70% as strong evidence, and ≥90% as very strong evidence of that trend. In cases where no category had ≥50% of bootstrap slopes we considered the trend to be inconclusive. Trends were assessed using six density estimates from 2002 to 2019 for all species, except Northern Cardinal, where trends were assessed using four density estimates, and ʻAkiapōlāʻau. There were only two recent density estimates for ʻAkiapōlāʻau, in 2005 and 2008. We compared the difference between the pair-wise bootstrap estimates for those years and tabulated the number of differences that fell between or exceed a 3% change in abundance over three years (analogous to the 25% over 25-year threshold used for the regressions). Trends were assessed within each subset of the survey area: low elevation (<1,500 m), high elevation (≥1,500 m), and total survey area. Trends of endangered species were assessed for their restricted range within the Kaʻū Rainforest.

# Results

## 2019 Landbird Detections

A total of 10,737 birds of 23 species (14 non-native and 9 native) were detected during 603 counts on 488 landbird monitoring stations (Tables 4 and 5). ʻApapane, Hawaiʻi ʻAmakihi, and ʻŌmaʻo accounted for the most detections and highest relative abundances at >2 BPC (Table 5). They were also the most widely distributed native birds detected with percent relative occurrence of >84%. ʻIʻiwi were detected at 36.5% of stations surveyed with a relative abundance of 0.67 BPC. At 0.16 BPC, Hawaiʻi ʻElepaio were detected at 13.7% of stations. The three endangered species detected during surveys—ʻAkiapōlāʻau, ʻAlawī, and Hawaiʻi ʻĀkepa—were detected in low numbers (94, 50, and 4 individuals, respectively). There were 8 detections of the recently federally delisted ʻIo (Hawaiian Hawk; *Buteo solitarius*). Non-native birds showed a wide range of relative occurrence and relative abundance (Table 5). Among non-natives, the Warbling White-eye had the highest relative occurrence of 73.4% and the highest relative abundance at nearly 2.0 BPC. The remaining non-native species occurred at <50% of stations surveyed.

There were sufficient detections of eight native species and three non-native species to estimate population density and abundance in the 2019 survey area. Densities, abundance, and trends are described at length in the sections below and we provide a summary for each species with links to maps of occurrence in Appendix E.

**Table 4.** List of species detected during the 2019 Kaʻū Rainforest landbird survey. Taxonomic classification follows the IOC World Bird List (Gill et al. 2023), except for ʻAlawī (Hawaiʻi Creeper) and ʻIo (Hawaiian Hawk), for which their Hawaiian name has not been recognized. The origin (E-endemic or NN-non-native) of each species are presented.

| Common Name | Scientific Name | Origin |
|---|---|---|
| ʻAkiapōlāʻau | *Hemignathus wilsoni* | E |
| ʻAlawī (Hawaiʻi Creeper) | *Loxops mana* | E |
| ʻApapane | *Himatione sanguinea* | E |
| Chinese Hwamei | *Garrulax canorus* | NN |
| Common Myna | *Acridotheres tristis* | NN |
| Common Waxbill | *Estrilda astrild* | NN |
| Erckel's Spurfowl | *Pternistis erckelii* | NN |
| Hawaiʻi ʻĀkepa | *Loxops coccineus* | E |
| Hawaiʻi ʻAmakihi | *Chlorodrepanis virens virens* | E |
| Hawaiʻi ʻElepaio | *Chasiempis sandwichensis* | E |
| House Finch | *Haemorhous mexicanus* | NN |
| ʻIʻiwi | *Drepanis coccinea* | E |
| ʻIo (Hawaiian Hawk) | *Buteo solitarius* | E |
| Japanese Bush Warbler | *Horornis diphone* | NN |

**Table 4 (continued).** List of species detected during the 2019 Kaʻū Rainforest landbird survey. Taxonomic classification follows the IOC World Bird List (Gill et al. 2023), except for ʻAlawī (Hawaiʻi Creeper) and ʻIo (Hawaiian Hawk), for which their Hawaiian name has not been recognized. The origin (E-endemic or NN-non-native) of each species are presented.

| Common Name | Scientific Name | Origin |
|---|---|---|
| Kalij Pheasant | *Lophura leucomelanos* | NN |
| Northern Cardinal | *Cardinalis cardinalis* | NN |
| ʻŌmaʻo | *Myadestes obscurus* | E |
| Red Junglefowl | *Gallus gallus* | NN |
| Red-billed Leiothrix | *Leiothrix lutea* | NN |
| Warbling White-eye | *Zosterops japonicus* | NN |
| Western Meadowlark | *Sturnella neglecta* | NN |
| Wild Turkey | *Meleagris gallopavo* | NN |
| Yellow-fronted Canary | *Crithagra mozambica* | NN |

**Table 5.** Indices of native and non-native bird detections for the 2019 Kaʻū Rainforest landbird survey. Total detections were the number of birds recorded during 603 counts at each of the 488 total stations surveyed. Stations occupied were the number of stations where one or more individuals of a species were detected. Percent occurrence was computed as stations occupied divided by total stations surveyed. Birds per station was computed by the total detections per species divided by total number of stations. Birds per count was computed by dividing total detections of each species by total number of counts.

| Species Name | Total Detections | Stations Occupied | Percent Occurrence | Birds Per Station | Birds Per Count |
|---|---|---|---|---|---|
| ʻAkiapōlāʻau | 4 | 4 | 0.8% | 0.01 | 0.01 |
| ʻAlawī | 94 | 53 | 10.9% | 0.19 | 0.16 |
| ʻApapane | 5,241 | 476 | 97.5% | 10.74 | 9.13 |
| Chinese Hwamei | 2 | 2 | 0.4% | <0.01 | <0.01 |
| Common Myna | 2 | 1 | 0.2% | <0.01 | <0.01 |
| Common Waxbill | 3 | 1 | 0.2% | 0.01 | 0.01 |
| Erckel's Spurfowl | 52 | 25 | 5.1% | 0.11 | 0.09 |
| Hawaiʻi ʻĀkepa | 50 | 29 | 5.9% | 0.10 | 0.09 |
| Hawaiʻi ʻAmakihi | 1,887 | 427 | 87.5% | 3.87 | 3.29 |
| Hawaiʻi ʻElepaio | 91 | 67 | 13.7% | 0.19 | 0.16 |
| House Finch | 3 | 2 | 0.4% | 0.01 | 0.01 |
| ʻIo | 8 | 6 | 1.2% | 0.02 | 0.01 |
| ʻIʻiwi | 387 | 178 | 36.5% | 0.79 | 0.67 |
| Japanese Bush Warbler | 115 | 74 | 15.2% | 0.24 | 0.20 |
| Kalij Pheasant | 15 | 9 | 1.8% | 0.03 | 0.03 |

**Table 5 (continued).** Indices of native and non-native bird detections for the 2019 Kaʻū Rainforest landbird survey. Total detections were the number of birds recorded during 603 counts at each of the 488 total stations surveyed. Stations occupied were the number of stations where one or more individuals of a species were detected. Percent occurrence was computed as stations occupied divided by total stations surveyed. Birds per station was computed by the total detections per species divided by total number of stations. Birds per count was computed by dividing total detections of each species by total number of counts.

| Species Name | Total Detections | Stations Occupied | Percent Occurrence | Birds Per Station | Birds Per Count |
|---|---|---|---|---|---|
| Northern Cardinal | 24 | 24 | 4.9% | 0.05 | 0.04 |
| ʻŌmaʻo | 1,233 | 413 | 84.6% | 2.53 | 2.15 |
| Red-billed Leiothrix | 493 | 239 | 49.0% | 1.01 | 0.86 |
| Red Junglefowl | 2 | 1 | 0.2% | <0.01 | <0.01 |
| Warbling White-eye | 967 | 358 | 73.4% | 1.98 | 1.68 |
| Western Meadowlark | 2 | 2 | 0.4% | <0.01 | <0.01 |
| Wild Turkey | 5 | 5 | 1.0% | 0.01 | 0.01 |
| Yellow-fronted Canary | 57 | 31 | 6.4% | 0.12 | 0.10 |

## Population Densities, Abundance, and Trends of Native Species

There were sufficient detections of eight native species in 2019 to estimate population density and abundance in each of the low, high, and total survey area combined stratum. For rare species, we provide estimates in their smaller restricted ranges. Species-specific densities and abundances for these species are provided in species summaries below, and links to native landbird trend graphics are provided in Appendix F. Also included is a summary for the ʻIo, a raptor for which insufficient detections were obtained to reliably estimate population size.

Upward trends of ʻApapane and Hawaiʻi ʻAmakihi were notable in each stratum. Trends were upward for the ʻAlawī, an endangered species that is range-restricted in the Kaʻū Rainforest. Trends were mixed for the ʻŌmaʻo—overall the population was stable with increasing densities in the low elevation stratum and downward trends in the high stratum. Evidence was strong for declines of the threatened ʻIʻiwi in each stratum. Also, trends of Hawaiʻi ʻElepaio were downward in each stratum. Trends of the endangered Hawaiʻi ʻĀkepa were inconclusive. There were not enough detections of ʻAkiapōlāʻau to estimate density in 2019.

**Table 6.** Native landbird trends within the Ka‘ū Rainforest (2002–2019) by species range or survey strata and total surveyed area. Strength of evidence for a trend is indicated by percentage of bootstrap slopes exceeding the threshold levels.

| Species | Elevation | # Years | Log-linear Regression | | Evidence for Trends | | |
|---|---|---|---|---|---|---|---|
| | | | Slope | Intercept | Downward | Stable | Upward |
| ‘Akiapōlā‘au [E] | Entire Ka‘ū Range | 2 | N/A | N/A | 56% [A] | 5% [D] | 39% [D] |
| ‘Apapane | High | 6 | 0.025 | 12.6 | 0% [D] | 0% [D] | 100% [C] |
| | Low | 4 | 0.024 | 12.4 | 0% [D] | 0% [D] | 100% [C] |
| | Total | 4 | 0.023 | 13.2 | 0% [D] | 0% [D] | 100% [C] |
| ‘Alawī | Entire Ka‘ū Range | 6 | 0.059 | 8.8 | 0% [D] | 0% [D] | 100% [C] |
| Hawai‘i ‘Ākepa | Entire Ka‘ū Range | 6 | -0.009 | 8.4 | 41% [D] | 47% [D] | 12% [D] |
| Hawai‘i ‘Amakihi | High | 6 | 0.049 | 11.4 | 0% [D] | 0% [D] | 100% [C] |
| | Low | 4 | 0.021 | 11.5 | 0% [D] | 1% [D] | 100% [C] |
| | Total | 4 | 0.038 | 12.2 | 0% [D] | 0% [D] | 100% [C] |
| Hawai‘i ‘Elepaio | High | 6 | -0.018 | 8.5 | 61% [A] | 26% [D] | 13% [D] |
| | Low | 3 | -0.025 | 9.7 | 84% [A] | 15% [D] | 1% [D] |
| | Total | 3 | -0.025 | 10.0 | 87% [A] | 13% [D] | 1% [D] |
| ‘I‘iwi | High | 6 | -0.014 | 10.3 | 60% [A] | 40% [D] | 0% [D] |
| | Low | 4 | -0.024 | 9.6 | 84% [A] | 16% [D] | 0% [D] |
| | Total | 4 | -0.029 | 10.7 | 100% [A] | 0% [D] | 0% [D] |
| ‘Ōma‘o | High | 6 | -0.026 | 10.2 | 100% [A] | 0% [D] | 0% [D] |
| | Low | 4 | 0.013 | 10.6 | 0% [D] | 26% [D] | 74% [C] |
| | Total | 4 | 0.000 | 11.2 | 0% [D] | **99%** [B] | 1% [D] |

[A] Threshold level is trending downward (also in dark red font and underlined).

[B] Threshold level is stable (**also in dark orange and bold font**).

[C] Threshold level is trending upward (also in dark blue-green font).

[D] Threshold level trends are inconclusive (also in dark blue font).

[E] The exception for threshold trend was for ‘Akiapōlā‘au, where there were only two estimates available (in 2005 and 2008), for which we compared the difference between the bootstrap estimates for those years and tabulated how many fell between or exceed a 3% change in abundance over three years.

## Native Species Summaries

### *ʻAkiapōlāʻau*

The federally endangered ʻAkiapōlāʻau had four detections on four stations. All the detections were within the northern section of KFR (Figure 17 in Appendix E). The detections were widely separated on Transects 6 and 10, occurring at approximately 1,500 m elevation. Three incidental detections were recorded on Transects 7 and 8 in 2019, which improved our confidence in determining the boundaries of the 4,730-ha inference area (Figure 13 in Appendix E). There were insufficient detections in 2010, 2016, and 2019 to estimate population size. The most recent abundance estimate was in 2008 with a total abundance of 691 ± 410 birds, and there was weak evidence of decline since 2005 (Table 6; Figure 40 in Appendix F) when there was an estimated abundance of 759 ± 340 birds (Table 7).

**Table 7.** ʻAkiapōlāʻau density and abundance estimates (± standard error [SE] and 95% confidence interval [CI]) in the species' estimated restricted range within the Kaʻū Rainforest survey area. Estimates of range are provided for each survey year with sufficient detections to determine density.

| Year | Kaʻū Rainforest Range (ha) | Density ± SE (95%CI) | Total Abundance ± SE (95%CI) |
|---|---|---|---|
| 1976 | 8,912 | 0.10 ± 0.04 (0.04–0.21) | 901 ± 375 (365–1,833) |
| 2005 | 4,730 | 0.16 ± 0.07 (0.06–0.34) | 759 ± 340 (282–1,613) |
| 2008 | 4,730 | 0.15 ± 0.09 (0.03–0.37) | 691 ± 410 (140–1,747) |

### *ʻAlawī*

The federally endangered ʻAlawī had 94 detections on 53 stations. The species occurred at 10.9% of the stations surveyed at 0.16 BPC (Table 5, Figure 18 in Appendix E). Occupancy was highest in the wet montane forests of KFR, where the canopy is co-dominated by large-stature ʻōhiʻa, koa, and ʻōlapa (*Cheirodendron trigynum*). We estimated the 2019 density at 1.34 ± 0.23 birds/ha with an abundance of 12,935 ± 2,225 birds in its 9,674-ha range (Table 8). Trends were upward, with very strong evidence of increasing densities (Table 6; Figure 41 in Appendix F), but the species had a notable reduction in range since 2002 (Table 8; Figure 14 in Appendix B).

**Table 8.** ‘Alawī density and abundance estimates (± SE and 95%CI) in the species’ entire estimated range within the Kaʻū Rainforest survey area.

| Year | Kaʻū Rainforest Range (ha) | Density ± SE (95%CI) | Abundance ± SE (95%CI) |
|---|---|---|---|
| 1976 | 16,368 | 0.15 ± 0.05 (0.08–0.26) | 2,488 ± 737 (1,288–4,176) |
| 1993 | 16,368 | 0.25 ± 0.08 (0.12–0.42) | 4,120 ± 1,246 (1,962–6,848) |
| 2002 | 12,064 | 0.49 ± 0.13 (0.28–0.78) | 5,880 ± 1,541 (3,330–9,372) |
| 2005 | 9,674 | 0.28 ± 0.08 (0.15–0.48) | 2,756 ± 818 (1,399–4,603) |
| 2008 | 9,674 | 0.75 ± 0.23 (0.39–1.30) | 7,283 ± 2,257 (3,757–12,605) |
| 2010 | 9,674 | 0.58 ± 0.22 (0.19–1.06) | 5,619 ± 2,137 (1,856–10,233) |
| 2016 | 9,674 | 0.84 ± 0.24 (0.43–1.36) | 8,152 ± 2,303 (4,145–13,174) |
| 2019 | 9,674 | 1.34 ± 0.23 (0.97–1.87) | 12,935 ± 2,225 (9,371–18,095) |

### *‘Apapane*

‘Apapane were the most broadly distributed and abundant native species detected in the 2019 survey, occurring at 97.5% of stations surveyed and at 9.13 BPC (Table 5; Figure 19 in Appendix E). Overall density was 19.84 ± 1.77 birds/ha for an estimated abundance of 653,190 ± 58,354 birds in the 32,917-ha survey area—the highest abundance estimated since 1993 (Table 9). In 2019, ‘Apapane density in the low elevation strata was 16.28 ± 1.63 birds/ha, while densities were higher at 24.93 ± 2.31 birds/ha in the high elevation strata (Table 9). There was very strong evidence of upward trends in both elevation strata and the total survey area (Table 6; Figure 42 in Appendix F).

**Table 9.** ʻApapane density and abundance estimates (± SE and 95%CI) in the low elevation (<1,500 m), high elevation (≥1,500 m), and total area combined. In 2010 and 2016 there were not enough detections to estimate densities in the low elevation stratum.

| Year | Low Elevation (19,369 ha) | | High Elevation (13,548 ha) | | Total Area (32,917 ha) | |
|---|---|---|---|---|---|---|
| | Density ± SE (95%CI) | Abundance ± SE (95%CI) | Density ± SE (95%CI) | Abundance ± SE (95%CI) | Density ± SE (95%CI) | Abundance ± SE (95%CI) |
| 1976 | 5.56 ± 0.52 (5.03–7.07) | 107,750 ± 10,060 (97,496–136,933) | 13.04 ± 1.16 (11.84–16.37) | 176,610 ± 15,661 (160,390–221,783) | 8.64 ± 0.69 (7.91–10.62) | 284,360 ± 22,727 (260,427–349,516) |
| 1993 | 19.26 ± 1.71 (17.66–24.38) | 373,130 ± 33,202 (342,052–472,205) | 26.05 ± 2.98 (22.63–34.32) | 352,900 ± 40,407 (306,527–464,923) | 22.06 ± 1.99 (19.93–27.75) | 726,030 ± 65,621 (656,169–913,404) |
| 2002 | 14.2 ± 1.42 (12.82–18.40) | 275,060 ± 27,559 (248,403–356,436) | 19.63 ± 1.86 (17.63–24.94) | 265,880 ± 2,5261 (238,812–337,835) | 16.43 ± 1.51 (14.95–20.86) | 540,940 ± 49,643 (492,082–686,683) |
| 2005 | 7.22 ± 1.17 (5.49–10.09) | 139,920 ± 22,709 (106,386–195,406) | 13.53 ± 1.09 (12.44–16.71) | 183,270 ± 14,748 (168,528–226,341) | 9.82 ± 1.02 (8.57–12.56) | 323,190 ± 33,509 (282,118–413,472) |
| 2008 | 12.10 ± 1.27 (10.78–15.76) | 234,410 ± 24,584 (208,884–305,252) | 21.71 ± 2.37 (19.25–28.53) | 294,130 ± 32,072 (260,728–386,449) | 16.06 ± 1.54 (14.50–20.53) | 528,540 ± 50,697 (477,184–675,915) |
| 2010 | – | – | 24.47 ± 2.08 (22.22–30.37) | 331,500 ± 281,85 (301,014–411,501) | – | – |
| 2016 | – | – | 25.27 ± 2.32 (22.72–31.82) | 342,330 ± 31,466 (307,758–431,104) | – | – |
| 2019 | 16.28 ± 1.63 (14.62–21.00) | 315,390 ± 31,549 (283,102–406,774) | 24.93 ± 2.31 (22.64–31.71) | 337,800 ± 31,341 (306,782–429,637) | 19.84 ± 1.77 (18.09–25.04) | 653,190 ± 58,354 (595,439–824,188) |

### *Hawai‘i ‘Ākepa*

The federally endangered Hawai‘i ‘Ākepa occurred at 5.9% of stations surveyed and at 0.09 BPC (Table 5). The detections straddled the HAVO and KFR boundary near the 1,600–1,900 m elevation range (Figure 20 in Appendix E). The species was detected in both subalpine woodlands and mature montane ‘ōhi‘a forests. There was one anomalous detection on Transect 2 in the southwest region of the KFR, in an area where there were no previous detections during any survey and which may be attributed to surveyor error. We estimated the 2019 density at 0.33 ± 0.08 birds/ha with an abundance of 4,169 ± 991 birds in its 12,495-ha range (Table 10). Trends were inconclusive for this species because of wide fluctuations in mean annual densities (ranging from 0.18 birds/ha in 2010 to 0.61 birds/ha in 2016) and high variance (coefficient of variation ranging from 0.19 to 0.33; Table 6; Figure 43 in Appendix F). The species' range had a notable contraction after 2002 resulting from no detections in the lowest elevations and along the lower edge of its previous range (Figure 15 in Appendix B).

**Table 10.** Hawai‘i ‘Ākepa density and abundance estimates (± SE and 95%CI) in the species' entire estimated range within the Ka‘ū Rainforest survey area.

| Year | Ka‘ū Rainforest Range (ha) | Density ± SE (95%CI) | Abundance ± SE (95%CI) |
|---|---|---|---|
| 1976 | 19,771 | 0.19 ± 0.05 (0.12–0.30) | 3,761 ± 912 (2,338–5,912) |
| 1993 | 19,771 | 0.66 ± 0.14 (0.44–1.00) | 13,047 ± 2,846 (8,592–19,748) |
| 2002 | 19,771 | 0.48 ± 0.13 (0.26–0.78) | 9,396 ± 2,631 (5,145–15,458) |
| 2005 | 12,495 | 0.31 ± 0.06 (0.20–0.44) | 3,813 ± 781 (2,486–5,549) |
| 2008 | 12,495 | 0.25 ± 0.08 (0.11–0.45) | 3,087 ± 1,061 (1,430–5,589) |
| 2010 | 12,495 | 0.18 ± 0.06 (0.08–0.31) | 2,190 ± 749 (986–3,921) |
| 2016 | 12,495 | 0.61 ± 0.14 (0.40–0.93) | 7,677 ± 1,707 (4,938–11,628) |
| 2019 | 12,495 | 0.33 ± 0.08 (0.21–0.52) | 4,169 ± 991 (2,596–6,479) |

### *Hawai‘i ‘Amakihi*

Hawai‘i ‘Amakihi were abundant and widespread throughout the study area, occurring at 87.5% of stations surveyed at 3.29 BPC (Table 5; Figure 21 in Appendix E). Overall density in 2019 was 8.34 ± 0.57 birds/ha for an estimated abundance of 274,600 ± 18,631 birds in the entire 32,917 ha survey area (Table 11). Density in the high elevation stratum was 11.31 ± 0.78 birds/ha, which was nearly twice the low elevation stratum estimate of 6.27 ± 0.49 birds/ha. The 2019 estimates were the highest throughout the Ka‘ū Rainforest survey timeseries. There was very strong evidence of upward trends in both elevation strata and the total survey area (Table 6; Figure 44 in Appendix F).

**Table 11.** Hawai'i 'Amakihi density and abundance estimates (± SE and 95%CI) in the low elevation (<1,500 m), high elevation (≥1,500 m), and total area combined. In 2010 and 2016 there were not enough detections to estimate separate densities in each inference area.

| Year | Low Elevation (19,369 ha) | | High Elevation (13,548 ha) | | Total Area (32,917 ha) | |
|---|---|---|---|---|---|---|
| | Density ± SE (95%CI) | Abundance ± SE (95%CI) | Density ± SE (95%CI) | Abundance ± SE (95%CI) | Density ± SE (95%CI) | Abundance ± SE (95%CI) |
| 1976 | 2.68 ± 0.24 (2.06–3.01) | 51,952 ± 4,697 (39,952–58,364) | 7.19 ± 0.60 (5.64–8.00) | 97,344 ± 8,171 (76,356–108,388) | 4.54 ± 0.36 (3.59–4.99) | 149,296 ± 11,745 (118,149–164,190) |
| 1993 | 3.66 ± 0.39 (2.75–4.28) | 70,931 ± 7,561 (53,281–82,919) | 6.38 ± 0.83 (4.43–7.67) | 86,462 ± 11,207 (60,010–103,940) | 4.78 ± 0.45 (3.63–5.41) | 157,393 ± 14,946 (119,416–178,006) |
| 2002 | 4.75 ± 0.48 (3.63–5.52) | 91,997 ± 9,340 (70,368–106,981) | 5.50 ± 0.60 (4.12–6.48) | 74,461 ± 8,179 (55,763–87,825) | 5.06 ± 0.43 (4.00–5.67) | 166,458 ± 14,080 (131,602–186,795) |
| 2005 | 3.92 ± 0.55 (2.64–4.81) | 75,904 ± 10,702 (51,139–93,090) | 3.51 ± 0.26 (2.81–3.85) | 47,540 ± 3,564 (38,123–52,095) | 3.75 ± 0.38 (2.80–4.30) | 123,444 ± 12,616 (92,200–141,656) |
| 2008 | 5.17 ± 0.51 (3.91–5.92) | 100,070 ± 9,914 (75,746–114,610) | 7.38 ± 0.78 (5.42–8.47) | 99,990 ± 10,532 (73,399–114,683) | 6.08 ± 0.52 (4.67–6.71) | 200,060 ± 17,147 (153,667–220,882) |
| 2010 | – | – | 4.92 ± 0.50 (3.68–5.62) | 66,694 ± 6,734 (49,792–76,190) | – | – |
| 2016 | – | – | 7.90 ± 0.60 (6.29–8.63) | 107,090 ± 8,076 (85,202–116,860) | – | – |
| 2019 | 6.27 ± 0.49 (4.97–6.90) | 121,410 ± 9,542 (96,278–133,682) | 11.31 ± 0.78 (9.14–12.19) | 153,190 ± 10,512 (123,883–165,092) | 8.34 ± 0.57 (6.76–8.98) | 274,600 ± 18,631 (222,669–295,703) |

### *Hawai‘i ‘Elepaio*

The Hawai‘i ‘Elepaio occurred at 13.7% of the stations surveyed and at 0.16 BPC (Table 5). The species was broadly distributed, occurring on most transects within seasonal mesic forests dominated by mixed koa and ‘ōhi‘a (Figure 22 in Appendix E). We estimated the 2019 density at 0.48 ± 0.10 birds/ha and an abundance of 15,753 ± 3,251 birds in the total survey area (Table 12). Density in the high elevation stratum (0.32 ± 0.08 birds/ha) was about half of the low elevation stratum density (0.59 ± 0.14 birds/ha). The 2019 density and abundance estimates were among the lowest recorded for the species, and evidence of population decline was strong in both elevation strata and the total survey area (Table 6; Figure 45 in Appendix F).

**Table 12.** Hawai‘i ‘Elepaio density and abundance estimates (± SE and 95%CI) in the low elevation (<1,500 m), high elevation (≥1,500 m), and total area combined. In 2005, 2010, and 2016 there were not enough detections to estimate separate densities in each inference area.

| | Low Elevation (19,369 ha) | | High Elevation (13,548 ha) | | Total Area (32,917 ha) | |
|---|---|---|---|---|---|---|
| Year | Density ± SE (95%CI) | Abundance ± SE (95%CI) | Density ± SE (95%CI) | Abundance ± SE (95%CI) | Density ± SE (95%CI) | Abundance ± SE (95%CI) |
| 1976 | 0.84 ± 0.16 (0.53–1.15) | 16,352 ± 3,038 (10,326–22,236) | 0.72 ± 0.15 (0.44–1.01) | 9,745 ± 1,989 (5,887–13,684) | 0.79 ± 0.14 (0.52–1.05) | 26,097 ± 4,484 (17,036–34,613) |
| 1993 | 0.92 ± 0.21 (0.54–1.34) | 17,884 ± 3,983 (10,379–25,990) | – | – | – | – |
| 2002 | 0.82 ± 0.18 (0.47–1.17) | 15,973 ± 3,485 (9,082–22,744) | 0.40 ± 0.18 (0.10–0.81) | 5,413 ± 2,460 (1,350–10,992) | 0.65 ± 0.15 (0.37–0.96) | 21,386 ± 4,998 (12,141–31,734) |
| 2005 | – | – | 0.25 ± 0.06 (0.13–0.38) | 3,324 ± 866 (1,761–5,154) | – | – |
| 2008 | 1.13 ± 0.24 (0.67–1.63) | 21,976 ± 4,710 (13,038–31,500) | 1.06 ± 0.28 (0.54–1.63) | 14,318 ± 3,769 (7,253–22,029) | 1.10 ± 0.23 (0.68–1.56) | 36,294 ± 7,429 (22,299–51,422) |
| 2010 | – | – | 0.27 ± 0.09 (0.11–0.47) | 3,720 ± 1,247 (1,442–6,328) | – | – |
| 2016 | – | – | 0.27 ± 0.08 (0.11–0.41) | 3,609 ± 1,045 (1,455–5,553) | – | – |
| 2019 | 0.59 ± 0.14 (0.33–0.87) | 11,367 ± 2,647 (6,385–16,763) | 0.32 ± 0.08 (0.17–0.49) | 4,386 ± 1,100 (2,289–6,600) | 0.48 ± 0.10 (0.29–0.68) | 15,753 ± 3,251 (9,567–22,311) |

***ʻIʻiwi***

The federally threatened ʻIʻiwi occurred at 36.5% of the stations surveyed and at 0.67 BPC (Table 5). Most detections occurred above 1,200 m elevation (Figure 23 in Appendix E). We estimated the 2019 density at 2.02 ± 0.16 birds/ha with an abundance of 44,189 ± 3,482 birds in the species' 21,826 ha range of the Kaʻū Rainforest (Table 13). Density in the species' 10,829-ha low elevation range was 1.47 ± 0.20 birds/ha and 2.58 ± 0.25 birds/ha in its 10,998-ha high elevation range. There was very strong evidence of downward trends across the species range and strong evidence for downward trends in both the low and high elevation portions of the survey area (Table 6; Figure 46 in Appendix F).

**Table 13.** ʻIʻiwi density and abundance estimates (± SE and 95%CI) in the low elevation (<1,500 m), high elevation (≥1,500 m), and total area combined. In 2010 and 2016 there were not enough detections to estimate separate densities in each inference area.

| Year | Low Elevation [A] | | High Elevation [B] | | Total Area [C] | |
|---|---|---|---|---|---|---|
| | Density ± SE (95%CI) | Abundance ± SE (95%CI) | Density ± SE (95%CI) | Abundance ± SE (95%CI) | Density ± SE (95%CI) | Abundance ± SE (95%CI) |
| 1976 | 1.84 ± 0.16 (1.54–2.18) | 25,126 ± 2,192 (21,059–29,652) | 3.88 ± 0.30 (3.31–4.49) | 42,716 ± 3,305 (36,394–49,348) | 2.75 ± 0.18 (2.41–3.12) | 67,842 ± 4,453 (59,330–76,786) |
| 1993 | 3.46 ± 0.35 (2.79–4.16) | 47,184 ± 4,761 (38,041–56,703) | 6.71 ± 0.94 (4.86–8.54) | 73,842 ± 10,330 (53,444–93,937) | 4.91 ± 0.49 (3.97–5.88) | 121,026 ± 11,981 (97,762–144,728) |
| 2002 | 1.48 ± 0.20 (1.09–1.89) | 20,148 ± 2,784 (14,872–25,784) | 5.61 ± 0.54 (4.58–6.71) | 61,738 ± 5,979 (50,383–73,820) | 3.32 ± 0.28 (2.79–3.91) | 81,886 ± 7,011 (68,726–96,210) |
| 2005 | 3.31 ± 0.69 (2.05–4.76) | 35,841 ± 7,467 (22,220–51,491) | 2.19 ± 0.15 (1.91–2.49) | 24,123 ± 1,635 (20,962–27,371) | 2.75 ± 0.36 (2.10–3.50) | 59,964 ± 7,780 (45,786–76,284) |
| 2008 | 0.55 ± 0.14 (0.30–0.87) | 5,956 ± 1,569 (3,224–9,372) | 1.69 ± 0.33 (1.06–2.34) | 18,639 ± 3,603 (11,662–25,784) | 1.13 ± 0.18 (0.77–1.49) | 24,595 ± 4,033 (16,802–32,613) |
| 2010 | -- | -- | 2.08 ± 0.31 (1.49–2.71) | 22,881 ± 3,428 (16,350–29,789) | -- | -- |
| 2016 | -- | -- | 3.39 ± 0.34 (2.76–4.10) | 37,240 ± 3,767 (30,338–45,104) | -- | -- |
| 2019 | 1.47 ± 0.20 (1.12–1.89) | 15,867 ± 2,134 (12,075–20,438) | 2.58 ± 0.25 (2.12–3.09) | 28,322 ± 2,725 (23,353–34,034) | 2.02 ± 0.16 (1.74–2.36) | 44,189 ± 3482 (37,895–51,546) |

[A] Low elevation range for years 1976 to 2002 was 13,633 ha and 10,829 ha for years 2005 to 2019.

[B] High elevation range was 10,998 ha for every survey year.

[C] Total range for years 1976 to 1994 was 24,630 ha and 21,826 ha for years 2002 to 2019.

### *ʻIo*

There were eight ʻIo detections on six stations in the Kaʻū Rainforest (Table 5). The raptor occurred at 1.2% of stations surveyed at 0.01 BPC, and was only detected below 1,500-m elevation in KFR and KCGMA (Figure 24 in Appendix E).

### *ʻŌmaʻo*

ʻŌmaʻo were broadly distributed throughout the survey area, occurring at 84.6% of stations surveyed and at 2.15 BPC (Table 5). Occurrence was highest in mesic and moderately wet climates co-dominated by ʻōhiʻa, koa, ʻōlapa, kāwaʻu, and hāpuʻu (*Cibotium* spp.) tree ferns (Figure 25 in Appendix E). We estimated the 2019 density at 2.35 ± 0.10 birds/ha and an abundance of 77,489 ± 3,383 birds in the total survey area (Table 14). Density between the elevation strata were similar with 2.25 ± 0.14 birds/ha in the high elevation stratum and 2.43 ± 0.13 birds/ha in the low elevation stratum. There was very strong evidence that trends remained stable in the total survey area, but there was very strong evidence of population declines in the high elevation stratum and strong evidence of increasing abundance in the larger low elevation stratum (Table 6; Figure 47 in Appendix F), which contributed to the overall stability in the trend of the Kaʻū Rainforest population.

**Table 14.** ʻŌmaʻo density and abundance estimates (± SE and 95%CI) in the low elevation (<1,500 m), high elevation (≥1,500 m), and total area combined. In 2010 and 2016 there were not enough detections to estimate separate densities in each inference area.

| Year | Low Elevation (19,369 ha) | | High Elevation (13,548 ha) | | Total Area (32,917 ha) | |
|---|---|---|---|---|---|---|
| | Density ± SE (95%CI) | Abundance ± SE (95%CI) | Density ± SE (95%CI) | Abundance ± SE (95%CI) | Density ± SE (95%CI) | Abundance ± SE (95%CI) |
| 1976 | 2.34 ± 0.11 (2.14–2.55) | 45,244 ± 2,061 (41,390–49,469) | 1.68 ± 0.12 (1.45–1.94) | 22,706 ± 1,686 (19,657–26,264) | 2.06 ± 0.09 (1.90–2.26) | 67,950 ± 3,014 (62,502–74,316) |
| 1993 | 3.31 ± 0.16 (3.00–3.63) | 64,073 ± 3,128 (58,125–70,388) | 3.10 ± 0.33 (2.48–3.77) | 42,065 ± 4,468 (33,591–51,106) | 3.22 ± 0.18 (2.88–3.58) | 106,138 ± 5,898 (94,741–117,860) |
| 2002 | 3.10 ± 0.19 (2.76–3.50) | 60,113 ± 3,656 (53,422–67,755) | 4.09 ± 0.31 (3.56–4.78) | 55,421 ± 4,211 (48,291–64,798) | 3.51 ± 0.18 (3.18–3.90) | 115,534 ± 6,051 (104,597–128,315) |
| 2005 | 0.85 ± 0.20 (0.43–1.27) | 16,435 ± 3,857 (9,544–24,665) | 1.53 ± 0.08 (1.40–1.70) | 20,772 ± 1,033 (18,971–23,022) | 1.13 ± 0.12 (0.91–1.39) | 37,207 ± 4,071 (29,899–45,857) |
| 2008 | 2.14 ± 0.15 (1.88–2.46) | 41,491 ± 2,884 (36,370–47,675) | 2.78 ± 0.20 (2.43–3.22) | 37,611 ± 2,756 (32,859–43,665) | 2.40 ± 0.13 (2.20–2.69) | 79,102 ± 4,130 (72,334–88,522) |
| 2010 | – | – | 0.91 ± 0.10 (0.74–1.11) | 12,300 ± 1,297 (9,988–15,072) | – | – |
| 2016 | – | – | 1.54 ± 0.12 (1.31–1.79) | 20,912 ± 1,666 (17,687–24,216) | – | – |
| 2019 | 2.43 ± 0.13 (2.21–2.70) | 47,028 ± 2,440 (42,740–52,304) | 2.25 ± 0.14 (2.00–2.54) | 30,461 ± 1,848 (27,146–34,389) | 2.35 ± 0.10 (2.17–2.58) | 77,489 ± 3,383 (71,575–84,836) |

### Population Densities, Abundance, and Trends of Non-Native Species

Detections of three non-native species in 2019 were sufficient to estimate population density and abundance in each low, high, and the total survey area combined strata. There was very strong evidence for downward trends of the Northern Cardinal in both elevation strata and for the Red-billed Leiothrix in the low elevation stratum (Table 15). There was weak evidence of a downward trend for the Red-billed Leiothrix in the total survey area, while trend in the high elevation stratum was inconclusive. There was very strong evidence of upward trends for the Warbling White-eye in each elevation stratum. Tables of estimated densities and abundances for each survey year are provided in the individual non-native species summaries below. Non-native landbird trend graphics are presented in Appendix F and are linked in the summaries. For the remaining 11 non-native species, we provide descriptions of relative abundance and link to occurrence maps in Appendix E.

**Table 15.** Non-native landbird trends within the Ka‘ū Rainforest (2002–2019). Strength of evidence for a trend is indicated by percentage of bootstrap slopes exceeding the threshold levels

| Species | Elevation | # Years | Log-linear Regression | | Evidence for Trends | | |
|---|---|---|---|---|---|---|---|
| | | | Slope | Intercept | Downward | Stable | Upward |
| Northern Cardinal | High | 4 | -0.091 | 6.4 | 98% [A] | 1% [C] | 1% [C] |
| | Low | 4 | -0.098 | 7.7 | 100% [A] | 0% [C] | 0% [C] |
| | Total | 3 | -0.102 | 7.9 | 100% [A] | 0% [C] | 0% [C] |
| Red-billed Leiothrix | High | 6 | 0.023 | 9.3 | 0% [C] | 10% [C] | 90% [B] |
| | Low | 4 | -0.025 | 10.7 | 96% [A] | 4% [C] | 0% [C] |
| | Total | 4 | -0.014 | 11.0 | 61% [A] | 39% [C] | 0% [C] |
| Warbling White-eye | High | 6 | 0.062 | 10.6 | 0% [C] | 0% [C] | 100% [B] |
| | Low | 4 | 0.028 | 11.8 | 0% [C] | 0% [C] | 100% [B] |
| | Total | 4 | 0.030 | 12.1 | 0% [C] | 0% [C] | 100% [B] |

[A] Threshold level is trending downward (also in dark red font and underlined).

[B] Threshold level is trending upward (also in dark blue-green font).

[C] Threshold level trends are inconclusive (also in dark blue font).

## Non-Native Species Summaries

### *Chinese Hwamei*

There were two detections on two stations of the Chinese Hwamei (*Garrulax canorus*; Table 5). The species occurred at 0.4% of the stations surveyed at less than 0.01 BPC. The two detections were near the bottom edge of the survey area on Transects 5 and 10 in a mix of open and closed canopy ʻōhiʻa forest with an understory of native shrubs and native ferns (Figure 26 in Appendix E).

### *Common Myna*

There were two detections on one station of the Common Myna (*Acridotheres tristis;* Table 5). The species occurred at 0.2% of the stations surveyed at less than 0.01 BPC. The detections were near the bottom edge of the survey area on Transect 11 in open canopy ʻōhiʻa forest with an understory of native shrubs and non-native grasses (Figure 27 in Appendix E).

### *Common Waxbill*

There were three detections on one station of the Common Waxbill (*Estrilda astrild*; Table 5). The species occurred at 0.2% of the stations surveyed at 0.01 BPC. The detections were near the bottom edge of the survey area on Transect 6 in open non-native canopy with an understory of non-native shrubs and grasses (Figure 28 in Appendix E).

### *Erckel's Spurfowl*

There were 52 detections of the Erckel's Spurfowl (*Pternistis erckelii*; Table 5). The game bird occurred at 5.1% of stations surveyed at 0.09 BPC. Most detections were above 1,600 m elevation, and in open montane areas dominated by native shrubs and grasses (Figure 29 in Appendix E).

### *House Finch*

There were three detections on two stations of the House Finch (*Haemorhous mexicanus*; Table 5). The species occurred at 0.4% of the stations surveyed at 0.01 BPC. The detections were on stations near the bottom of Transect 6 in open non-native canopy with an understory of non-native shrubs and grasses (Figure 30 in Appendix E).

### *Japanese Bush Warbler*

There were 115 detections of the Japanese Bush Warbler (*Horornis diphone*; Table 5). The species was detected at 15.2% of the stations surveyed at 0.20 BPC. Detections occurred broadly throughout the survey area, mostly in closed canopy forest below 1,700-m elevation (Figure 31 in Appendix E).

### *Kalij Pheasant*

There were 15 detections on 9 stations of the Kalij Pheasant (*Lophura leucomelanos*; Table 5). The gamebird occurred at 1.8% of stations surveyed at 0.03 BPC. Most detections were above 1,500 m elevation in closed canopy ʻōhiʻa forest within KFR (Figure 32 in Appendix E).

### *Northern Cardinal*

There were 24 detections on 24 stations of the Northern Cardinal. The species was detected at 4.9% of stations surveyed at 0.04 BPC (Table 5). Most detections were near the edges of the survey area, in closed canopy forests with mixed native and non-native trees and shrubs (Figure 33 in Appendix E). We estimated the 2019 density at 0.03 ± 0.01 birds/ha with an abundance of 1,133 ± 400 birds in

the total survey area (Table 16). There was very strong evidence of downward trends in both elevation strata and the total survey area (Table 15; Figure 48 in Appendix E).

**Table 16.** Northern Cardinal density and abundance estimates (± SE and 95%CI) in the low elevation (<1,500 m), high elevation (≥1,500 m), and total area combined. In 1993, 2002, 2010, and 2016 there were not enough detections to estimate separate densities in each inference area.

| Year | Low Elevation (19,369 ha) | | High Elevation (13,548 ha) | | Total Area (32,917 ha) | |
|---|---|---|---|---|---|---|
| | Density ± SE (95%CI) | Abundance ± SE (95%CI) | Density ± SE (95%CI) | Abundance ± SE (95%CI) | Density ± SE (95%CI) | Abundance ± SE (95%CI) |
| 1976 | 0.07 ± 0.03 (0.04–0.14) | 1,407 ± 504 (798–2,772) | 0.01 ± 0.01 (<0.01–0.03) | 183 ± 109 (32–460) | 0.05 ± 0.02 (0.03–0.09) | 1,590 ± 554 (927–3,099) |
| 1993 | 0.11 ± 0.04 (0.06–0.22) | 2,139 ± 778 (1,165–4,215) | – | – | – | – |
| 2002 | 0.26 ± 0.08 (0.16–0.48) | 5,017 ± 1,611 (3,050–9,364) | – | – | – | – |
| 2005 | 0.17 ± 0.08 (0.05–0.38) | 3,284 ± 1,594 (1,032–7,281) | 0.06 ± 0.02 (0.03–0.12) | 819 ± 299 (443–1,614) | 0.12 ± 0.05 (0.05–0.26) | 4,103 ± 1,688 (1,769–8,388) |
| 2008 | 0.19 ± 0.06 (0.11–0.34) | 3,677 ± 1,142 (2,155–6,630) | 0.07 ± 0.04 (0.02–0.18) | 972 ± 576 (229–2,487) | 0.14 ± 0.04 (0.09–0.26) | 4,649 ± 1,439 (2,785–8,426) |
| 2010 | – | – | – | – | – | – |
| 2016 | – | – | 0.04 ± 0.02 (0.01–0.09) | 531 ± 279 (102–1,196) | – | – |
| 2019 | 0.05 ± 0.02 (0.02–0.10) | 918 ± 355 (442–1,833) | 0.02 ± 0.01 (<0.01–0.04) | 215 ± 121 (45–519) | 0.03 ± 0.01 (0.02–0.07) | 1,133 ± 400 (580–2,147) |

***Red-billed Leiothrix***

The Red-billed Leiothrix was detected at 49% of the stations surveyed and at 0.86 BPC (Table 5). Most detections were in native dominated habitats below 1,800 m elevation within KFR (Figure 34 in Appendix E). Detections in the Kahuku Unit were in closed ‘ōhi‘a forest near the boundary of KFR. In 2019, we estimated a density of 1.56 ± 0.14 birds/ha and an abundance of 51,261 ± 4,755 birds in the total survey area (Table 17). Density in the high elevation stratum was 1.10 ± 0.14 birds/ha and 1.88 ± 0.21birds/ha in the low elevation stratum. Evidence of a downward trend in the low elevation stratum was very strong while evidence of a downward trend in the total survey area was weak, and trends were upward in the high elevation stratum (Table 15; Figure 49 in Appendix F).

**Table 17.** Red-billed Leiothrix density and abundance estimates (± SE and 95%CI) in the low elevation (<1,500 m), high elevation (≥1,500 m), and total area combined. In 2010 and 2016 there were not enough detections to estimate separate densities in each inference area.

| Year | Low Elevation (19,369 ha) | | High Elevation (13,548 ha) | | Total Area (32,917 ha) | |
|---|---|---|---|---|---|---|
| | Density ± SE (95%CI) | Abundance ± SE (95%CI) | Density ± SE (95%CI) | Abundance ± SE (95%CI) | Density ± SE (95%CI) | Abundance ± SE (95%CI) |
| 1976 | 1.28 ± 0.11 (1.09–1.53) | 24,865 ± 2,206 (21,073–29,721) | 0.42 ± 0.07 (0.30–0.56) | 5,665 ± 905 (4,018–7,565) | 0.93 ± 0.08 (0.79–1.09) | 30,530 ± 2,522 (26,019–35,907) |
| 1993 | 2.73 ± 0.27 (2.30–3.35) | 52,866 ± 5,195 (44,494–64,860) | 0.92 ± 0.30 (0.40–1.59) | 12,482 ± 4,099 (5,423–21,491) | 1.99 ± 0.22 (1.63–2.48) | 65,348 ± 7,083 (53,719–81,485) |
| 2002 | 2.81 ± 0.27 (2.34–3.41) | 54,497 ± 5,294 (45,361–66,115) | 0.81 ± 0.19 (0.47–1.20) | 10,955 ± 2,507 (6,364–16,192) | 1.99 ± 0.19 (1.67–2.43) | 65,452 ± 6,367 (54,876–79,834) |
| 2005 | 2.73 ± 0.34 (2.09–3.43) | 52,831 ± 6,630 (40,400–66,391) | 0.55 ± 0.07 (0.44–0.71) | 7,487 ± 961 (5,902–9,669) | 1.83 ± 0.21 (1.45–2.29) | 60,318 ± 7,023 (47,790–75,319) |
| 2008 | 2.65 ± 0.25 (2.22–3.18) | 51,235 ± 4,760 (43,010–61,671) | 0.81 ± 0.16 (0.51–1.15) | 10,942 ± 2,220 (6,878–15,581) | 1.89 ± 0.17 (1.60–2.26) | 62,177 ± 5,573 (52,602–74,448) |
| 2010 | – | – | 0.72 ± 0.14 (0.47–1.00) | 9,717 ± 1,847 (6,315–13,556) | – | – |
| 2016 | – | – | 0.84 ± 0.13 (0.58–1.11) | 11,328 ± 1,827 (7,888–15,049) | – | – |
| 2019 | 1.88 ± 0.21 (1.52–2.34) | 36,412 ± 4,056 (29,453–45,354) | 1.10 ± 0.14 (0.86–1.40) | 14,849 ± 1,835 (11,715–18,908) | 1.56 ± 0.14 (1.32–1.89) | 51,261 ± 4,755 (43,515–62,154) |

### *Red Junglefowl*

There were two detections of Red Junglefowl (*Gallus gallus*; Table 5). The species was detected at 0.2% of stations surveyed at <0.01 BPC. The detections were within KFR, at the bottom of Transect 6 in open non-native canopy with an understory of non-native shrubs and grasses (Figure 35 in Appendix E).

### *Warbling White-eye*

The Warbling White-eye was the most broadly distributed and abundant of the non-native species detected in 2019. The species was detected at 73.4% of the stations surveyed and at 1.68 BPC (Table 5). The species occurred broadly at all elevations and vegetation types throughout the survey area (Figure 36). We estimated a density of 6.17 ± 0.33 birds/ha with an abundance of 203,114 ± 10,714 birds in the total survey area (Table 18). Density in the high elevation stratum (3.28 ± 0.25 birds/ha) was less than half the density in the low elevation stratum at 8.20 ± 0.49 birds/ha. Evidence of upward trends in both elevation strata and the total survey area was very strong (Table 15; Figure 50 in Appendix F).

**Table 18.** Warbling White-eye density and abundance estimates (± SE and 95%CI) in the low elevation (<1,500 m), high elevation (≥1,500 m), and total area combined. In 2010 and 2016 there were not enough detections to estimate separate densities in each inference area.

| Year | Low Elevation (19,369 ha) | | High Elevation (13,548 ha) | | Total Area (32,917 ha) | |
|---|---|---|---|---|---|---|
| | Density ± SE (95%CI) | Abundance ± SE (95%CI) | Density ± SE (95%CI) | Abundance ± SE (95%CI) | Density ± SE (95%CI) | Abundance ± SE (95%CI) |
| 1976 | 6.06 ± 0.38 (5.44–6.92) | 117,470 ± 7,349 (105,313–134,120) | 1.41 ± 0.16 (1.14–1.76) | 19,156 ± 2,154 (15,397–23,841) | 4.15 ± 0.24 (3.75–4.70) | 136,626 ± 8,049 (123,286–154,836) |
| 1993 | 5.52 ± 0.54 (4.60–6.73) | 106,930 ± 10,551 (89,091–130,450) | 1.75 ± 0.47 (0.92–2.78) | 23,742 ± 6,422 (12,517–37,689) | 3.97 ± 0.38 (3.35–4.82) | 130,672 ± 12,404 (110,139–158,765) |
| 2002 | 5.06 ± 0.42 (4.36–6.01) | 97,972 ± 8,168 (84,394–116,413) | 1.04 ± 0.29 (0.54–1.69) | 14,144 ± 3,980 (7,282–22,885) | 3.41 ± 0.28 (2.93–4.03) | 112,116 ± 9,270 (96,285–132,624) |
| 2005 | 5.26 ± 0.76 (3.94–6.91) | 101,830 ± 14,676 (76,258–133,789) | 3.53 ± 0.20 (3.20–3.97) | 47,787 ± 2,653 (43,372–53,772) | 4.55 ± 0.46 (3.75–5.56) | 149,617 ± 15,223 (123,501–1831,77) |
| 2008 | 8.54 ± 0.53 (7.67–9.76) | 165,480 ± 10,362 (148,515–189,135) | 2.82 ± 0.47 (1.99–3.82) | 38,234 ± 6,326 (26,965–51,764) | 6.19 ± 0.38 (5.56–7.05) | 203,714 ± 12,585 (182,855–232,187) |
| 2010 | – | – | 2.05 ± 0.25 (1.59–2.59) | 27,769 ± 3,451 (21,566–35,094) | – | – |
| 2016 | – | – | 6.39 ± 0.49 (5.59–7.50) | 86,634 ± 6,583 (75,759–101,563) | – | – |
| 2019 | 8.20 ± 0.49 (7.43–9.35) | 158,740 ± 9,456 (143,972–181,040) | 3.28 ± 0.25 (2.86–3.83) | 44,374 ± 3,362 (38,687–51,867) | 6.17 ± 0.33 (5.70–6.97) | 203,114 ± 10,714 (187,589–229,588) |

### *Western Meadowlark*

There were two detections of the Western Meadowlark (*Sturnella neglecta*; Table 5). The species was detected at 0.4% of stations surveyed at <0.01 BPC. There was one detection in KPFR and one in KCGMA (Figure 37 in Appendix E). The species was detected in open non-native grassland.

### *Wild Turkey*

There were five detections of Wild Turkey (*Meleagris gallopavo*; Table 5). The game bird occurred at 1% of stations surveyed at 0.01 BPC (Table 4). The detections were above 1,800 m elevation in open native scrubland in the Kahuku Unit portion of the survey area (Figure 38 in Appendix E).

### *Yellow-fronted Canary*

The Yellow-fronted Canary (*Crithagra mozambica*) had 57 detections and was detected at 6.4% of stations surveyed at 0.10 BPC (Table 5). The detections were near the periphery of the survey area, with a relatively high occurrence in open montane woodlands in an understory of predominantly non-native grasses in the Kahuku Unit (Figure 39 in Appendix E).

## Habitat Surveys

Habitat variables were measured at 488 landbird monitoring stations in 2019. Of the 488 stations surveyed, 329 were classified within the wet moisture zone, of which 324 were within the KFR survey area (Table 44 in Appendix G, Figure 51 in Appendix G). The mesic moisture zone was recorded at 100 of the stations and the remaining 59 stations were either in the dry or unknown moisture zone. Canopy height and canopy cover were recorded at 472 and 457 of the stations, respectively (Table 45 in Appendix G; Figures 52 and 53 in Appendix G). Stations having a dominant canopy height of over 10 m were recorded at 325 stations. Stations with a closed canopy cover classification were recorded at 320 stations. Shorter tree heights and open to scattered canopy cover classifications occurred within the subalpine and montane woodland survey areas of the Kahuku Unit. *Metrosideros polymorpha* was the dominant canopy species at >80% of the 488 stations surveyed (Table 46 in Appendix G, Figure 54 in Appendix G). The remaining stations were co-dominated by *M. polymorpha* and either *Acacia koa*, *Cheirodendron trigynum*, *Ilex anomala*, or grouped classes of native trees or native ferns. Non-native *Eucalyptus* trees dominated one habitat plot near the bottom of KFR. Other non-native canopy species recorded included non-native trees *Schinus terebinthifolia* and *Psidium cattleianum,* and non-native treefern *Sphaeropteris cooperi*. Surveyors noted dead and dying trees, likely due to Rapid ʻŌhiʻa Death, on Transects 1 and 2 in the west of KFR and on Transects 9 and 10 in the eastern areas of KFR. A wide variety of understory classifications were recorded at 472 of the 488 stations (Table 47 in Appendix G). Native ferns (e.g., *Cibotium menziesii*, *Sadleria* spp.) were the dominant understory class for >25% of the stations surveyed (Figure 55 in Appendix G). Native shrubs (e.g., *Hydrangea arguta, Dodonaea viscosa, Leptecophylla tameiameiae*), matted ferns (*Dicranopteris linearis*), native grasses, and bare ground accounted for the most dominant and co-dominant classifications. Several classes varied in order of dominance and resulted in 177 classifications in the entire survey area, each occurring at less than 10% of stations within the survey area.

In addition to habitat variables that were collected in the field in 2019, we summarized the Jacobi (1989) vegetation classifications for each of the 488 stations surveyed (Table 48 in Appendix G,

Figure 56 in Appendix G). Within the Kahuku Unit, 25 of the 70 stations surveyed (35.7%) were classified as mesic (moist) environment, with a canopy dominated by *M. polymorpha* and then by a mixture of native trees, with an understory dominated by native shrubs followed by matted ferns (coded as M:Me, nt(ns,mf) in Jacobi [1989]). In KFR, nearly half of the 371 stations surveyed had a vegetation classification of a wet environment, with a canopy of *M. polymorpha* and then by a mixture of native trees, with an understory predominated by tree ferns and then native shrubs to a lesser extent (coded as W:Me,nt(tf,ns) in Jacobi [1989]). Summaries of the vegetation classifications extracted from the Jacobi (1989) maps are provided in Table 48 in Appendix G. Note the definitions of each code are provided in the footnotes under the table. The classifications are also displayed on Figure 56 in Appendix G. Evidence of ungulates were recorded on every transect surveyed. Sign of pigs, sheep, and cattle were recorded on Transects 10 and 11. Signs of pigs and cattle were recorded on Transect 9, while evidence of just pigs was recorded on each of the other transects surveyed.

### Vegetation Covariates

Preliminary analysis revealed that 10 vegetation covariates were evaluated with seven improving the detection function model fit for one or more species (Table 19). Covariates and model fits for each species are presented in Appendix D. Models with only vegetation covariates did not have lower AIC values than models with observation and weather covariates. For nine of the eleven species, one or more vegetation covariates combined with observation and weather covariates improved detection function model fit (Table 20), except for ʻAkiapōlāʻau where vegetation covariates did not improve model fit and ʻAlawī where the model with Detect 2,4 and model with Detect 2,4 + Height19 were within two AIC units (Table 20; Appendix D).

**Table 19.** Vegetation covariates used to improve detection function model. Also shown is the number of distinct levels used in the evaluation.

| Variable Abbreviation | Description | Evaluated | Levels Used | Significant in a Model |
|---|---|---|---|---|
| Jacobi | 1983 (Jacobi 1989) vegetation category | Yes | 8 | Yes |
| Env | Wet, dry, mesic (moist) forest, or unclassified | Yes | 4 | Yes |
| Canopy | Closed vs. open vs. scattered forest from 1983 classification | Yes | 3 | No |
| Overstory | Dominant overstory species from 1983 classification | Yes | 4 | Yes |
| Understory | Dominant understory species from 1983 classification | Yes | 5 | Yes |
| Green | Green et al. (2015) habitat association | No | N/A | N/A |
| Cover | Closed, open, scattered, or very scattered forest | Yes | 4 | Yes |
| Canopy19 | Dominant canopy species and height recorded in 2019 | No | N/A | N/A |
| Under19 | Predominant understory species recorded in 2019 | Yes | 5 | No |
| Height19 | Canopy height category recorded in 2019 | Yes | 4 | Yes |

**Table 19 (continued).** Vegetation covariates used to improve detection function model. Also shown is the number of distinct levels used in the evaluation.

| Variable Abbreviation | Description | Evaluated | Levels Used | Significant in a Model |
|---|---|---|---|---|
| Hcan19 | Canopy height + dominant species recorded in 2019 | Yes | 5 | No |
| Undom | Dominant understory species recorded in 2019 | Yes | 9 | Yes |

**Table 20.** Bird models and species detection functions that were improved with vegetation covariates. Refer to Table 19 for vegetation covariate abbreviations. Truncation (Trunc) is the distance at which the detection probability was <10% using a preliminary half-normal detection function model.

| Species | Trunc. | Key | Best Model with Vegetation Covariates | Abundance Change |
|---|---|---|---|---|
| ʻAkiapōlāʻau | None | Half-normal | None | N/A |
| ʻAlawī | None | Half-normal | Detect 2,4 | N/A |
| ʻApapane | 10% | Hazard-rate | Detect 2,4 + Jacobi + Undom | +0.5% |
| Hawaiʻi ʻĀkepa | None | Hazard-rate | Year (grouped) + Undom19 | +1.0% |
| Hawaiʻi ʻAmakihi | 10% | Hazard-rate | Detection + Env + Undom | +3.3% |
| Hawaiʻi ʻElepaio | None | Hazard-rate | Detection + Overstory | -8.6% |
| ʻIʻiwi | 5% | Half-normal | Detection + Overstory | +0.4% |
| ʻŌmaʻo | 10% | Hazard-rate | Detect 2,4 + Jacobi + Cover | +7.8% |
| Northern Cardinal | 5% | Hazard-rate | Detection + Undom | +5.3% |
| Red-billed Leiothrix | 5% | Hazard-rate | Detection + Jacobi | +5.4% |
| Warbling White-eye | 10% | Hazard-rate | Detection + Env | +5.4% |

Abundances for most species were revised upward, with only slight increases in estimates from models that included vegetation covariates compared to the detection function models without vegetation covariates. The maximum increase was 7.8% for ʻŌmaʻo with a detection function model that included the Jacobi (1989) vegetation classification and cover covariates. The sole decrease in abundance was for the Hawaiʻi ʻElepaio that declined 8.6% with the detection function that included the overstory covariate.

# Discussion

## Landbirds

We estimated distribution, status, and trends for eight native and three non-native landbird species observed during the 2019 landbird survey within the Kaʻū Rainforest. ʻApapane and Hawaiʻi ʻAmakihi were the most abundant and widespread native species. Both species exhibited strong evidence of upward trends throughout the entire survey area since 2002. Both species are generalist foragers and can exploit a wide variety of habitats and have higher fecundity than most foraging specialists (e.g., ʻIʻiwi and ʻAkiapōlāʻau; Banko and Banko 2009b). Generalist traits likely contributed to the Hawaiʻi ʻAmakihi's capacity to develop a resistance or tolerance to avian malaria in forests where mosquitoes and disease are abundant (Woodworth et al. 2005, Foster et al. 2007, Atkinson et al. 2013). ʻApapane are also generalists and less susceptible to avian malaria than specialists (Atkinson et al. 1995), but there is little evidence the species has developed resistance to the disease. Indirectly, however, the species increased in low elevation strata in areas where Gaudioso et al. (2015) found disease prevalence as high as 70% of ʻApapane tested. Trends were also upward in the elevation strata, near sites where prevalence was approximately 10% of ʻApapane tested.

ʻIʻiwi were broadly distributed in elevations above 1,200 m, but across the species' range in the Kaʻū Rainforest there was strong evidence the population declined between 2002 and 2019. The species' range had been reduced in this area by almost 3,000 ha since 2005. Contractions in range occurred along the lower elevations of the species' range, where the species is increasingly vulnerable to avian malaria transmission (Paxton et al. 2013). Avian malaria generally restricts ʻIʻiwi to elevations above 1,500 m elevation where the presence of malaria and *Culex* mosquitoes drops due to cold temperature intolerance (Atkinson et al. 2000). ʻIʻiwi are nectarivorous and obligated to foraging on resources provided by ʻōhiʻa and other plants (Fancy and Ralph 2020). Mature ʻōhiʻa occur throughout the survey area, thus ʻIʻiwi may be attracted to trees in bloom in areas below 1,500 m, increasing their exposure to disease (Hart et al. 2011, Guillaumet et al. 2017). The declines of ʻIʻiwi population in the Kaʻū Rainforest that overlaps with the malaria-mosquito range are consistent with trends on other Hawaiian Islands. On the island of Kauaʻi, ʻIʻiwi have contracted from the lower elevations of its recent range (extending down to 900 m elevation in 1968 but now limited to >1,100 m elevation) and abundances in its existing range decreased by 86% from 2000 to 2012 (Paxton et al. 2016, 2020). ʻIʻiwi are at risk of extirpation on the islands of Oʻahu and Molokaʻi, where surveys have detected few birds (Paxton et al. 2013, S. Judge and L. Smith, NPS, unpublished data). The Island of Hawaiʻi and Maui have substantial native forest habitat above 1,500 m and are the only islands where upward trends in ʻIʻiwi populations have been observed (Camp et al. 2009a, Paxton et al. 2013, Judge et al. 2017a, Kendall et al. 2024).

Only four ʻAkiapōlāʻau were detected during the 2019 survey. The species' range in the Kaʻū Rainforest has decreased by 22% since 2002 and by nearly 50% since the first survey in 1979 (Table 7). Densities declined significantly from 2005 to 2008 when there were an estimated 691 ± 410 birds. Densities were not estimated for subsequent surveys due to insufficient detections. ʻAkiapōlāʻau prey primarily on the larvae of the koa long-horned beetle (*Aegolipton reflexa*) which are only found in

koa trees (Ralph and Fancy 1996, Goldsmith et al. 2007). Koa was relatively sparse in the Kaʻū Rainforest, which may be a limiting factor for ʻAkiapōlāʻau in the area. ʻAkiapōlāʻau responded positively to reforestation efforts at Hakalau Forest National Wildlife Refuge (HFNWR), where crews outplanted koa in pastures previously grazed by ungulates (Paxton et al. 2018, Kendall et al. 2024). Birds quickly took advantage of new foraging opportunities in young koa trees and densities increased in the afforested pasture. This reforestation strategy has potential to benefit ʻAkiapōlāʻau at the upper limits of their range in the Kaʻū Rainforest, where ʻōhiʻa dominated montane woodlands could be enhanced with koa outplantings to benefit the species. DLNR and DOFAW designated ~509 ha of native mesic montane forest within the northeast portion of KFR called the Kapāpala Koa Canoe Management Area (KKCMA). The 2023 draft management plan (State of Hawaiʻi-DLNR 2023b) states that one of the primary objectives is providing a sustainable, long-term supply of koa for constructing traditional koa canoes. The unit was fenced and there has been ongoing ungulate control, along with silviculture practices to enhance the growth and regeneration of koa trees for selective harvest, while providing habitat for native forest birds, including ʻAkiapōlāʻau, which have been sighted near the northwest boundary of the unit (State of Hawaiʻi-DLNR 2023b).

Abundance and trends were more favorable for the endangered ʻAlawī and Hawaiʻi ʻĀkepa. Evidence of increasing densities of ʻAlawī was very strong. We estimated the 2019 abundance at 12,935 ± 2,225 birds (Table 8), which was the highest abundance reported for the species in the four decades of Kaʻū Rainforest surveys, and slightly larger than the 2019 ʻAlawī population in HFNWR with an estimated 9,888 ± 2,270 birds (Kendall et al. 2024). Trends were inconclusive for the Hawaiʻi ʻĀkepa, but our 2019 estimate of 4,169 ± 991 birds (Table 10) confirmed that the Kaʻū Rainforest population was the second largest subpopulation on the Island of Hawaiʻi (Judge et al. 2018, Kendall et al. 2024). Both species overlap throughout most of their ranges, but ʻAlawī are restricted to mature and large stature ʻōhiʻa, while the range of Hawaiʻi ʻĀkepa extends above the closed canopy ʻōhiʻa forest into open montane woodlands (Judge et al. 2018). It is notable, however, that ʻAlawī densities, like ʻAkiapōlāʻau, also responded positively to reforestation efforts in pastures within HFNWR (Kendall et al. 2024). In 2015, TMA finished enclosing an ~800 ha area of important ʻAlawī and Hawaiʻi ʻĀkepa habitat within KFR called the Hōʻili Wai Unit, and the ~800 ha Nā Manu Unit to the west of Hōʻili Wai is expected to be completely fenced by 2025 (Corie Yanger-TMA September 2023, written communication). Furthermore, plans are underway to fence and control ungulates in an additional unit to the northeast of Hōʻili Wai to enhance more native plant and forest bird habitat (Kaʻū Forest Reserve Management Plan 2012). Ungulate and weed control efforts within each unit are expected to provide long-term protection of native forest bird habitat within the Kaʻū Rainforest.

The Hawaiʻi ʻElepaio exhibited strong evidence of a downward trend throughout the entire 2019 survey area. We estimated an abundance of 15,753 ± 3,251 birds, which was a 56% reduction from the highest estimate in 2008 (Table 12). Unlike most Hawaiian honeycreepers, the Hawaiʻi ʻElepaio, a monarch flycatcher, is less vulnerable to avian malaria (van Riper et al.1986, VanderWerf et al. 2006). The Hawaiʻi species, as well as the Kauaʻi ʻElepaio (*C. sclateri*) and the endangered Oʻahu ʻElepaio (*C. ibidis*), are, however, vulnerable to mammalian predators. Eggs and nestlings are especially vulnerable to depredation. For instance, black rats caused failures in 53% of nests in a

mesic forest of HAVO (Sarr et al. 1997) and black rats were the leading cause of mortality and endangerment of the Oʻahu ʻElepaio (VanderWerf 2020). The threats of mammalian predators are not unique to the Hawaiʻi ʻElepaio—declines of ʻŌmaʻo in the high elevation stratum, Northern Cardinal in both strata, and the Red-billed Leiothrix in the low elevation stratum could also be attributed to predation, not only by black rats and feral cats, but also by Norway rats, Polynesian rats, and mongooses. Predator control can be locally successful in native forests (VanderWerf 2001, Banko et al. 2019), but landscape controls have rarely been implemented in native bird habitats on the main Hawaiian Islands due to expense, logistical constraints, and concerns about public perceptions of non-target impacts.

The Warbling White-eye remained the most widespread and abundant non-native species detected in the 2019 survey, and there was very strong evidence of increasing abundance throughout the Kaʻū Rainforest. This generalist forager can take advantage of both native and non-native resources. The impact of competition of the Warbling White-eye to native species has been difficult to demonstrate (Mountainspring and Scott 1985) but the species occurred in densities equivalent to or higher than other generalist species, such as the Hawaiʻi ʻAmakihi. The extent that either of those species are limited by foraging resources is uncertain, but Banko et al. (2015) estimated varying degrees of overlap in the diets of several native species to those of the Warbling White-eye and Red-billed Leiothrix. The Red-billed Leiothrix also co-occurred with most native species detected in 2019 and as a generalist species that forages on arthropods and fruits, also likely competes with native birds for resources (Foster 2005). The Japanese Bush Warbler recently irrupted in the survey area and neither Tweed et al. (2007) nor Gorresen et al. (2007) detected the species during their surveys in the Kaʻū region. Japanese Bush Warblers and other non-native generalists disperse invasive plants (Foster 2005, Vizentin-Bugoni et al. 2019, Chimera and Drake 2010) and influence disease transmission to native species because they can serve as a reservoir for the avian malaria parasite (Hobbelen et al. 2012, McClure et al. 2020).

Upward trends of native forest birds, in part, can be explained by the ongoing protection of one of the largest native forests in the state of Hawaiʻi. The control of ungulates and weeds has ameliorated degradation of important forest bird habitat (Pratt and Jacobi 2009, Price et al. 2009, Kendall et al. 2024). However, many species of Hawaiian plants are vulnerable to climate change (Fortini et al. 2013), and climate-envelope models predict reductions in species richness by the end of the 21$^{st}$ century (Camp et al. 2018). The greatest native plant range contractions are projected to occur in wet and mesic forests that predominate the low elevation stratum of the Kaʻū Rainforest, thus habitat suitability for native forest birds will likely be affected in areas where we demonstrated declines in native bird densities. The climate models projected minimal to moderate range expansion for select native plant species, particularly in the subalpine and alpine environments of HAVO, where forest birds have the potential to expand in range. However, these gains are relatively small compared to the predicted expansion in range of disease vectors under current climate change scenarios. Climate models predict that species vulnerable to disease, such as ʻAkiapōlāʻau, ʻAlawī, and Hawaiʻi ʻĀkepa, will lose more than 75% of their current range by 2100 (Fortini et al. 2015). ʻIʻiwi, which is already restricted to elevations above 1,500 m due to mosquitoes and avian malaria, are predicted to lose 60% of their current range (Fortini et al. 2015). It's clear that the application and development of

tools that suppress the transmission of avian malaria remains a priority for preventing extinction (Paxton et al. 2022). Pursuing this goal via the Incompatible Insect Technique (Zheng et al. 2019) has become a viable technique on the islands of Maui and Kauaʻi (Haleakalā National Park 2023, State of Hawaiʻi-DLNR 2023a). The technique, if successful, could also be used to suppress avian malaria transmission within the Kaʻū Rainforest.

### Habitats

Our habitat survey followed the methods developed by Jacobi (1989). We used this habitat information to identify influencing factors (covariates) in modeling detection functions for estimating bird densities. For example, the model for Hawaiʻi ʻAmakihi included moisture and understory dominant species covariates, indicating that the moisture zone (i.e., wet, mesic, or dry) and dominant species in the understory strongly influenced Hawaiʻi ʻAmakihi detectability. Incorporating sampling and vegetation covariates generally reduces estimator variability, thus increasing confidence in the density and abundance estimates. In addition, incorporating the vegetation covariates adjusted the abundance estimates upward for most species compared to estimates from best-fit models without vegetation covariates. We observed that these adjustments, however, were only modest and well within the 95% CIs, with a maximum increase of 7.8% for ʻŌmaʻo and a decrease of 8.6% for Hawaiʻi ʻElepaio.

Information gained from the habitat surveys did not substantially improve abundance estimates. However, habitat surveys are an important component of the landbird monitoring effort because the information can be used to better understand the dynamics of bird populations and habitat structures. Habitat conditions such as canopy cover and density influence food availability, which in turn may affect foraging bird population densities in the area (Fretz 2002). If we detect changes in bird populations, having long-term habitat information may permit identifying causative factors driving those changes. Furthermore, the information gathered from the habitat surveys serves as an overview and provided general descriptions of habitat conditions at our study plots. With continuous monitoring, habitat surveys provide the needed clues for effective future management, such as ungulate and alien grass control. Lastly, the habitat information can also be incorporated into other programs of vital signs monitoring. Canopy information may complement satellite imagery to improve knowledge of the vegetation composition in an area. Understory vegetation information may reveal habitat structures that cannot be surveyed using remote sensing methods. Canopy and understory vegetation information may help to locate and monitor the spread of invasive plants, which have already become an acute problem in Hawaiʻi for the preservation of native ecosystem and bird habitats (Loope et al. 2001).

Our 2019 habitat survey covered a wide area of the Kaʻū Rainforest and surveyors may detect invasive plants such as banana poka (*Passiflora tripartita* var. *mollissima*), night-blooming jasmine (*Cestrum nocturnum*), Koster's curse (*Miconia crenata*), and others at their incipient stage before a major infestation strikes. In 2019, >80% of stations sampled were dominated by native trees and shrubs. Surveyors noted the presence of *C. nocturnum* and *P. cattleianum* at the lowest stations in the survey area. Surveyors indicated presence of ʻōhiʻa trees that appeared to be infected by the fungal pathogens *Ceratocystis lukuohia* or *Ceratocystis huliohia* in areas of KFR. The pathogens can cause

"Rapid ʻŌhiʻa Death" (Barnes et al. 2018) and negatively impact native forest birds through habitat loss (Camp et al. 2019). Occurrence of the disease has been recorded in other areas the Kaʻū Rainforest (Vaughn et al. 2023). However, state and federal land managers have implemented protocols and outreach campaigns to help reduce the spread and impact of Rapid ʻŌhiʻa Death (Cannon et al. 2022). Future habitat surveys can help update land managers on the status of important landbird habitat and potential threats to the ecosystem.

## Conclusion

The 2019 Kaʻū Rainforest landbird survey was an increasingly common example of an interagency collaboration working towards the shared goal of tracking populations of native avifauna and identifying their threats. Participants were a mix of academic, federal and state government, and non-government organizations, each with unique insights into avian ecology, quantitative ecology, and the management of natural resources. This partnership has contributed to the protection and conservation of over 30,000 ha of continuous native landbird habitat, which may not have been possible by a single management entity given the scale of the Kaʻū Rainforest. Working together, HAVO, DOFAW, and TNC have individually managed areas of old-growth ʻōhiʻa and koa forest, allowing managers to budget, procure funding, and implement fence construction, ungulate control, and monitoring efforts. This strategy has allowed agencies to scale up levels of land management to protect more of the ecosystem. These collaborative management efforts help preserve native habitat at landscape scales.

# Literature Cited


Ahumada, J. A., D. A. LaPointe, and M. D. Samuel. 2004. Modeling the population dynamics of *Culex quinquefasciatus* (Diptera: Culicidae), along an elevational gradient in Hawai‘i. Journal of Medical Entomology 41(6):1157–1170.

Atkinson, I. A. E. 1977. A reassessment of factors, particularly *Rattus rattus L*., that influenced the decline of endemic forest birds in the Hawaiian Islands. Pacific Science 31(2):109–133.

Atkinson, C. T., J. K. Lease, R. J. Dusek, and M. D. Samuel. 2005. Prevalence of pox-like lesions and malaria in forest bird communities on leeward Mauna Loa Volcano, Hawai‘i. Condor 107:537–546.

Atkinson, C. T., K. L. Woods, R. J. Dusek, L. S. Sileo, and W. M. Iko. 1995. Wildlife disease and conservation in Hawai‘i: pathogenecity of avian malaria (*Plasmodium relictum*) in experimentally infected ‘I‘iwi (*Vestiaria coccinea*). Parasitology 111:S59–S69.

Atkinson, C. T., R. B. Utzurrum, D. A. Lapointe, R. J. Camp, L. H. Crampton, J. T. Foster, and T. W. Giambelluca. 2014. Changing climate and the altitudinal range of avian malaria in the Hawaiian Islands–an ongoing conservation crisis on the island of Kaua‘i. Global Change Biology 20(8):2426–2436.

Banko, P. C. 1992. Constraints on productivity of wild Nēnē or Hawaiian Geese *Branta sandvicensis*. Wildfowl 43(43):99–106.

Banko, P. C., R. E. David, J. D. Jacobi, and W. E. Banko. 2001. Conservation status and recovery strategies for endemic Hawaiian birds. Studies in Avian Biology 22:359–376.

Banko, W. E., and P. C. Banko 2009a. Historic decline and extinction. Pages 25–58 *in* Conservation Biology of Hawaiian Forest Birds: Implications for Island Avifauna (T. K. Pratt, C. T. Atkinson P. C. Banko, J. D Jacobi, and B. L. Woodworth, editors). Yale University Press, New Haven, Connecticut.

Banko, W. E., and P. C. Banko. 2009b. Evolution and ecology of food exploitation. Pages 159–193 *in* Conservation Biology of Hawaiian Forest Birds: Implications for Island Avifauna (T. K. Pratt, C. T. Atkinson, P. C. Banko, J. D Jacobi, and B. L. Woodworth, editors). Yale University Press, New Haven, Connecticut.

Banko, P. C., K. A. Jaenecke, R. W. Peck, and K. W. Brinck. 2019. Increased nesting success of Hawai‘i ‘Elepaio in response to the removal of invasive black rats. The Condor 121(2):1–12.

Banko, P. C., R. W. Peck, K. Brinck, and D. Leonard. 2015. Richness, diversity, and similarity of arthropod prey consumed by a community of Hawaiian forest birds. Technical Report HCSU-066. Hawai‘i Cooperative Studies Unit.

Barnes, I., A. Fourie, M. J. Wingfield, T. C. Harrington, D. L. McNew, L. S. Sugiyama, B. C. Luiz, W. P. Heller, and L. M. Keith. 2018. New *Ceratocystis* species associated with rapid death of *Metrosideros polymorpha* in Hawai‘i. Persoonia-Molecular Phylogeny and Evolution of Fungi 40(1):154–181.

Best, L. B. 1981. Seasonal changes in detection of individual bird species. Pages 252–261 *in* Estimating numbers of terrestrial birds (C. J. Ralph and J. M. Scott, editors). Studies in Avian Biology No. 6.

Buckland, S. T., D. R. Anderson, K. P. Burnham, J. L. Laake, D. L. Borchers, and L. Thomas. 2001. Introduction to distance sampling: estimating abundance of biological populations. Oxford University Press, Oxford, England, United Kingdom.

Buckland, S. T., E. A. Rexstad, T. A. Marques, and C. S. Oedekoven. 2015. Distance Sampling: Methods and Applications. Springer, London, United Kingdom.

Camp, R. J., P. M. Gorresen, T. K. Pratt, and B. L. Woodworth. 2009a. Population trends of native Hawaiian forest birds, 1976–2008: the data and statistical analyses. Hawai‘i Cooperative Studies Unit Technical Report HCSU-012. University of Hawai‘i at Hilo, Hilo, Hawai‘i.

Camp, R. J., D. A. LaPointe, P. J. Hart, D. E. Sedgwick, and L. K. Canale. 2019. Large-scale tree mortality from Rapid ‘Ōhi‘a Death negatively influences avifauna in lower Puna, Hawai‘i Island, USA. The Condor 121(2):duz007.

Camp, R. J., R. Loh, P. Berkowitz, K. W. Brinck, J. D. Jacobi, J. Price, S. McDaniel, and L. Fortini. 2018. Potential impacts of projected climate change on vegetation management in Hawai‘i Volcanoes National Park. Park Science 34(1):22–32.

Camp, R. J., T. K. Pratt, C. Bailey, and D. Hu. 2011. Landbirds vital sign monitoring protocol – Pacific Island Network. Natural Resources Report NPS/PACN/NRR—2011/402. National Park Service, Fort Collins, Colorado.

Camp, R. J., M. H. Reynolds, B. L. Woodworth, P. M. Gorresen, and T. K. Pratt. 2009b. Monitoring Hawaiian forest birds. Pages 83–107 *in* Conservation Biology of Hawaiian Forest Birds: Implications for insular avifauna (T. K. Pratt, C. T. Atkinson, P. C. Banko, J. D. Jacobi, and B. L. Woodworth, editors). Yale University Press, New Haven, Connecticut.

Camp, R. J., N. Seavey, M. H. Reynolds, and P. M. Gorresen. 2008. A statistical test to show negligible trend: comment. Ecology 89(5):1469–1472.

Cannon, P., J. B. Friday, T. Harrington, L. Keith, M. Hughes, R. Hauff, F. Hughes, R. Perroy, D. Benitez, K. Roy, and R. Peck. 2022. Rapid ‘Ōhi‘a Death in Hawai‘i. Pages 267–289 *in* Forest Microbiology, Volume 2: Forest Tree Health (F. O. Asiegbu and A. Kovalchuk, editors). Academic Press, San Diego, California.

Chesser, R. T., S. M. Billerman, K. J. Burns, C. Cicero, J. L. Dunn, B. E. Hernández-Baños, R. A. Jiménez, A. W. Kratter, N. A. Mason, P. C. Rasmussen, J. V. Remsen, Jr., and K. Winker. 2023. Check-list of North American Birds (online). American Ornithological Society. https://checklist.americanornithology.org/taxa/

Chimera, C. G., and D. R. Drake. 2010. Patterns of seed dispersal and dispersal failure in a Hawaiian dry forest having only introduced birds. Biotropica 42(4):493–502.

Elphick, C. S., D. L. Roberts, and J. M. Reed. 2010. Estimated dates of recent extinctions for North American and Hawaiian birds. Biological Conservation 143:617–624.

Fancy, S. G. and C. J. Ralph. 2020.ʻIʻiwi (*Drepanis coccinea*), version 1.0. *in* Birds of the World (A. F. Poole and F. B. Gill, editors). Cornell Lab of Ornithology, Ithaca, New York. https://doi.org/10.2173/bow.iiwi.01

Fortini, L. B., A. E. Vorsino, F. A. Amidon, E. H. Paxton, and J. D. Jacobi. 2015. Large-scale range collapse of Hawaiian forest birds under climate change and the need 21st century conservation options. PloS One 10(10):e0140389.

Foster, J. T. 2005. Exotic bird invasions into forests of Hawaiʻi: Demography, competition, and seed dispersal. PhD. Dissertation. University of Illinois, Urbana-Champaign, Illinois.

Foster, J. T., B. L. Woodworth, L. E. Eggert, P. J. Hart, D. Palmer, D. C. Duffy, and R. C. Fleischer. 2007. Genetic structure and evolved malaria resistance in Hawaiian honeycreepers. Molecular Ecology 16(22):4738–4746.

Fretz, J. S. 2002. Scales of food availability for an endangered insectivore, the Hawaiʻi ʻĀkepa. The Auk 119(1):166–174.

Gaudioso, J., D. Lapointe, C. T. Atkinson, and A. N. Egan. 2015. Avian disease and mosquito vectors in the Kahuku unit of Hawaiʻi Volcanoes National Park and Kaʻū Forest Reserve. Hawaiʻi Cooperative Studies Unit Technical Report HCSU-070, University of Hawaiʻi at Hilo, Hilo, Hawaiʻi.

Gill, F., D. Donsker, and P. Rasmussen (editors). 2023. IOC World Bird List (v13.1). doi: 10.14344/IOC.ML.13.1

Goldsmith, S., H. Gillespie, and C. Weatherby. 2007. Restoration of Hawaiian montane wet forest: endemic Longhorned Beetles (Cerambycidae: *Plagithmysus*) in Koa (Fabaceae: *Acacia koa*) plantations and in intact forest. The Southwestern Naturalist 52(3):356–363.

Gorresen, P. M., R. J Camp, and T. K. Pratt. 2007. Forest bird distribution, density and trends in the Kaʻū region of Hawaiʻi Island. U.S. Geological Survey, Biological Resources Discipline, Open-File Report 2007-10. U.S. Department of the Interior, Washington, D.C.

Green, K., M. Hall, C. Lopez, A. Ainsworth, M. Selvig, K. Akamine, S. Fugate, K. Schulz, D. Benitez, M. Wasser, And G. Kudray. 2015. Vegetation mapping inventory project: Hawai‘i Volcanoes National Park. Natural Resource Report NPS/PACN/NRR—2015/966, National Park Service, Fort Collins, Colorado.

Guillaumet, A., W. A. Kuntz, M. D. Samuel, and E. H. Paxton. 2017. Altitudinal migration and the future of an iconic Hawaiian honeycreeper in response to climate change and management. Ecological Monographs 87(3):410–428.

Haleakalā National Park. 2023. Suppression of invasive mosquito populations to reduce transmission of avian malaria to threatened and endangered forest birds on East Maui environmental assessment. https://parkplanning.nps.gov/projectHome.cfm?projectID=102795.

Hart, P. J., B. L. Woodworth, R. J. Camp, K. Turner, K. McClure, K. Goodall, C. Henneman, C. Spiegel, J. Lebrun, E. Tweed, and M. Samuel. 2011. Temporal variation in bird and resource abundance across an elevational gradient in Hawai‘i. The Auk 128(1):113–126.

Hays, W. S., and S. Conant. 2007. Biology and impacts of Pacific Island invasive species. 1. A worldwide review of effects of the small Indian mongoose, *Herpestes javanicus* (Carnivora: Herpestidae). Pacific Science 61(1):3–16.

Hess, S., B. Kawakami, Jr., D. Okita, and K. Medeiros. 2006. A preliminary assessment of mouflon abundance at the Kahuku unit of Hawai‘i Volcanoes National Park: U.S. Geological Survey Open-File Report 2006-1193.

Hobbelen, P. H., M. D. Samuel, D. A. LaPointe, and C. T. Atkinson. 2012. Modeling future conservation of Hawaiian honeycreepers by mosquito management and translocation of disease-tolerant ‘Amakihi. PLoS One 7(11):p.e49594.

Jacobi, J. D. 1989. Vegetation maps of the upland plant communities of the islands of Hawai‘i, Maui, Molokai, and Lanai. Technical Report 68. Cooperative National Park Resources Studies Unit, Department of Botany. University of Hawai‘i, Honolulu, Hawai‘i.

James, H. F., and S. L. Olson. 1991. Descriptions of thirty-two new species of birds from the Hawaiian Islands: Part II. Passeriformes. Ornithological Monographs (46):1–88.

Judge, S. W., R. J. Camp, D. E. Sedgwick, C. L. Squibb, and P. J. Hart. 2017a. Pacific Island landbird monitoring report, Hawai‘i Volcanoes National Park, 2015-2016: Tract groups 1 and 2. Natural Resource Report NPS/PACN/NRR—2017/1407. National Park Service, Fort Collins, Colorado.

Judge, S. W., S. C. Hess, J. K. Faford, D. Pacheco, and C. R. Leopold. 2017b. Monitoring the eradication of European mouflon sheep (*Ovis gmelini musimon*) from the Kahuku Unit of Hawai‘i Volcanoes National Park. Pacific Science 71(4):425–436.

Judge, S. W., J. Gaudioso, B. Hsu, R. Camp, and P. Hart. 2011. Pacific Island landbird monitoring annual report, Hawai‘i Volcanoes National Park, tract group 1 and 2, 2010. Natural Resource Technical Report NPS/PACN/NRTR—2011/486. National Park Service, Fort Collins, Colorado.

Judge, S. W., R. J. Camp, P. J. Hart, and S. T. Kichman. 2018. Population estimates of the endangered Hawai‘i ‘Ākepa (*Loxops coccineus*) in different habitats on windward Mauna Loa. Journal of Field Ornithology 89(1):11–21.

Kaholoaa, R. L., C. N. Bailey, E. K. Kekiwi, K. K. Purdy, S. W. Judge, J. A. Tamayose, and C. J. Schwarz. 2019. Predator control management plan Haleakalā National Park. Natural Resource Report NPS/HALE/NRR—2019/2005. National Park Service, Fort Collins, Colorado.

Ka‘ū Forest Reserve Management Plan. 2012. State of Hawai‘i Department of Land and Natural Resources, Division of Forestry and Wildlife. https://dlnr.hawaii.gov/forestry/files/2013/02/Kau_FR_Mgnt_Plan_2012.pdf

Ka‘ū Preserve, Hawai‘i Island, Hawai‘i, Long-Range Management Plan, Fiscal Years 2013–2018. 2011. The Nature Conservancy- Hawai‘i Operating Unit. https://dlnr.hawaii.gov/ecosystems/files/2013/09/Kau-LRMP-FY13-18FinalDraft47.pdf

Kendall, S. J., R. A. Rounds, R. J. Camp, A. S. Genz, T. Cady, and D. L. Ball. 2024. Forest bird populations at the Big Island National Wildlife Refuge Complex, Hawai‘i. Journal of Fish and Wildlife Management 14(2):410–432.

Kirch, P. V. 1982. The impact of the prehistoric Polynesians on the Hawaiian ecosystem. Pacific Science 36(1):1–4.

Kirch, P. V. 2011. When did the Polynesians settle Hawai‘i? A review of 150 years of scholarly inquiry and a tentative answer. Hawaiian Archaeology 12:3–26.

LaPointe, D. A., M. L. Goff, and C. T. Atkinson. 2010. Thermal constraints to the sporagonic development and altitudinal distribution of avian malaria *Plasmodium relictum* in Hawai‘i. Journal of Parasitology 96(2):318–324.

Leopold, C. R., and S. C. Hess. 2017. Conversion of native terrestrial ecosystems in Hawai‘i to novel grazing systems: a review. Biological Invasions 19(1):161–177.

Loope, L. L., F. G. Howarth, F. Kraus, and T. K. Pratt. 2001. Newly emergent and future threats of alien species to Pacific landbirds and ecosystems. Studies in Avian Biology 22:291–294.

Marques, F. F. C., and S. T. Buckland. 2004. Covariate models for the detection function. Pages 31–47 *in* Advanced Distance Sampling (S. T. Buckland, D. R. Anderson, K. P. Burnham, J. L. Laake, D. L. Borchers, and L. Thomas, editors). Oxford University Press, Oxford, England, United Kingdom.

McClure, K. M., R. C. Fleischer, and A. M. Kilpatrick. 2020. The role of native and introduced birds in transmission of avian malaria in Hawai‘i. Ecology 101(7):p.e03038.

McKenzie, M. M., T. W. Giambelluca, and H. F. Diaz. 2019. Temperature trends in Hawai‘i: A century of change, 1917–2016. International Journal of Climatology 39(10):3987–4001.

Mountainspring, S., and J. M. Scott. 1985. Interspecific competition among Hawaiian forest birds. Ecological Monographs 55(2):219–239.

National Park Service. 2016. Hawai‘i Volcanoes National Park general management plan. https://www.nps.gov/havo/learn/management/upload/Hawaii-Volcanoes-General-Management-Plan_2016_508.pdf.

Olson, S. L., and H. F. James. 1982. Fossil birds from the Hawaiian Islands: evidence for wholesale extinction by man before Western contact. Science 217(4560):633–635.

Olson, S. L., and H. F. James. 1984. The role of Polynesians in the extinction of the avifauna of the Hawaiian Islands. Pages 768–780 *in* Quaternary Extinctions: A Prehistoric Revolution (P. S. Martin, and R. G. Klein, editors). University of Arizona Press, Tucson, Arizona.

Olson, S. L., and H. F. James. 1991. Descriptions of thirty-two new species of birds from the Hawaiian Islands: Part I. Non-Passeriformes. Ornithological Monographs (45):1–88.

Paxton, E. H., K. W. Brinck, L. H. Crampton, J. Hite, and M. Costantini. 2020. Kaua‘i forest bird population estimates and trends. Hawai‘i Cooperative Studies Unit Technical Report HCSU-098. University of Hawai‘i at Hilo.

Paxton, E. H., R. J. Camp, P. M. Gorresen, L. H. Crampton, D. L. Leonard, and E. A. VanderWerf. 2016. Collapsing avian community on a Hawaiian island. Science Advances 2:e1600029.

Paxton, E. H., P. M. Gorresen, and R. J. Camp. 2013. Abundance, distribution, and population trends of the iconic Hawaiian honeycreeper, the ‘I‘iwi (*Vestiaria coccinea*) throughout the Hawaiian Islands. U.S. Geological Survey Open-File Report 2013-1150, Reston, Virginia.

Paxton, E. H., M. Laut, S. Enomoto, and M. Bogardus. 2022. Hawaiian forest bird conservation strategies for minimizing the risk of extinction: Biological and biocultural considerations. Hawai‘i Cooperative Studies Unit Technical Report HCSU-103. University of Hawai‘i at Hilo, Hawai‘i.

Paxton, E. H., S. G. Yelenik, T. E. Borneman, E. T. Rose, R. J. Camp, and S. J. Kendall. 2018. Rapid colonization of a Hawaiian restoration forest by a diverse avian community. Restoration Ecology 26(1):165–173.

Pratt, L. W., and J. D. Jacobi. 2009. Loss, degradation, and persistence of habitats. Pages 137–158 *in* Conservation Biology of Hawaiian Forest Birds: Implications for Island Avifauna (T. K. Pratt, C. T. Atkinson, P. C. Banko, J. D. Jacobi, and B. L. Woodworth, editors). Yale University Press, New Haven, Connecticut.

Price, J., S. M. Gon III, J. D. Jacobi, and D. Matsuwaki. 2007. Mapping plant species ranges in the Hawaiian Islands: Developing a methodology and associated GIS layers. Hawai‘i Cooperative Studies Unit Technical Report HCSU-008. University of Hawai‘i at Hilo, Hilo, Hawai‘i.

Pyle, R. L., and P. Pyle. 2017. The birds of the Hawaiian islands: occurrence, history, distribution, and status. B. P. Bishop Museum, Honolulu, Hawai‘i. http://hbs.bishopmuseum.org/birds/rlp-monograph.

Price, J, P, J. D. Jacobi, L. W. Pratt, F. R. Warshauer, and C. W. Smith. 2009. Protecting forest bird populations across landscapes. Pages 381–404 *in* Conservation Biology of Hawaiian Forest Birds: Implications for island avifauna (T. K. Pratt, C. T. Atkinson, P. C. Banko, J. D. Jacobi, and B. L. Woodworth, editors). Yale University Press, New Haven, Connecticut.

Ralph, C. J., and S. G. Fancy. 1994. Timing of breeding and molting in six species of Hawaiian honeycreepers. Condor 96:151–161.

Ralph, C. J., and S. G. Fancy. 1996. Aspects of the life history and foraging ecology of the endangered ‘Akiapōlā‘au. Condor 98:312–321.

Reynolds, R. T., J. M. Scott, and R. A. Nussbaum. 1980. A variable circular-plot method for estimating bird numbers. Condor 82(3):309–313.

Samuel, M. D., P. H. F.Hobbelen, F. DeCastro, J. A. Ahumada, D. A. LaPointe, C. T. Atkinson, B. L. Woodworth, P. J. Hart, and D. C. Duffy. 2011. The dynamics, transmission, and population impacts of avian malaria in native Hawaiian birds: a modeling approach. Ecological Applications 21(8):2960–2973.

Sarr, Z., C. P. Stone, and N. P. Shema. 1997. Nesting success and population status of the ‘Elepaio (*Chasiempis sandwichensis*) in the Mauna Loa strip section of Hawai‘i Volcanoes National Park. Cooperative National Park Studies Unit Technical Report 112.

Scott, J. M., S. Mountainspring, F. L. Ramsey, and C. B. Kepler. 1986. Forest bird communities of the Hawaiian Islands: their dynamics, ecology, and conservation. Studies in Avian Biology No. 9. Cooper Ornithological Society.

Simon, J. C., T. K. Pratt, K. E. Berlin, J. R. Kowalsky, S. G. Fancy, and J. S. Hatfield. 2002. Temporal variation in bird counts within a Hawaiian rainforest. Condor 104(4):469–481.

State of Hawai‘i Department of Land and Natural Resources. 2023a. Environmental assessment for use of Wolbachia-based incompatible insect technique for the suppression of nonnative southern house mosquito populations on Kaua‘i. https://files.hawaii.gov/dbedt/erp/Doc_Library/2023-06-23-KA-DEA-Wolbachia-based-Suppression-of-Mosquitoes-on-Kauai.pdf.

State of Hawai‘i Department of Land and Natural Resources. 2023b. Draft Kapāpala koa canoe management area plan. https://dlnr.hawaii.gov/forestry/files/2023/03/Draft-Kapapala-Koa-Canoe-Management-Area-Plan-April-2023.pdf.

Thomas, L, S. T. Buckland, E. A. Rexstad, J. L. Laake, S. Strindberg, S. L. Hadley, J. R. B. Bishop, T. A. Marques, and K. P. Burnham. 2010. Distance software: Design and analysis of distance sampling surveys for estimating population size. Journal of Applied Ecology 47(1):5–14.

Tomich, P. Q. 1986. Mammals in Hawai‘i: a synopsis and notational bibliography. Bishop Museum special publication, 76.

Tweed, E., P. M. Gorresen, R. J. Camp, P. J. Hart, and T. K. Pratt. 2007. Forest bird inventory of the Kahuku unit of Hawai‘i Volcanoes National Park. The Pacific Cooperative Studies Unit Technical Report #143, University of Hawai‘i, Hilo, Hawai‘i.

U.S. Fish and Wildlife Service (USFWS). 2023a. ECOS environmental conservation online system. https://ecos. Fws. Gov/ecp/ (accessed on 14 May 2024).

U.S. Fish and Wildlife Service (USFWS). 2023b. Endangered and threatened wildlife and plants; removal of 21 species from the list of endangered and threatened wildlife. Federal Register 88(199):71644–71682.

VanderWerf, E. A. 2020. Hawai‘i ‘Elepaio (*Chasiempis sandwichensis*), version 1.0. In Birds of the World (P. G. Rodewald, editor). Cornell Lab of Ornithology, Ithaca, New York.

VanderWerf, E. A., M. D. Burt, J. L. Rohrer, and S. M. Mosher. 2006. Distribution and prevalence of mosquito-borne diseases in O‘ahu ‘Elepaio. The Condor 108 (4):770–777.

VanderWerf, E. A., R. E. David, P. Donaldson, R. May, H. D. Pratt, P. Pyle, and L. Tanino. 2018. First report of the Hawai‘i bird records committee. Western Birds 49(1):2–23.

van Riper, C., III, S. G. van Riper, M. L. Goff, and M. Laird. 1986. The Epizootiology and Ecological significance of malaria in Hawaiian land birds. Ecological Monographs 56(4):327–344.

Vaughn, N. R., R. F. Hughes, and G. P. Asner. 2023. Multi-scale remote sensing-based landscape epidemiology of the spread of rapid ‘Ōhi‘a Death in Hawai‘i. Forest Ecology and Management 538:120983.

Vizentin-Bugoni, J., C. E. Tarwater, J. T. Foster, D. R. Drake, J. M. Gleditsch, A. M. Hruska, J. P. Kelley, and J. H. Sperry. 2019. Structure, spatial dynamics, and stability of novel seed dispersal mutualistic networks in Hawai‘i. Science 364(6435):78–82.

Wagner W. L., D. R. Herbst, and S. H. Sohmer. 1990. Manual of the flowering plants of Hawai‘i, Vol. 1. Honolulu: Bishop Museum.

Warner, R. E. 1968. The role of introduced diseases in the extinction of the endemic Hawaiian avifauna. The Condor 70(2):101–120.

Witmer, G. W., and A. B. Shiels. 2017. Ecology, impacts, and management of invasive rodents in the United States. Pages 193–219 *in* Ecology and Management of Terrestrial Vertebrate Invasive Species in the United States (W. C Pitt, J. C. Beasley, and G. W. Witmer, editors). CRC Press, Boca Raton, Florida.

Wolfe, E. W., and J. Morris. 1996. Geologic map of the island of Hawai‘i. U.S. Geologic Survey IMAP I-252. https://doi.org/10.3133/i2524A.

Woodworth, B. L., C. T. Atkinson, D. A. LaPointe, P. J. Hart, C. S. Spiegel, E. J. Tweed, C. Henneman, J. LeBrun, T. Denette, R. DeMots, K. L. Kozar, D. Triglia, D. Lease, A. Gregor, T. Smith, and D. Duffy. 2005. Host population persistence in the face of introduced vector-borne diseases: Hawai‘i ‘Amakihi and avian malaria. Proceedings of the National Academy of Sciences 102(5):1531–1536.

Zheng, X., D. Zhang, Y. Li, C. Yang, Y. Wu, X. Liang, Y. Liang, X. Pan, L. Hu, Q. Sun, X. Wang, Y. Wei, J. Zhu, W. Qian, Z. Yan, A.G. Parker, et al. 2019. Incompatible and sterile insect techniques combined eliminate mosquitoes. Nature 572(7767):56–61.

# Appendix A. Hawai‘i Volcanoes National Park and Ka‘ū Forest Reserve Landbird Monitoring Field Report (2019)


## Abstract

The National Park Service Pacific Island Inventory and Monitoring Program (PACN), Hawai‘i Volcanoes National Park (HAVO), the State of Hawai‘i Department of Land and Natural Resources Division of Forestry and Wildlife (DOFAW), the Three Mountain Alliance, and The Nature Conservancy collaborated to conduct surveys in the Ka‘ū Rainforest of Hawai‘i Island. Surveys were conducted within the Kahuku Unit of HAVO, the Ka‘ū Forest Reserve (KFR), Kapāpala Forest Reserve, and the Kapāpala Cooperative Game Management Area. The effort accomplished the goals of surveying HAVO and KFR every 5 years.

A total of 11 permanently established legacy transects and 5 one-time-only randomly transects, totaling 488 stations were surveyed to monitor the landbird composition and status, and the composition and characteristics of the landbird habitat. PACN, HAVO, and DOFAW personnel established and maintained survey transects in January and February of 2019, prior to the landbird survey. Surveys for landbirds and habitat was conducted from 5 March through 18 April 2019. A total of 14 primary surveyors conducted surveys, which took place over 17 calendar days totaling 63 survey days. The transect preparation and maintenance required approximately the same effort in the field and there were several days of planning and training. Many of the transects required supply drops via helicopter to assist crews camping for multiple nights. This appendix documents the field effort and describes the logistical needs and considerations for future sample efforts in the Ka‘ū Rainforest.



## Acknowledgements

This large undertaking had multiple surveyors from many programs at State of Hawai‘i Division of Forestry and Wildlife (DOFAW), National Park Service (NPS), U.S. Fish and Wildlife Services (USFWS) and other agencies. We would like to thank the following surveyors from the Wildlife Program and Natural Area Reserve System: Jason Omick, Ian Cole, Lila Fried, Tom Dement, Josh Pang-Ching and Bret Mossman. Many thanks to Jermy Uowolo, Joe Kern, and Kalā Lindsey-Asing of the Mauna Kea Forest Restoration Project. Thanks to Laura Berthold, Chris Warren, and Kristi Fukanaga of the Maui Forest Bird Recovery Project. Thanks to our partners at USFWS: John Vetter, Steve Kendall, Rachel Rounds, and Eldridge Naboa. Special thanks to Colleen Cole of Three Mountain Alliance. Many thanks to Lester Gebin, Shalan Crysdale, and others from The Nature Conservancy who assisted with survey effort, site access, and logistics. Many thanks to Cari Lynn Squibb of the Hawai‘i Cooperative Studies Unit. Thanks to the volunteer efforts of Jacob Drucker. Special thanks to trail clearers and habitat surveyors who braved the elements in one of the most remote areas of Hawai‘i. Thanks for the support from Nick Agorastos of the State of Hawai‘i Natural Area Reserves System (NARS), and the following from DOFAW Operations: Jen Tietjen, Isaih Reynolds, Ron Miyahsiro, Jason Flemming, Damien Arcangel, Aaron Osorio, and Kristine “Chico” Mihara. Mahalo nui loa and hope to see many of you again in 5 years to repeat this survey!

## Introduction

The National Park Service Pacific Island Inventory and Monitoring Program (PACN) conducts landbird monitoring surveys in Hawai‘i Volcanoes National Park (HAVO) every five years. Surveys are conducted in eight separate tracts, each with discrete boundaries defined by elevation, habitat characteristics, and management units. The PACN Landbird Monitoring Protocol (hereafter, Protocol; Camp et al. 2011) described methods for conducting point-transect distance sampling and defined the survey schedule. The first PACN landbird survey was in 2010, when a team of three primary surveyors and three field technicians prepared transects and surveyed each of the eight tracts over a four-month period (Judge et al. 2011). To reduce the substantial effort, which required 5-6 people, the HAVO survey effort was split into two years. The Old HAVO tract group, which includes three tracts, was again surveyed in 2015, and the Kahuku Unit tract group, which includes five tracts, was surveyed in 2016. Survey results and transect logistics for both tract groups were detailed in Judge et al. (2017).

The Kahuku Tract, which is the largest monitoring tract in PACN landbird monitoring protocol, was surveyed by teams in 2010 and 2016. The tract lies primarily within the Ka‘ū Forest Reserve (KFR), with the top portions of permanently established Legacy Transects beginning within the HAVO Kahuku Unit (Figure 2). HAVO acquired the Kahuku Unit in 2003 and initiated landbird surveys in 2005, in partnership with the U.S. Geological Survey (USGS) Pacific Island Ecosystems Research Center (PIERC) and the University of Hawai‘i at Manoa Pacific Cooperative Studies Unit. Tweed et al. (2007) established and surveyed 25 transects in the Kahuku Tract in 2005. The Protocol prioritized five of those transects for PACN landbird monitoring. The numbering of the transects remained the same as the Tweed et al. (2007) designations.

The Division of Forest and Wildlife (DOFAW) conducts surveys irregularly in the Ka‘ū District of Hawai‘i Island. Many of the Ka‘ū transect locations and numbering were based off the initial Hawai‘i Forest Bird Survey (Scott et al. 1986). DOFAW coordinated and conducted Ka‘ū landbird surveys in 1993, 2002, and 2008, and those results were reported for the “Ka‘ū Region” by Gorresen et al. (2007) and Camp et al. (2009). DOFAW had intended to resurvey the Ka‘ū Region as early as 2013, but other management and survey needs elsewhere delayed the effort.

In 2019, DOFAW, PACN, the Three Mountain Alliance, and The Nature Conservancy collaborated to conduct surveys in the Ka‘ū Region and the Kahuku Tract. At approximately 35,000 hectares, the survey area is one of the largest native forests in the State of Hawai‘i. The survey area covered portions of HAVO, KFR, Kapāpala Forest Reserve (KPFR), and the Kapāpala Cooperative Game Management Area (KCGMA) and were collectively named the Ka‘ū Rainforest for this field report. PACN landbird monitoring adjusted their survey schedule for the collaborative survey effort by repeating most of the 2016 Kahuku Tract survey effort after 3 years instead of the scheduled 5 years. Many of the PACN legacy transects were relabeled and extended to align with HFBS transects. Those changes and specific transect logistics are detailed in this field report.

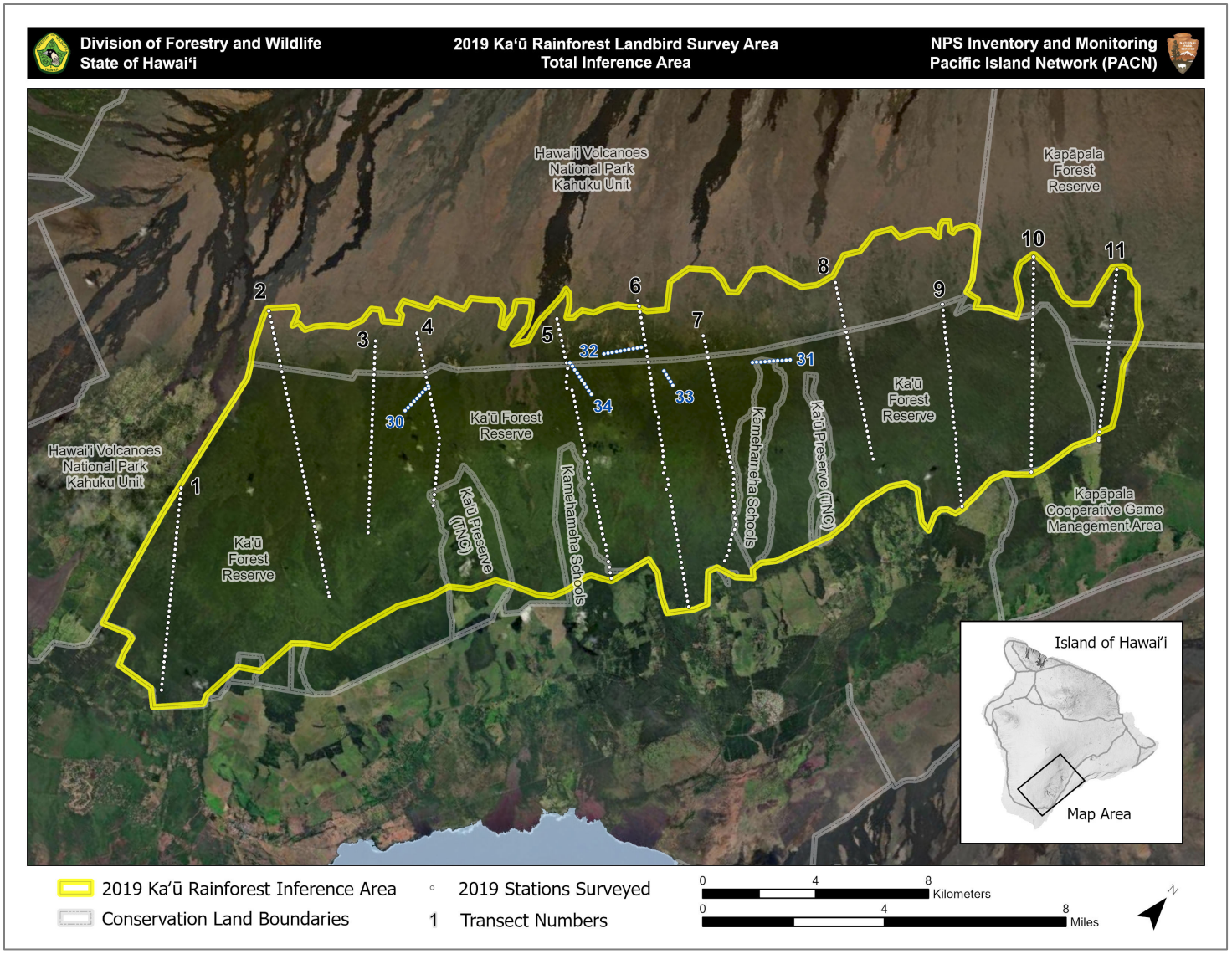



**Figure 2.** The 2019 Ka'ū Rainforest survey area and transects surveyed in 2019.

## Methods

### *Training*

Bird Identification

Training for bird identification and calibration for distance measurements were conducted according to the Protocol (Camp et al. 2011). Primary point counters had multiple years of experience counting birds and conducting avian research on the Island of Hawai‘i. Nevertheless, all of the field crews participated in the training and calibration to standardize bird identification and distance measurements. Training and calibration were conducted in HAVO and areas of Waiakea Forest Reserve. Additionally, most surveyors participated in annual point counts in the USFWS Hakalau Forest National Wildlife Refuge surveys coordinated by USFWS, Keauhou-Kulani Forest surveys coordinated by the Three Mountain Alliance, and the Mauna Kea surveys coordinated by DOFAW. During surveys, inexperienced point counters, or secondary counters, were paired with the primary counters and both discussed what was heard and seen after each count to facilitate species identification learning. Additionally, surveyors explored areas of HAVO where forest birds could be readily seen and heard. Common birds such as ‘Apapane (*Himatione sanguinea*), Hawai‘i ‘Amakihi (*Chlorodrepanis virens virens*), Warbling White-eye (*Zosterops japonicus*), and other common species were focused on until observers were comfortable identifying those species. Rarer species were then sought out in the field for observation. Surveys did not commence until each primary counter was confident of identifying birds visually and aurally.

Distance Measurement Training

In addition to bird identification, crews practiced estimating distances. Distance calibration training followed procedures detailed in the Protocol (Camp et al. 2011). Training for distance measurements was conducted repeatedly at sites with varying habitat characteristics on the Island of Hawai‘i. Between 6 and 30 strips of colored flagging were tied to objects about the station, typically trees, and each counter estimated the distance, in meters, from the station center-point to the flagging. The differences between the actual and estimated distance were calculated and recorded in field books. Calibration was continued until each crewmember obtained an accuracy of less than 10% difference between the actual and estimated distances for more than 80% of all measurements. It was important to practice distance measurements in a variety of habitats, such as open shrubland or dense forest. Distance measurements varied by habitat, thus requiring counters to make mental adjustments to accommodate for the surroundings. Surveyors also carried range finders in the field and spent a minute or two before each survey to familiarize themselves with the surroundings and gain accurate distances to trees or other features within the survey area.

Habitat Identification

Training for habitat data collection followed methods outlined in the Protocol (Camp et al. 2011). Each primary point counter had several years of field experience on the Island of Hawai‘i and already knew many of the dominant plants encountered in survey areas. Plant guides by Wagner et al. (1990) and others were used to accurately identify species in the field, and any unknown plants encountered in the field were not assigned a vegetation class. Surveyors were instructed to identify dominant or codominant plants to species within a 50-m radius of the survey station. If plots were

codominated by several species, surveyors could lump groups of canopy and understory species into broad native or non-native vegetation classifications (e.g., Native Trees, Native Ferns, Non-native Shrubs).

### *Field Preparation*

Field gear was purchased according to the Protocol (Camp et al. 2011) with minor exceptions and additions. Field equipment not itemized in the Protocol such as backpacks, rubber boots, rain pants, and rain jackets were purchased for crews or made available from collaborators. Essential camping gear was also purchased for extended stays in the field including kitchenware, camp stove, camp chairs, tarpaulins, white gas, propane, and lanterns. Surveyors were also provided with a measuring tape and range finder to assist with distance measurements.

### *Helicopter Assistance*

Transect maintenance crews and surveyors were shuttled to the top of Transects 8, 9, and 10 because of the remoteness of those areas. Because most of the helicopter operations were in the early morning hours, surveyors were able to commence the survey soon after they landed. Transect maintenance crews and surveyors were supplied water, flagging, and some food near the middle of most of the transects. Those details and transect logistics are described in the transect description section below.

### *Transect and Station Maintenance*

All PACN legacy transects and stations were established for long term monitoring during the field season of 2010 (Judge et al. 2011). Flagging was refreshed during the 2016 survey effort and again in 2019. No flagging was placed on randomly prescribed landbird transects. Blue flagging marked the length and path of transects. Orange flagging was placed approximately 5 and 10 m away from the station to prevent surveyors from accidentally missing the station. In 2010, stations on legacy transects were marked with a 1 m length of ¾ inch PVC pipe with a metal tag indicating transect and station number as prescribed in the Protocol (Camp et al. 2011). PVC poles were still in good condition in 2016 and 2019.and only pink flagging was added to each pole and the nearest tree. Stations that extended past the PACN established transects were not marked with a pole but with pink flagging, an aluminum station tag denoting transect and station number, and the orange "warning" flags.

Transects were navigated using Global Positioning Systems (GPS) units and magnetic compasses as prescribed in the Protocol (Camp et al. 2011). When establishing new transects and stations, crews found it more accurate to keep transects straight in closed canopy forests by reading the bearing in degrees from the GPS and then following that bearing using a magnetic compass. The Garmin 60CSX units typically had an accuracy of 3 to 6 meters, depending on canopy, weather, and satellite coverage. Random stations were surveyed as close as possible to the GPS waypoint.

### *2019 Transect Relabelling and Realignment*

As part of the PACN Landbird Monitoring protocol to survey the Kahuku Tract, five legacy transects were permanently established during the intitial effort in 2010 (Judge et al. 2011). Legacy Transects 7, 12, 17, and 22 were relabeled to coincide with the Hawai‘i Forest Bird Survey (HFBS) transect numbers (Table 21), and the landbird monitoring database was updated to reflect these changes.

**Table 21.** PACN legacy transect numbering in the Kahuku Tract during the 2010 and 2016 landbird monitoring surveys and the new relabeled numbers updated during the 2019 survey. These changes will be adopted by the PACN landbird monitoring protocol for future PACN surveys and/or DOFAW surveys.

| PACN (2010–2016) Legacy Transect Number | 2019 Kaʻū Survey Relabeled Number |
|---|---|
| 2 | 2 |
| 7 | 4 |
| 12 | 5 |
| 17 | 7 |
| 22 | 8 |

### *Data Collection*

Point-transect distance sampling methods were used to survey landbirds and followed techniques described in the Protocol (Camp et al. 2011). Surveys were conducted at sampling stations established on transects. Stations were spaced either 150 or 200 m apart depending on location or the transect type (legacy or random). All birds seen or heard at each station were recorded during an 8-minute sampling period. The species, method of detection, and distance between observer and bird, measured to the nearest meter, were recorded. Rounding of measurements to the nearest 5 or 10 m was strictly avoided to eliminate "heaping." Unnecessary noise and movement were avoided during counts to prevent altering bird behavior. Binoculars were used to facilitate species identification and rangefinders were used to accurately estimate distances to detection. Counts were temporarily stopped during wind gusts >6 on the Beaufort scale or disturbances (e.g., helicopters, barking dogs, power tools). There were no differences between the Protocol prescribed and applied sampling methods.

Habitat data were collected as described in the Protocol (Camp et al. 2011). Surveyors reviewed plant guides to identify species or families in the field. Each primary counter also had several years of field experience on the Island of Hawaiʻi and already knew many of the dominant plants encountered in the landbird monitoring tracts.

### *Survey Area*

Kahuku Tract of Hawaiʻi Volcanoes National Park

The Kahuku Tract was the largest of the eight PACN landbird monitoring tracts and the only PACN tract surveyed in 2019. Five legacy transects totaling 93 stations and 5 random transects were surveyed during the 2010 and 2016 landbird surveys. Transects were approached at higher elevations inside HAVO by the upper Kahuku Road (refer to Transect Logisitcs and Descriptions below for more details).

The tract was accessed through the lower HAVO Kahuku Unit gate off Highway 11 between the 70 and 71-mile markers. Field operations were based out of the Nēnē Cabin or CCC Cabin, approximately an hour and half drive past the lower Kahuku gate. The Nēnē cabin was small with three bunks so some of the crew slept outside in tents. The CCC Cabin was larger and more ideal for

large field crews. Both cabins were outfitted with a propane stove and some utensils, the crews brought all other camping gear including potable water and cookware. The cabins were reserved through the HAVO Kahuku Unit Manager, usually in coordination with the Three Mountain Alliance (TMA) who used the CCC Cabin often. It was important to coordinate to avoid interfering with HAVO Resource Management hunters during the control effort of invasive ungulates. Fieldwork was prohibited during hunting activities for safety concerns.

The transects in the Kahuku Tract were long and difficult to walk, especially the lower halves of the transect where vegetation was thick and impeded navigation. Kanawao (*Hydrangea arguta*) was especially dense in areas of the KFR. In 2010 and 2016, surveyors would double-back on the transect to return to the road for pickup. In 2019, crews continued down the transects to survey the lower portions of KFR and required multiple days to survey. Crews rarely finished their daily duties in under eight hours and occasionally were unable to finish the transect before 11 am. The road up to and past the Nēnē cabin required a 4x4 truck and was very slow going.

Kamehameha Schools Land Assets Division

Approximately 1,200 ha of Kamehameha Schools Land Assets Division (KS) properties fell within the 2019 landbird survey area, which included three separate parcels: Punaluʻu, Mohokea, and Pāʻauʻau. Each of the parcels were managed for agriculture (https://www.ksbe.edu/aina/), but the parcels were ʻōhiʻa (*Metrosideros polymorpha*) dominated with eucalyptus (*Eucalyptus* spp.) plantations near the lower survey area boundary. The parcels were near Transect 5 and Transect 7. Access to KS land requires permission from the Land Assests Division, which can be time consuming and the result uncertain. Thus, access to those areas was avoided, and the bearing of Transect 7 was altered to remain within KFS boundaries, just outside of the KS parcel.

Kapāpala Forest Reserve

KPFR, at 15,085 ha, was established in 1930, and supports public access for birdwatching, hiking, and hunting. The top sections of Transect 10 and Transect 11 lie within the reserve. In 2019, access was via helicopter or vehicle through Kapāpala Ranch. Specific roads and field logistics are described at length in the Transect Logistics and Descriptions sections below.

Kapāpala Cooperative Game Management Area

The Kapāpala Cooperative Game Management Area (KCGMA) is a lease agreement with State of Hawaiʻi's Department of Land and Natural Resources (DLNR) and Kapāpala Ranch, the ranch being the lessee of the ~9,700-ha state parcel. KCGMA is located adjacent to HAVO and KFR and managed for bird hunting and ranching. The bird hunting season extends from the first Saturday of November through the last weekend of January with hunting permitted on weekends and holidays. KCGMA supports six species of game birds: Erckel's Spurfowl (*Pternistis erckelii*), Kalij Pheasant (*Lophura leucomelanos*), California Quail (*Callipepla californica*), Zebra Dove (*Geopelia striata*), Spotted Dove (*Spilopelia chinensis*), and Wild Turkey (*Meleagris gallopavo*). The Common Pheasant (*Phasianus colchicus*) and Chukar Partridge (*Alectoris chukar*) have been reared and released when available. DOFAW manages seven water guzzlers for game bird, removes predators, and improves habitat by mowing and mulching areas important for game birds. Access is coordinated with ranch managers to allow access through two gates off Highway 11. Being an active ranch, the

area provides many four-wheel drive roads, which surveyors used to access Transect 11, and consideration to livestock is essential. Specific roads and field logistics are described at length in the "Transect Logistics and Descriptions" sections below.

Ka‘ū Forest Reserve

KFR is one of the largest reserves in the state of Hawai‘i, and at 24,945 ha, the reserve dominates the forested southeast region of Mauna Loa. Established in 1906, the reserve maintains water supply for agricultural lands and communities in the Ka‘ū District (Ka‘ū Forest Reserve Management Plan 2012). Approximately 4,900 ha are fenced and prioritized for the protection of rare native plants and animals through invasive species control. In 2015, TMA installed a fence to enclose the 810-ha Hō‘ili Wai Unit in the upper portions of KFR near Transect 5 and Transect 6. Plans to enclose an additional 4,000 ha were initiated and, as of 2023, the effort is still ongoing. Ungulate control usually coincided with fencing efforts.

TMA bases field efforts from the CCC cabin, which served for an important field site for the 2019 survey. Field crews accessed the top sections of transects through the HAVO Kahuku Unit via 4x4 vehicles or helicopter. Crews were extracted from the lower sections of transects via 4x4 vehicles from public roads including Lorenzo Road, Kiolaka‘a Road, Mountain House Road, Waterfall Road (known as Galimba access at Pu‘u One), Honanui Road, and ‘Āinapō Road. ‘Āinapō and Honanui roads have locked gates and permission for access was arranged with Kāpapala Ranch. Specific roads and field logistics are described at length in the Transect Logistics and Descriptions sections below.

Ka‘ū Preserve

The Nature Conservancy's (TNC) Ka‘ū Preserve consists of four separate units that are adjacent to KFR. Only portions of the Kaiholena, Keaīwa, and Kāhilipali Units fell within the 2019 survey area. The Kāhilipali Unit is just outside the survey area and was not included for inference. Surveyors and field crews coordinated with the TNC office in the Ka‘ū District to coordinate extraction from the bottom of Transect 4, which was near the top section of the Kaiholena Unit (discussed below). Refer to the "Ka‘ū Preserve, Hawai‘i Island, Hawai‘i, Long-Range Management Plan, Fiscal Years 2013–2018" for more details regarding each unit and management objectives.

### *Transect Logistics and Descriptions*

Transect 1

Transect 1 at 37 stations long was entirely within KFR boundaries. Station 1 began approximately 80 m from the HAVO boundary (Figure 2). The transect closely aligned with aspect and station positions to the original HFBS and subsequent surveys. The top of the transect was accessed through the HAVO Kahuku gate, which is between mile markers 70 and 71, off Highway 11 (a.k.a. Mamalahoa Highway). Transect maintenance crews and surveyors were dropped off via vehicle on 4x4 roads within the "Lower Kahuku Paddocks" by permission from HAVO managers. The transect required two nights and three days to cut and flag. The survey was conducted on a separate effort and also required two nights and three days. The transect ended near the DOFAW Kioloka‘a Cabin, a short hike from station 37 (Figure 3).

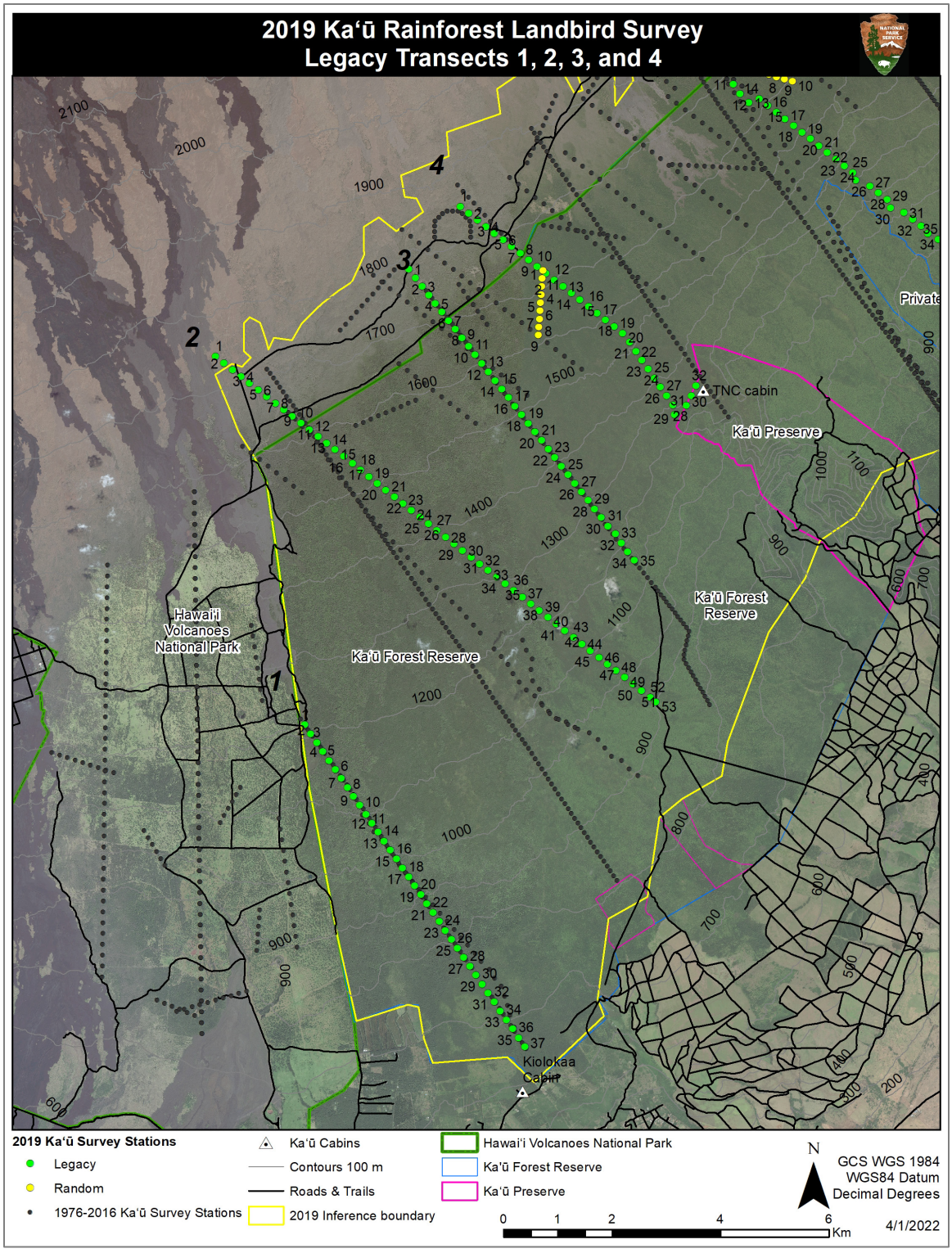



**Figure 3.** Legacy transects 1, 2, 3, and 4 and stations surveyed during the 2019 Ka‘ū Rainforest landbird survey (in green). Yellow stations indicate the one-time-only random transects prescribed in 2019.

Transect 2

Transect 2 began within HAVO and extended 53 stations down into KFR. The first 17 stations of the transect were surveyed by the PACN Landbird Monitoring project in 2010 and 2016. In 2019, the aspect of the transect and station positions were realigned from the HFBS alignment and the transect was extended to total 53 stations (Figure 3). The transect was accessed through the HAVO Kahuku entrance off Highway 11. An approximate one-hour drive led up to the Upper Kahuku Road to the transect near Station 10. One group of surveyors could survey uphill from the road to survey stations 1 through 10 in a day. Surveyors working down the transect from Station 11 would need to backpack overnight. Stations 1–17 were regularly maintained, but the transect needed flagging and trail cutting from stations 18 through 53, an effort that required one night of camping and two full days of transect maintenance. The bird survey also required two nights of camping to survey stations 10 through 53. In 2019, surveyors departed Hilo early in the morning to have time to reach Station 10 and survey that same day. The top 9 stations were surveyed opportunistically. The transect ended near the Mountain House Road where maintenance crews and surveyors were extracted by vehicle (UTM:  5Q 225126 2117956; Figure 4).

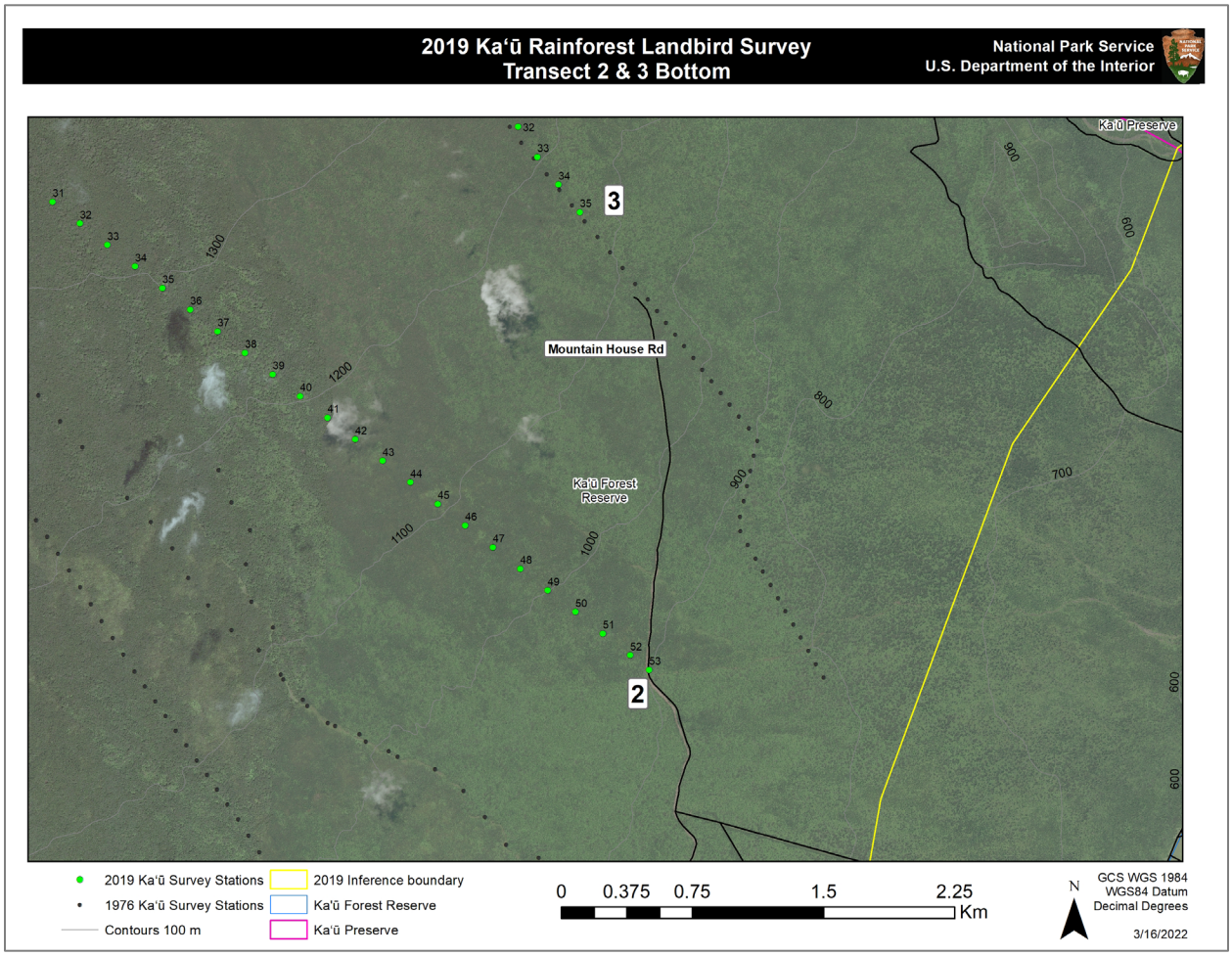



**Figure 4.** Exit routes for the bottom of Transect 2 and Transect 3 within the Ka'ū Forest Reserve.

Transect 3

Transect 3 began within HAVO and extended 37 stations down into KFR (Figure 2). The transect was positioned near the original HFBS locations and was not previously surveyed by PACN. The transect was accessed through the Kahuku entrance, and the Upper Kahuku Road crossed the transect between Stations 6 and 7. In 2019, surveyors drove to the CCC cabin and stayed the night there. They started the survey the next morning on Station 7 and Stations 1–6 were surveyed opportunistically later. Surveyors camped on the transect and completed the survey on a second field day. The transect ended 180 m from the Mountain House Road (UTM: 5Q 225045 2120081; Figure 3). Cutting and flagging the transect required a similar plan, where a team camped one-night mid-way down the transect. The top portion of the transect was flagged during a separate training effort.

Transect 4

PACN Legacy Transect 7 was renamed to Transect 4 in 2019. The 20 station long transect was surveyed by the PACN Landbird Monitoring project in 2010 and 2016. In 2019, the transect was extended down through KFR to the TNC Preserve Boundary (Appendix A–Figure 2). At Station 21, the aspect of the transect was redirected to lengthen the transect and facilitate exit. Surveyors cut and surveyed the transect in the same effort and redirected Stations 30–32 in a Northeast direction following the TNC Preserve boundary (Figure 4). Prior to the survey, water and supplies were dropped near Station 25, where surveyors camped and accessed the supplies. From Station 32, the surveyors hiked down a short trail to a TNC Cabin, where they overnighted and hiked to where they were picked up by vehicle. The lower half of the transect was difficult to cut and survey because of dense uluhe (*Dicranopteris linearis*), which caused the 2019 team to redirect the transect and camp an additional night at the TNC Maka‘alia Cabin (Appendix A–Figure 4).

Transect 5

PACN Transect 12 was renamed to Transect 5 following HFBS numbering. The PACN legacy transect was 21 stations long and was surveyed and maintained in 2010 and 2016. In 2019, the transect was extended an additional 27 stations to a total of 48 total stations (Figure 5). The transect started within HAVO with Station 1 approximately 570 m southwest from the Nēnē cabin. The CCC cabin was approximately 200 m northeast from Station 6. The transect crossed through the fenced Hō‘ili Wai on KFR which is managed by TMA. Prior to the survey, a maintenance crew cut and flagged the transect over a three-day period. Water and supplies were dropped via helicopter near Station 27, where both the maintenance crew and surveyors camped. Initially prescribed at 46 stations, two more stations were added in 2019, which allowed surveyors to finish closer to “Clouds Rest Road,” where they were extracted via 4x4 vehicle.

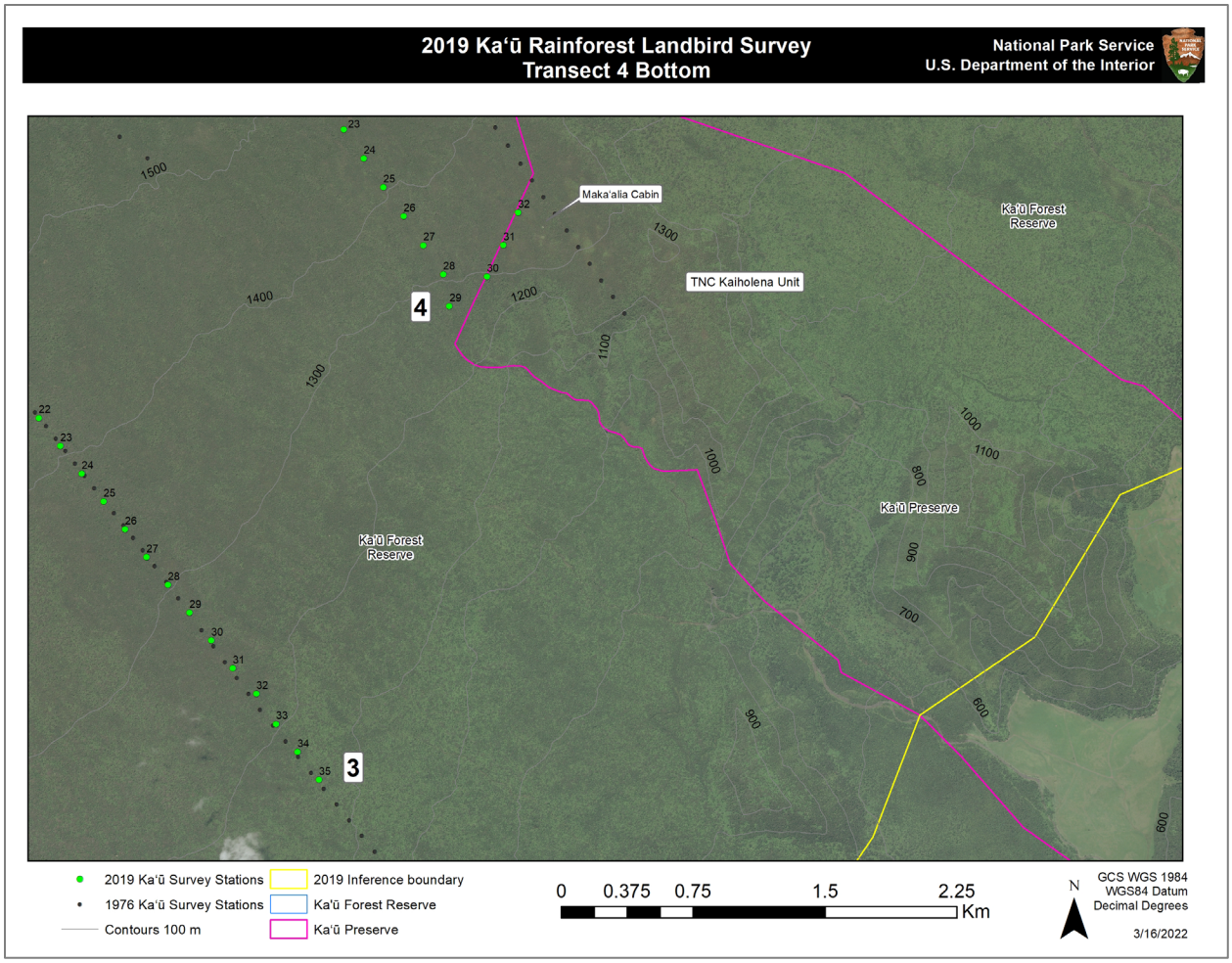



**Figure 5.** Exit route for Transect 4 and The Nature Conservancy Kaiholena Unit Preserve. Surveyors changed direction of the transect to intersect the Ka‘ū Forest Reserve and Kaiholena Unit fenceline. Surveyors then continued to the Maka‘alia Cabin and exited the preserve along the fenceline to a small parking area within the unit.

Transect 6

Transect 6 was positioned in the same aspect as the original HFBS transect and many stations were closely located. At 56 stations long Transect 6 was one of the longest transects surveyed in 2019 (Figure 5). It required a substantial effort to flag and clear because there was no existing flagging. The transect began within HAVO in mixed lava and open canopy woodland. Station 1 was adjacent to the Upper Kahuku 4x4 road, which was approximately a 20-minute drive past the CCC cabin. The first 11 stations were within HAVO, with Station 12 just beyond the KFR/HAVO boundary. Water and supplies were dropped via helicopter close to the Hō‘ili Wai fence line near Station 23 (UTM: 5Q 230118 2130179) where maintenance and survey crews camped and accessed supplies. Both maintenance and survey crews required two nights of camping to finish the effort. Crews exited the transect from Station 50 via “George’s Trail” which started closer to the bottom of Transect 7 on private land (Figure 6).

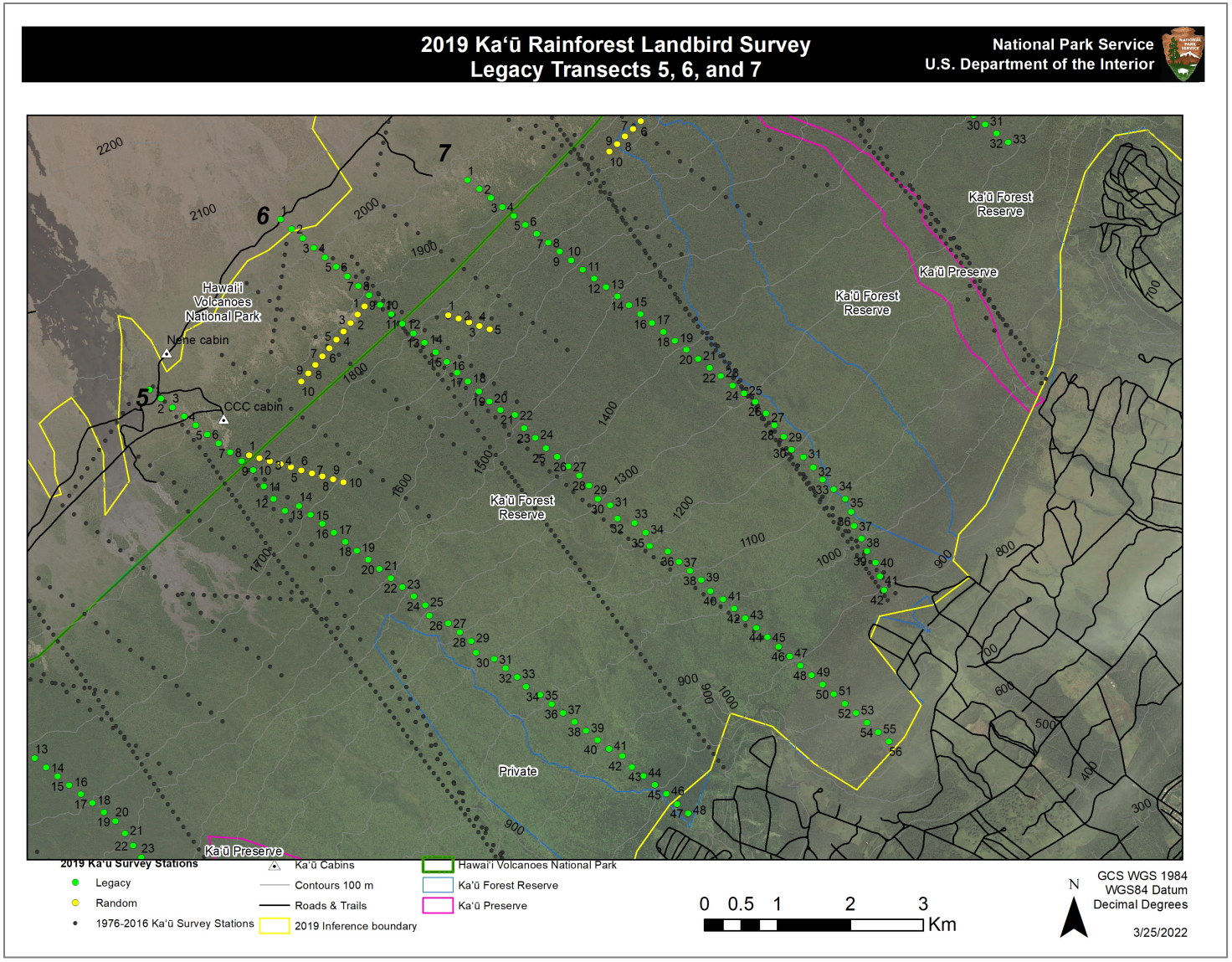



**Figure 6.** Transects 5, 6, and 7 and stations surveyed during the 2019 Ka‘ū Rainforest landbird survey (in green). Yellow stations indicate the one-time-only random transects prescribed in 2019.

Transect 7

PACN Transect 17 was renamed to the HFBS Transect 7 for continuity. The PACN legacy transect was 12 stations long and was surveyed and maintained in 2010 and 2016. The PACN transect did not align with the original HFBS transect, which started more to the northeast (Figure 5). Only four stations were within the HAVO boundary, with Station 5 positioned within KFR approximately 60 m from the boundary fence. Transect 7 intersected the original HFBS stations near Station 26, where we adjusted the aspect slightly so it would align more closely with the original HFBS station locations. The transect consists of 42 stations. Maintenance and survey crews each needed two nights of camping on the transect to finish the effort. Water and supplies were dropped off via helicopter near Station 24. Crews exited Transect 7 at Station 42, by proceeding 55 m at bearing of 211 degrees to the pickup near the start of George's Trail (Figure 6).

Transect 8

PACN Transect 22 was renumbered Transect 8 for continuity (Figure 7). Stations 1 through 25 were maintained and surveyed by PACN in 2010 and 2016. In 2019, the transect was extended to a total of 36 stations. Stations 1 through 9 fell within HAVO and the remaining stations were within KFR. The top of the transect was accessed via the rough 4x4 road that continued past the Nēnē cabin. In 2019, the bird surveyors were shuttled to the top of the transect via helicopter with operations coordinated for Transects 9 and 10. The maintenance crew flagged and cleared to Station 28. The survey crew flagged and cleared the remainder of the transect and conducted the survey over two days. They camped near Station 30 where water and supplies had been dropped via helicopter. Surveyors stopped counting at Station 33 and exited the transect at Station 36 by traversing to a KFR trail that meandered south and connected to two bridges and a parking area that could be accessed from the Ka‘ū Coffee Mill (Figure 8).

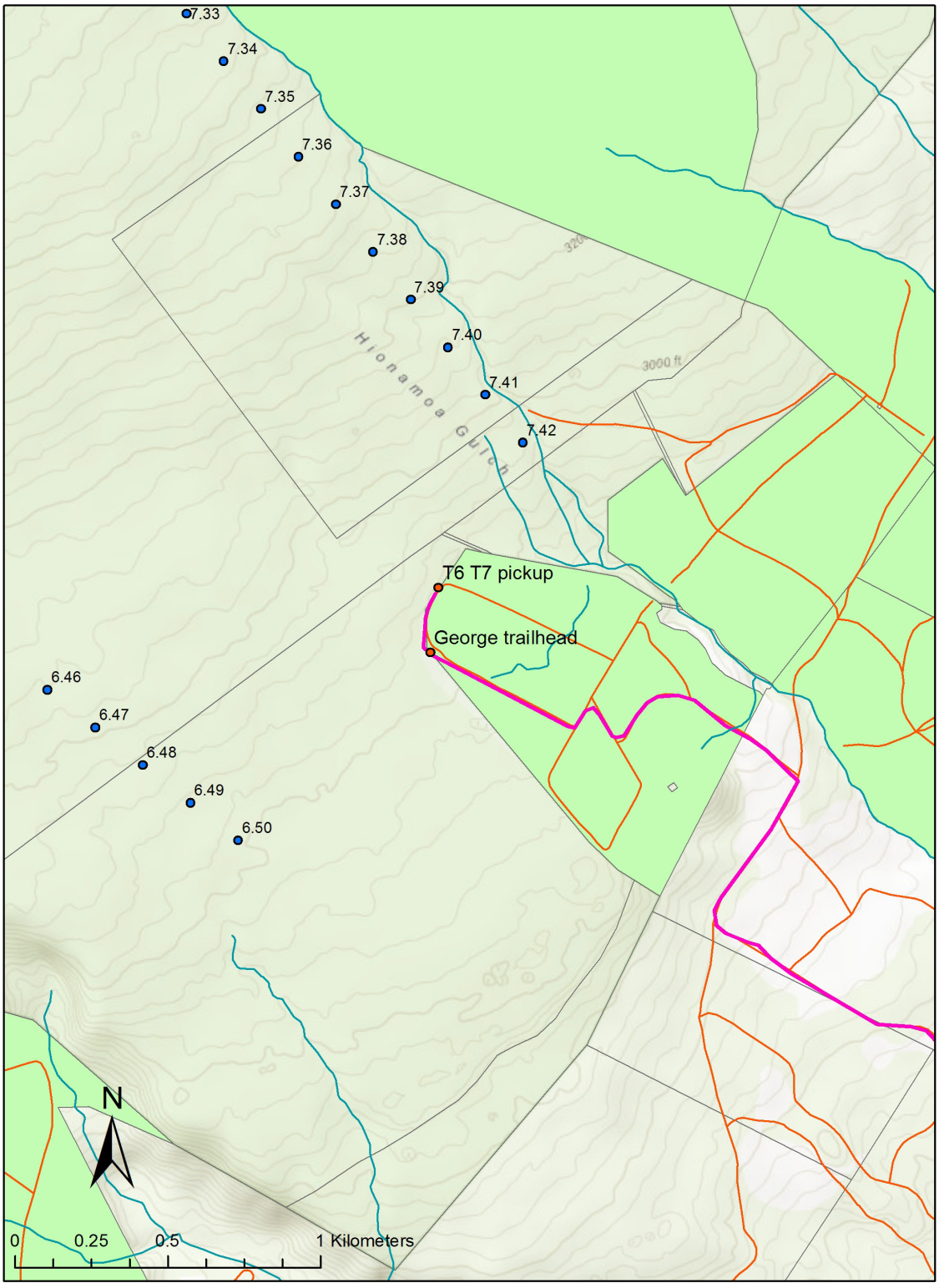



**Figure 7.** Exit routes for Transect 6 and Transect 7 surveyed in 2019. Surveyors and maintenance crews on either transect were extracted from a parking area near “George‘s Trail”.

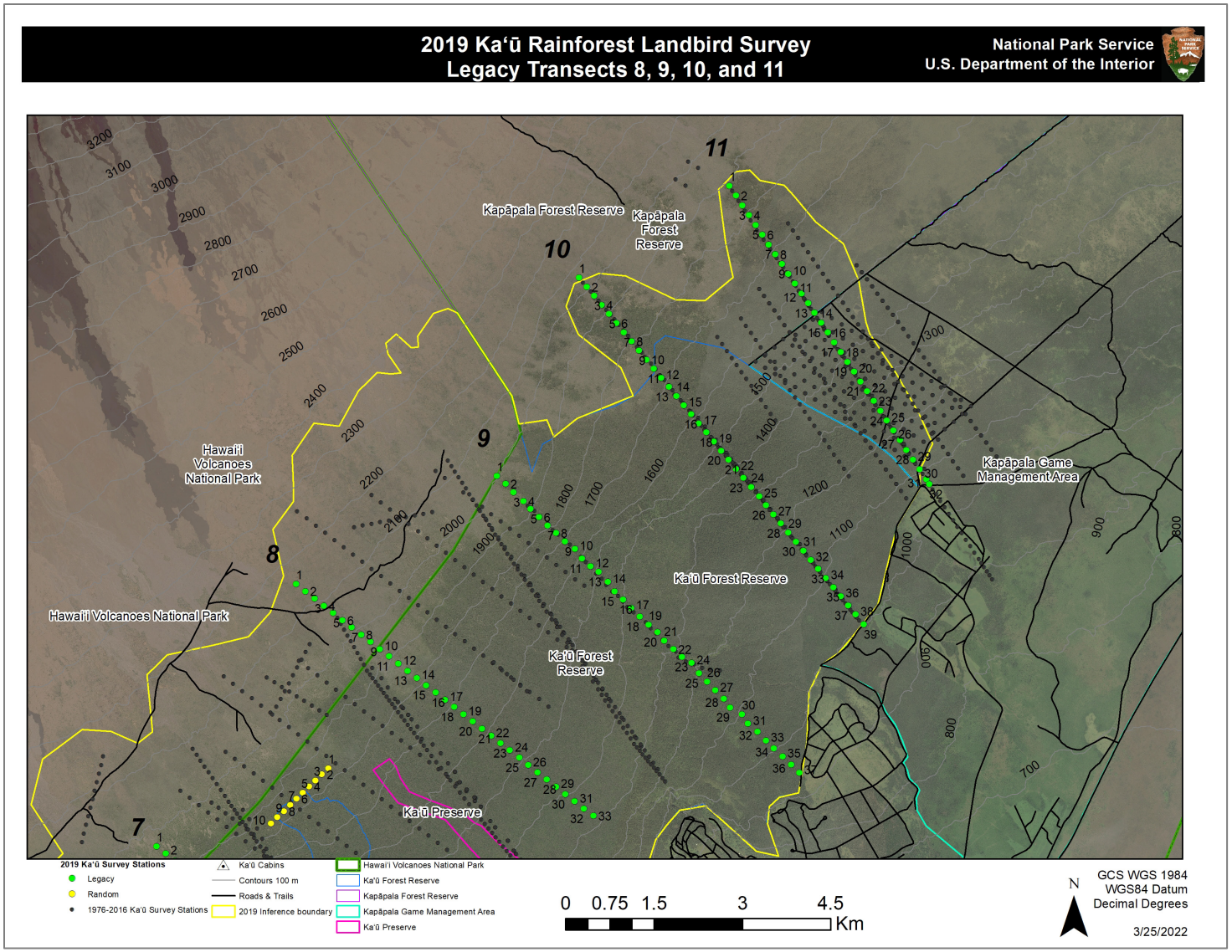



**Figure 8.** Ka‘ū Rainforest Transects 8, 9, 10, and 11 and stations surveyed in 2019 (in green). Yellow stations indicate the one-time-only random transects prescribed in 2019.

Transect 9

Transect 9 was newly established, flagged, and surveyed in 2019. The station positions and aspect of transect aligned closely with the original HFBS Transect 9 and subsequent surveys. At 37 stations long, the entire transect fell within KFR with Station 1 positioned close to the KFR/HAVO boundary (Figure 7). The top of the transect was remote and required helicopter transport to shuttle maintenance and survey crews to a landing zone near Station 1. Water and supplies were dropped off prior to the survey near Station 23 (UTM:  5Q 238222 2136621). Transect maintenance and surveying both required two nights camping on the transect. Crews exited the transect from Station 37 (refer to instructions on Appendix A–Figure 9, Figure 10).

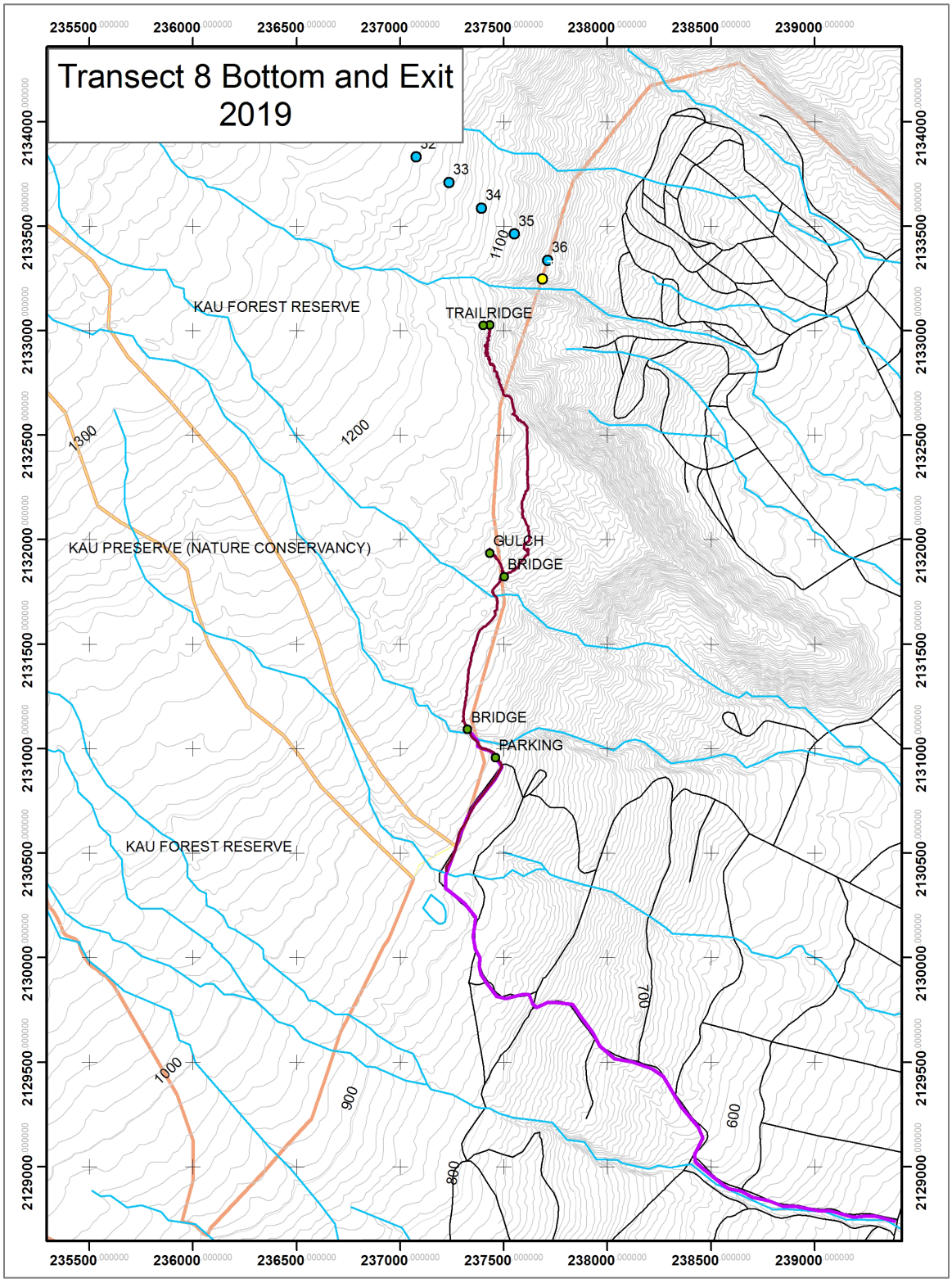



**Figure 9.** Exit route of Transect 8 surveyed in 2019. UTM axes are provided for reference.

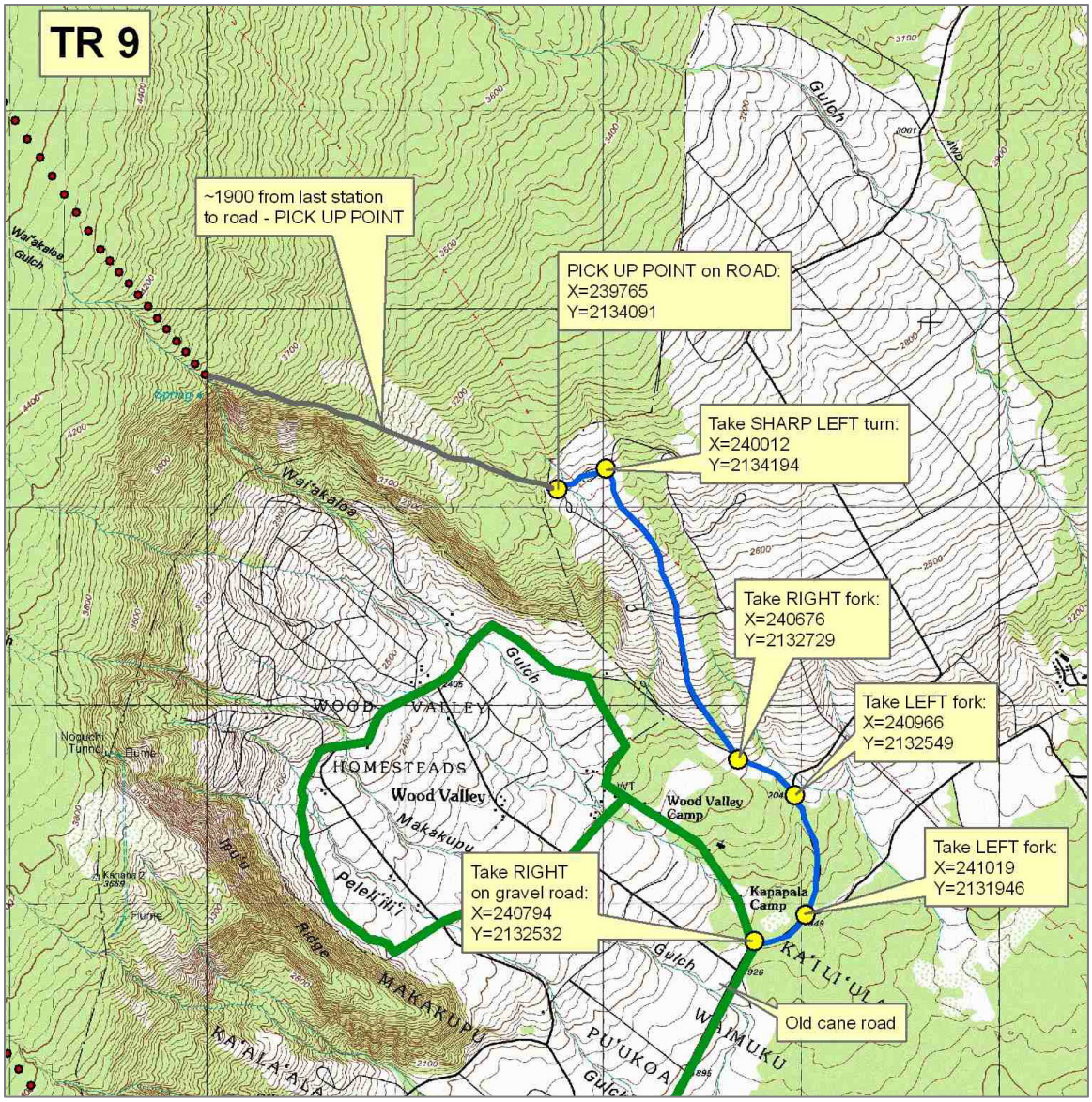



**Figure 10.** Access and exit routes of Transect 9 surveyed in 2019.

Transect 10

Transect 10 was newly flagged and surveyed in 2019. Most station positions and the aspect of transect aligned closely with the original HFBS survey and subsequent surveys (Figure 7). The first 10 stations fell within KPFR and then it continued into KFR and ended at Station 39. Water and supplies were dropped off prior to the survey near Station 22 (UTM: 5Q 238803 2140283). Transect maintenance and surveying both required two nights camping on the transect. Crews exited the transect from Station 39 (refer to instructions on Figure 11).

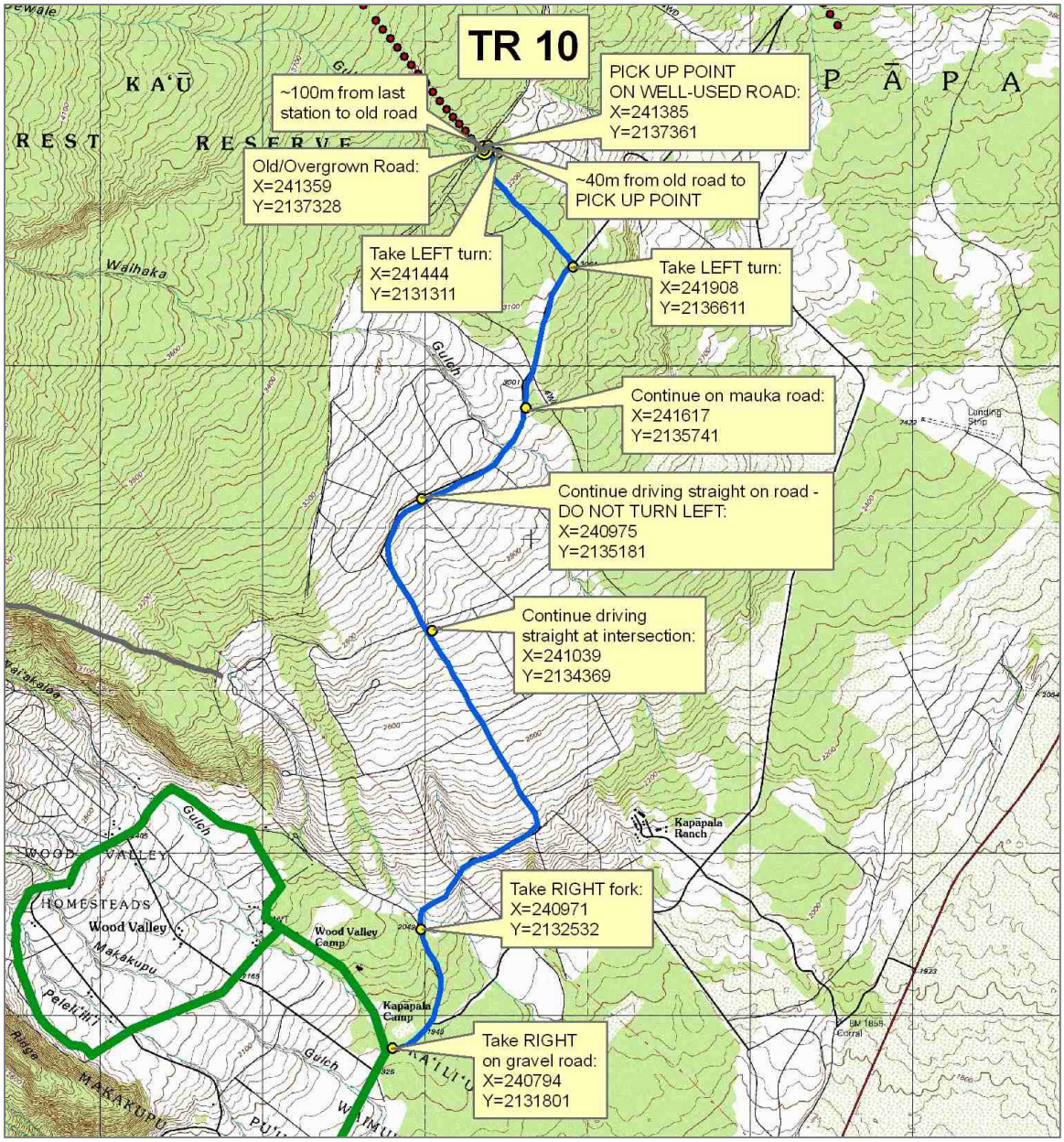



**Figure 11.** Access and exit routes of Transect 10 surveyed in 2019.

Transect 11

Transect 11 was newly cut and flagged in 2019. Most station positions and aspect of transect aligned closely with the original HFBS survey and subsequent surveys (Figure 7). The first 14 stations fell within KPFR. The transect continued into the KCGMA and continued to Station 32. The transect was flagged and brushed during bird and habitat surveys. The transect was accessed through the Kapāpala Ranch gate off Highway 11 via a 4x4 road that traversed the KFR and KCGMA boundary, crossing the transect near Station 14. Surveyors surveyed uphill to Station 1 and then returned to the vehicle. Surveys proceeded downhill from Station 14 into KCGMA. The transect crossed 4x4 roads near Stations 25 and 30 and can be exited from Station 32 by traversing southeast to another access road.

Random Transects

Five randomly prescribed transects were surveyed in 2019. The transects were numbered 30 through 34 (Figure 2). One transect fell within the HAVO boundary and the remaining were within KFR. Transects were not prepped before the surveys and surveyors required one day to access, survey, and exit each transect.

## Summary

The 2019 Kaʻū Rainforest Survey was conducted safely and efficiently. The transects and permanent stations were marked clearly with flagging following Protocol procedures. It should be noted that flagging often degrades in windy and sunny conditions and crews should expect to replace flagging on subsequent surveys. To maintain the every 5-years survey schedule, the Kaʻū Rainforest survey would be repeated in 2024.The PACN 5-year survey schedule was adjusted for just the Kahuku Tract, which was surveyed in 2016 and again in 2019, which normally would have been surveyed in 2021, along with the four other monitoring tracts within the Kahuku Unit (Judge et al. 2017). We anticipate that the Kahuku Tract will be surveyed subsequently on the adjusted schedule as to coincide with the larger Kaʻū Rainforest survey in 2024, provided DOFAW and partners have the available resources to do so. It is expected that the next Kaʻū Rainforest survey will require less effort because of the 2019 transect preparation and survey.

# Appendix B. Methods for Determining Inference Area of Range Restricted Species

### Kaʻū Rainforest Survey Area

The upper bounds of the Kaʻū Rainforest survey area were defined primarily by transect location and vegetation classes described by the Pacific Island Inventory and Monitoring Program (PACN) vegetation mapping project (Green et al. 2015). Within Hawaiʻi Volcanoes National Park (HAVO), the highest stations range between elevations of 1,800 m to approximately 2,150 m (Figure 12). The HAVO transects primarily lie within montane woodland, which Green et al. (2015) described as open canopy (20–50% cover) *Metrosideros polymorpha* (hereafter: ʻōhiʻa) with a predominate shrub cover of *Leptecophylla tameiameiae* and *Dodonaea viscosa*, and to a lesser extent *Coprosma* spp., *Vaccinium* spp., and *Myrsine sandwicensis*. Montane woodland supports several species of Hawaiian landbirds, including relatively high densities of Hawaiʻi ʻĀkepa (*Loxops coccineus;* Judge et al. 2018). The upper edges of montane woodland are bordered by bare lava, montane dry shrubland, and sparsely vegetated subalpine shrubland, which offer minimal forest bird foraging opportunities and are not important breeding habitat due to the absence of ʻōhiʻa and koa (*Acacia koa*). These areas were excluded for abundance estimates unless these classes were interspersed within larger vegetation classes predominated by ʻōhiʻa. The western boundary of the inference area followed the HAVO park boundary, starting near 750-m elevation and extending in a nearly straight line to the top of the montane woodland edge near Station 3 on Transect 2 at approximately 1,750-m elevation (Figure 12). The upper edge boundary then roughly contours the montane woodland in a northeast direction approximately 25 km to the HAVO and KFR boundary near 2,350-m elevation, where it then descends along the boundary to the edge of the closed ʻōhiʻa vegetation class described by Jacobi (1989). The eastern edge then extends around Transect 11 and includes areas that were surveyed in 1993. The lower edge then continues to trace the closed ʻōhiʻa forest edge and the boundary between Kaʻū Forest Reserve (KFR) and Kapāpala Forest Reserve (KPFR) The lower edge follows the forest-agriculture boundary or bottom of the transects, avoiding privately owned properties composed of disturbed ranchland and plantations.

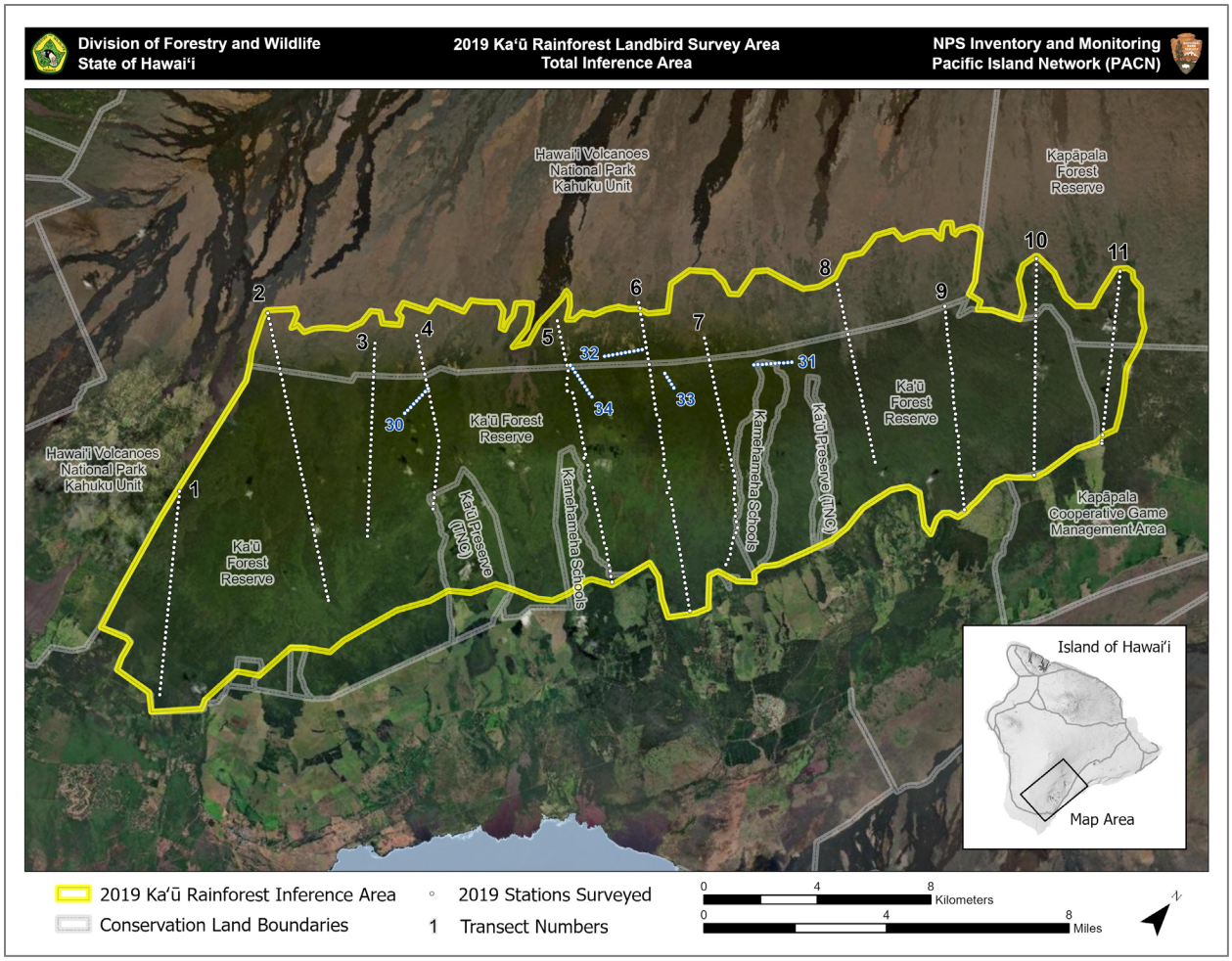



**Figure 12.** The 2019 Ka‘ū Rainforest landbird survey inference area.

## ‘Akiapōlā‘au Range

The range of ‘Akiapōlā‘au (*Hemignathus wilsoni*) in the Ka‘ū Rainforest survey area was based on location of detections from all the previous surveys (Figure 13). Scott et al. (1986) estimated an initial range of 6,000 ha in the Ka‘ū Rainforest. Gorresen et al. (2007) and Tweed et al. (2007) estimated the ‘Akiapōlā‘au range to be 5,555 ha in the Ka‘ū Rainforest, a range that was based on 38 detections during surveys conducted from 1976 to 2005. We updated the post-2005 range by examining detection locations from the 2008, 2010, and 2019 surveys. Tweed et al. (2007) included an area on the western edge of the range that extended towards Transect 5, but no ‘Akiapōlā‘au were detected west of Transect 6 during subsequent surveys. With the additional survey data, we relocated the western edge of the range eastward to Transect 6 where two birds were detected during the survey and one bird was heard incidentally in 2019. The upper edge followed the closed ‘ōhi‘a forest to near the top of Transect 9 and then eastward towards Transect 10. The boundary then followed a more northerly direction to include areas of Transect 10 where two birds were detected during the 2019 survey, and where another was heard incidentally near Station 5. Our revisions reduced the ‘Akiapōlā‘au range to 4,730 ha; however, because of restoration efforts in Kapāpala Forest Reserve (KPFR), areas near Transect 11 may be included in the future.

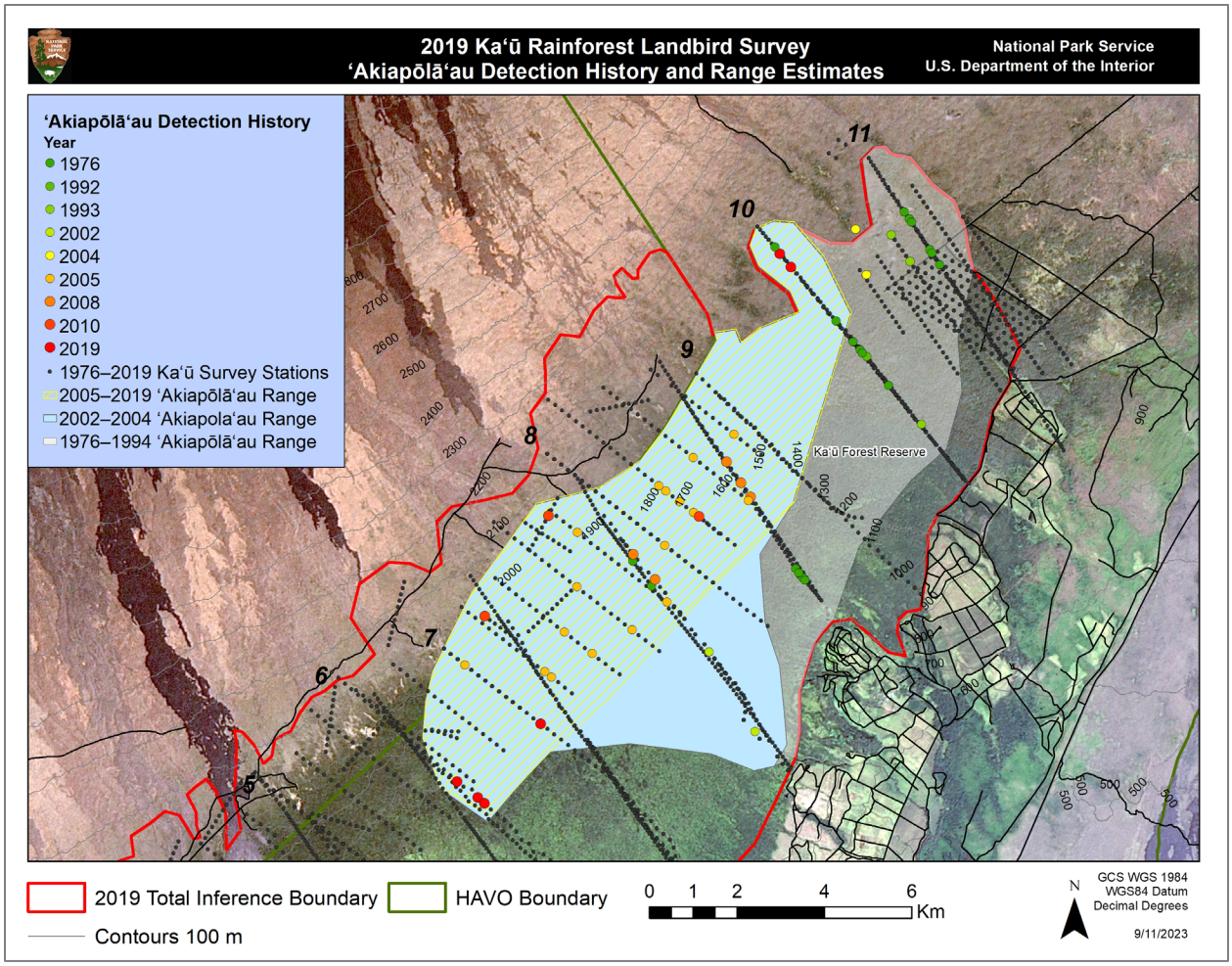



**Figure 13.** ‘Akiapōlā‘au detection history and estimated ranges within the Ka‘ū Rainforest survey area. Ranges cover portions of the Ka‘ū Forest Reserve, Kapāpala Forest Reserve, and the Kahuku Unit of Hawai‘i Volcanoes National Park.

## ‘Alawī Range

Scott et al. (1986) estimated the 1976 ‘Alawī (*Loxops mana*) range at 18,900 ha in the Ka‘ū Rainforest survey area. The range extended down to 700-m elevation, which was the lowest elevation recorded for the species throughout its survey history. Improvements in GIS technology and subsequent detections helped revise the 1976 range. Surveys in 1992, 1993, and 1994 were relatively consistent with previous records and we used the location of those detections to define a 1976–1994 range of 16,396 ha. The upper bound of the 1976–1994 range was demarcated by the edge of the closed ‘ōhi‘a forest and open montane woodland near 1,900-m elevation (Figure 14). Subsequent surveys in 2002 and 2004 indicated a contraction from the western portion of their range and in areas below the 1,100 m elevation, with most of low elevation detections occurring on Transect 7. Detections in these years were unique to the entire survey period, thus we defined a 2002–2004 range that totaled 12,064 ha. Because of the infrequency of surveys in the eastern area of the inference area, some detections in KPFR were excluded in the estimated ranges. We expect additional survey efforts and off-count detections in this area to facilitate future revisions of ‘Alawī range. Surveys from 2005

through 2019 indicated few birds below the 1,300 m and 1,400 m contours and more evidence of range contraction in the western portions of the survey area. We estimated the 2005–2019 range as 9,674 ha. In 2019, there was one anomalous detection on Transect 11 near 1,050-m elevation that we excluded from the range. The upper bound of the ranges stayed consistent for each survey period, using the closed ʻōhiʻa and open montane habitat strata edge defined by Jacobi (1989) and Green et al. (2015).

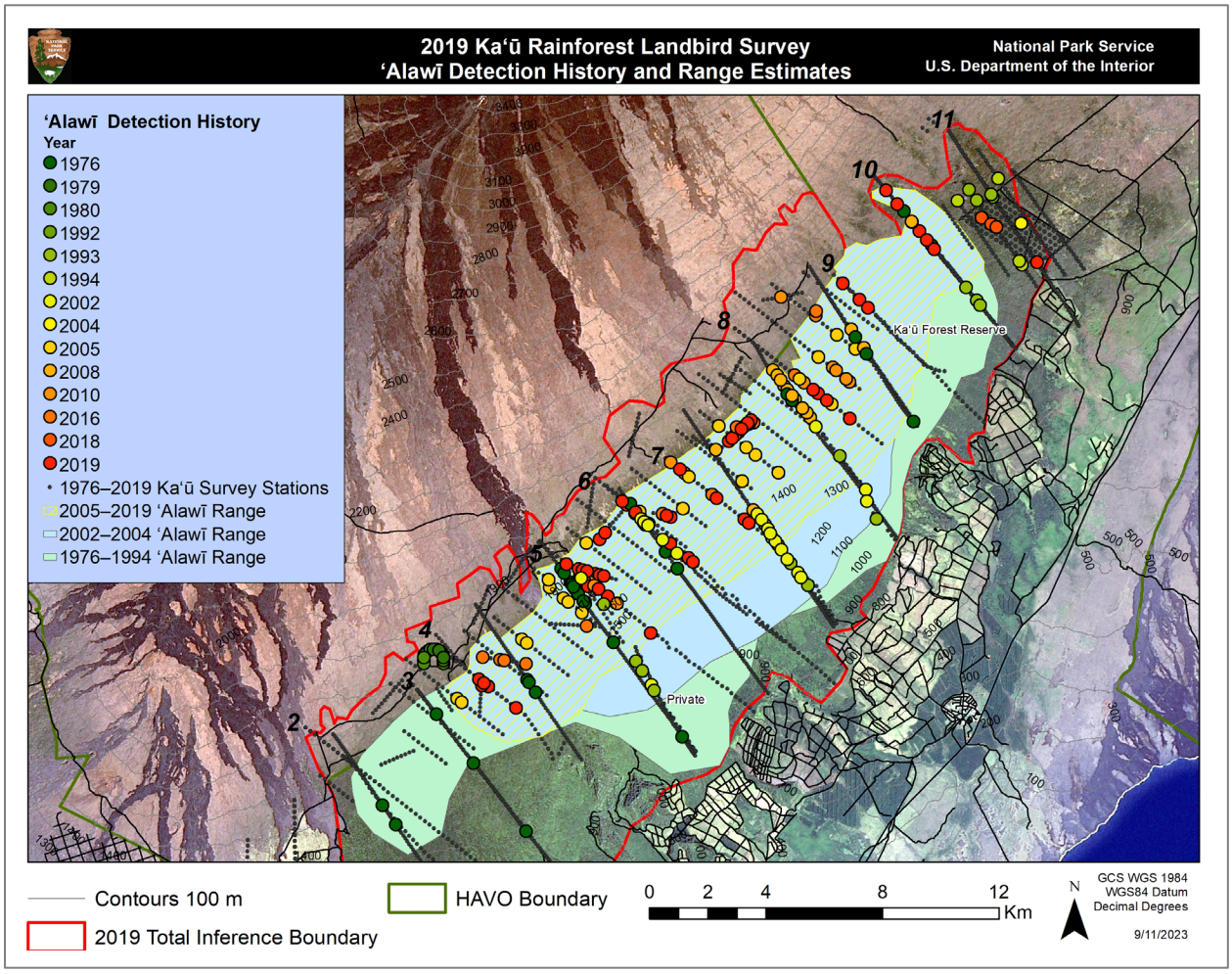



**Figure 14.** ʻAlawī detection history and estimated ranges within the Kaʻū Rainforest survey area. The species' range covers portions of the Kaʻū Forest Reserve, Kapāpala Forest Reserve, and the Kahuku Unit of Hawaiʻi Volcanoes National Park.

## Hawaiʻi ʻĀkepa Range

Scott et al. (1986) estimated the Hawaiʻi ʻĀkepa range in the Kaʻū Rainforest at 18,000 ha based on survey detections during the 1976 Hawaiʻi Forest Bird Survey (HFBS). The lower boundary extended to 1,100 m elevation and 19% of the Kaʻū Rainforest population ranged below 1,500 m elevation. Hawaiʻi ʻĀkepa contracted upslope after 1976 and no detections below 1,500 m elevation occurred during the 1993, 2002, and 2005 surveys (Figure 15). Gorresen et al. (2005) and Tweed et al. (2007) estimated the range at 7,958 ha. The 2010 Pacific Island Inventory and Monitoring

Program (PACN) survey revised the range to an estimated 10,982 ha area (Judge et al. 2011). The expanded range included the previously underrepresented montane woodland habitat near the upper limits of the species' range. That estimate was improved by expanded survey coverage and vegetation maps produced by Jacobi (1989) and Green et al. (2015). In 2019, we revised the previous ranges to reflect survey coverage, habitat types, and history of detections within the Kaʻū Rainforest survey area. The 1976–2004 range was revised to 19,771 ha, and we estimated a 2005–2019 range of 12,495 ha.

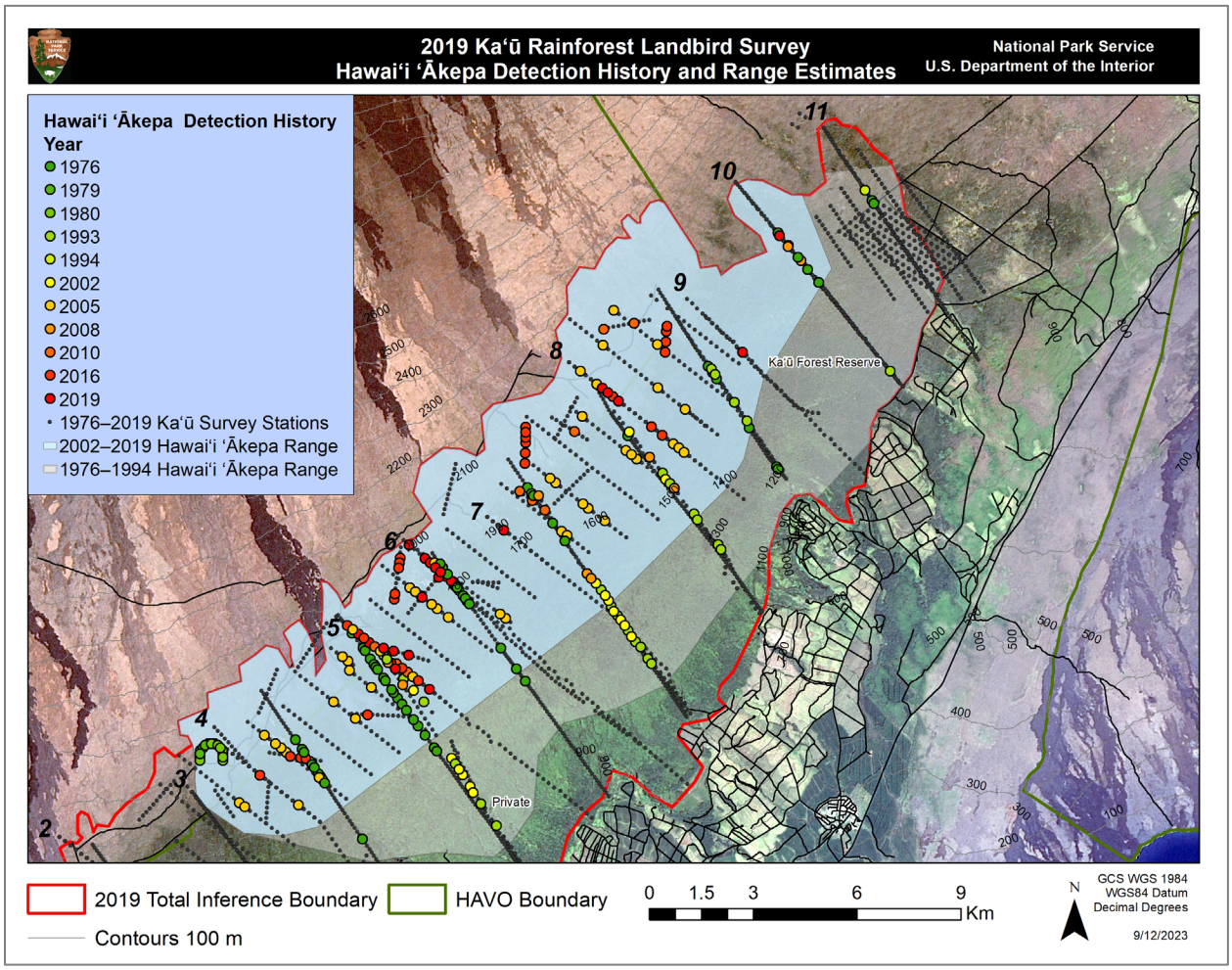



**Figure 15.** Hawaiʻi ʻĀkepa detection history and estimated ranges within the Kaʻū Rainforest survey area. Ranges cover portions of the Kaʻū Forest Reserve, Kapāpala Forest Reserve, and the Kahuku Unit of Hawaiʻi Volcanoes National Park.

### ʻIʻiwi Range

Scott et al. (1986) estimated the 1976 ʻIʻiwi (*Drepanis coccinea*) range at 28,000 ha in the Kaʻū Rainforest survey area. The species' range is continuous to the east to the Central Windward region of the island (Gorresen et al. 2005) and to the west to the Mauna Loa South Flank tract of HAVO (Judge et al. 2017); thus, the eastern and western boundaries were demarcated by the survey transect locations and 2019 inference area (Figure 16). The upper limit extended upslope to the woodland and

barren lava and shrubland vegetation classes delineated by Green et al. (2015). The lower boundary of the species' range had followed a history of detections since 2005 in the 1,000–1,300 m elevation range. We estimated a range of 24,630 ha for the 1976 to 2002 period, which included detections as low as 800 m. After 2002 there were few detections below 1,000 m, so we revised the Kaʻū Rainforest range to 21,826 ha, a range that remained consistent from 2005 to 2019.

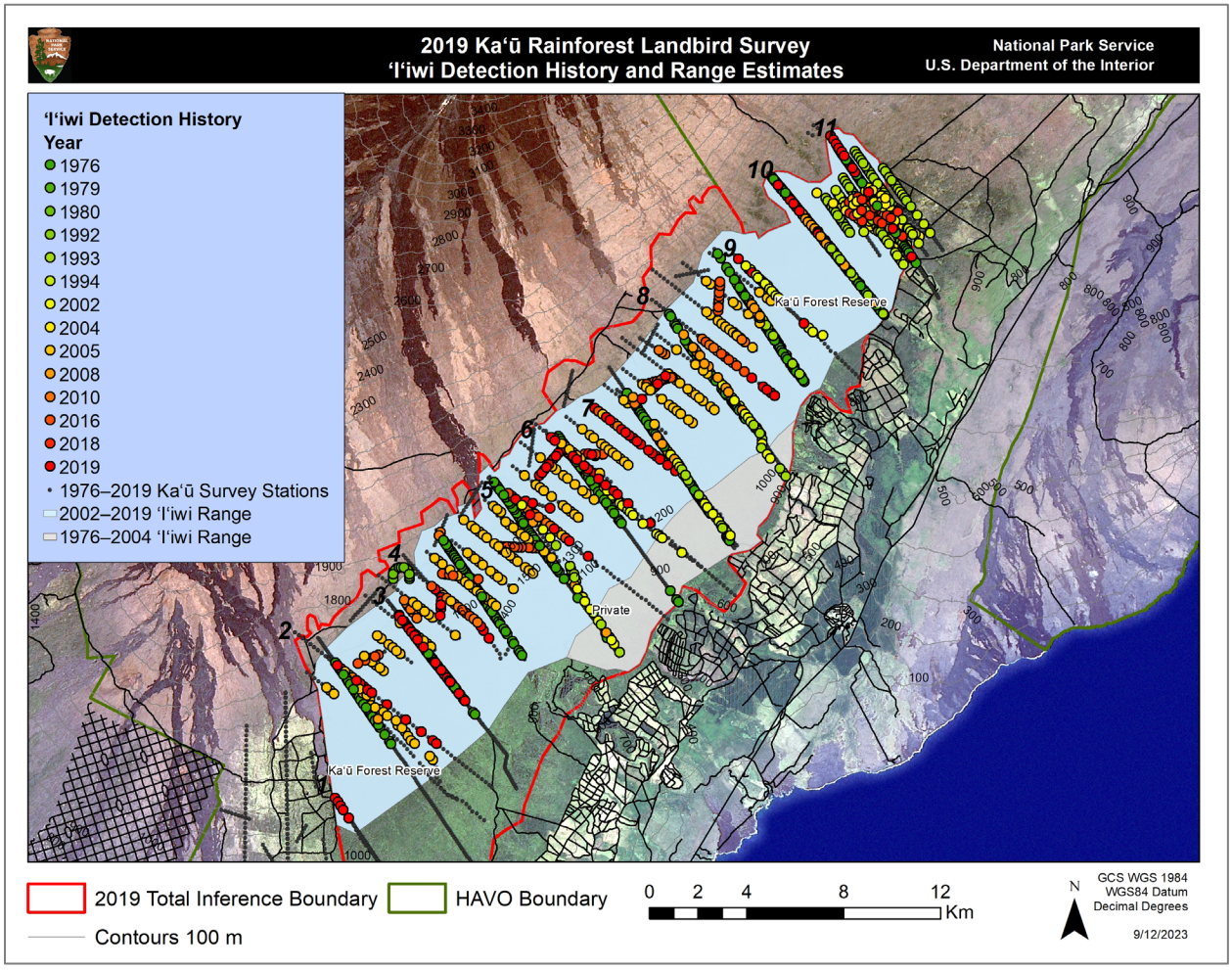



**Figure 16.** ʻIʻiwi detection history and estimated ranges within the Kaʻū Rainforest survey area. Ranges cover portions of the Kaʻū Forest Reserve, Kapāpala Forest Reserve, and the Kahuku Unit of Hawaiʻi Volcanoes National Park.

# Appendix C. Akaike's Information Criterion (AIC) Statistics- Weather, Temporal, and Observer Covariates

Model parameters and model-selection results for forest birds of the 2019 Kaʻū Rainforest survey are presented in this appendix. Within each species analysis, models were sorted by differences in second-order Akaike's information criterion corrected for small sample size (ΔAIC) between each candidate model and the model with the lowest AIC value. Models examined included half-normal and hazard-rate key detection functions and with cosine (COS), Hermite polynomial (Hpoly), and simple polynomial (Spoly) series expansions. Covariates were incorporated with the most parsimonious model to improve model precision. Covariates included the categorical variables cloud cover (Cloud), amount of rain (Rain), Beaufort wind scale (Wind), Beaufort gust scale (Gust), observer (Obs), time of day (Time), survey month (Month), survey year (Year [factor]). Detection type (1=heard, 2=seen, 4=heard and seen) was also evaluated as a categorical variable, indicated as "Detection", and based on pooling detection type by combination of types (e.g., "Detect 2, 4" pools all detections that were seen and both heard and seen, while "Detect 1, 4" pools detections that were heard and both heard and seen). Time of day (Time) and survey year (Year [continuous]) were evaluated as a continuous variable. The number of estimated parameters (Num params), and negative log-likelihood (-LogL) are presented. The Akaike model weight (w) is the likelihood that each model is the best of the converged models evaluated for each species.

### Model Selection- Weather, Temporal, and Observer Covariates

Model selection criteria are provided in Tables 22–32 below.

**Table 22.** Model selection based on AIC for ʻAkiapōlāʻau (*Hemignathus wilsoni*)

| Model | Series Expansion | Covariate | # Params | AIC | ∆ AIC | w | Justification |
|---|---|---|---|---|---|---|---|
| Half-normal | Cos | – | 2 | 472.21 | 0.00 | 0.29348 | – |
| | None | – | 1 | 472.31 | 0.10 | 0.27911 | – |
| Hazard-rate | None | – | 2 | 472.84 | 0.63 | 0.21370 | – |
| | S-poly | – | 2 | 472.84 | 0.63 | 0.21370 | – |
| Half-normal | H-poly | – | – | – | – | – | Parameters highly correlated |
| Hazard-rate | Cos | – | – | – | – | – | Maximum probability of detection > 1 |

**Table 23.** Model selection based on AIC for ʻAlawī (*Loxops mana*).

| Model | Series Expansion | Covariate | # Params | AIC | ∆ AIC | w | Justification |
|---|---|---|---|---|---|---|---|
| Half-normal | None | Detect 2,4 | 2 | 2030.66 | 0.00 | 0.63053 | – |
| | None | Detection | 3 | 2031.73 | 1.07 | 0.36947 | – |
| | None | Wind | 3 | 2073.26 | 42.60 | 0.00000 | – |
| | None | Cloud | 4 | 2073.96 | 43.30 | 0.00000 | – |
| | None | Detect 1,4 | 2 | 2075.70 | 45.04 | 0.00000 | – |
| | None | Rain | 3 | 2079.80 | 49.14 | 0.00000 | – |
| | None | Time | 2 | 2084.57 | 53.91 | 0.00000 | – |
| | None | Observer | 2 | 2089.36 | 58.70 | 0.00000 | – |
| | Cos | – | 1 | 2096.88 | 66.22 | 0.00000 | – |
| | None | – | 1 | 2096.88 | 66.22 | 0.00000 | – |
| | None | Gust | 5 | 2098.13 | 67.47 | 0.00000 | – |
| | None | Year (continuous) | 2 | 2098.86 | 68.20 | 0.00000 | – |
| Hazard-rate | S-poly | – | 4 | 2100.10 | 69.44 | 0.00000 | – |
| | None | – | 2 | 2104.43 | 73.77 | 0.00000 | – |

**Table 23 (continued).** Model selection based on AIC for ‘Alawī (*Loxops mana*).

| Model | Series Expansion | Covariate | # Params | AIC | ∆ AIC | w | Justification |
|---|---|---|---|---|---|---|---|
| Half-normal | H-poly | – | – | – | – | – | Parameters highly correlated |
| | None | Year (factor) | – | – | – | – | Failed to converge |
| Hazard-rate | Cos | – | – | – | – | – | Parameters highly correlated |

**Table 24.** Model selection based on AIC for ‘Apapane (Himatione sanguinea).

| Model | Series Expansion | Covariate | # Params | AIC | ∆ AIC | w | Justification |
|---|---|---|---|---|---|---|---|
| Hazard-rate | Cos(2,3) | Detect 2,4 | 5 | 149739.40 | 0.00 | 1.00000 | – |
| | Cos(2,3) | Detect 1,4 | 5 | 151017.00 | 1277.59 | 0.00000 | – |
| | Cos(2,3) | Wind | 8 | 152427.00 | 2687.59 | 0.00000 | – |
| | Cos(2,3) | Time | 5 | 152432.90 | 2693.50 | 0.00000 | – |
| | Cos | – | 4 | 152441.90 | 2702.50 | 0.00000 | – |
| | Cos(2,3) | Cloud | 15 | 152456.90 | 2717.50 | 0.00000 | – |
| | Cos(2,3) | Rain | 7 | 152459.90 | 2720.50 | 0.00000 | – |
| | S-poly | – | 4 | 152460.60 | 2721.19 | 0.00000 | – |
| Half-normal | Cos | – | 3 | 152464.00 | 2724.59 | 0.00000 | – |
| | H-poly | – | 1 | 152477.50 | 2738.09 | 0.00000 | – |
| | None | – | 1 | 152477.50 | 2738.09 | 0.00000 | – |
| Hazard-rate | None | – | 2 | 152509.60 | 2770.19 | 0.00000 | – |
| | Cos(2,3) | Detection | – | – | – | – | Maximum probability of detection > 1 |
| | Cos(2,3) | Year (Factor) | – | – | – | – | Maximum probability of detection > 1 |
| | Cos(2,3) | Year (Continuous) | – | – | – | – | Parameters highly correlated |
| | Cos(2,3) | Observer | – | – | – | – | Maximum probability of detection > 1 |
| | Cos(2,3) | Gust | – | – | – | – | Maximum probability of detection > 1 |

**Table 25.** Model selection based on AIC for Hawai‘i ‘Amakihi (*Chlorodrepanis virens virens*).

| Model | Series Expansion | Covariate | # Params | AIC | ∆ AIC | w | Justification |
|---|---|---|---|---|---|---|---|
| Hazard-rate | None | Detection | 4 | 42284.29 | 0.00 | 0.77899 | – |
| | None | Detect 2,4 | 3 | 42286.81 | 2.52 | 0.22101 | – |
| | None | Detect 1,4 | 3 | 42845.39 | 561.10 | 0.00000 | – |
| | None | Observer | 20 | 42864.41 | 580.12 | 0.00000 | – |
| | None | Year (Factor) | 9 | 43249.97 | 965.68 | 0.00000 | – |
| | None | Time | 3 | 43342.42 | 1058.13 | 0.00000 | – |
| | None | Gust | 7 | 43364.33 | 1080.04 | 0.00000 | – |
| | None | Wind | 5 | 43375.02 | 1090.73 | 0.00000 | – |
| | None | Rain | 5 | 43385.20 | 1100.91 | 0.00000 | – |
| | None | Cloud | 6 | 43385.99 | 1101.70 | 0.00000 | – |
| | None | – | 2 | 43442.82 | 1158.53 | 0.00000 | – |
| | S-poly | – | 2 | 43442.82 | 1158.53 | 0.00000 | – |
| | Cos | – | 2 | 43442.82 | 1158.53 | 0.00000 | – |
| Half-normal | None | – | 1 | 43508.31 | 1224.02 | 0.00000 | – |
| Hazard-rate | None | Year (Continuous) | – | – | – | – | Parameters highly correlated |
| Half-normal | Cos | – | – | – | – | – | Maximum probability of detection > 1 |
| | H-poly | – | – | – | – | – | Parameters highly correlated |

**Table 26.** Model selection based on AIC for Hawai‘i ‘Elepaio (*Chasiempis sandwichensis*).

| Model | Series Expansion | Covariate | # Params | AIC | ∆ AIC | w | Justification |
|---|---|---|---|---|---|---|---|
| Hazard-rate | None | Detection | 4 | 4600.40 | 0.00 | 0.99998 | – |
| | None | Detect 2,4 | 3 | 4621.92 | 21.52 | 0.00002 | – |
| | None | Year (Factor) | 9 | 4745.85 | 145.44 | 0.00000 | – |
| | None | – | 2 | 4761.67 | 161.27 | 0.00000 | – |
| | Cos | – | 2 | 4761.67 | 161.27 | 0.00000 | – |
| | None | Time | 3 | 4771.67 | 171.27 | 0.00000 | – |
| | None | Observer | 3 | 4772.10 | 171.70 | 0.00000 | – |
| | None | Detect 1,4 | 3 | 4772.12 | 171.72 | 0.00000 | – |
| | None | Rain | 4 | 4774.09 | 173.69 | 0.00000 | – |
| | None | Wind | 5 | 4775.66 | 175.26 | 0.00000 | – |
| | None | Cloud | 5 | 4775.98 | 175.57 | 0.00000 | – |
| | None | Gust | 6 | 4776.68 | 176.28 | 0.00000 | – |
| Half-normal | H-poly | – | 1 | 4783.82 | 183.42 | 0.00000 | – |
| | None | – | 1 | 4783.82 | 183.42 | 0.00000 | – |
| | Cos | – | – | – | – | – | Parameters constrained |
| Hazard-rate | S-poly | – | – | – | – | – | Parameters highly correlated |
| | None | Year (Continuous) | – | – | – | – | Parameters highly correlated |

**Table 27.** Model selection based on AIC for Hawai‘i ‘Ākepa (*Loxops coccineus*). The best fit model was a Hazard-rate detection function with blocked years as a covariate. The years were pooled into three groups: (1) 1976; (2) 1993, 2005, 2008, 2010, and 2016; (3) 2002 and 2019.

| Model | Series Expansion | Covariate | # Params | AIC | ∆ AIC | w | Justification |
|---|---|---|---|---|---|---|---|
| Hazard-rate | None | Year Block | 4 | 3209.87 | 0.00 | 0.98922 | – |
| | None | Year (Factor) | 9 | 3219.02 | 9.16 | 0.01017 | – |
| | None | Detect 2,4 | 3 | 3225.28 | 15.41 | 0.00045 | – |
| | None | Detection | 4 | 3227.37 | 17.51 | 0.00016 | – |
| | None | Cloud | 5 | 3234.21 | 24.34 | 0.00001 | – |
| | None | Wind | 5 | 3235.64 | 25.77 | 0.00000 | – |
| | None | Time | 3 | 3235.92 | 26.05 | 0.00000 | – |
| | None | Rain | 4 | 3251.57 | 41.71 | 0.00000 | – |
| | None | Gust | 6 | 3269.95 | 60.08 | 0.00000 | – |
| | None | – | 2 | 3278.81 | 68.95 | 0.00000 | – |
| | None | Detect 1,4 | 3 | 3280.74 | 70.87 | 0.00000 | – |
| | None | Observer | 3 | 3280.82 | 70.95 | 0.00000 | – |
| Half-normal | None | – | 1 | 3293.99 | 84.12 | 0.00000 | – |
| | Cos | – | – | – | – | – | Parameters constrained |
| Hazard-rate | Cos | – | – | – | – | – | Parameters constrained |
| | S-poly | – | – | – | – | – | Parameters constrained |
| | None | – | – | – | – | – | Parameters highly correlated |
| Half-normal | H-poly | – | – | – | – | – | Parameters highly correlated |

**Table 28.** Model selection based on AIC for ʻIʻiwi (*Drepanis coccinea*).

| Model | Series Expansion | Covariate | # Params | AIC | ∆ AIC | w | Justification |
|---|---|---|---|---|---|---|---|
| Hazard-rate | None | Detection | 4 | 18727.37 | 0.00 | 1.00000 | – |
| | None | Year (Factor) | 9 | 19019.28 | 291.91 | 0.00000 | – |
| | None | Observer | 14 | 19041.82 | 314.45 | 0.00000 | – |
| | None | – | 2 | 19143.82 | 416.45 | 0.00000 | – |
| | S-poly | – | 2 | 19143.82 | 416.45 | 0.00000 | – |
| | None | Time | 3 | 19176.42 | 449.05 | 0.00000 | – |
| | None | Detect 2,4 | 3 | 19176.79 | 449.42 | 0.00000 | – |
| | None | Detect 1,4 | 3 | 19176.88 | 449.51 | 0.00000 | – |
| | None | Rain | 4 | 19178.79 | 451.42 | 0.00000 | – |
| | None | Wind | 5 | 19180.81 | 453.44 | 0.00000 | – |
| | None | Gust | 6 | 19182.82 | 455.45 | 0.00000 | – |
| | None | Cloud | 6 | 19182.85 | 455.48 | 0.00000 | – |
| Half-normal | None | – | 1 | 19209.13 | 481.76 | 0.00000 | – |
| Hazard-rate | Cos | – | – | – | – | – | Parameters constrained |
| Half-normal | Cos | – | – | – | – | – | Parameters constrained |
| Hazard-rate | None | Year (Continuous) | – | – | – | – | Parameters highly correlated |
| Half-normal | H-poly | – | – | – | – | – | Parameters highly correlated |

**Table 29.** Model selection based on AIC for Northern Cardinal (*Cardinalis cardinalis*).

| Model | Series Expansion | Covariate | # Params | AIC | ∆ AIC | w | Justification |
|---|---|---|---|---|---|---|---|
| Hazard-rate | None | Detection | 4 | 2285.39 | 0.00 | 0.56248 | – |
| | None | Detect 2,4 | 3 | 2286.14 | 0.75 | 0.38677 | – |
| | None | Detect 1,4 | 3 | 2290.21 | 4.81 | 0.05075 | – |
| | None | Year (Factor) | 9 | 2312.67 | 27.27 | 0.00000 | – |
| | None | Gust | 6 | 2315.06 | 29.67 | 0.00000 | – |
| | None | – | 2 | 2316.00 | 30.60 | 0.00000 | – |
| | None | Rain | 3 | 2316.55 | 31.16 | 0.00000 | – |
| Half-normal | Cos | – | 1 | 2316.56 | 31.17 | 0.00000 | – |
| | None | – | 1 | 2316.56 | 31.17 | 0.00000 | – |
| Hazard-rate | None | Time | 3 | 2318.05 | 32.66 | 0.00000 | – |
| | None | Wind | 5 | 2318.45 | 33.05 | 0.00000 | – |
| | None | Cloud | 5 | 2321.84 | 36.45 | 0.00000 | – |
| | S-poly | – | – | – | – | – | Parameters constrained |
| Half-normal | H-poly | – | – | – | – | – | Parameters highly correlated |
| Hazard-rate | None | Year (Continuous) | – | – | – | – | Parameters highly correlated |

**Table 30.** Model selection based on AIC for ʻŌmaʻo (*Myadestes obscurus*).

| Model | Series Expansion | Covariate | # Params | AIC | ∆ AIC | w | Justification |
|---|---|---|---|---|---|---|---|
| Hazard-rate | None | Detect 2,4 | 3 | 44069.40 | 0.00 | 1.00000 | – |
| | None | Detection | 4 | 44113.29 | 43.89 | 0.00000 | – |
| | None | Detect 1,4 | 3 | 44367.35 | 297.95 | 0.00000 | – |
| | None | Observer | 14 | 44461.57 | 392.17 | 0.00000 | – |

**Table 30 (continued).** Model selection based on AIC for ‘Ōma‘o (*Myadestes obscurus*).

| Model | Series Expansion | Covariate | # Params | AIC | Δ AIC | w | Justification |
|---|---|---|---|---|---|---|---|
| Hazard-rate (continued) | None | Year (Factor) | 9 | 44472.09 | 402.69 | 0.00000 | – |
| | None | Gust | 7 | 44527.25 | 457.85 | 0.00000 | – |
| | None | Cloud | 6 | 44532.56 | 463.16 | 0.00000 | – |
| | None | Time | 3 | 44541.82 | 472.42 | 0.00000 | – |
| | None | Wind | 5 | 44544.63 | 475.23 | 0.00000 | – |
| | None | – | 2 | 44544.95 | 475.55 | 0.00000 | – |
| | None | Rain | 4 | 44545.43 | 476.03 | 0.00000 | – |
| Half-normal | None | – | 1 | 44791.84 | 722.44 | 0.00000 | – |
| Hazard-rate | S-poly | – | – | – | – | – | Parameters constrained |
| | Cos | – | – | – | – | – | Parameters constrained |
| | None | Year (Continuous) | – | – | – | – | Parameters highly correlated |
| Half-normal | Cos | – | – | – | – | – | Parameters constrained |
| | H-poly | – | – | – | – | – | Parameters constrained |

**Table 31.** Model selection based on AIC for Red-billed Leiothrix (*Leiothrix lutea*).

| Model | Series Expansion | Covariate | # Params | AIC | Δ AIC | w | Justification |
|---|---|---|---|---|---|---|---|
| Hazard-rate | None | Detection | 4 | 19131.13 | 0.00 | 0.72894 | – |
| | None | Detect 2,4 | 3 | 19133.11 | 1.98 | 0.27106 | – |
| | None | Observer | 11 | 19379.45 | 248.32 | 0.00000 | – |
| | None | Detect 1,4 | 3 | 19380.20 | 249.07 | 0.00000 | – |
| | None | Year (Factor) | 9 | 19394.86 | 263.73 | 0.00000 | – |
| | None | Gust | 6 | 19426.31 | 295.18 | 0.00000 | – |

**Table 31 (continued).** Model selection based on AIC for Red-billed Leiothrix (*Leiothrix lutea*).

| Model | Series Expansion | Covariate | # Params | AIC | Δ AIC | w | Justification |
|---|---|---|---|---|---|---|---|
| Hazard-rate (continued) | None | Wind | 5 | 19447.35 | 316.22 | 0.00000 | – |
| | None | Time | 3 | 19464.87 | 333.74 | 0.00000 | – |
| | None | Cloud | 6 | 19468.00 | 336.87 | 0.00000 | – |
| | None | Rain | 4 | 19470.20 | 339.07 | 0.00000 | – |
| | None | – | 2 | 19483.29 | 352.16 | 0.00000 | – |
| Half-normal | None | – | 1 | 19514.35 | 383.22 | 0.00000 | – |
| Hazard-rate | S-poly | – | – | – | – | – | Parameters constrained |
| | Cos | – | – | – | – | – | Parameters constrained |
| | None | Year (Continuous) | – | – | – | – | Parameters highly correlated |
| Half-normal | Cos | – | – | – | – | – | Parameters constrained |
| | H-poly | – | – | – | – | – | Parameters constrained |

**Table 32.** Model selection based on AIC for Warbling White-eye (*Zosterops japonicus*).

| Model | Series Expansion | Covariate | # Params | AIC | Δ AIC | w | Justification |
|---|---|---|---|---|---|---|---|
| Hazard-rate | None | Detection | 4 | 27274.24 | 0.00 | 0.65178 | – |
| | None | Detect 2,4 | 3 | 27275.50 | 1.26 | 0.34717 | – |
| | None | Observer | 18 | 27287.10 | 12.86 | 0.00105 | – |
| | None | Year (Factor) | 9 | 27490.07 | 215.83 | 0.00000 | – |
| | None | Detect 1,4 | 3 | 27490.16 | 215.92 | 0.00000 | – |
| | None | Time | 3 | 27602.59 | 328.35 | 0.00000 | – |
| | None | Gust | 6 | 27617.29 | 343.05 | 0.00000 | – |
| | None | Rain | 4 | 27617.50 | 343.26 | 0.00000 | – |

**Table 32 (continued).** Model selection based on AIC for Warbling White-eye (*Zosterops japonicus*).

| Model | Series Expansion | Covariate | # Params | AIC | Δ AIC | w | Justification |
|---|---|---|---|---|---|---|---|
| Hazard-rate (continued) | None | Cloud | 6 | 27618.93 | 344.69 | 0.00000 | – |
| | None | Wind | 5 | 27620.82 | 346.58 | 0.00000 | – |
| | None | – | 2 | 27666.07 | 391.83 | 0.00000 | – |
| Half-normal | None | – | 1 | 27848.07 | 573.83 | 0.00000 | – |
| Hazard-rate | S-poly | – | – | – | – | – | Parameters constrained |
| | Cos | – | – | – | – | – | Parameters constrained |
| | None | Year (Continuous) | – | – | – | – | Parameters highly correlated |
| Half-normal | Cos | – | – | – | – | – | Parameters constrained |
| | H-poly | – | – | – | – | – | Parameters constrained |

# Appendix D. Akaike's Information Criterion (AIC) Statistics- Vegetation Covariates

Model parameters and model-selection results for forest birds of the 2019 Kaʻū Rainforest survey are presented in this appendix. Within each species analysis, models were sorted by differences in second-order Akaike's information criterion corrected for small sample size ($\Delta AIC_c$) between each candidate model and the model with the lowest AIC value. Models examined included half-normal (HN) and hazard-rate (HR) key detection functions and with cosine (Cos), Hermite polynomial (Hpoly), and simple polynomial (Spoly) series expansions. Covariates were incorporated with the most parsimonious model to improve model precision. Vegetation covariate descriptions and abbreviation in parentheses are described as follows: dominant understory species from Jacobi (1989; Understory), dominant understory from Jacobi (1989; Undom), Jacobi (1989) vegetation category (Jacobi), dominant canopy composition from Jacobi (1989; Overstory), moisture regime (Env), Jacobi (1989) canopy cover (Canopy), canopy cover classification recorded in 2019 (Cover), canopy height recorded in 2019 (Height19), canopy height and dominant species recorded in 2019 (Hcan19), predominant understory species recorded in 2019 (Under19), dominant understory species recorded in 2019 (Undom). Covariates also include detection type (Detection and Detect 2,4) and survey year. The number of estimated parameters (Num params), and negative log-likelihood (-LogL) are presented. The Akaike model weight (AIC weights) is the likelihood that each model is the best of the converged models evaluated for each species.

### Model Selection- Vegetation Covariates

Model selection criteria are provided in Tables 33–43 below

**Table 33.** Model selection based on AIC for ‘Akiapōlā‘au (*Hemignathus wilsoni*).

| Model | Covariate | # Params | AIC | ∆ AIC | Weight | Justification |
|---|---|---|---|---|---|---|
| Half-normal | Cos(1) + Understory | 4 | 196.43 | 0.00 | 0.33 | No clear best vegetation covariate so none chosen. |
| | Cos(1) + Cover | 2 | 197.51 | 1.09 | 0.19 | – |
| | Cos(1) + Undom | 6 | 198.54 | 2.12 | 0.12 | – |
| | Null (Cos(1) only) | 1 | 199.01 | 2.58 | 0.09 | – |
| | Cos(1) + Overstory | 5 | 199.47 | 3.04 | 0.07 | – |
| | Cos(1) + Jacobi | 6 | 199.80 | 3.38 | 0.06 | – |
| | Cos(1) + Height19 | 2 | 200.26 | 3.84 | 0.05 | – |
| | Cos(1) + Env | 4 | 201.13 | 4.71 | 0.03 | – |
| | Cos(1) + Overstory | 3 | 201.41 | 4.98 | 0.03 | – |
| | Cos(1) + Canopy | 3 | 202.12 | 5.70 | 0.02 | – |

**Table 34.** Model selection based on AIC for ‘Apapane (*Himatione sanguinea*).

| Model | Covariate | # Params | AIC | ∆ AIC | Weight | Justification |
|---|---|---|---|---|---|---|
| Hazard-rate | Cos(2, 3) + Detect 2,4 + Jacobi + Undom | 18 | 90179.05 | 0.00 | 1.00 | Jacobi + Undom chosen as a candidate post hoc |
| | Cos(2, 3) + Detect 2,4 + Undom | 11 | 90218.47 | 39.42 | 0.00 | – |
| | Cos(2, 3) + Detect 2,4 + Jacobi | 10 | 90221.27 | 42.22 | 0.00 | – |
| | Cos(2, 3) + Detect 2,4 + Understory | 7 | 90229.47 | 50.42 | 0.00 | – |
| | Cos(2, 3) + Detect 2,4 + Env | 6 | 90231.27 | 52.22 | 0.00 | – |
| | Cos(2, 3) + Detect 2,4 + Hcan19 | 7 | 90286.17 | 107.12 | 0.00 | – |
| | Cos(2, 3) + Detect 2,4 + Cover | 6 | 90291.15 | 112.10 | 0.00 | – |
| | Cos(2, 3) + Detect 2,4 + Height19 | 6 | 90321.79 | 142.74 | 0.00 | – |
| | Cos(2, 3) + Detect 2,4 + Overstory | 6 | 90340.94 | 161.89 | 0.00 | – |
| | Cos(2, 3) + Detect 2,4 | 3 | 90344.61 | 165.57 | 0.00 | – |

**Table 34 (continued).** Model selection based on AIC for ʻApapane (*Himatione sanguinea*).

| Model | Covariate | # Params | AIC | ∆ AIC | Weight | Justification |
|---|---|---|---|---|---|---|
| Hazard-rate (continued) | Cos(2, 3) + Detect 2,4 + Canopy | 5 | 90348.04 | 168.99 | 0.00 | – |
| | Cos(2, 3) + Jacobi + Undom | 17 | 92138.00 | 1958.95 | 0.00 | – |
| | Cos(2, 3) + Undom | 10 | 92160.61 | 1981.56 | 0.00 | – |
| | Cos(2, 3) + Jacobi | 9 | 92183.44 | 2004.40 | 0.00 | – |
| | Cos(2, 3) + Env | 5 | 92195.34 | 2016.29 | 0.00 | – |
| | Cos(2, 3) + Understory | 6 | 92202.64 | 2023.59 | 0.00 | – |
| | Cos(2, 3) + Cover | 5 | 92209.90 | 2030.85 | 0.00 | – |
| | Cos(2, 3) + Detect 2,4 + Overstory | 6 | 92225.32 | 2046.27 | 0.00 | – |
| | Cos(2, 3) + Overstory | 5 | 92227.97 | 2048.92 | 0.00 | – |
| | Null (Cos(2, 3) only) | 3 | 92235.32 | 2056.28 | 0.00 | – |
| | Cos(2, 3) + Height19 | 5 | 92241.59 | 2062.54 | 0.00 | – |
| | Cos(2, 3) + Canopy | 4 | 92260.10 | 2081.05 | 0.00 | – |

**Table 35.** Model selection based on AIC for Hawaiʻi ʻĀkepa (*Loxops coccineus*).

| Model | Covariate | # Params | AIC | ∆ AIC | Weight | Justification |
|---|---|---|---|---|---|---|
| Hazard-rate | Year (grouped) + Undom | 11 | 2009.99 | 0.00 | 0.98 | – |
| | Year (grouped) + Overstory | 5 | 2020.48 | 10.49 | 0.01 | – |
| | Year (grouped) | 3 | 2020.80 | 10.81 | 0.00 | – |
| | Year (grouped) + Understory | 7 | 2020.84 | 10.85 | 0.00 | – |
| | Year (grouped) + Jacobi | 10 | 2021.25 | 11.26 | 0.00 | – |
| | Year (grouped) + Env | 5 | 2022.50 | 12.51 | 0.00 | – |
| | Year (grouped) + Height19 | 4 | 2022.80 | 12.81 | 0.00 | – |
| | Year (grouped) + Canopy | 4 | 2022.80 | 12.81 | 0.00 | – |
| | Year (grouped) + Cover | 6 | 2025.95 | 15.96 | 0.00 | – |

**Table 35 (continued).** Model selection based on AIC for Hawai‘i ‘Ākepa (*Loxops coccineus*).

| Model | Covariate | # Params | AIC | ∆ AIC | Weight | Justification |
|---|---|---|---|---|---|---|
| Hazard-rate (continued) | Year (grouped) + Hcan19 | 7 | 2027.08 | 17.09 | 0.00 | – |
| | Undom | 10 | 2041.78 | 31.79 | 0.00 | – |
| | Null (+adj) | 2 | 2056.87 | 46.88 | 0.00 | – |
| | Env | 4 | 2057.40 | 47.41 | 0.00 | – |
| | Height19 | 3 | 2058.54 | 48.55 | 0.00 | – |
| | Canopy | 3 | 2058.87 | 48.88 | 0.00 | – |
| | Overstory | 4 | 2059.82 | 49.83 | 0.00 | – |
| | Jacobi | 9 | 2061.01 | 51.02 | 0.00 | – |
| | Year (grouped) + Overstory | 6 | 2061.79 | 51.80 | 0.00 | – |
| | Cover | 5 | 2062.11 | 52.12 | 0.00 | – |
| | Understory | 6 | 2097.38 | 87.39 | 0.00 | – |

**Table 36.** Model selection based on AIC for Hawai‘i ‘Amakihi (*Chlorodrepanis virens virens*).

| Model | Covariate | # Params | AIC | ∆ AIC | Weight | Justification |
|---|---|---|---|---|---|---|
| Hazard-rate | Detection + Env + Undom | 15 | 28435.87 | 0.00 | 0.88 | Env + Undom chosen as a candidate post-hoc |
| | Detection + Env | 7 | 28441.02 | 5.15 | 0.07 | – |
| | Detection + Undom | 12 | 28442.16 | 6.29 | 0.04 | – |
| | Detection + Jacobi | 11 | 28445.02 | 9.15 | 0.01 | – |
| | Detection + Understory | 8 | 28447.99 | 12.13 | 0.00 | – |
| | Detection + Hcan19 | 8 | 28461.94 | 26.08 | 0.00 | – |
| | Detection + Height19 | 7 | 28466.24 | 30.37 | 0.00 | – |
| | Detection + Cover | 7 | 28467.67 | 31.81 | 0.00 | – |
| | Detection + Canopy | 6 | 28467.82 | 31.95 | 0.00 | – |

**Table 36 (continued).** Model selection based on AIC for Hawai‘i ‘Amakihi (*Chlorodrepanis virens virens*).

| Model | Covariate | # Params | AIC | ∆ AIC | Weight | Justification |
|---|---|---|---|---|---|---|
| Hazard-rate (continued) | Detection | 4 | 28471.03 | 35.17 | 0.00 | – |
| | Detection + Overstory | 7 | 28472.53 | 36.66 | 0.00 | – |
| | Env + Undom | 13 | 29246.27 | 810.40 | 0.00 | – |
| | Env | 5 | 29246.40 | 810.53 | 0.00 | – |
| | Canopy | 4 | 29250.05 | 814.19 | 0.00 | – |
| | Height19 | 5 | 29254.34 | 818.48 | 0.00 | – |
| | Overstory | 5 | 29258.13 | 822.26 | 0.00 | – |
| | Undom | 10 | 29258.31 | 822.44 | 0.00 | – |
| | Null (+adj) | 2 | 29259.50 | 823.63 | 0.00 | – |
| | Cover | 5 | 29263.95 | 828.08 | 0.00 | – |
| | Detection + Overstory | 6 | 29264.84 | 828.97 | 0.00 | – |
| | Understory | 6 | 29265.29 | 829.43 | 0.00 | – |
| | Jacobi | 9 | 29269.08 | 833.21 | 0.00 | – |

**Table 37.** Model selection based on AIC for Hawai‘i ‘Elepaio (*Chasiempis sandwichensis*).

| Model | Covariate | # Params | AIC | ∆ AIC | Weight | Justification |
|---|---|---|---|---|---|---|
| Hazard-rate | Detection + Overstory | 7 | 2569.63 | 0.00 | 0.69 | – |
| | Detection + Cover | 7 | 2573.31 | 3.68 | 0.11 | – |
| | Detection + Height19 | 7 | 2574.27 | 4.64 | 0.07 | – |
| | Detection + Canopy | 6 | 2575.07 | 5.44 | 0.05 | – |
| | Detection | 4 | 2575.16 | 5.53 | 0.04 | – |
| | Detection + Undom | 12 | 2576.13 | 6.50 | 0.03 | – |
| | Detection + Hcan19 | 8 | 2578.91 | 9.28 | 0.01 | – |
| | Detection + Env | 7 | 2579.20 | 9.57 | 0.01 | – |

**Table 37 (continued).** Model selection based on AIC for Hawai‘i ‘Elepaio (*Chasiempis sandwichensis*).

| Model | Covariate | # Params | AIC | ∆ AIC | Weight | Justification |
|---|---|---|---|---|---|---|
| Hazard-rate (continued) | Detection + Jacobi | 11 | 2579.94 | 10.31 | 0.00 | – |
| | Detection + Understory | 8 | 2582.06 | 12.43 | 0.00 | – |
| | Height19 | 5 | 2673.12 | 103.49 | 0.00 | – |
| | Overstory | 5 | 2673.32 | 103.69 | 0.00 | – |
| | Null | 2 | 2676.04 | 106.41 | 0.00 | – |
| | Cover | 5 | 2677.25 | 107.62 | 0.00 | – |
| | Canopy | 4 | 2679.46 | 109.83 | 0.00 | – |
| | Detection + Overstory | 6 | 2679.91 | 110.28 | 0.00 | – |
| | Jacobi | 9 | 2680.62 | 111.00 | 0.00 | – |
| | Env | 5 | 2681.26 | 111.63 | 0.00 | – |
| | Undom | 10 | 2682.09 | 112.46 | 0.00 | – |
| | Understory | 6 | 2683.50 | 113.87 | 0.00 | – |

**Table 38.** Model selection based on AIC for ‘Alawī (*Loxops mana*).

| Model | Covariate | # Params | AIC | ∆ AIC | Weight | Justification |
|---|---|---|---|---|---|---|
| Half-normal | Detect 2,4 + Height19 | 3 | 1178.08 | 0.00 | 0.44 | Height19 chosen |
| | Detect 2,4 | 2 | 1178.92 | 0.84 | 0.29 | – |
| | Detect 2,4 + Canopy | 3 | 1180.65 | 2.57 | 0.12 | – |
| | Detect 2,4 + Env | 4 | 1182.28 | 4.21 | 0.05 | – |
| | Detect 2,4 + Cover | 5 | 1183.45 | 5.38 | 0.03 | – |
| | Detect 2,4 + Overstory | 5 | 1183.72 | 5.64 | 0.03 | – |
| | Detect 2,4 + Hcan19 | 6 | 1183.93 | 5.85 | 0.02 | – |
| | Detect 2,4 + Understory | 6 | 1185.05 | 6.97 | 0.01 | – |
| | Detect 2,4 + Jacobi | 9 | 1188.98 | 10.91 | 0.00 | – |

**Table 38 (continued).** Model selection based on AIC for ‘Alawī (*Loxops mana*).

| Model | Covariate | # Params | AIC | ∆ AIC | Weight | Justification |
|---|---|---|---|---|---|---|
| Half-normal (continued) | Detect 2,4 + Undom | 10 | 1190.85 | 12.77 | 0.00 | – |
| | Null | 1 | 1219.81 | 41.73 | 0.00 | – |
| | Height19 | 2 | 1221.02 | 42.94 | 0.00 | – |
| | Canopy | 2 | 1221.66 | 43.58 | 0.00 | – |
| | Env | 3 | 1223.03 | 44.95 | 0.00 | – |
| | Cover | 4 | 1223.74 | 45.66 | 0.00 | – |
| | Overstory | 4 | 1224.35 | 46.27 | 0.00 | – |
| | Understory | 5 | 1225.30 | 47.23 | 0.00 | – |
| | Detect 2,4 + Overstory | 5 | 1226.90 | 48.82 | 0.00 | – |
| | Jacobi | 8 | 1227.98 | 49.91 | 0.00 | – |
| | Undom | 9 | 1233.87 | 55.79 | 0.00 | – |

**Table 39.** Model selection based on AIC for ‘I‘iwi (*Drepanis coccinea*).

| Model | Covariate | # Params | AIC | ∆ AIC | Weight | Justification |
|---|---|---|---|---|---|---|
| Half-normal | Detection + Overstory | 6 | 12807.49 | 0.00 | 0.49 | Overstory chosen |
| | Detection + Jacobi | 10 | 12807.75 | 0.26 | 0.43 | – |
| | Detection + Understory | 7 | 12811.74 | 4.24 | 0.06 | – |
| | Detection + Env | 6 | 12814.04 | 6.54 | 0.02 | – |
| | Detection + Canopy | 5 | 12814.82 | 7.33 | 0.01 | – |
| | Detection | 3 | 12822.92 | 15.43 | 0.00 | – |
| | Detection + Undom | 11 | 12823.06 | 15.57 | 0.00 | – |
| | Detection + Cover | 6 | 12827.59 | 20.09 | 0.00 | – |
| | Detection + Height19 | 6 | 12827.68 | 20.19 | 0.00 | – |
| | Detection + Hcan19 | 7 | 12828.43 | 20.93 | 0.00 | – |

**Table 39 (continued).** Model selection based on AIC for ʻIʻiwi (*Drepanis coccinea*).

| Model | Covariate | # Params | AIC | ∆ AIC | Weight | Justification |
|---|---|---|---|---|---|---|
| Half-normal (continued) | Jacobi | 8 | 12986.02 | 178.53 | 0.00 | – |
| | Overstory | 4 | 12988.55 | 181.06 | 0.00 | – |
| | Canopy | 3 | 12996.45 | 188.96 | 0.00 | – |
| | Undom | 9 | 12996.69 | 189.20 | 0.00 | – |
| | Understory | 5 | 12998.02 | 190.53 | 0.00 | – |
| | Env | 4 | 12999.73 | 192.23 | 0.00 | – |
| | Null | 1 | 13006.75 | 199.26 | 0.00 | – |
| | Detection + Overstory | 5 | 13010.02 | 202.53 | 0.00 | – |
| | Height19 | 4 | 13010.10 | 202.60 | 0.00 | – |
| | Cover | 4 | 13010.12 | 202.63 | 0.00 | – |

**Table 40.** Model selection based on AIC for ʻŌmaʻo (*Myadestes obscurus*).

| Model | Covariate | # Params | AIC | ∆ AIC | Weight | Justification |
|---|---|---|---|---|---|---|
| Hazard-rate | Detect 2,4 + Jacobi + Cover | 13 | 27161.66 | 0.00 | 0.99 | – |
| | Detect 2,4 + Jacobi | 10 | 27171.73 | 10.08 | 0.01 | – |
| | Detect 2,4 + Cover | 6 | 27174.93 | 13.27 | 0.00 | – |
| | Detect 2,4 + Understory | 7 | 27176.86 | 15.20 | 0.00 | – |
| | Detect 2,4 + Env | 6 | 27178.31 | 16.66 | 0.00 | – |
| | Detect 2,4 + Undom | 11 | 27184.99 | 23.33 | 0.00 | – |
| | Detect 2,4 | 3 | 27185.06 | 23.40 | 0.00 | – |
| | Detect 2,4 + Height19 | 6 | 27187.24 | 25.59 | 0.00 | – |
| | Detect 2,4 + Canopy | 5 | 27187.93 | 26.27 | 0.00 | – |
| | Detect 2,4 + Overstory | 6 | 27188.80 | 27.15 | 0.00 | – |
| | Detect 2,4 + Hcan19 | 7 | 27191.54 | 29.88 | 0.00 | – |

**Table 40 (continued).** Model selection based on AIC for ʻŌmaʻo (*Myadestes obscurus*).

| Model | Covariate | # Params | AIC | ∆ AIC | Weight | Justification |
|---|---|---|---|---|---|---|
| Hazard-rate (continued) | Jacobi + Cover | 12 | 27458.48 | 296.83 | 0.00 | – |
| | Jacobi | 9 | 27469.99 | 308.33 | 0.00 | – |
| | Understory | 6 | 27481.45 | 319.79 | 0.00 | – |
| | Cover | 5 | 27482.25 | 320.59 | 0.00 | – |
| | Env | 5 | 27483.90 | 322.25 | 0.00 | – |
| | Undom | 10 | 27488.47 | 326.81 | 0.00 | – |
| | Null | 2 | 27494.25 | 332.60 | 0.00 | – |
| | Canopy | 4 | 27496.28 | 334.62 | 0.00 | – |
| | Height19 | 5 | 27496.62 | 334.96 | 0.00 | – |
| | Overstory | 5 | 27497.10 | 335.44 | 0.00 | – |
| | Detect 2,4 + Overstory | 6 | 27500.97 | 339.32 | 0.00 | – |

**Table 41.** Model selection based on AIC for Northern Cardinal (*Cardinalis cardinalis*).

| Model | Covariate | # Params | AIC | ∆ AIC | Weight | Justification |
|---|---|---|---|---|---|---|
| Hazard-rate | Detection + Undom | 11 | 1187.58 | 0.00 | 0.69 | – |
| | Undom | 10 | 1190.02 | 2.44 | 0.20 | – |
| | Detection + Canopy | 5 | 1194.11 | 6.53 | 0.03 | – |
| | Canopy | 4 | 1195.37 | 7.79 | 0.01 | – |
| | Detection + Understory | 7 | 1196.07 | 8.50 | 0.01 | – |
| | Jacobi | 9 | 1196.30 | 8.72 | 0.01 | – |
| | Detection + Env | 6 | 1196.48 | 8.90 | 0.01 | – |
| | Detection + Overstory | 6 | 1196.64 | 9.06 | 0.01 | – |
| | Detection + Hcan19 | 7 | 1197.05 | 9.47 | 0.01 | – |
| | Detection + Cover | 6 | 1197.58 | 10.00 | 0.00 | – |

**Table 41 (continued).** Model selection based on AIC for Northern Cardinal (*Cardinalis cardinalis*).

| Model | Covariate | # Params | AIC | ∆ AIC | Weight | Justification |
|---|---|---|---|---|---|---|
| Hazard-rate (continued) | Overstory | 5 | 1197.89 | 10.31 | 0.00 | – |
| | Detection | 3 | 1198.23 | 10.65 | 0.00 | – |
| | Detection + Overstory | 6 | 1198.42 | 10.84 | 0.00 | – |
| | Detection + Height19 | 6 | 1199.46 | 11.88 | 0.00 | – |
| | Null | 2 | 1199.71 | 12.13 | 0.00 | – |
| | Cover | 5 | 1199.93 | 12.35 | 0.00 | – |
| | Height19 | 5 | 1200.81 | 13.23 | 0.00 | – |
| | Detection + Jacobi | 10 | 1203.16 | 15.58 | 0.00 | – |
| | Env | 5 | 1234.93 | 47.35 | 0.00 | – |
| | Understory | 6 | 1251.58 | 64.00 | 0.00 | – |

**Table 42.** Model selection based on AIC for Red-billed Leiothrix (*Leiothrix lutea*).

| Model | Covariate | # Params | AIC | ∆ AIC | Weight | Justification |
|---|---|---|---|---|---|---|
| Hazard-rate | Detection + Jacobi | 11 | 11498.68 | 0.00 | 1.00 | – |
| | Detection + Overstory | 7 | 11523.90 | 25.22 | 0.00 | – |
| | Detection + Undom | 12 | 11536.52 | 37.84 | 0.00 | – |
| | Detection + Env | 7 | 11554.35 | 55.67 | 0.00 | – |
| | Detection + Understory | 8 | 11559.13 | 60.45 | 0.00 | – |
| | Detection + Canopy | 6 | 11564.74 | 66.06 | 0.00 | – |
| | Detection + Hcan19 | 8 | 11581.19 | 82.51 | 0.00 | – |
| | Detection | 4 | 11584.23 | 85.55 | 0.00 | – |
| | Detection + Cover | 7 | 11586.07 | 87.39 | 0.00 | – |
| | Detection + Height19 | 7 | 11586.63 | 87.95 | 0.00 | – |
| | Jacobi | 9 | 11704.72 | 206.04 | 0.00 | – |

**Table 42 (continued).** Model selection based on AIC for Red-billed Leiothrix (*Leiothrix lutea*).

| Model | Covariate | # Params | AIC | ∆ AIC | Weight | Justification |
|---|---|---|---|---|---|---|
| Hazard-rate (continued) | Overstory | 5 | 11720.78 | 222.10 | 0.00 | – |
| | Undom | 10 | 11742.99 | 244.31 | 0.00 | – |
| | Env | 5 | 11759.91 | 261.23 | 0.00 | – |
| | Canopy | 4 | 11762.80 | 264.12 | 0.00 | – |
| | Understory | 6 | 11766.94 | 268.26 | 0.00 | – |
| | Detection + Overstory | 6 | 11772.20 | 273.52 | 0.00 | – |
| | Null | 2 | 11783.28 | 284.61 | 0.00 | – |
| | Cover | 5 | 11783.33 | 284.65 | 0.00 | – |
| | Height19 | 5 | 11783.45 | 284.77 | 0.00 | – |

**Table 43.** Model selection based on AIC for Warbling White-eye (*Zosterops japonicus*).

| Model | Covariate | # Params | AIC | ∆ AIC | Weight | Justification |
|---|---|---|---|---|---|---|
| Hazard-rate | Detection + Env | 7 | 14098.61 | 0.00 | 0.89 | – |
| | Detection + Jacobi | 11 | 14102.95 | 4.34 | 0.10 | – |
| | Detection + Understory | 8 | 14107.30 | 8.69 | 0.01 | – |
| | Detection + Undom | 12 | 14112.12 | 13.51 | 0.00 | – |
| | Detection + Hcan19 | 8 | 14114.38 | 15.77 | 0.00 | – |
| | Detection + Height19 | 7 | 14116.08 | 17.47 | 0.00 | – |
| | Detection + Overstory | 7 | 14120.57 | 21.96 | 0.00 | – |
| | Detection + Cover | 7 | 14123.89 | 25.28 | 0.00 | – |
| | Detection | 4 | 14124.56 | 25.95 | 0.00 | – |
| | Detection + Canopy | 6 | 14127.24 | 28.63 | 0.00 | – |
| | Undom | 10 | 14272.67 | 174.06 | 0.00 | – |
| | Env | 5 | 14272.76 | 174.15 | 0.00 | – |

**Table 43 (continued).** Model selection based on AIC for Warbling White-eye (*Zosterops japonicus*).

| Model | Covariate | # Params | AIC | ∆ AIC | Weight | Justification |
|---|---|---|---|---|---|---|
| Hazard-rate (continued) | Jacobi | 9 | 14275.48 | 176.87 | 0.00 | – |
| | Height19 | 5 | 14279.70 | 181.09 | 0.00 | – |
| | Detection + Overstory | 6 | 14283.59 | 184.98 | 0.00 | – |
| | Overstory | 5 | 14284.05 | 185.44 | 0.00 | – |
| | Null | 2 | 14285.85 | 187.24 | 0.00 | – |
| | Cover | 5 | 14286.31 | 187.70 | 0.00 | – |
| | Understory | 6 | 14323.17 | 224.56 | 0.00 | – |
| | Canopy | 4 | 14325.40 | 226.79 | 0.00 | – |

# Appendix E. Landbird Occurrence Maps

### Native Species

Occurrence maps for native landbird species can be seen in Figures 17–25.

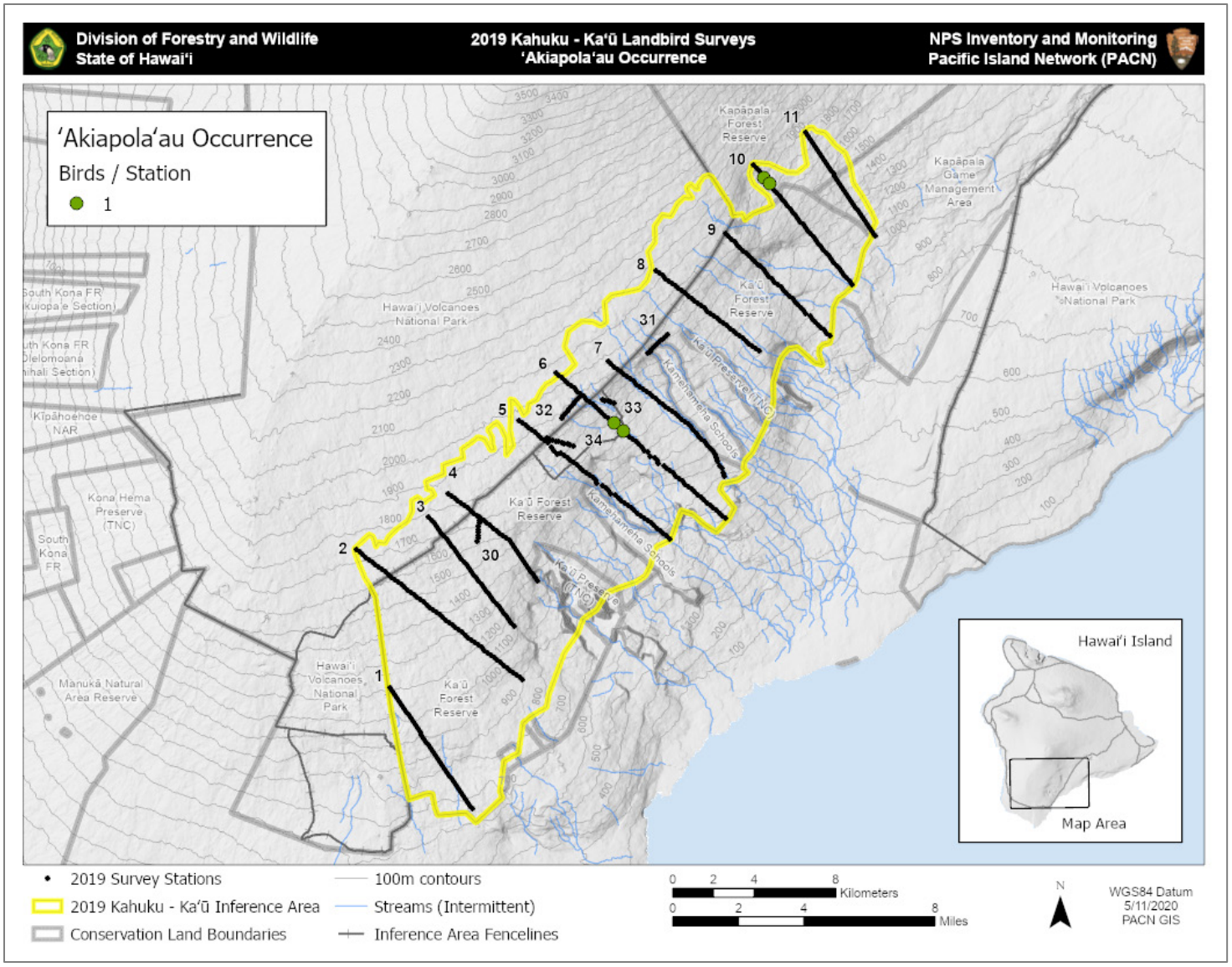



**Figure 17.** ʻAkiapōlāʻau (*Hemignathus wilsoni*) detections during the 2019 Kaʻū Rainforest landbird survey. The number of birds per station was divided by the number of counts at each station where species was detected.

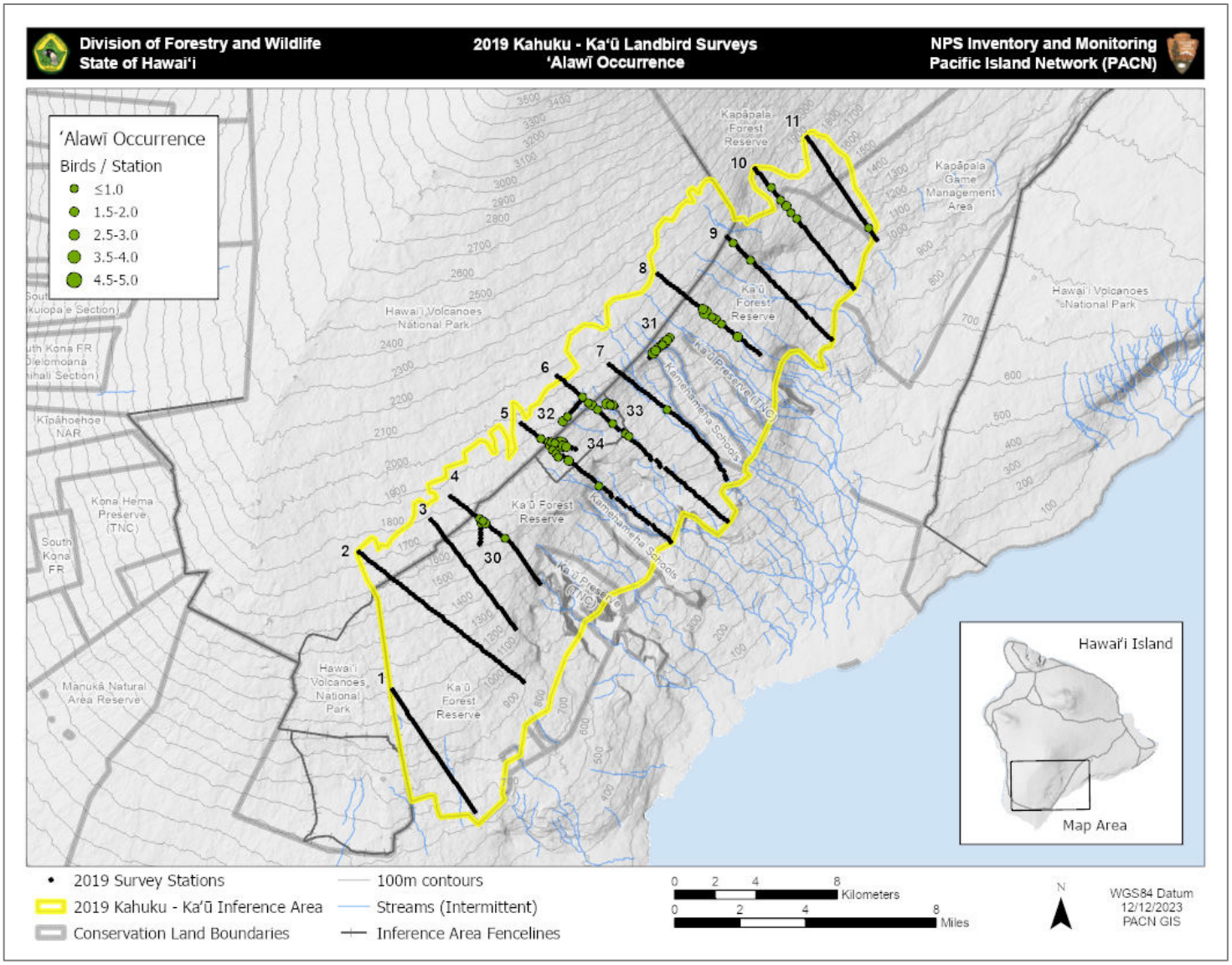



**Figure 18.** ʻAlawī (*Loxops* mana) detections during the 2019 Kaʻū Rainforest landbird survey. The number of birds per station was divided by the number of counts at each station where species was detected.

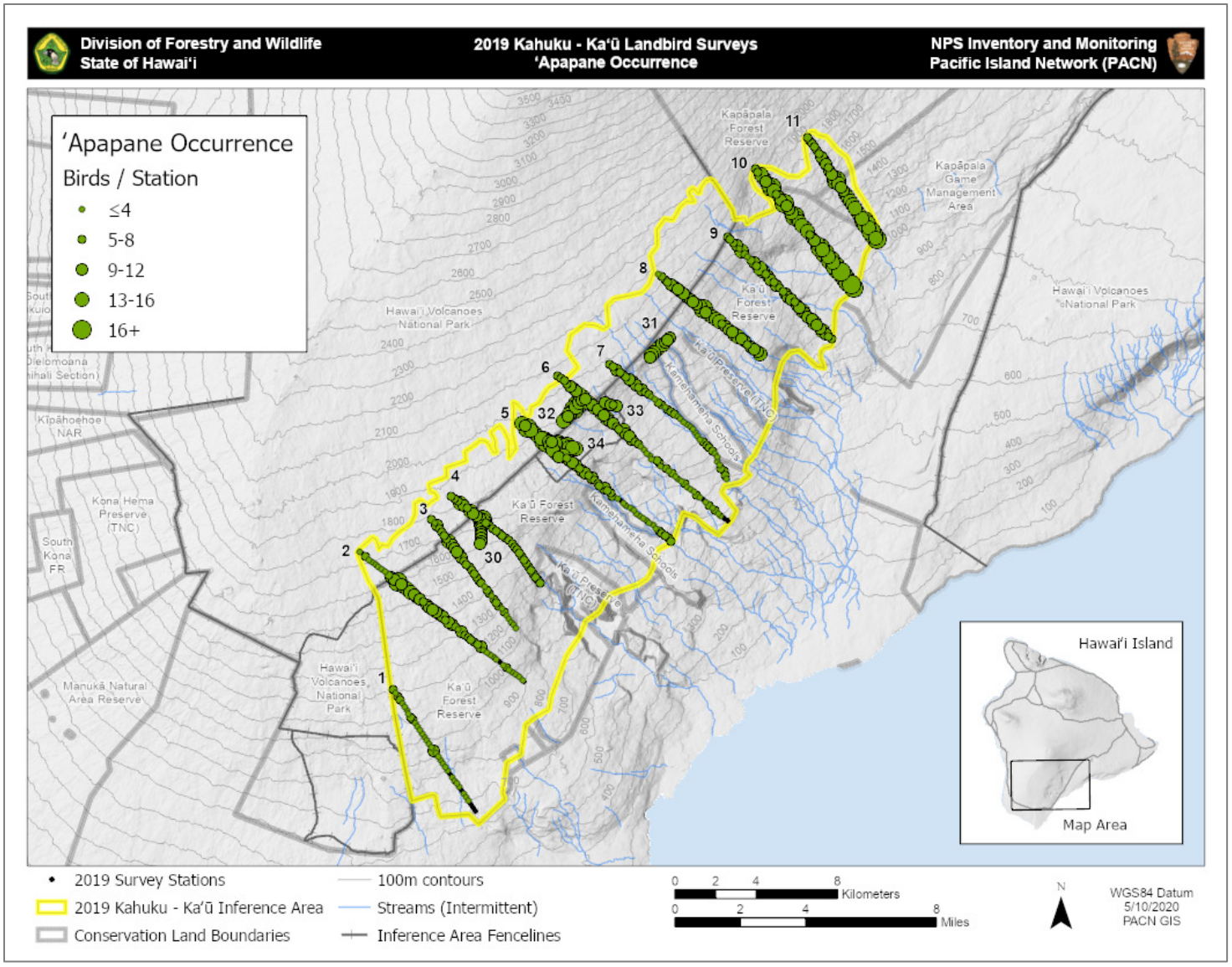



**Figure 19.** ʻApapane (*Himatione sanguinea*) detections during the 2019 Kaʻū Rainforest landbird survey. The number of birds per station was divided by the number of counts at each station where species was detected.

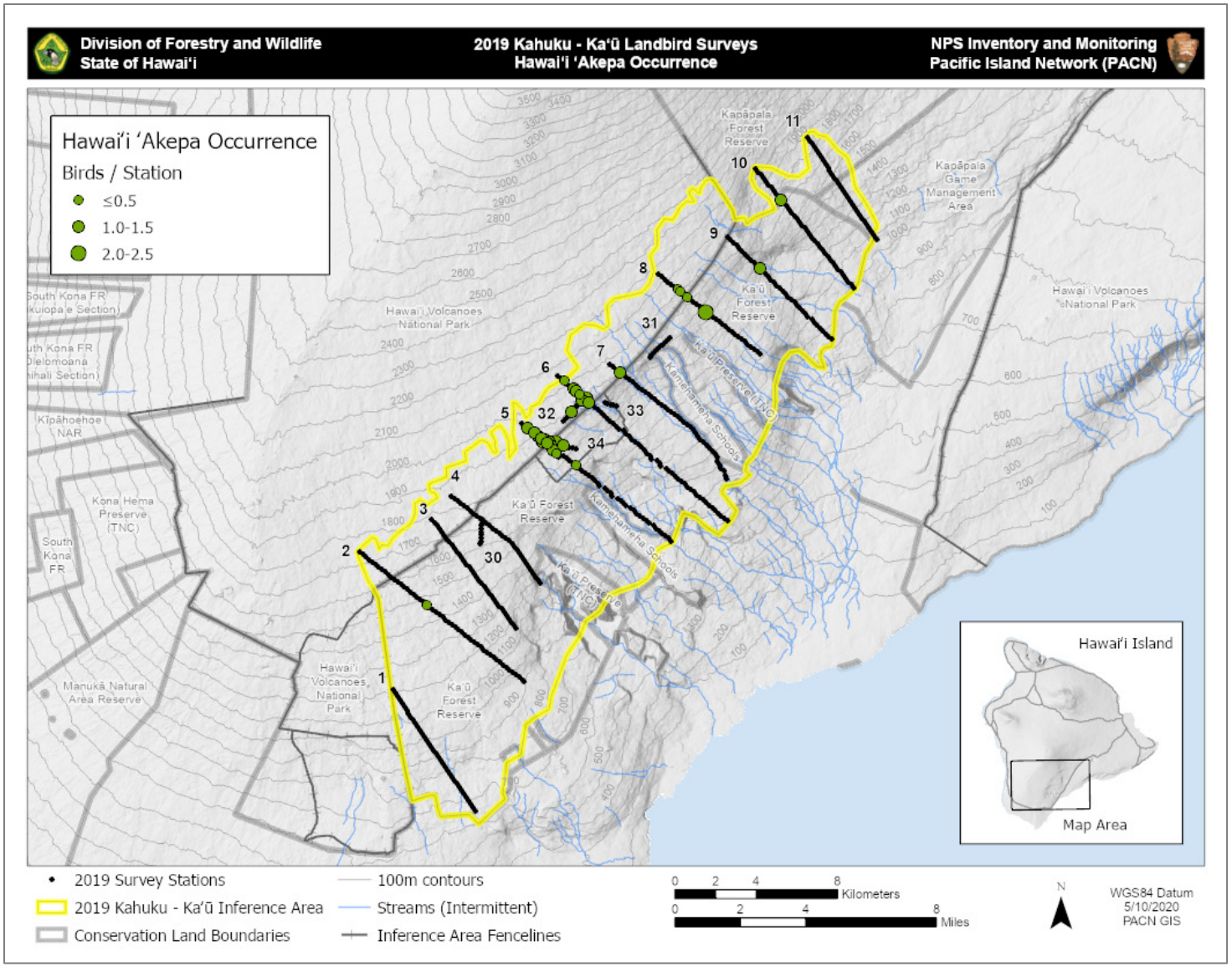



**Figure 20.** Hawai'i 'Ākepa (*Loxops coccineus*) detections during the 2019 Ka'ū Rainforest landbird survey. The number of birds per station was divided by the number of counts at each station where species was detected.

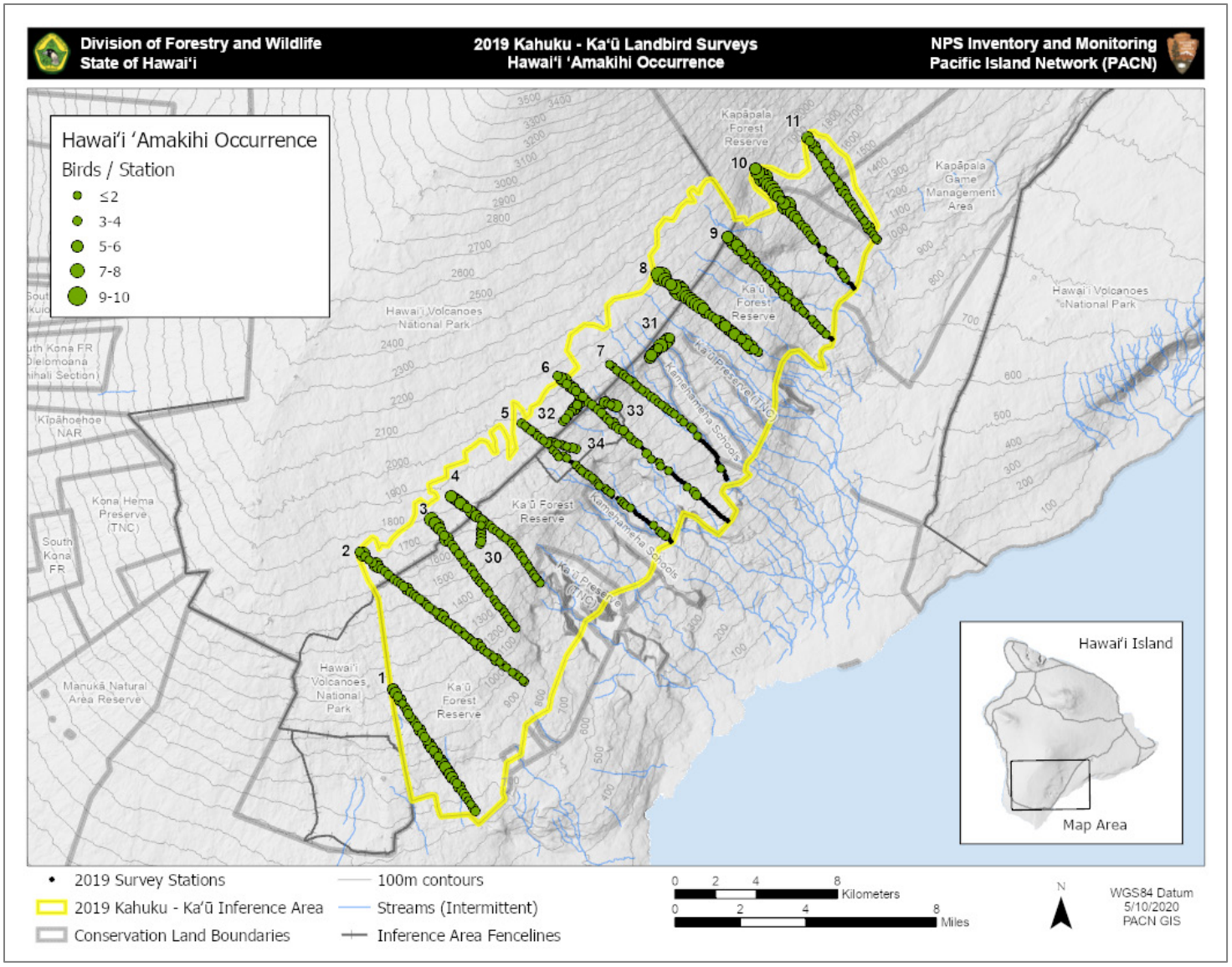



**Figure 21.** Hawai'i 'Amakihi (*Chlorodrepanis virens virens*) detections during the 2019 Ka'ū Rainforest landbird survey. The number of birds per station was divided by the number of counts at each station where species was detected.

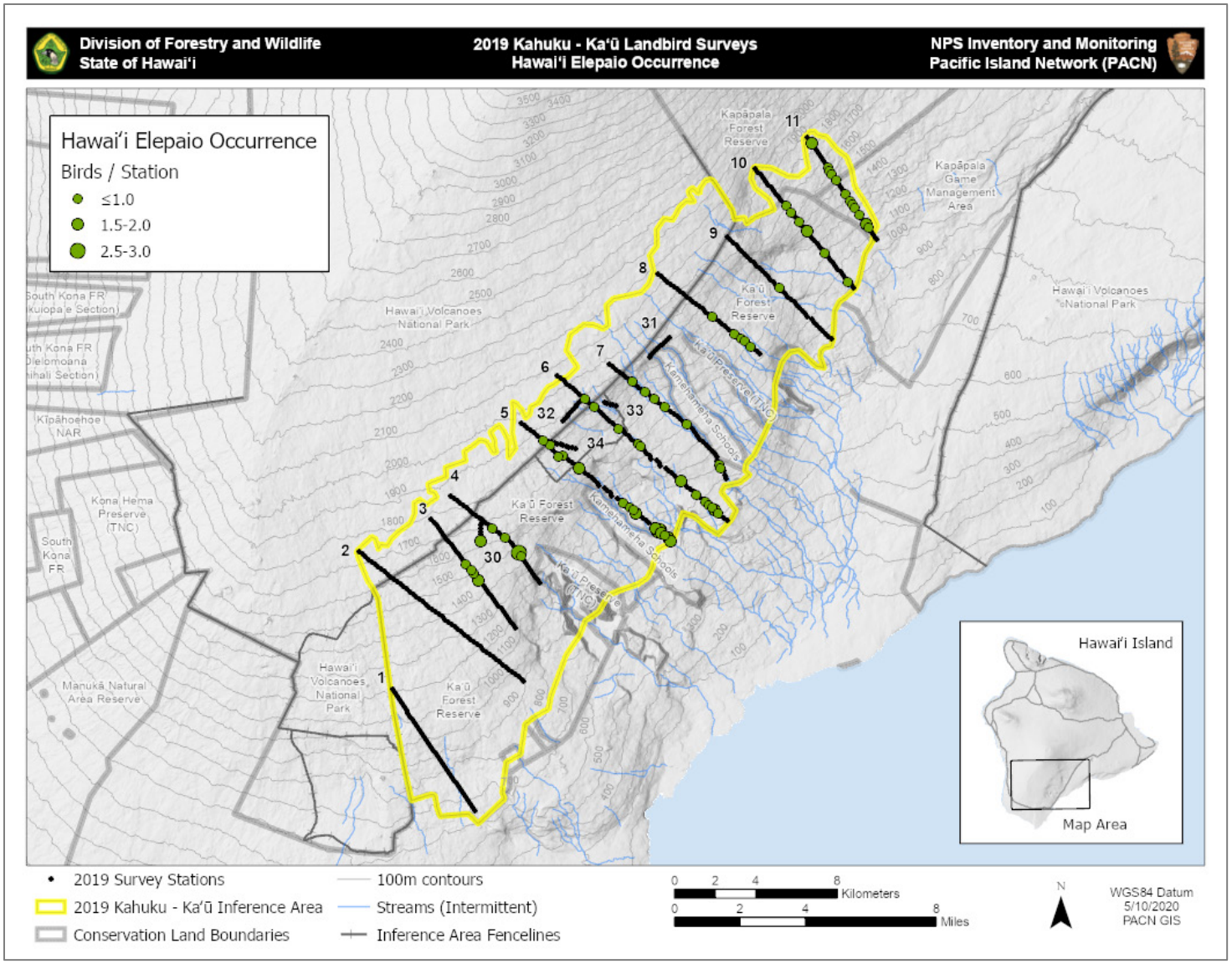



**Figure 22.** Hawai'i 'Elepaio (*Chasiempis sandwichensis*) detections during the 2019 Ka'ū Rainforest landbird survey. The number of birds per station was divided by the number of counts at each station where species was detected.

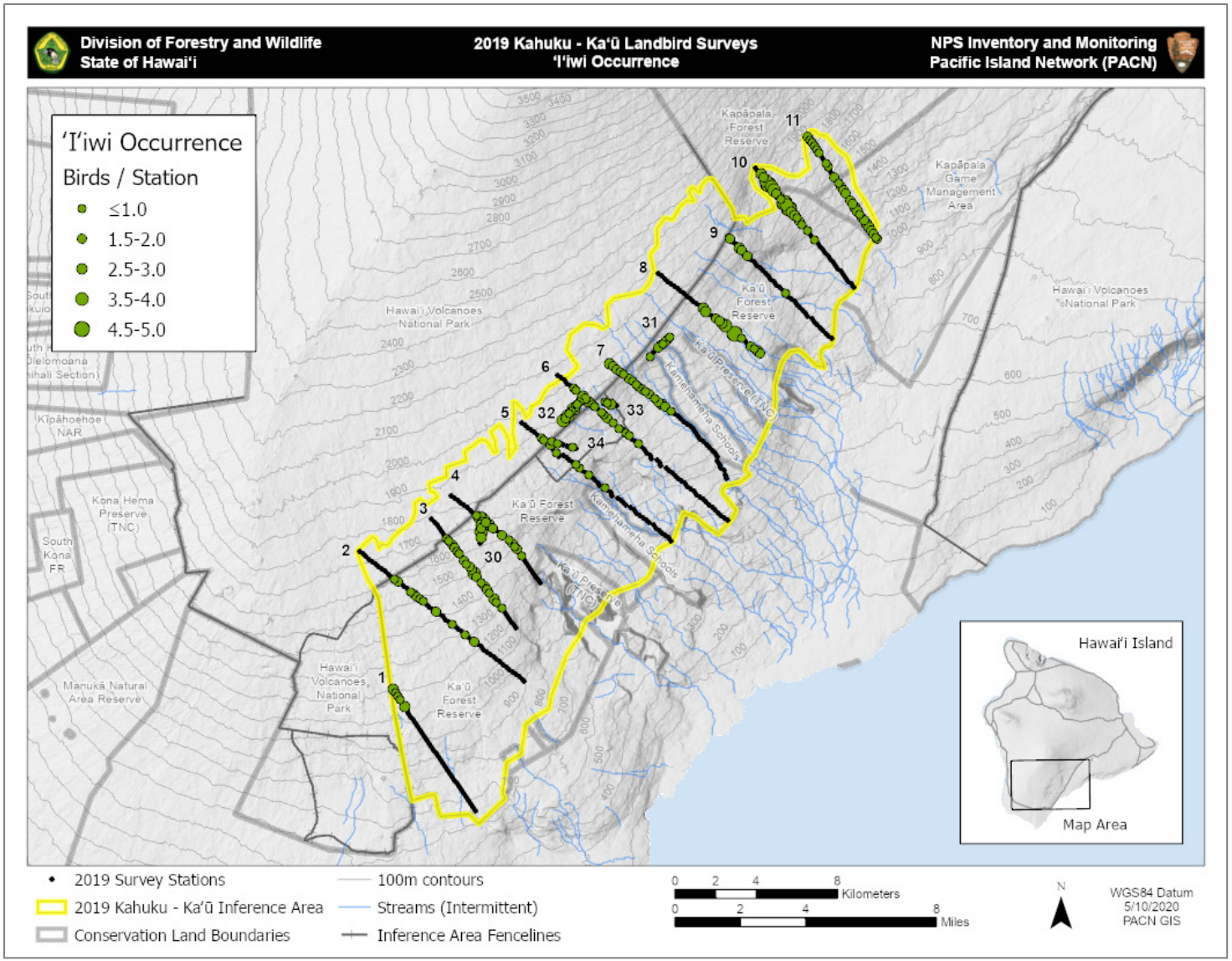



**Figure 23.** ʻIʻiwi (*Drepanis coccinea*) detections during the 2019 Kaʻū Rainforest landbird survey. The number of birds per station was divided by the number of counts at each station where species was detected.

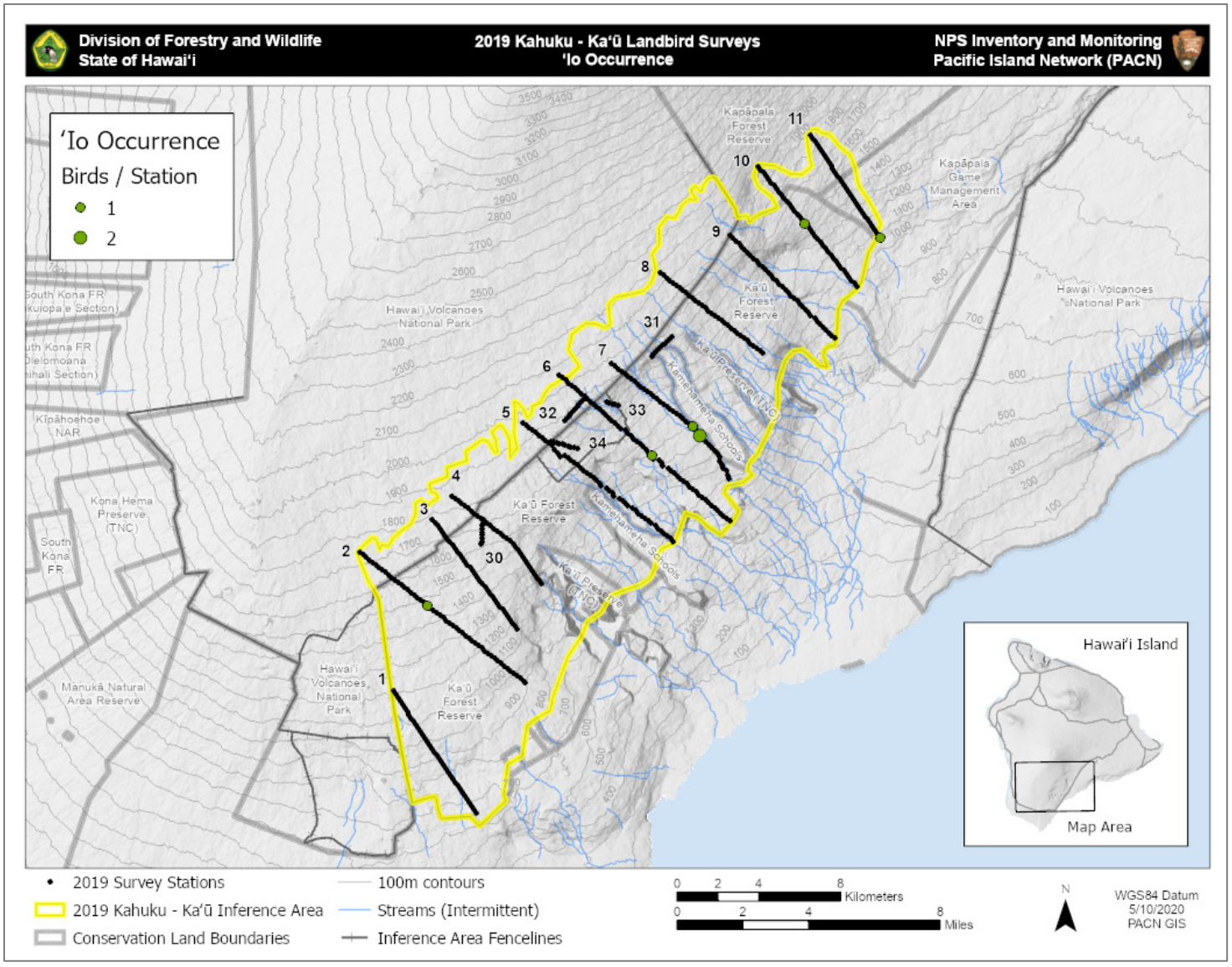



**Figure 24.** ʻIo (*Buteo solitarius*) detections during the 2019 Kaʻū Rainforest landbird survey.

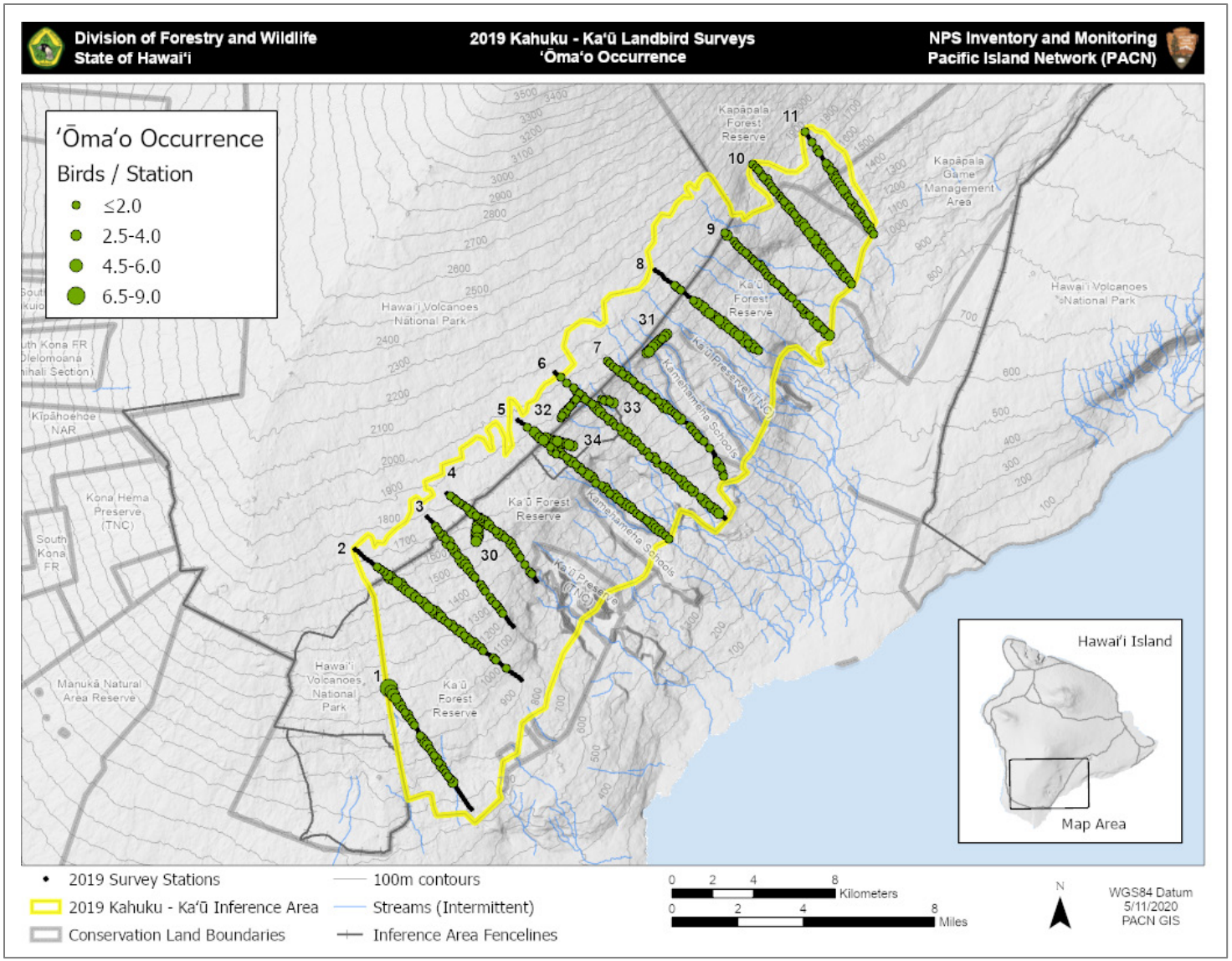



**Figure 25.** ʻŌmaʻo (*Myadestes obscurus*) detections during the 2019 Kaʻū Rainforest landbird survey. The number of birds per station was divided by the number of counts at each station where species was detected.

### Non-Native Species

Occurrence maps for non-native landbird species can be seen in Figures 26–39.

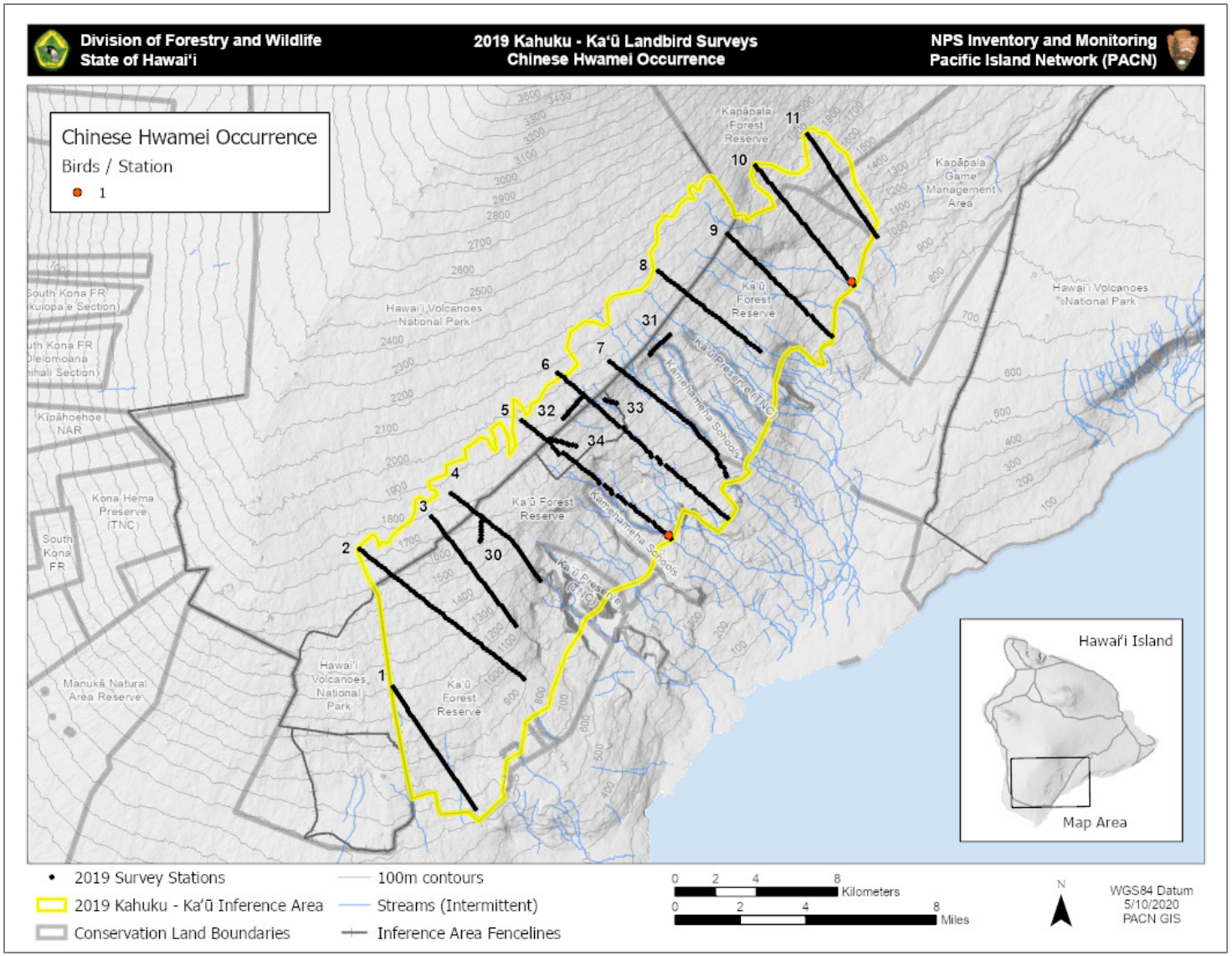



**Figure 26.** Chinese Hwamei (*Garrulax canorus*) detections during the 2019 Ka'ū Rainforest landbird survey.

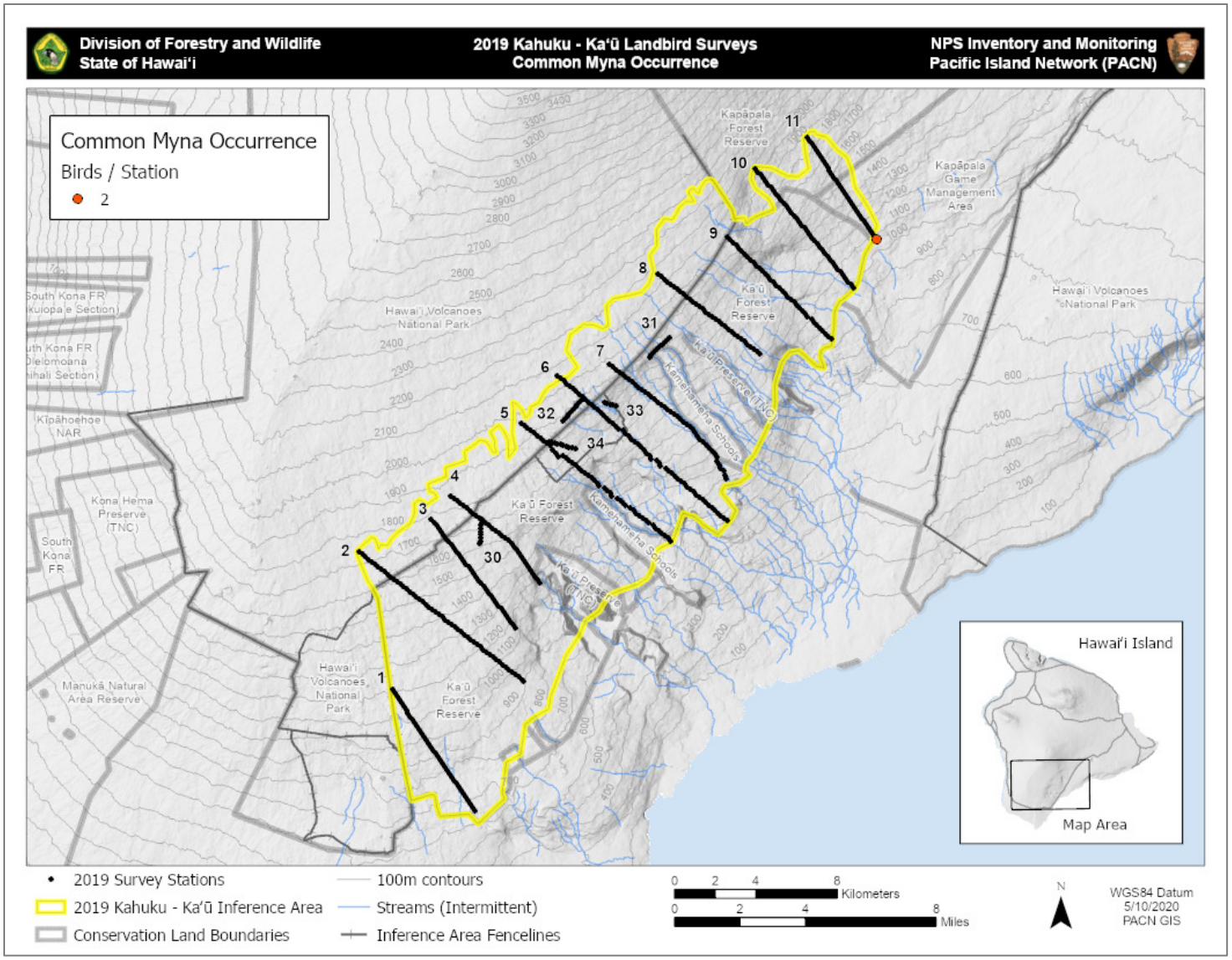



**Figure 27.** Common Myna (*Acridotheres tristis*) detections during the 2019 Ka‘ū Rainforest landbird survey.

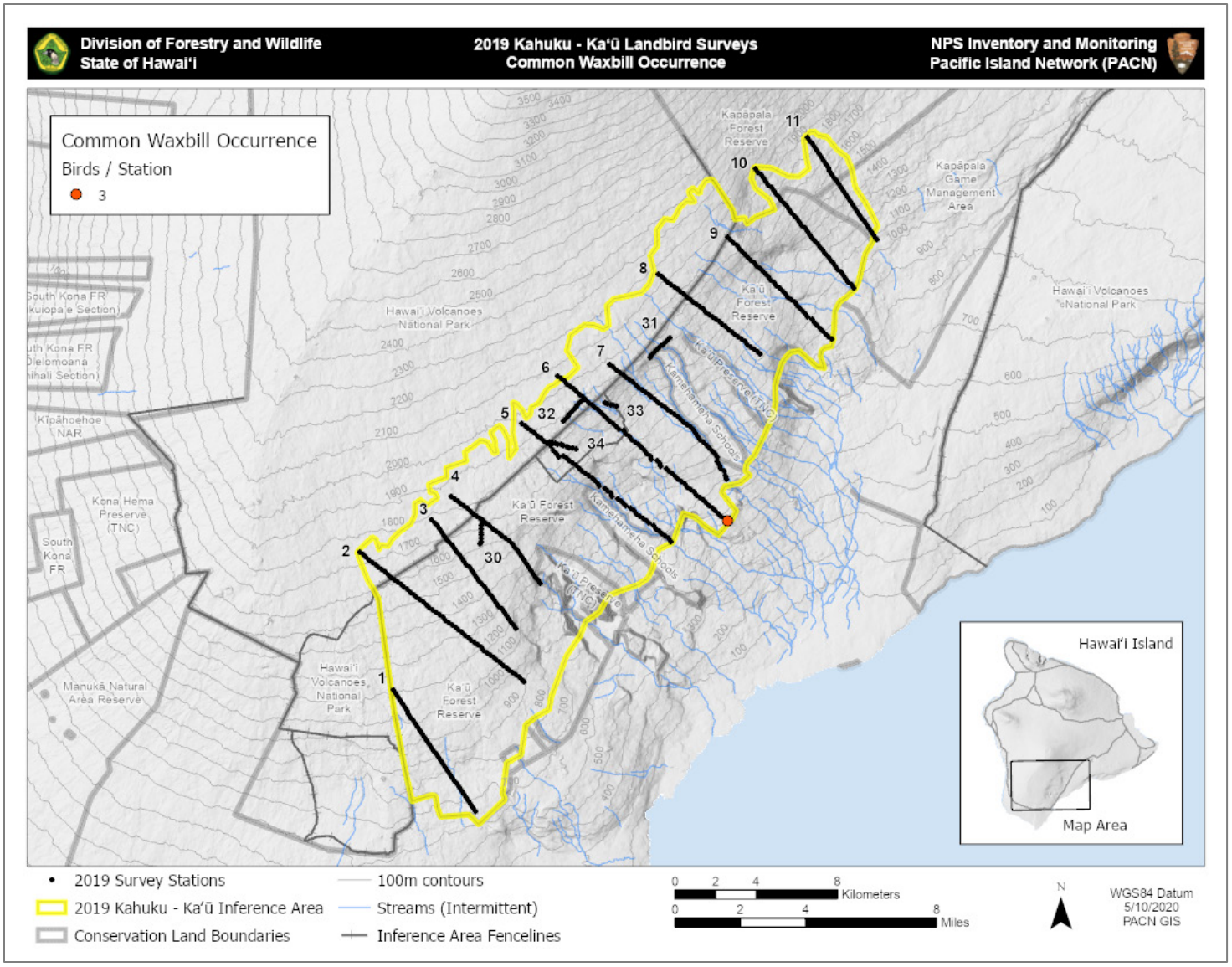



**Figure 28.** Common Waxbill (*Estrilda astrild*) detections during the 2019 Ka'ū Rainforest landbird survey.

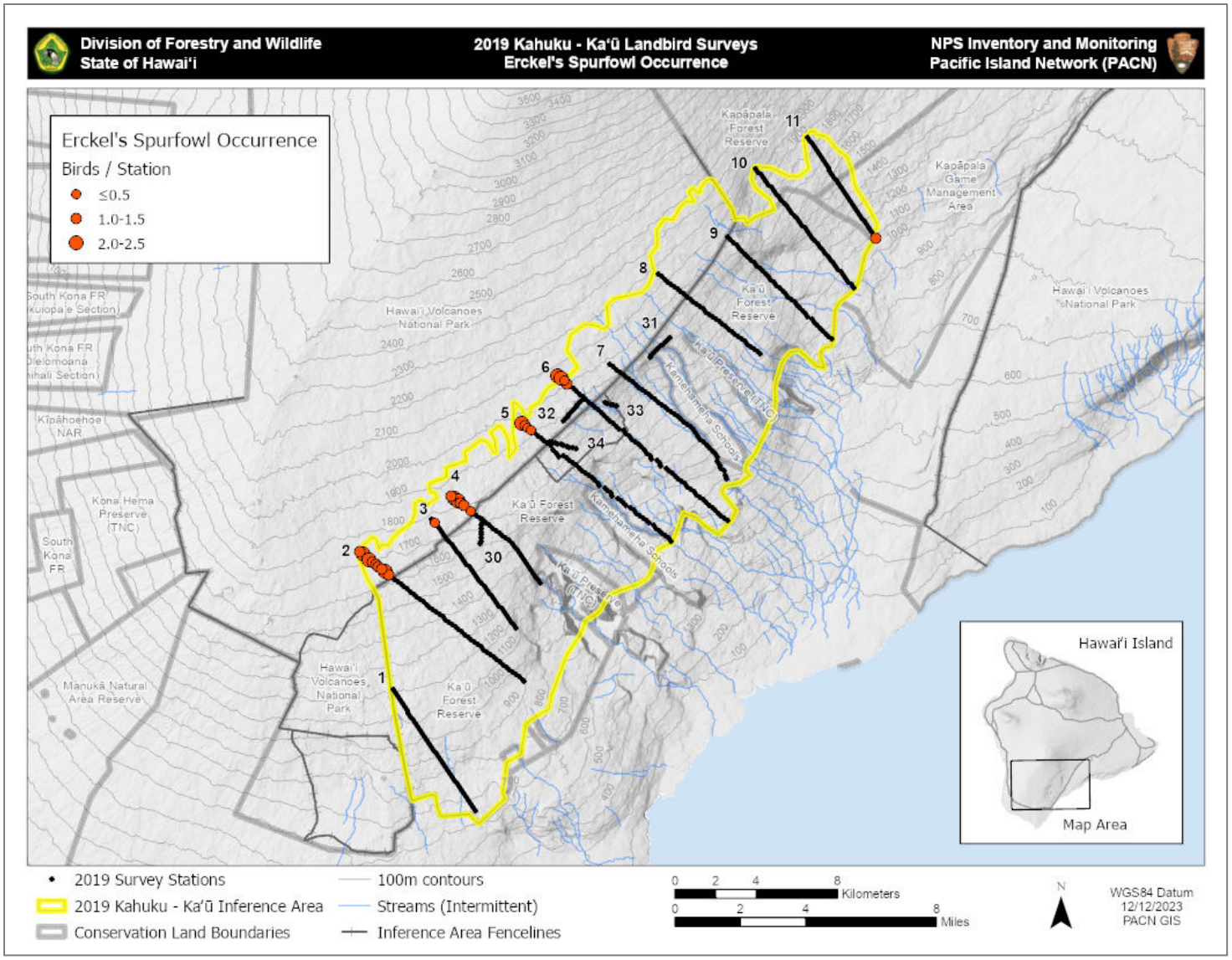



**Figure 29.** Erckel's Spurfowl (*Pternistis erckelii*) detections during the 2019 Ka'ū Rainforest landbird survey. The number of birds per station was divided by the number of counts at each station where species was detected.

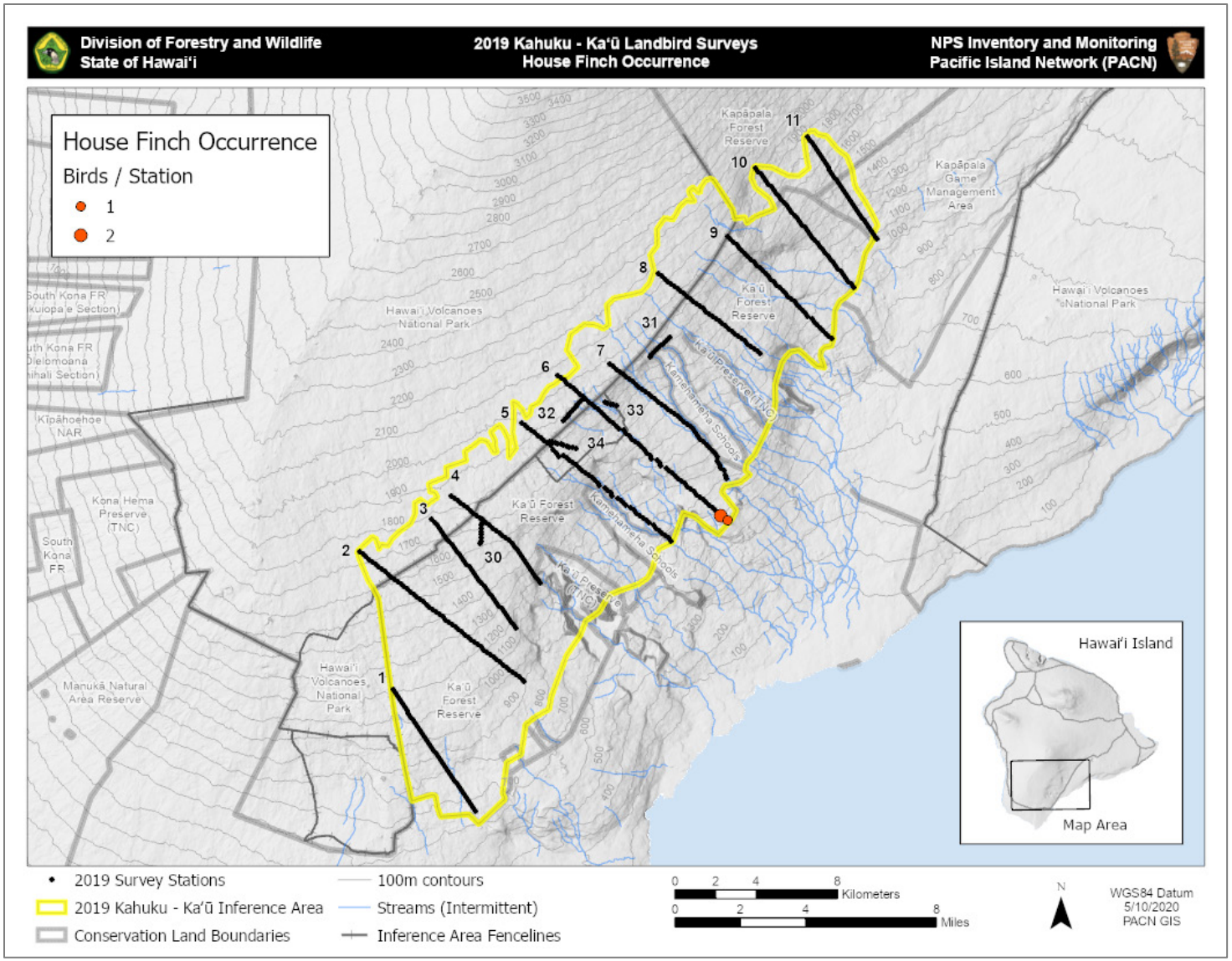



**Figure 30.** House Finch (*Haemorhous mexicanus*) detections during the 2019 Ka‘ū Rainforest landbird survey.

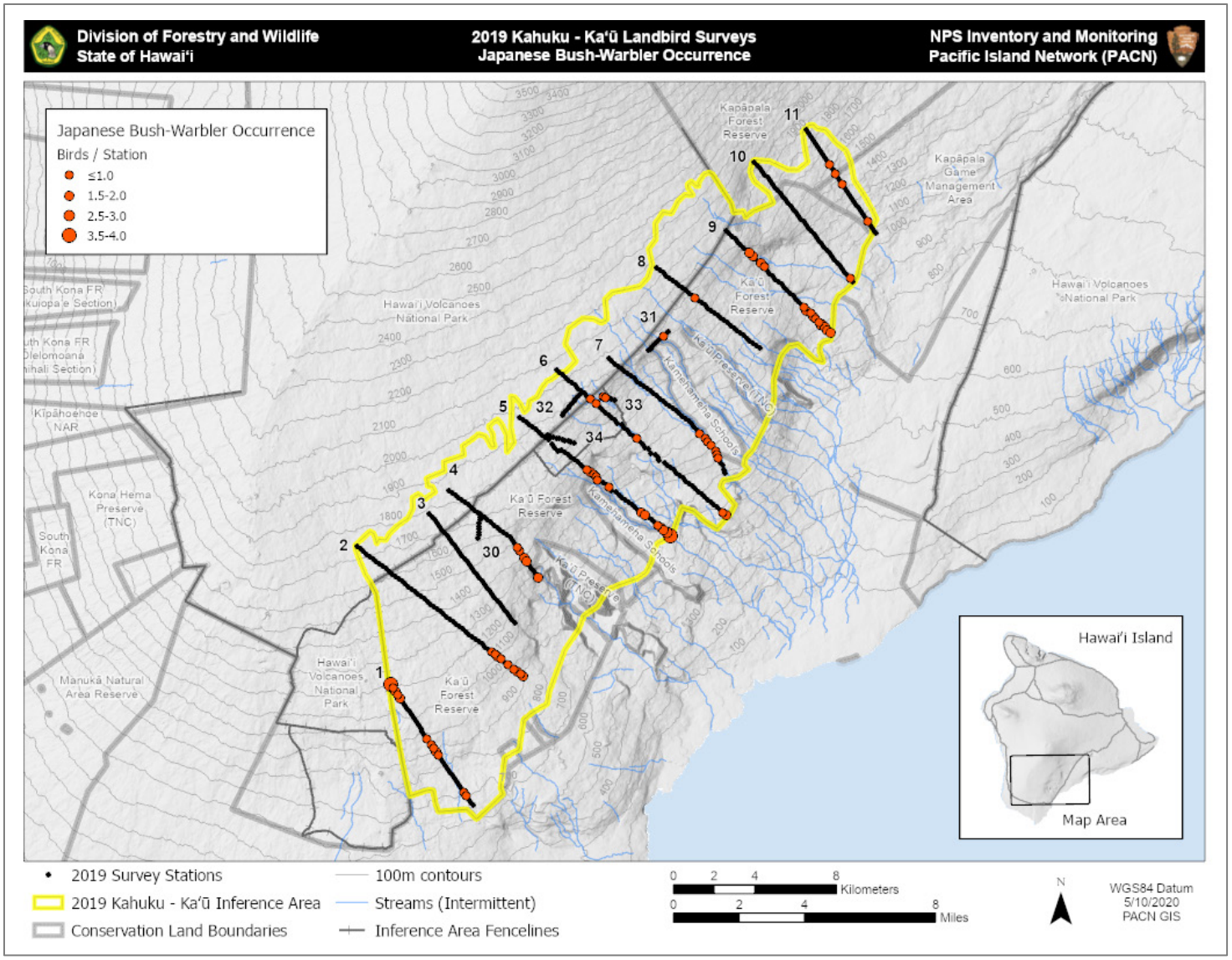



**Figure 31.** Japanese Bush Warbler (*Horornis diphone*) detections during the 2019 Ka‘ū Rainforest landbird survey. The number of birds per station was divided by the number of counts at each station where species was detected.

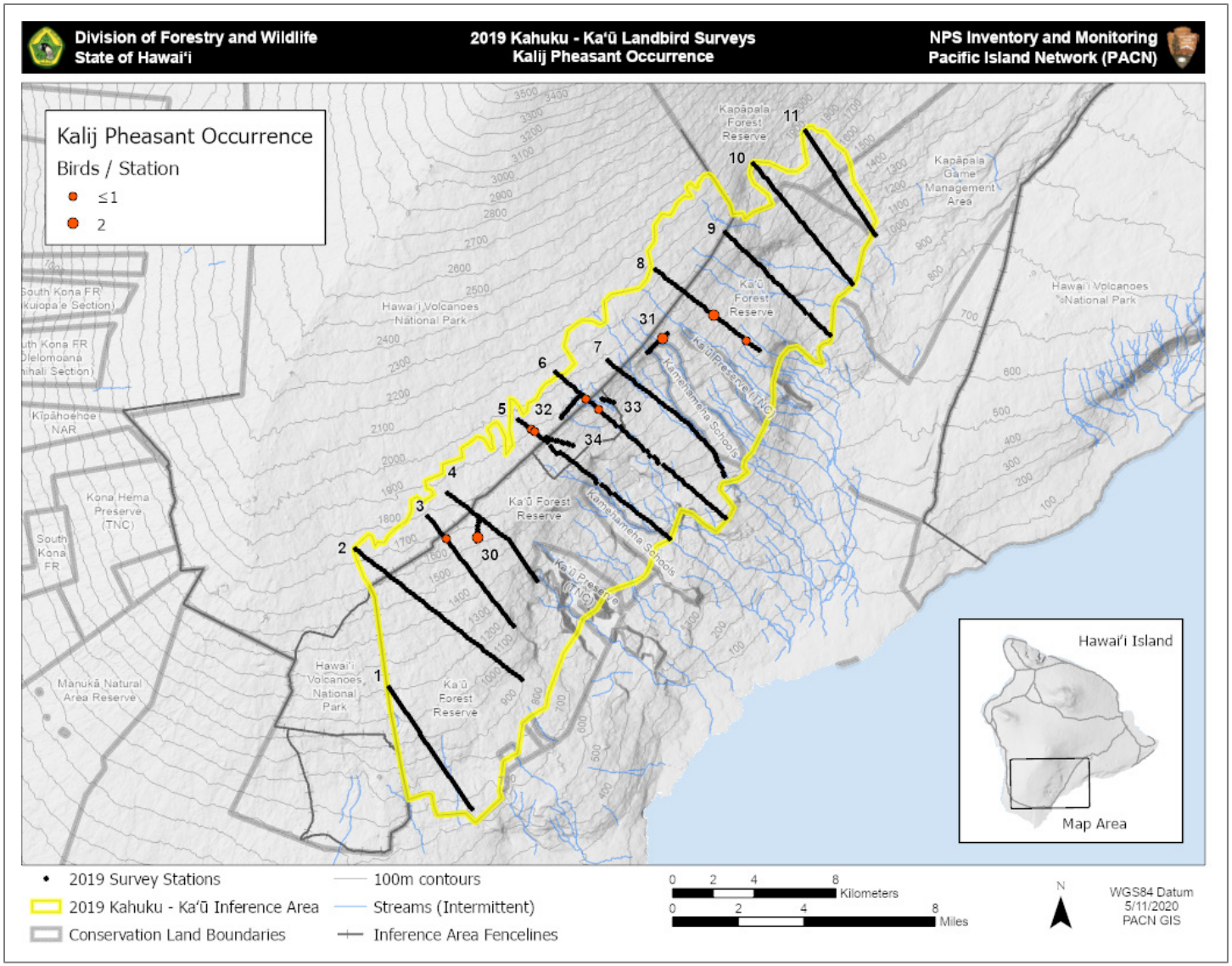



**Figure 32.** Kalij Pheasant (*Lophura leucomelanos*) detections during the 2019 Ka'ū Rainforest landbird survey. The number of birds per station was divided by the number of counts at each station where species was detected. The number of birds per station was divided by the number of counts at each station where species was detected.

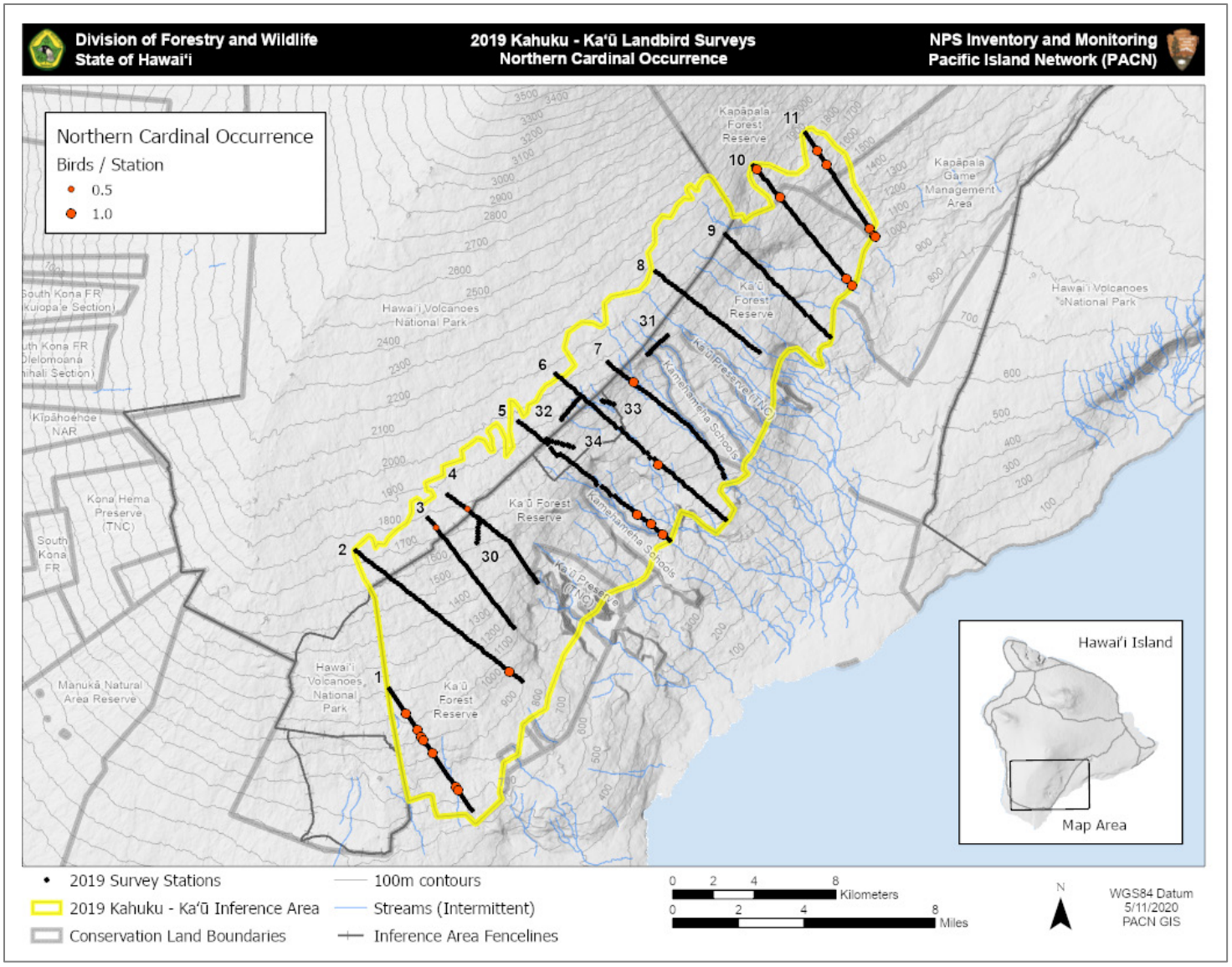



**Figure 33.** Northern Cardinal (*Cardinalis cardinalis*) detections during the 2019 Ka'ū Rainforest landbird survey. The number of birds per station was divided by the number of counts at each station where species was detected.

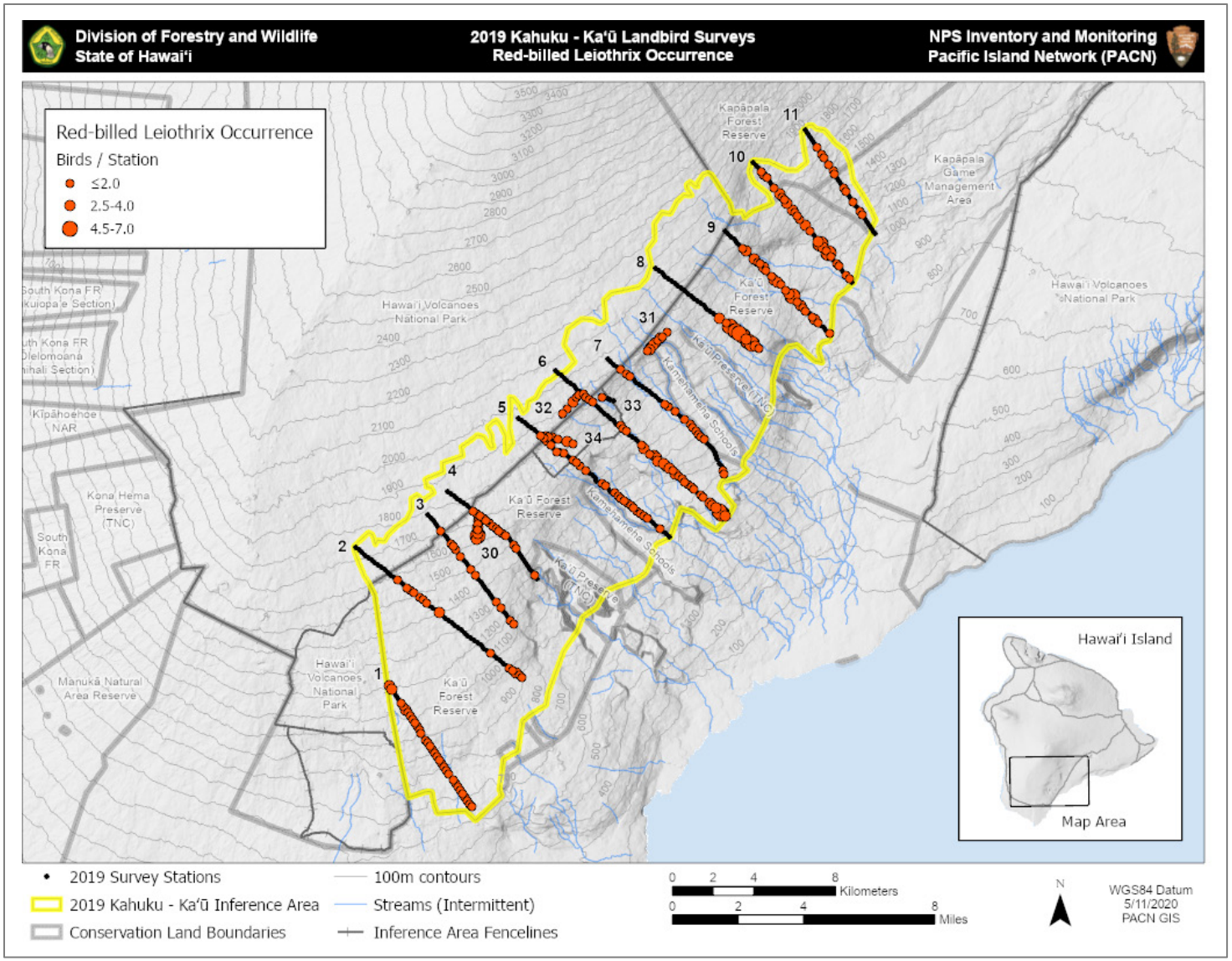



**Figure 34.** Red-billed Leiothrix (*Leiothrix lutea*) detections during the 2019 Kaʻū Rainforest landbird survey. The number of birds per station was divided by the number of counts at each station where species was detected.

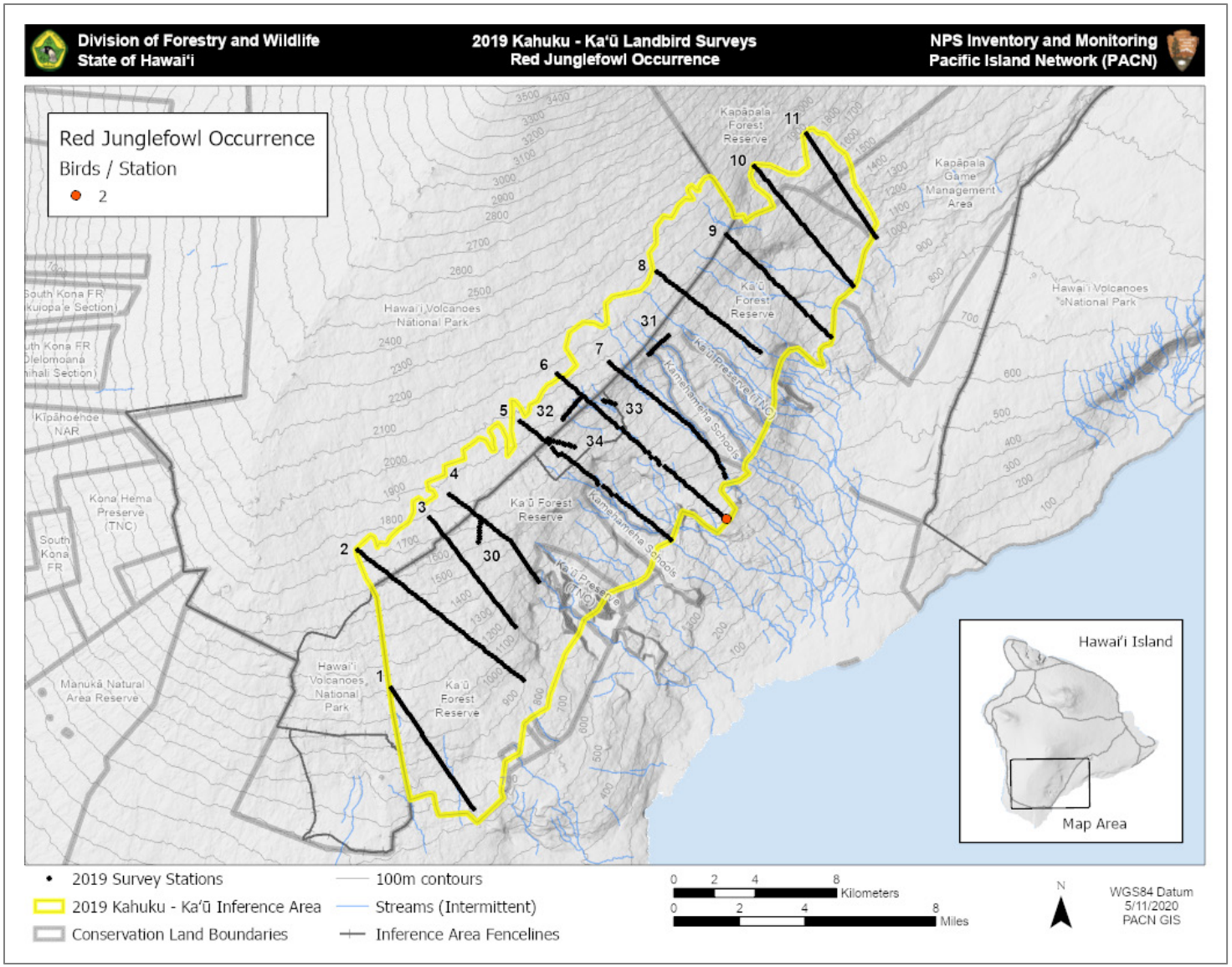



**Figure 35.** Red Junglefowl (*Gallus gallus*) detections during the 2019 Ka'ū Rainforest landbird survey.

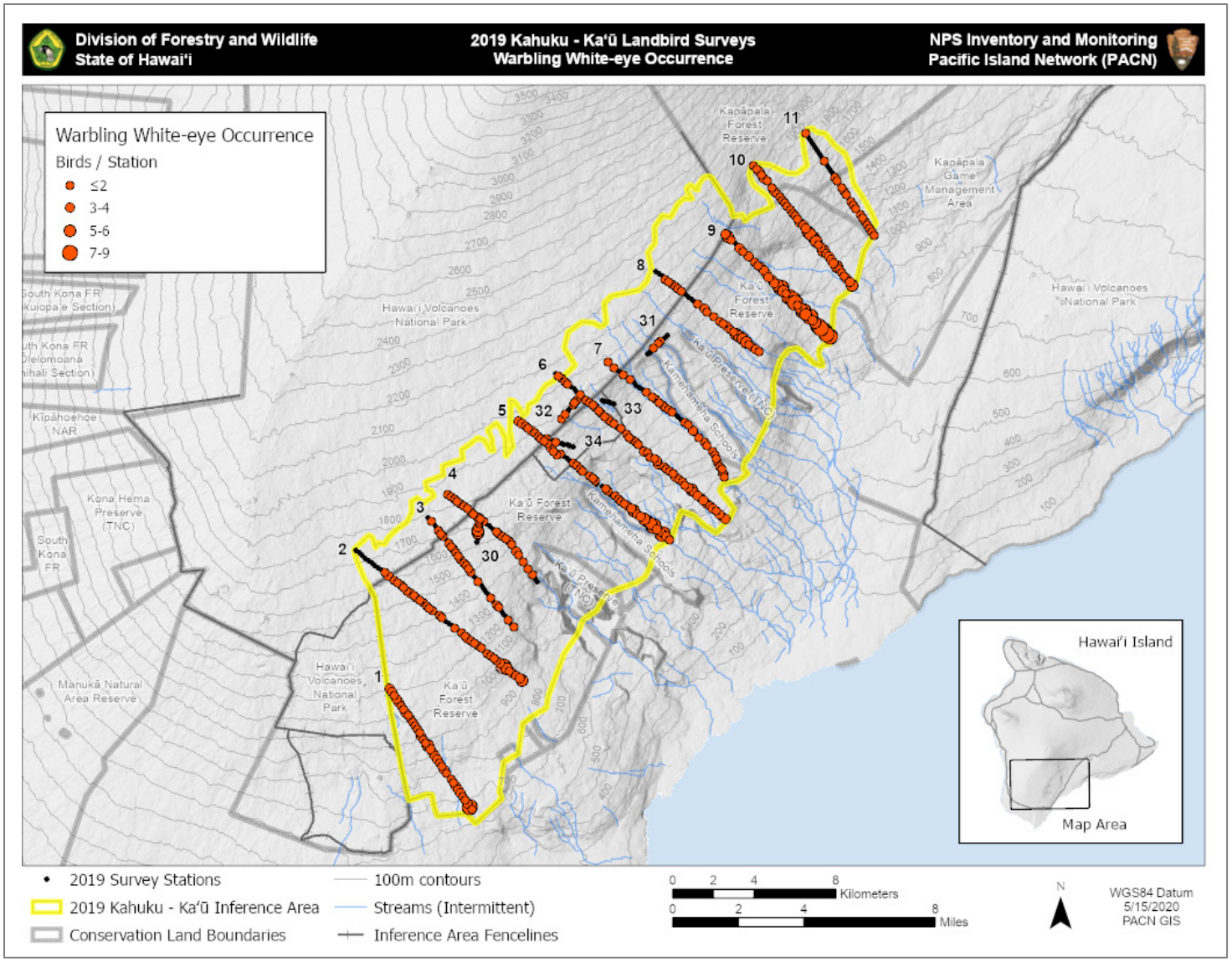



**Figure 36.** Warbling White-eye (*Zosterops japonicus*) detections during the 2019 Ka‘ū Rainforest landbird survey. The number of birds per station was divided by the number of counts at each station where species was detected.

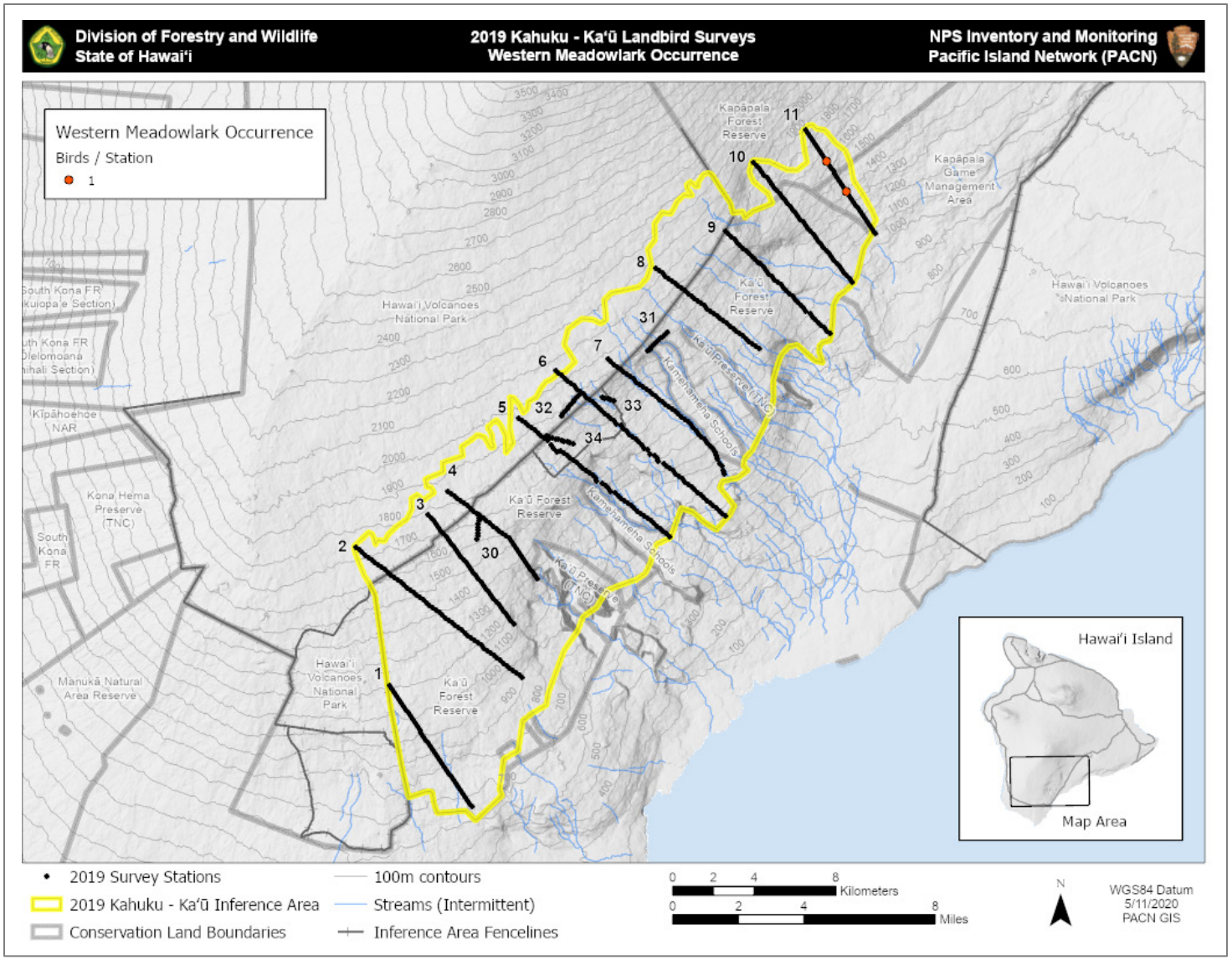



**Figure 37.** Western Meadowlark (*Sturnella neglecta*) detections during the 2019 Ka'ū Rainforest landbird survey.

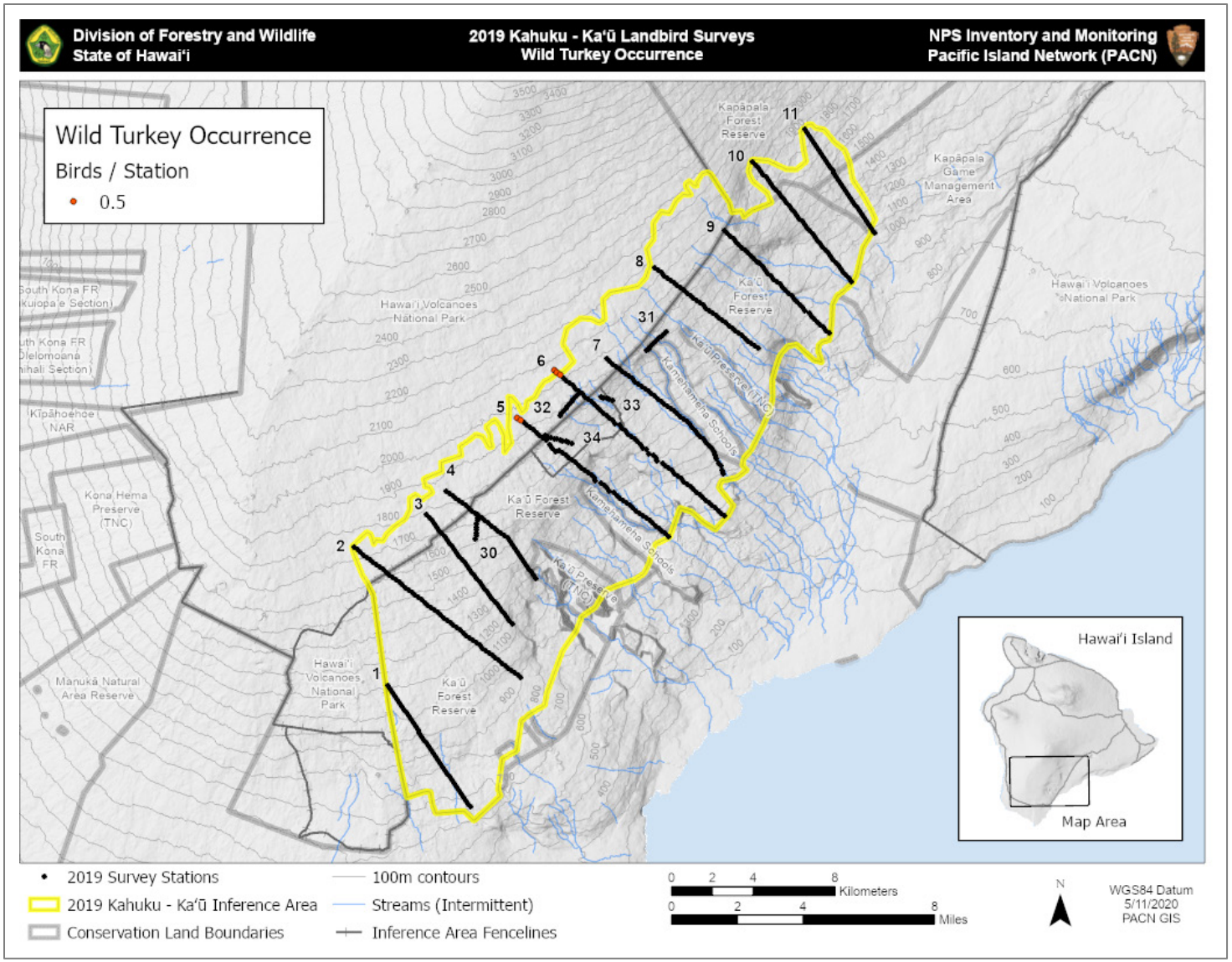



**Figure 38.** Wild Turkey (*Meleagris gallopavo*) detections during the 2019 Ka'ū Rainforest landbird survey. The number of birds per station was divided by the number of counts at each station where species was detected.

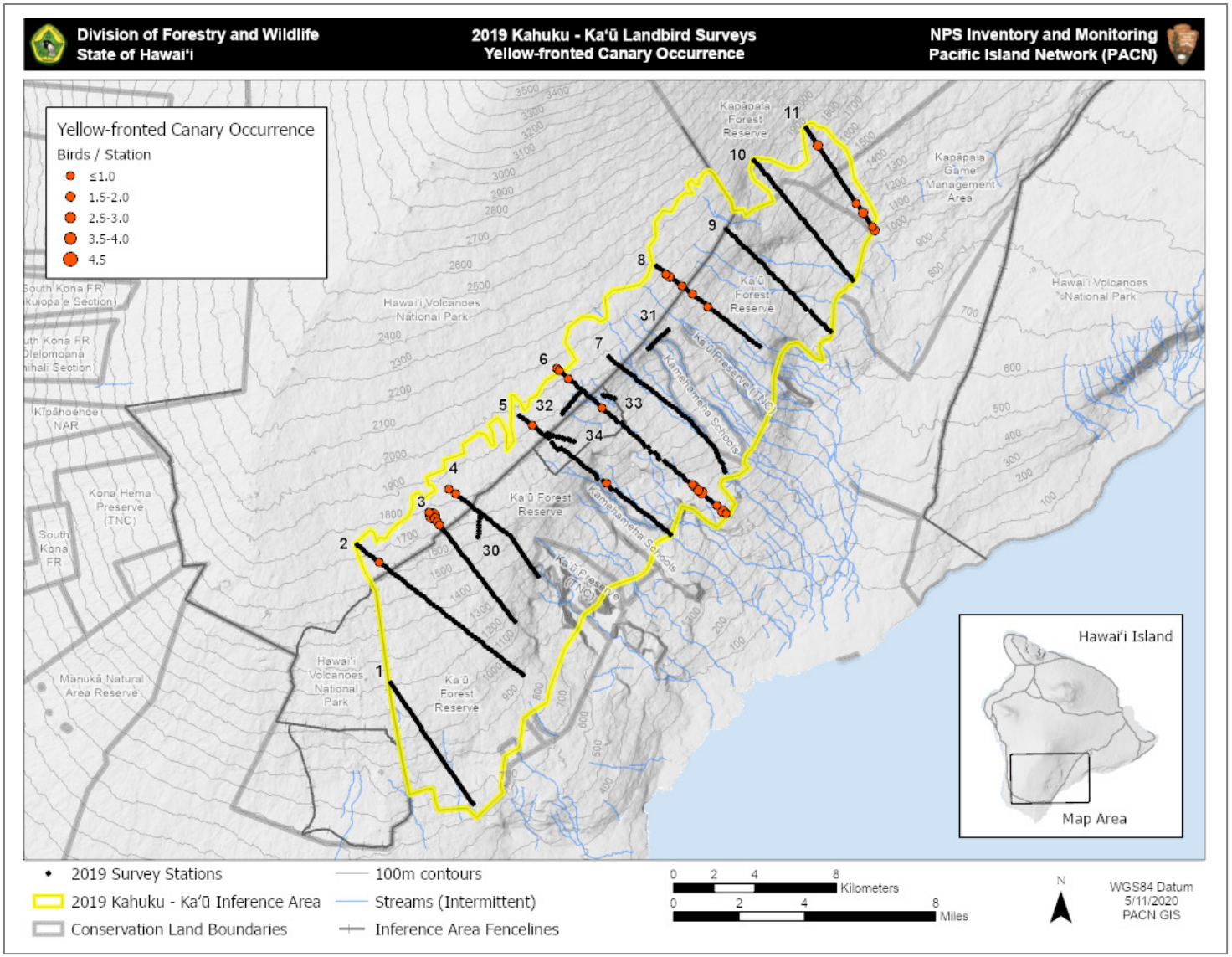



**Figure 39.** Yellow-fronted Canary (*Crithagra mozambica*) detections during the 2019 Ka'ū Rainforest landbird survey. The number of birds per station was divided by the number of counts at each station where species was detected.

# Appendix F. Kaʻū Rainforest Landbird Trend Graphics

Figures 40–50 show the trends observed for the Kaʻū rainforest landbirds.

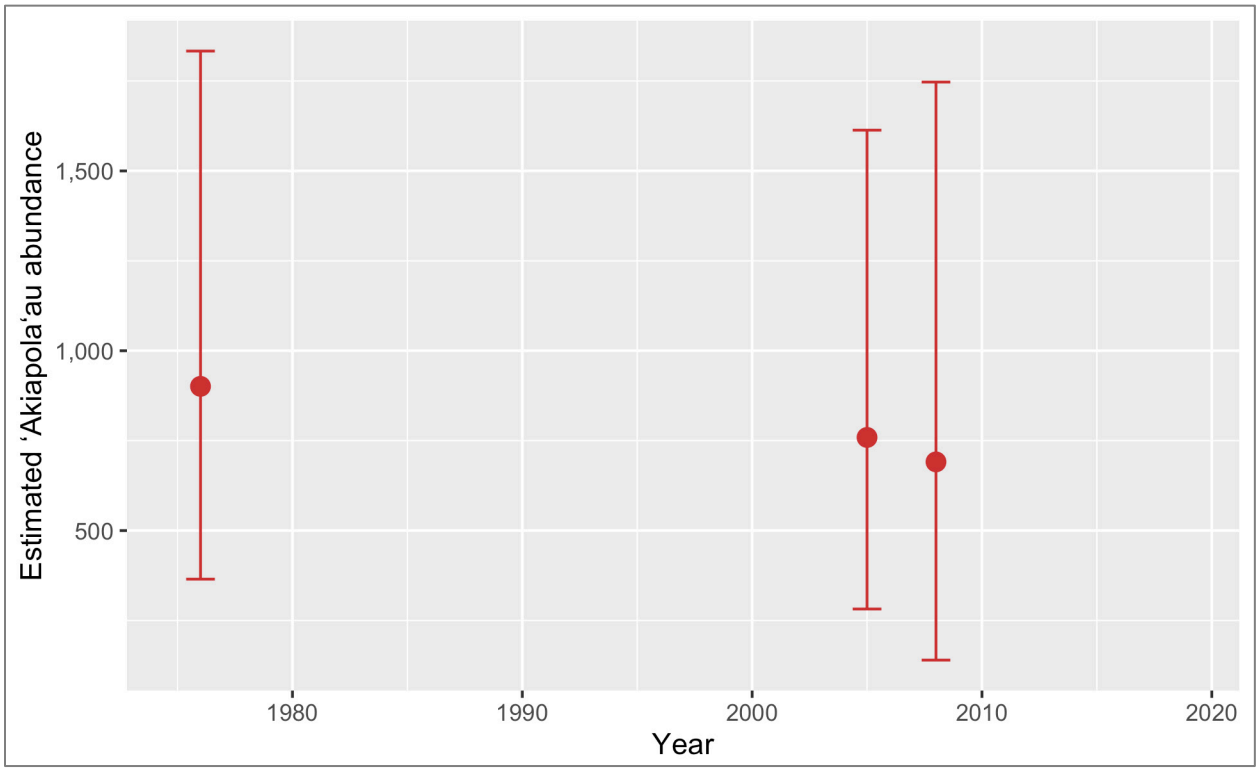



**Figure 40.** ʻAkiapōlāʻau (*Hemignathus wilsoni*) population estimates from surveys conducted in the Kaʻū Rainforest from 1976 to 2019. Point estimates are shown with 95% confidence intervals derived from bootstrap procedures. Estimates are for the species' range assuming a uniform density throughout.

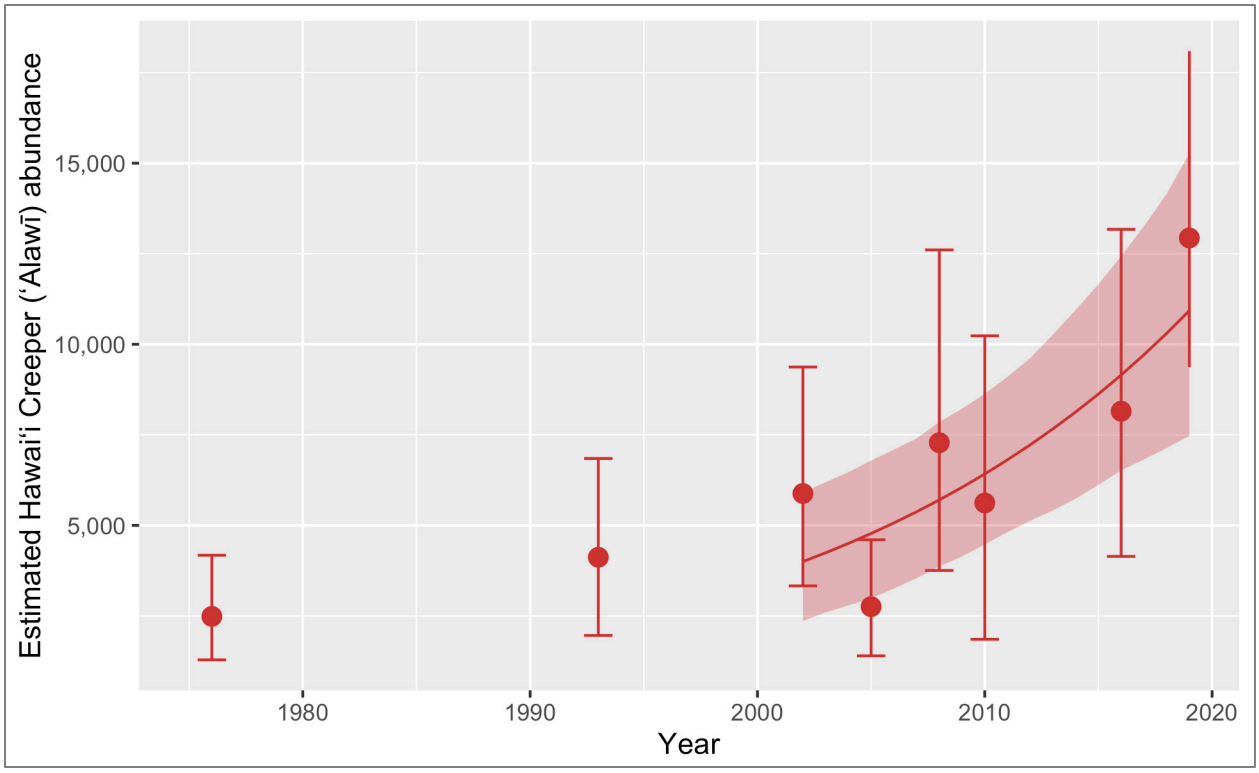



**Figure 41.** ʻAlawī (*Loxops mana*) population estimates from 1976 to 2019 and trends from 2002 to 2019. Point estimates are shown with 95% bootstrap uncertainty boundaries, along with log-linear trendlines and shaded 95% bootstrap confidence envelopes. Estimates and trend are for the species' range assuming a uniform density throughout.

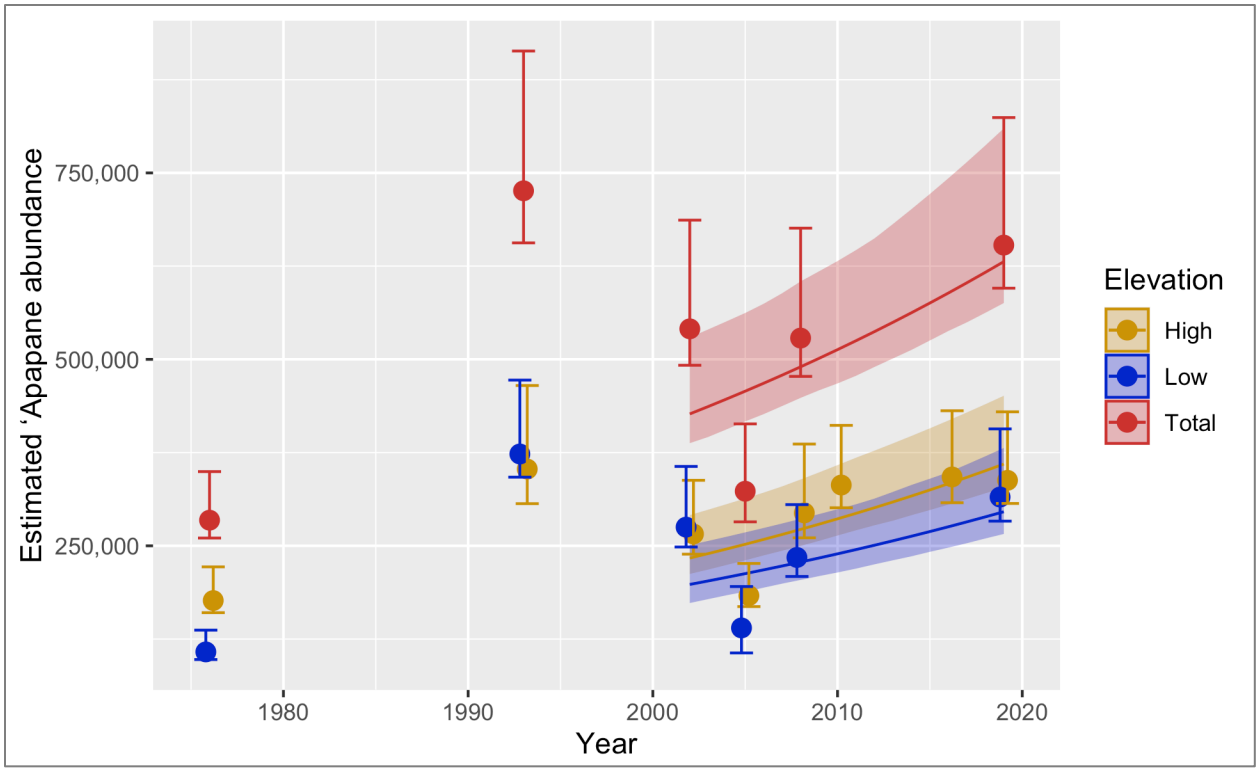



**Figure 42.** ‘Apapane (*Himatione sanguinea*) population estimates from 1976 to 2019 and trends from 2002 to 2019. Point estimates are shown with 95% bootstrap uncertainty boundaries, along with log-linear trendlines and shaded 95% bootstrap confidence envelopes. Blue color indicates estimates for the population in the low elevation stratum (<1,500 m) and yellow indicates the high elevation stratum (≥1,500 m). The red color indicates estimates and trend for the entire survey area assuming a uniform density throughout.

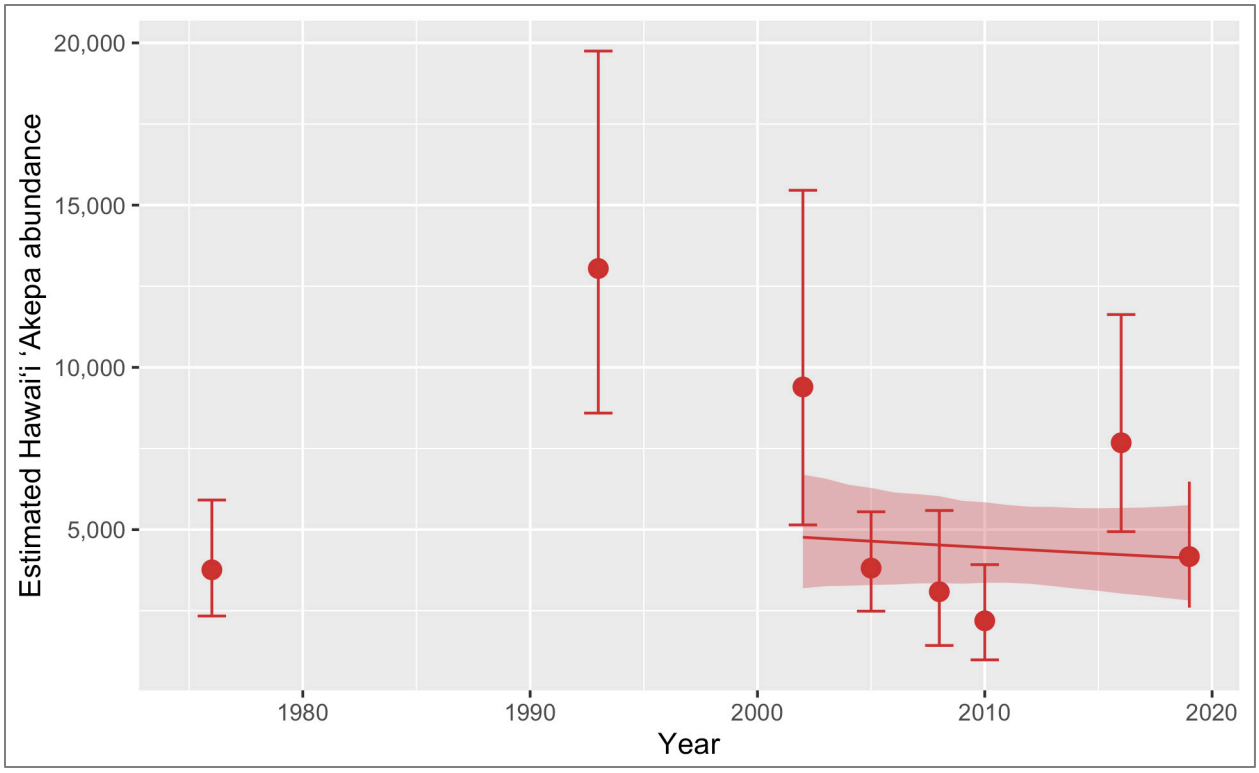



**Figure 43.** Hawai'i 'Ākepa (*Loxos coccineus*) population estimates from 1976 to 2019 and trends from 2002 to 2019. Point estimates are shown with 95% bootstrap uncertainty boundaries, along with log-linear trendlines and shaded 95% bootstrap confidence envelopes. Estimates and trend are for the species' range assuming a uniform density throughout.

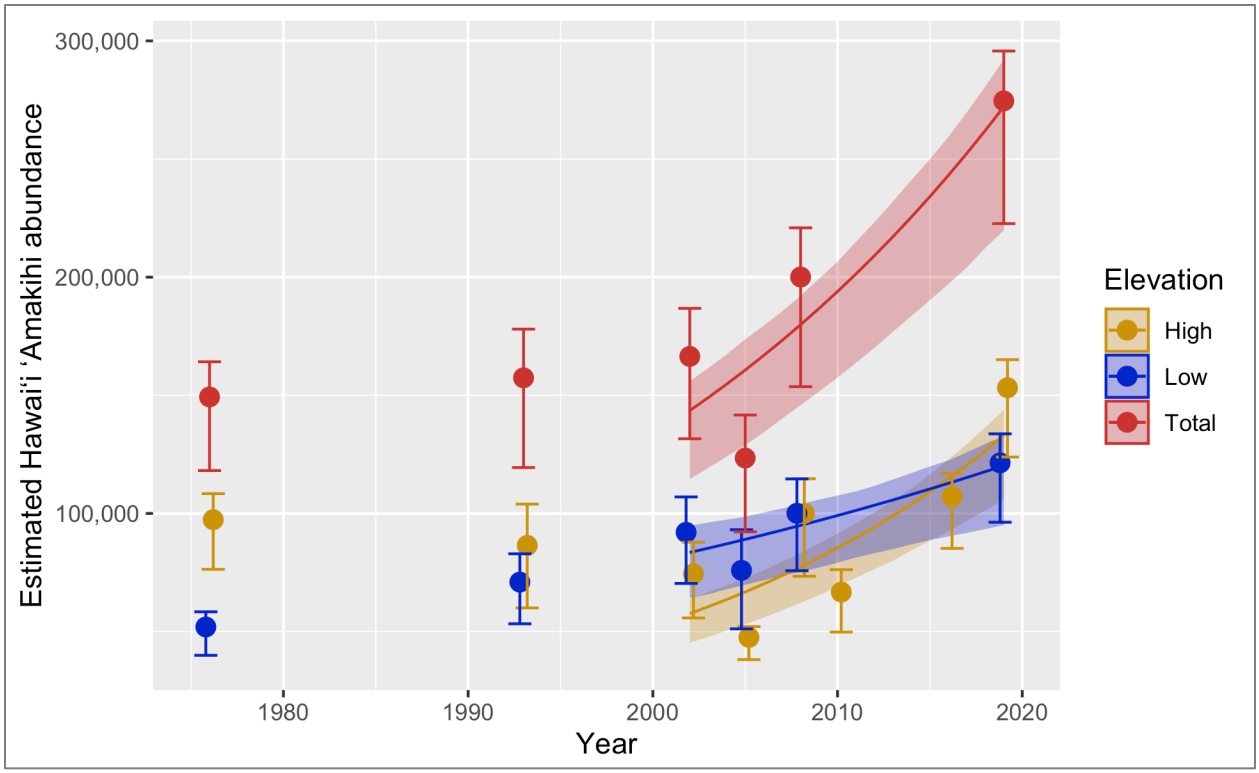



**Figure 44.** Hawai'i 'Amakihi (*Chlorodrepanis virens virens*) population estimates from 1976 to 2019 and trends from 2002 to 2019. Point estimates are shown with 95% bootstrap uncertainty boundaries, along with log-linear trendlines and shaded 95% bootstrap confidence envelopes. Blue color indicates estimates for the population in the low elevation stratum (<1,500 m) and yellow indicates the high elevation stratum (≥1,500 m). The red color indicates estimates and trend for the entire survey area assuming a uniform density throughout.

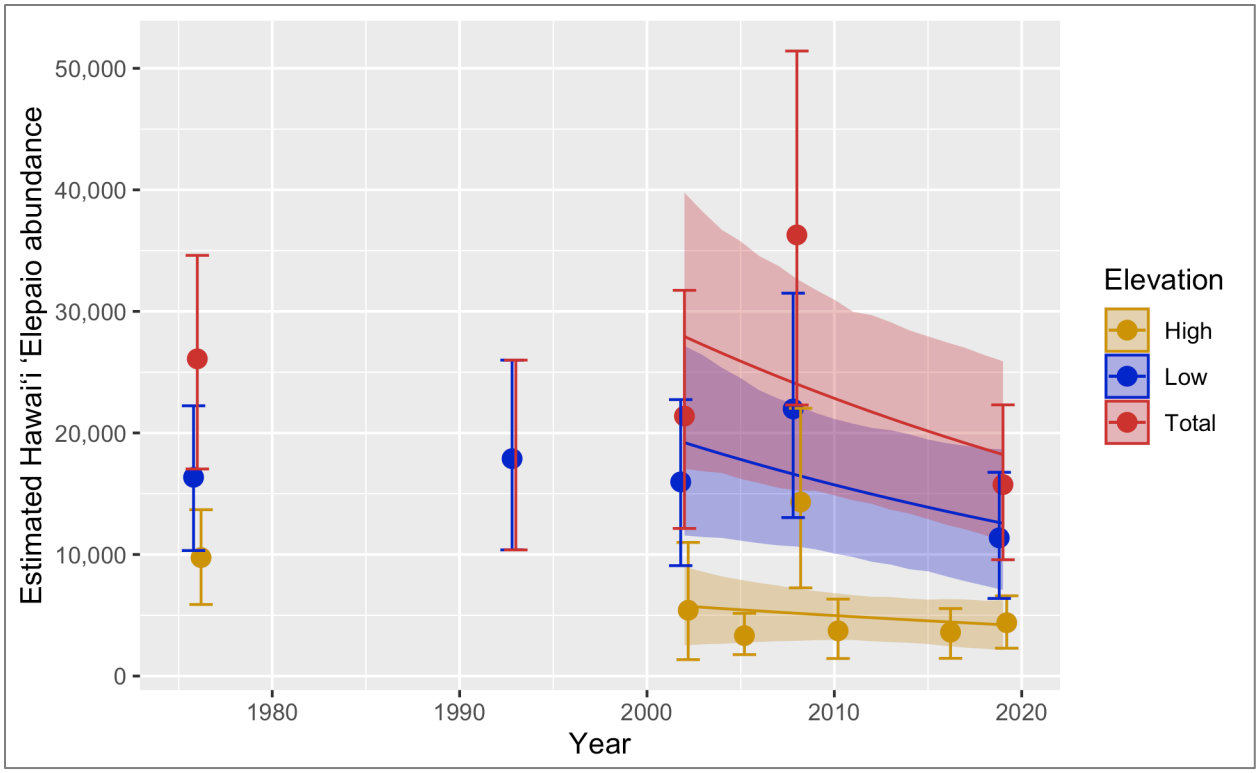



**Figure 45.** Hawai'i 'Elepaio (*Chasiempis sandwichensis*) population estimates from 1976 to 2019 and trends from 2002 to 2019. Point estimates are shown with 95% bootstrap uncertainty boundaries, along with log-linear trendlines and shaded 95% bootstrap confidence envelopes. Blue color indicates estimates for the population in the low elevation stratum (<1,500 m) and yellow indicates the high elevation stratum (≥1,500 m). The red color indicates estimates and trend for the entire survey area assuming a uniform density throughout.

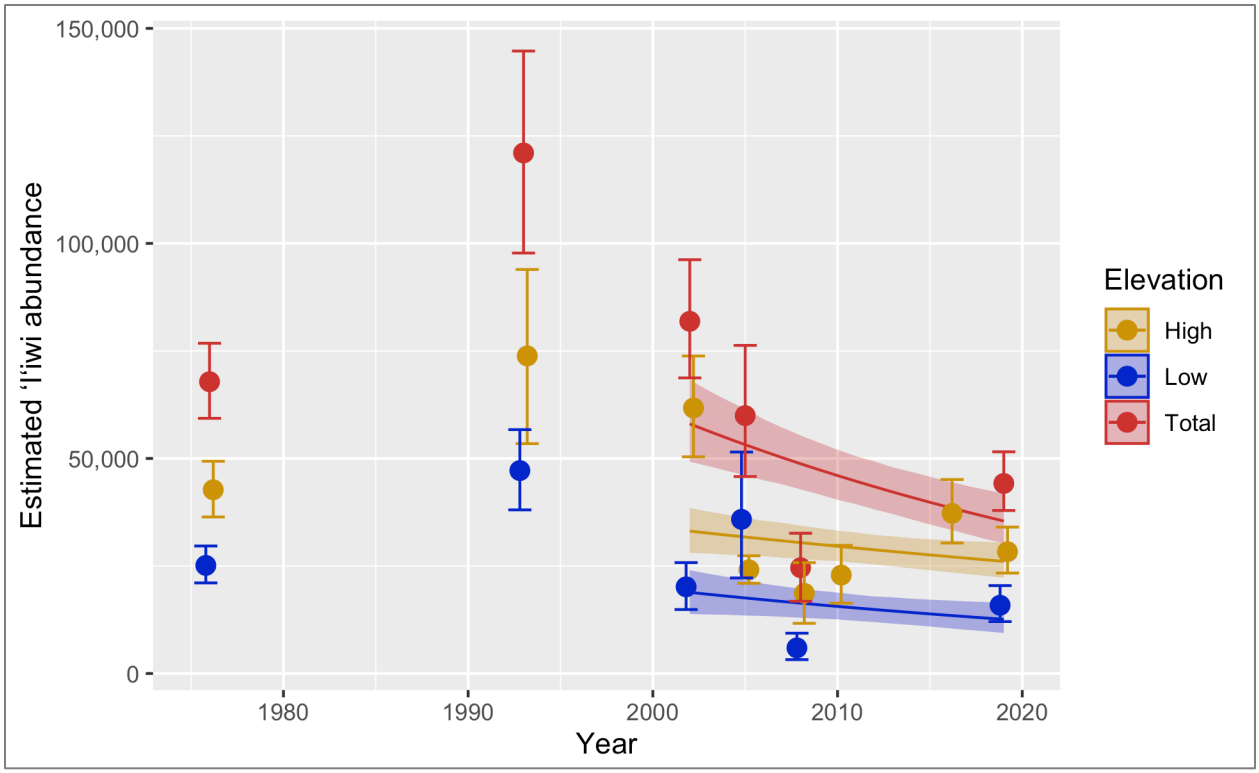



**Figure 46.** ʻIʻiwi (*Drepanis coccinea*) population estimates from 1976 to 2019 and trends from 2002 to 2019. Point estimates are shown with 95% bootstrap uncertainty boundaries, along with log-linear trendlines and shaded 95% bootstrap confidence envelopes. Blue color indicates estimates for the population in the low elevation stratum (<1,500 m) and yellow indicates the high elevation stratum (≥1,500 m). The red color indicates estimates and trend for the entire survey area assuming a uniform density throughout.

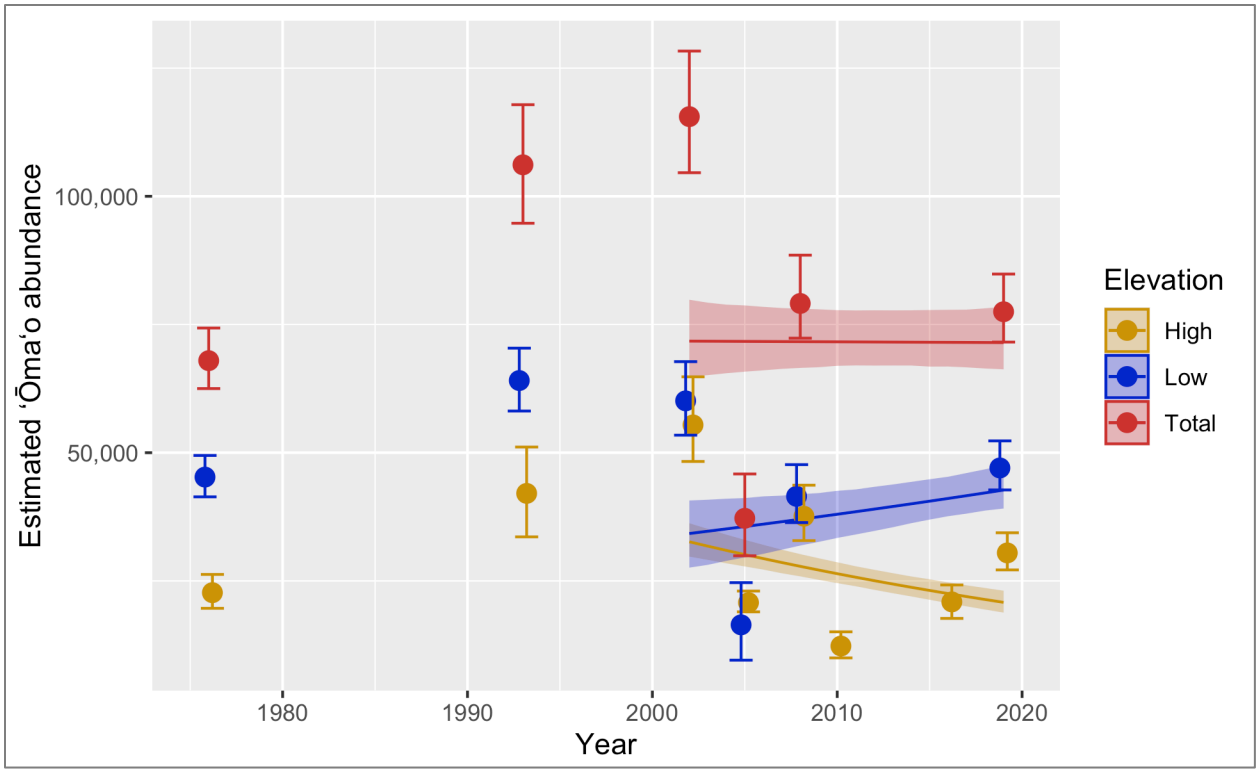



**Figure 47.** ʻŌmaʻo (*Myadestes obscurus*) population estimates from 1976 to 2019 and trends from 2002 to 2019. Point estimates are shown with 95% bootstrap uncertainty boundaries, along with log-linear trendlines and shaded 95% bootstrap confidence envelopes. Blue color indicates estimates for the population in the low elevation stratum (<1,500 m) and yellow indicates the high elevation stratum (≥1,500 m). The red color indicates estimates and trend for the entire survey area assuming a uniform density throughout.

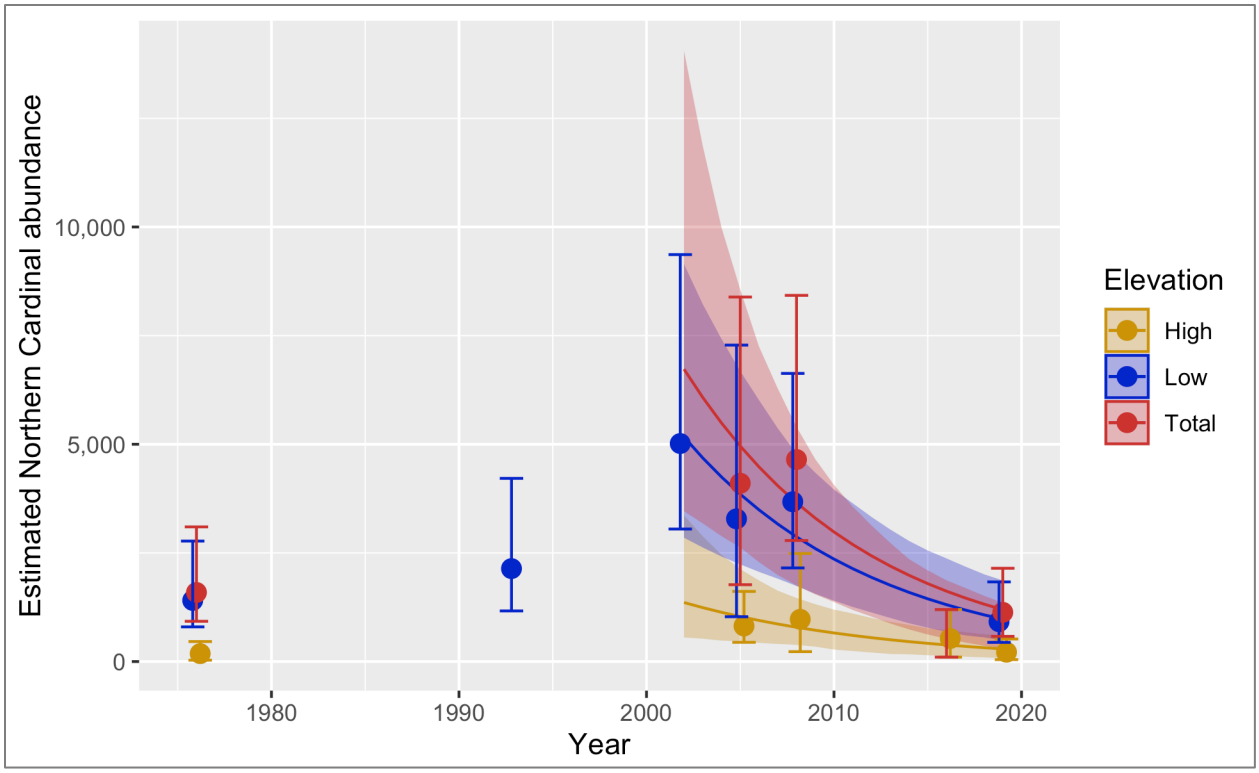



**Figure 48.** Northern Cardinal (*Cardinalis cardinalis*) population estimates from 1976 to 2019 and trends from 2002 to 2019. Point estimates are shown with 95% bootstrap uncertainty boundaries, along with log-linear trendlines and shaded 95% bootstrap confidence envelopes. Blue color indicates estimates for the population in the low elevation stratum (<1,500 m) and yellow indicates the high elevation stratum (≥1,500 m). The red color indicates estimates and trend for the entire survey area assuming a uniform density throughout.

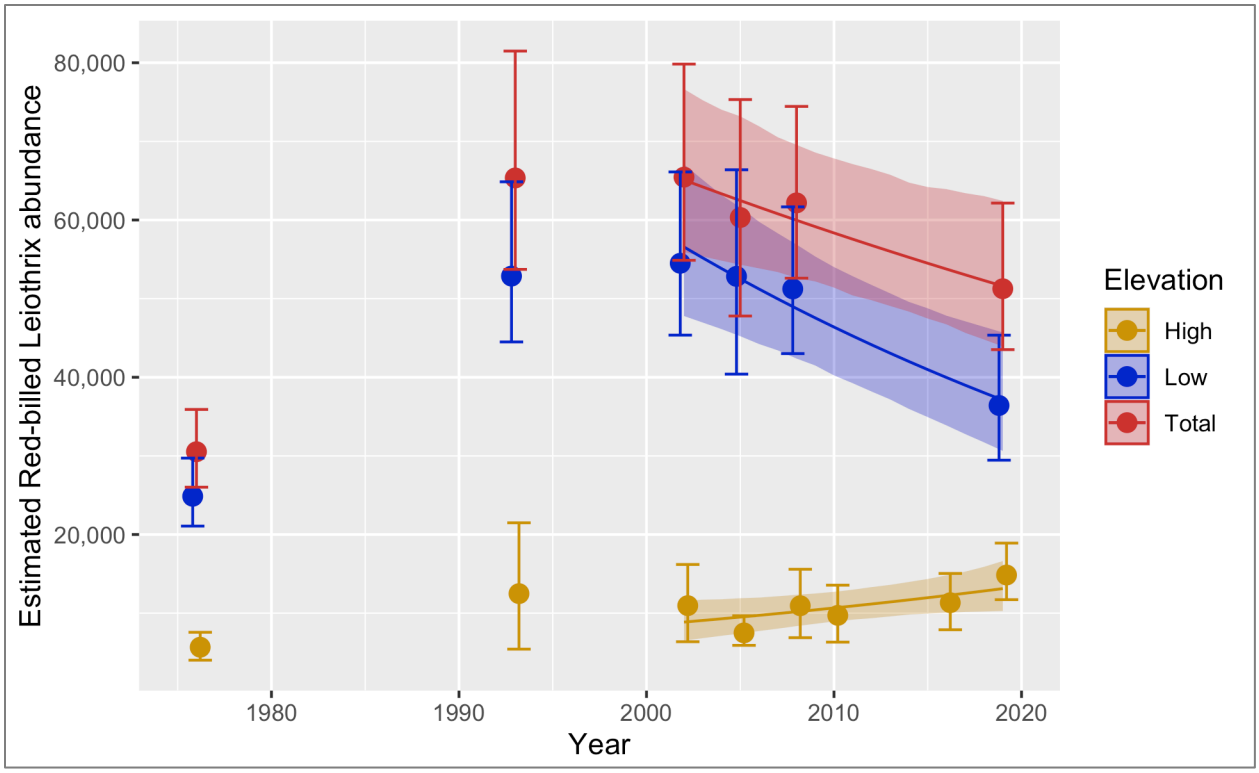



**Figure 49.** Red-billed Leiothrix (*Leiothrix lutea*) trends population estimates from 1976 to 2019 and from 2002 to 2019. Point estimates are shown with 95% bootstrap uncertainty boundaries, along with log-linear trendlines and shaded 95% bootstrap confidence envelopes. Blue color indicates estimates for the population in the low elevation stratum (<1,500 m) and yellow indicates the high elevation stratum (≥1,500 m). The red color indicates estimates and trend for the entire survey area assuming a uniform density throughout.

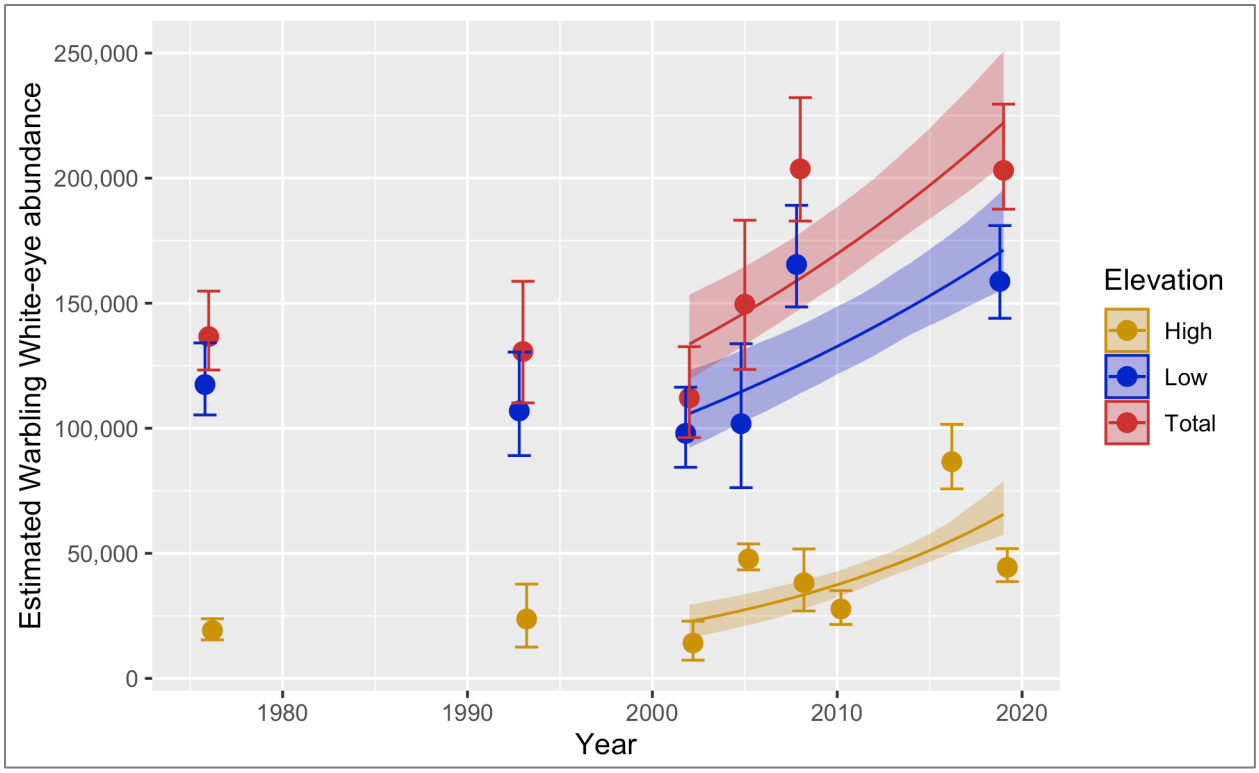



**Figure 50.** Warbling White-eye (*Zosterops japonicus*) population estimates from 1976 to 2019 and trends from 2002 to 2019. Point estimates are shown with 95% bootstrap uncertainty boundaries, along with log-linear trendlines and shaded 95% bootstrap confidence envelopes. Blue color indicates estimates for the population in the low elevation stratum (<1,500 m) and yellow indicates the high elevation stratum (≥1,500 m). The red color indicates estimates and trend for the entire survey area assuming a uniform density throughout.

# Appendix G. 2019 Habitat Survey Results

Tables 44–48 and Figures 51–56 show the habitat survey results for 2019.

**Table 44.** Moisture zones of 2019 Kaʻū Rainforest survey stations per each study area. Classifications were determined post hoc by examining the vegetation maps provided by Jacobi (1989) and Green et al. (2015). Moisture zone limits were defined by Wagner et al. (1991). The percent of classes recorded per each management area and per total stations surveyed are presented.

| Survey Area | Moisture Zone (annual rainfall) | Count | % |
|---|---|---|---|
| Hawaiʻi Volcanoes National Park (Kahuku Unit) | Dry (<1,200 mm) | 31 | 44.3% |
| | Mesic (1,200–2,500 mm) | 37 | 52.9% |
| | Wet (>2,500 mm) | 2 | 2.9% |
| Kapāpala Cooperative Game Management Area | Dry (<1,200 mm) | 0 | 0.0% |
| | Mesic (1,200–2,500 mm) | 17 | 89.5% |
| | Wet (>2,500 mm) | 0 | 0.0% |
| | Unknown | 2 | 10.5% |
| Kapāpala Forest Reserve | Dry (<1,200 mm) | 14 | 56.0% |
| | Mesic (1,200–2,500 mm) | 11 | 44.0% |
| | Wet (>2,500 mm) | 0 | 0.0% |
| Kaʻū Forest Reserve | Dry (<1,200 mm) | 3 | 0.8% |
| | Mesic (1,200–2,500 mm) | 35 | 9.4% |
| | Wet (>2,500 mm) | 324 | 87.3% |
| | Unknown | 9 | 2.4% |
| Kaʻū Preserve (The Nature Conservancy) | Dry (<1,200 mm) | 0 | 0.0% |
| | Mesic (1,200–2,500 mm) | 0 | 0.0% |
| | Wet (>2,500 mm) | 3 | 100% |
| | Unknown | 0 | 0.0% |
| **Total** | **Dry (<1,200 mm)** | **48** | **9.8%** |
| | **Mesic (1,200–2,500 mm)** | **100** | **20.5%** |
| | **Wet (>2,500 mm)** | **329** | **67.4%** |
| | **Unknown** | **11** | **2.3%** |
| **Grand Total** | **N/A** | **488** | **N/A** |

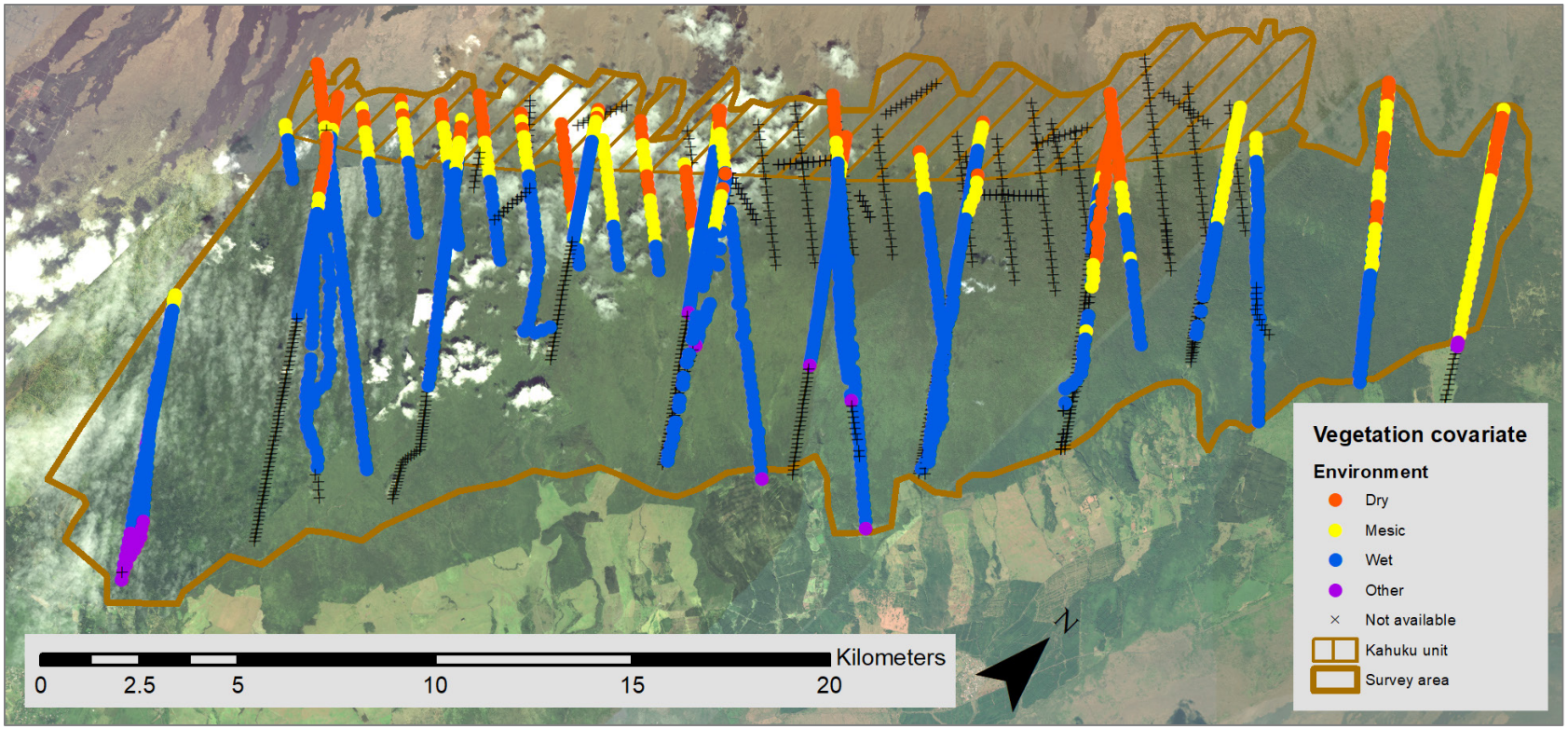



**Figure 51.** Environment classifications recorded at stations surveyed in 2019 and in previous years. Stations that were classified as dry, mesic (moist), wet, or other. “Other” categories were stations classified as straddling two categories.

**Table 45.** Canopy height and cover classes recorded during the 2019 Kaʻū Rainforest Survey. The sum of each class recorded at each survey station are provided per survey area and for the total survey area.

| 2019 Survey Area | Canopy Height Class | Count of Height Class | % | Cover Class | Count of Cover Class | % |
|---|---|---|---|---|---|---|
| Hawaiʻi Volcanoes National Park (Kahuku Unit) | 2-5 m | 11 | 15.7% | Closed | 22 | 31.4% |
| | 6-10 m | 40 | 57.1% | Open | 31 | 44.3% |
| | > 10 m | 19 | 27.1% | Scattered | 10 | 14.3% |
| | – | – | – | Very Scattered | 7 | 10.0% |
| Kapāpala Cooperative Game Management Area | 2-5 m | 0 | 0.0% | Closed | 12 | 63.2% |
| | 6-10 m | 0 | 0.0% | Open | 7 | 36.8% |
| | > 10 m | 19 | 100.0% | Scattered | 0 | 0.0% |
| | – | – | – | Very Scattered | 0 | 0.0% |
| Kapāpala Forest Reserve | 2-5 m | 1 | 4.0% | Closed | 10 | 40.0% |
| | 6-10 m | 12 | 48.0% | Open | 5 | 20.0% |
| | > 10 m | 12 | 48.0% | Scattered | 10 | 40.0% |
| | – | – | – | Very Scattered | 0 | 0.0% |
| Kaʻū Forest Reserve | 2-5 m | 6 | 1.7% | Closed | 273 | 80.3% |
| | 6-10 m | 74 | 20.8% | Open | 55 | 16.2% |
| | > 10 m | 275 | 77.5% | Scattered | 8 | 2.4% |
| | – | – | – | Very Scattered | 4 | 1.2% |
| Kaʻū Preserve (The Nature Conservancy) | 2-5 m | 0 | 0.0% | Closed | 3 | 100.0% |
| | 6-10 m | 3 | 100.0% | Open | 0 | 0.0% |
| | > 10 m | 0 | 0.0% | Scattered | 0 | 0.0% |
| | – | – | – | Very Scattered | 0 | 0.0% |

**Table 45 (continued).** Canopy height and cover classes recorded during the 2019 Kaʻū Rainforest Survey. The sum of each class recorded at each survey station are provided per survey area and for the total survey area.

| 2019 Survey Area | Canopy Height Class | Count of Height Class | % | Cover Class | Count of Cover Class | % |
|---|---|---|---|---|---|---|
| Total | 2-5 m | 18 | 3.8% | Closed | 320 | 70.0% |
| | 6-10 m | 129 | 27.3% | Open | 98 | 21.4% |
| | > 10 m | 325 | 68.9% | Scattered | 28 | 6.1% |
| | – | – | – | Very Scattered | 11 | 2.4% |
| Grand Total | N/A | 472 | N/A | N/A | 457 | N/A |

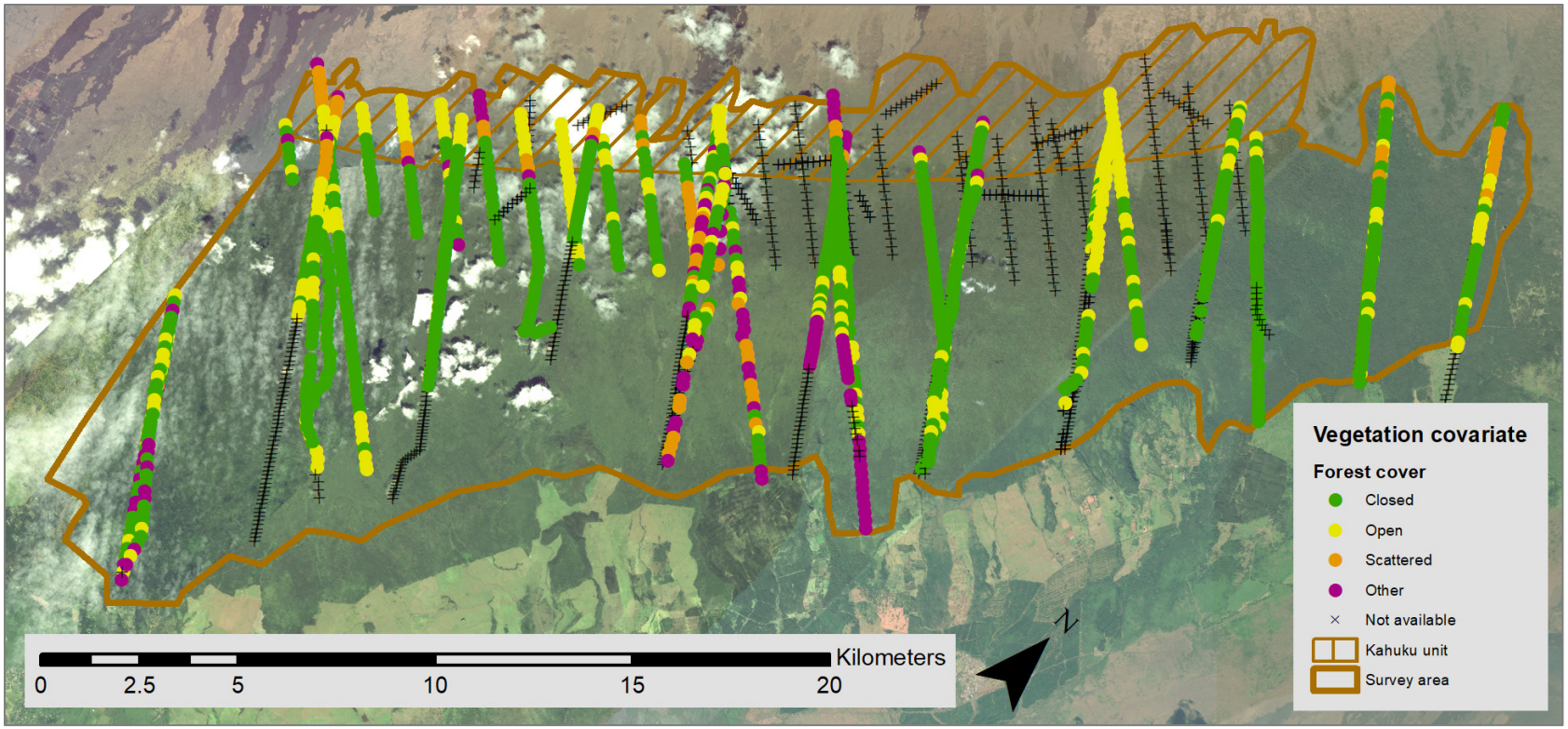



**Figure 52.** Forest cover classifications recorded at stations surveyed in 2019 and in previous years. Stations were classified as closed, scattered, open, or other. “Other” categories were stations classified as more than one structure.

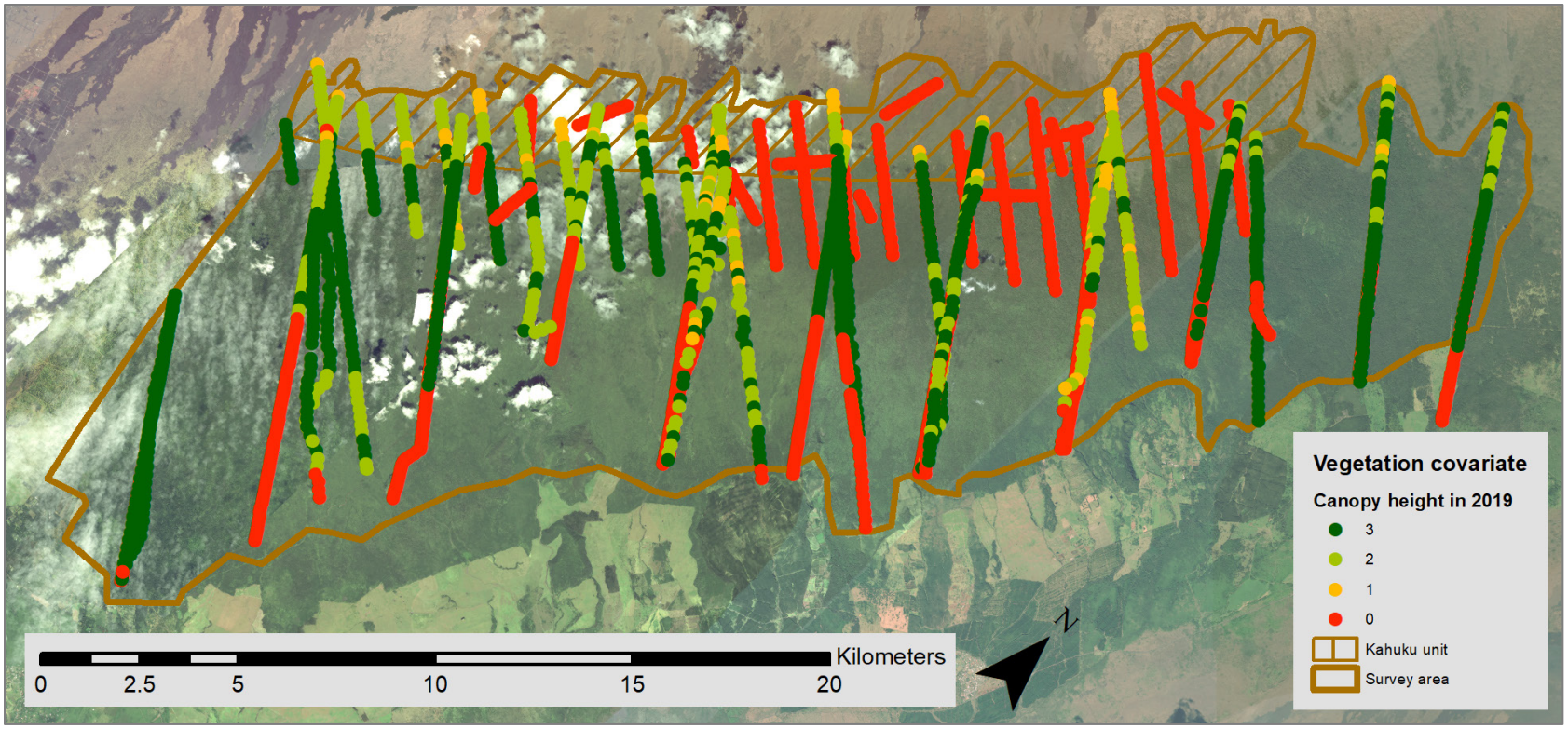



**Figure 53.** Canopy height classes recorded at each station during the 2019 Kaʻū Rainforest landbird survey and for transects surveyed in previous years. Canopy height classes: 3= >10 m, 2= 6–10 m, 1= ≤ 5 m, 0= not recorded or unknown (most stations in red on map were not surveyed in 2019).

**Table 46.** Dominant canopy classes recorded within each survey area during the 2019 Kaʻū Rainforest landbird survey. Tree species or grouped classes (e.g., Native trees) that are separated by a dash are codominant with the other species, meaning both occurred equally throughout the habitat plot around the survey station. Percent of each class recorded per survey area are presented.

| 2019 Survey Area | Dominant Canopy Class | Count | % |
|---|---|---|---|
| Hawaiʻi Volcanoes National Park (Kahuku Unit) | *Metrosideros polymorpha* | 70 | 100% |
| Kapāpala Cooperative Game Management Area | *Acacia koa-Metrosideros polymorpha* | 11 | 57.9% |
| | *Metrosideros polymorpha-Ilex anomala* | 3 | 15.8% |
| | *Metrosideros polymorpha* | 2 | 10.5% |
| | *Acacia koa* | 1 | 5.3% |
| | *Metrosideros polymorpha-Cheirodendron trigynum* | 1 | 5.3% |
| | *Metrosideros polymorpha-Myoporum sandwicense* | 1 | 5.3% |
| Kapāpala Forest Reserve | *Acacia koa-Metrosideros polymorpha* | 14 | 56% |
| | *Metrosideros polymorpha* | 10 | 40% |
| | *Acacia koa* | 1 | 4% |
| Kaʻū Forest Reserve | *Metrosideros polymorpha* | 311 | 86.1% |
| | *Metrosideros polymorpha-Cheirodendron trigynum* | 17 | 4.7% |
| | Unknown | 16 | 4.4% |
| | *Metrosideros polymorpha-Acacia koa* | 3 | 0.8% |
| | *Acacia koa* | 5 | 1.4% |
| | *Metrosideros polymorpha*-Native ferns | 2 | 0.6% |
| | *Metrosideros polymorpha-Ilex anomala* | 2 | 0.6% |
| | *Metrosideros polymorpha*-Native trees | 2 | 0.6% |
| | *Acacia koa-Cheirodendron trigynum* | 1 | 0.3% |
| | *Cheirodendron trigynum* | 1 | 0.3% |
| | *Eucalyptus* spp. | 1 | 0.3% |
| Kaʻū Preserve (The Nature Conservancy) | *Metrosideros polymorpha* | 3 | 100% |
| **Grand Total** | **N/A** | **488** | **N/A** |

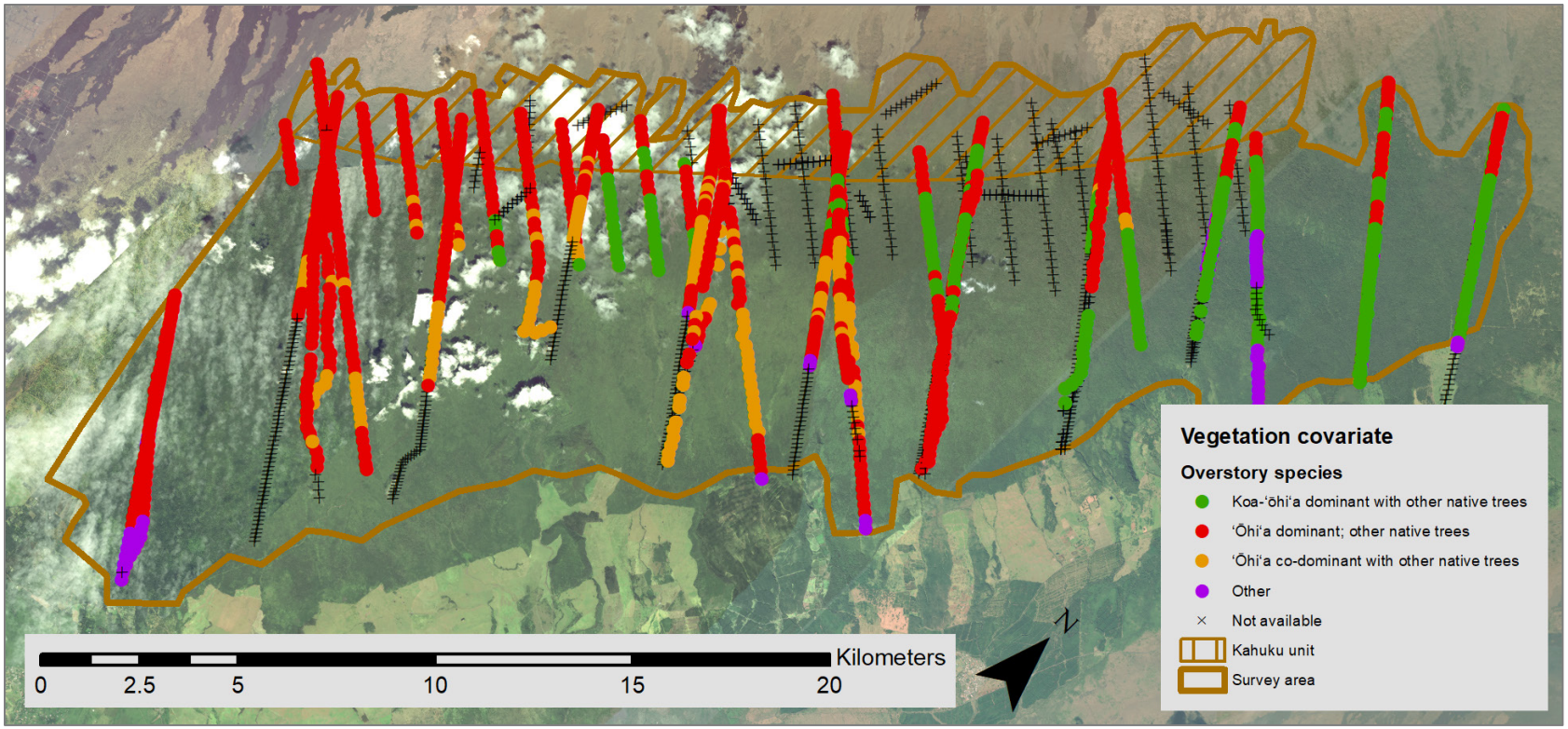



**Figure 54.** The predominant canopy species recorded at each station surveyed in 2019 and for transects surveyed in previous years.

**Table 47.** Understory classes recorded within each survey area during the 2019 Kaʻū Rainforest landbird survey. Classes are separated by a comma in order of dominance. Classes separated by a dash are codominant within the habitat plot around the survey station. The percent of classes recorded within each survey area are presented.

| 2019 Survey Area | Understory Class | Count | % |
|---|---|---|---|
| Hawaiʻi Volcanoes National Park (Kahuku Unit) | Native Shrubs, Non-native Grasses | 12 | 17.1% |
| | Native Shrubs, Native Grasses | 7 | 10.0% |
| | Native Shrubs, Native Grasses, Non-native Grasses | 4 | 5.7% |
| | Native Shrubs, Bare Ground | 3 | 4.3% |
| | Native Shrubs, Matted Ferns, Non-native Grasses | 3 | 4.3% |
| | Native Ferns-Non-native Grasses, Native Trees (saplings) | 2 | 2.9% |
| | Native Shrubs, Native Grasses | 2 | 2.9% |
| | Native Shrubs, Native Sedges, Bare Ground | 2 | 2.9% |
| | *Coprosma* spp., Native Ferns, Bare Ground | 2 | 2.9% |
| | *Classes Occurring less than 2%* | 33 | 47.1% |
| Kapāpala Cooperative Game Management Area | Non-native Grasses | 4 | 21.1% |
| | Matted Ferns, Native Shrubs, Non-native Grasses, | 2 | 10.5% |
| | *Classes Occurring Less than 10%* | 13 | 68.4% |
| Kapāpala Forest Reserve | Non-native Grasses, Native Shrubs | 6 | 24.0% |
| | Native Shrubs, Matted Ferns | 4 | 16.0% |
| | Native Shrubs, Native Grasses | 4 | 16.0% |
| | Native Shrubs, Bare Ground, Native Grasses | 3 | 12.0% |
| | Native Shrubs, Matted Ferns, Bare Ground | 2 | 8.0% |
| | *Classes occurring less than 8%* | 6 | 24.0% |
| Kaʻū Forest Reserve | Native Ferns, Native Shrubs | 20 | 5.6% |
| | Native Ferns, *Hydrangea arguta* | 11 | 3.1% |
| | Tree Ferns, Native Shrubs | 10 | 2.8% |
| | Tree Ferns, *Hydrangea arguta* | 9 | 2.5% |
| | *Hydrangea arguta*, Native Ferns | 7 | 2.0% |
| | Native Ferns, Matted Ferns | 7 | 2.0% |
| | Native Shrubs, Native Ferns | 7 | 2.0% |
| | *Classes occurring less than 2%* | 144 | 40.6% |

**Table 47 (continued).** Understory classes recorded within each survey area during the 2019 Kaʻū Rainforest landbird survey. Classes are separated by a comma in order of dominance. Classes separated by a dash are codominant within the habitat plot around the survey station. The percent of classes recorded within each survey area are presented.

| 2019 Survey Area | Understory Class | Count | % |
|---|---|---|---|
| Kaʻū Preserve (The Nature Conservancy) | Native Ferns, Tree Ferns, Matted Ferns | 1 | 33.3% |
| | Native Shrubs, Tree Ferns | 1 | 33.3% |
| | Native Shrubs, Tree Ferns, Matted Ferns | 1 | 33.3% |
| **Grand Total** | **N/A** | **472** | **N/A** |

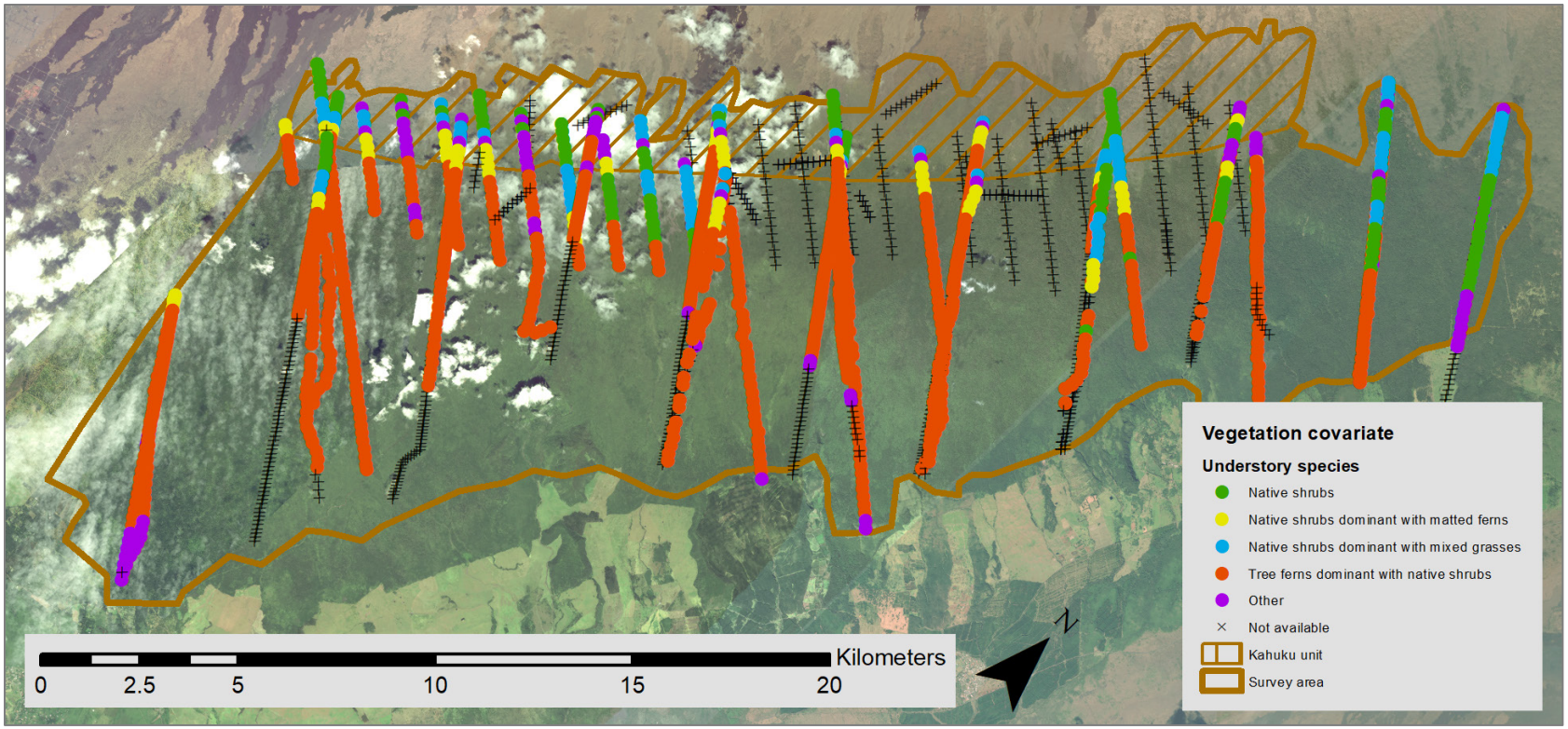



**Figure 55.** The predominant understory species or class recorded at each station surveyed in 2019 and for some transects surveyed in previous years.

**Table 48.** Vegetation classification codes (Jacobi 1989) recorded for each station surveyed in 2019. The codes encompass many aspects of forest structure including species association, tree canopy composition, and undergrowth composition in order of dominance or co-dominance. Classifications were determined post hoc from Jacobi (1989) vegetation maps. Percent of each code recorded for stations within each survey area are presented.

| 2019 Survey Area | Vegetation Classification Codes (Jacobi 1989) * | Count | % |
|---|---|---|---|
| Hawai‘i Volcanoes National Park (Kahuku Unit) | M:Me,nt(ns,mf) | 25 | 35.7% |
| | D:(ns)Me,nt | 19 | 27.1% |
| | D:Me,nt(ns,mg) | 12 | 17.1% |
| | M:Me,nt(mf-ns) | 6 | 8.6% |
| | M:Me,nt(ns-xg-xs) | 3 | 4.3% |
| | M:Me,nt(mf-ns) pilo | 2 | 2.9% |
| | W:Me,nt(tf,ns) | 2 | 2.9% |
| | M:Me,nt(mf-ns) | 1 | 1.4% |
| Kapāpala Cooperative Game Management Area | M:Ac-Me,nt(ns) | 10 | 52.6% |
| | M:Ac-Me,nt(ns-xg-xs) | 7 | 36.8% |
| | unknown | 2 | 10.5% |
| Kapāpala Forest Reserve | D:Me,nt(ns,mg) | 14 | 56.0% |
| | M:Ac-Me,nt(ns) | 9 | 36.0% |
| | M:Ac-Me,nt(ns-xg-xs) | 2 | 8.0% |
| Ka‘ū Forest Reserve | W:Me,nt(tf,ns) | 179 | 48.2% |
| | W:Ac-Me,nt(tf,ns) | 79 | 21.3% |
| | W:(tf,ns)Me-nt | 63 | 17.0% |
| | M:Me,nt(ns,mf) | 17 | 4.6% |
| | M:Ac-Me,nt(ns) | 16 | 4.3% |
| | unknown | 9 | 2.4% |
| | D:Me,nt(ns,mg) | 3 | 0.8% |
| | W:Me,nt(ns/mf) | 2 | 0.5% |
| | M:Me,nt(mf-ns) | 1 | 0.3% |
| | M:Me,nt(mf-ns) | 1 | 0.3% |
| | W:xt,nt(xs) | 1 | 0.3% |
| Ka‘ū Preserve (The Nature Conservancy) | W:(tf,ns)Me-nt | 3 | 100.0% |
| **Grand Total** | **N/A** | **488** | **N/A** |

* Codes for Jacobi (1989) rapid habitat assessment classification: Species association type (D=dry, M=mesic (moist), W=wet), Tree canopy cover (Me=Metrosideros polymorpha, Ac=Acacia koa, nt=native trees, tf=tree ferns, xt=exotic trees), Understory species composition (ns=native shrubs, xs=exotic shrubs, mf=matted ferns, tf=tree ferns, mg=mixed grasses, pilo=Coprosma spp.). Refer to Jacobi (1989) for descriptions of codes not listed in table.

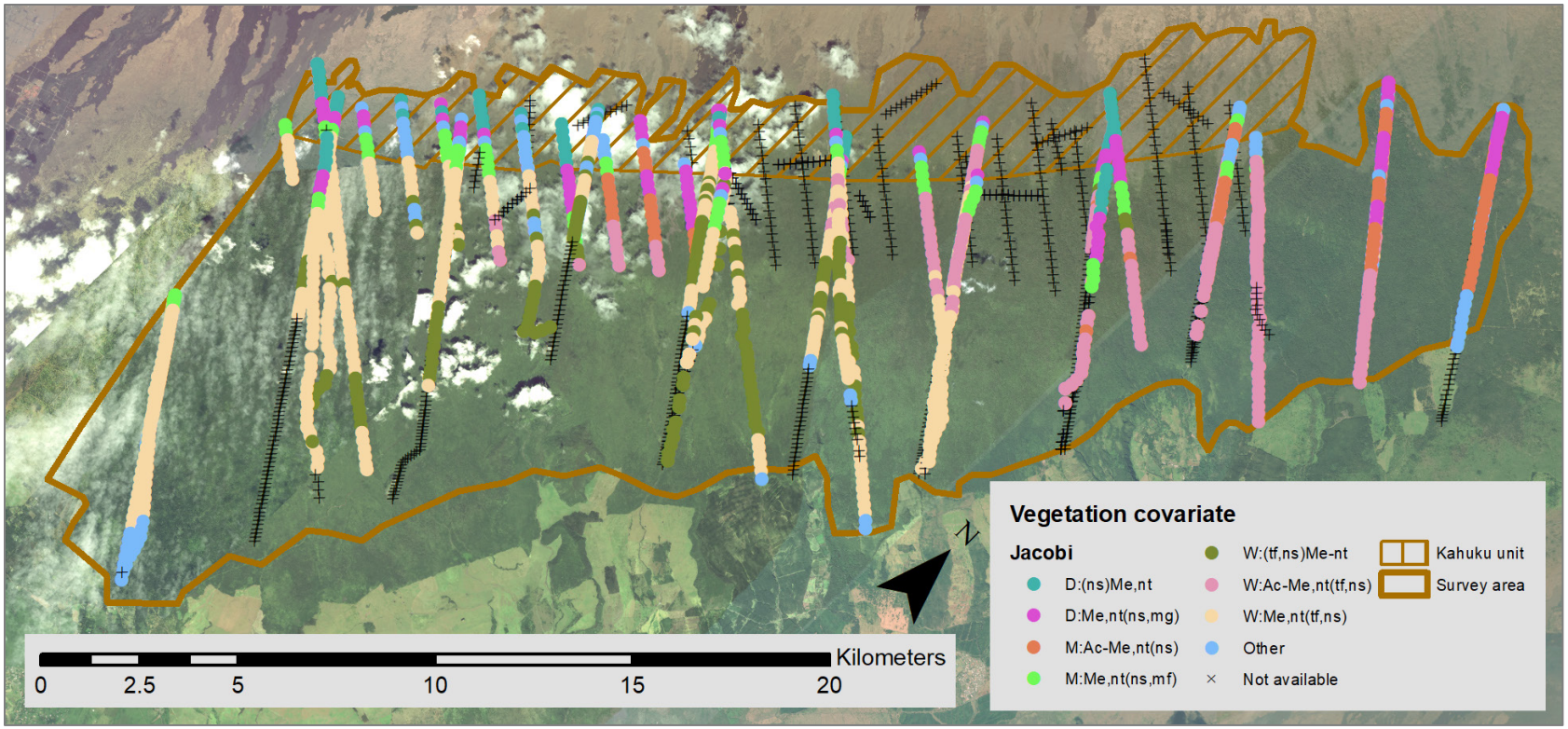



**Figure 56.** The Jacobi (1989) vegetation code recorded for each station surveyed in 2019 and previous survey years. The code encompasses many aspects of forest structure including environment, canopy height, and dominant canopy and undergrowth species, and so is a combination of many other vegetation covariates. Refer to footnotes in table above for code definitions and in Jacobi (1989) for more details.

**National Park Service**
**U.S. Department of the Interior**

**Science Report NPS/SR—2024/141**
https://doi.org/10.36967/2303786




**Natural Resource Stewardship and Science**
1201 Oakridge Drive, Suite 150
Fort Collins, CO 80525

NPS 124/193811, June 2024